Fakultät für Medizin

Institut für Virologie

Activation of CTL against Poxviral Antigens depends on Time of Expression and Subcellular Localization during Infection

Sha Tao

Vollständiger Abdruck der von der Fakultät für Medizin der Technischen Universität München zur Erlangung des akademischen Grades eines

Doctor of Philosophy (Ph.D.)

genehmigten Dissertation.

Vorsitzender: Univ.-Prof. Dr. Jürgen Ruland

Betreuer: Univ.-Prof. Dr. Ingo Drexler

Prüfer der Dissertation:

1. apl. Prof. Dr. Volker Bruß

2. Priv.-Doz. Dr. Oliver Ebert

3. Univ.-Prof. Dr. Gerd Sutter (Ludwig-Maximilians-Universität München)

Die Dissertation wurde am 05.06.2013 bei der Fakultät für Medizin der Technischen Universität München eingereicht und durch die Fakultät für Medizin am 22.10.2013 angenommen.

Contents

Abstract

Recombinant modified vaccinia virus Ankara (recMVA) vectors provide a high-level gene expression and have proven to be immunogenic when delivering antigens in animals and humans. Since cytotoxic CD8+ T cells (CTL) have an important role in clearing acute viral infections, we were interested in defining criteria for optimal activation conditions for these cells by MVA vector vaccines. Our group has previously shown that antigen presentation of late viral gene products to CTL is substantially delayed and dramatically shapes the CTL repertoire in secondary expansion due to T cell competition (Kastenmuller *et al*., 2007; Meyer *et al*., 2008). Thereby, the timing of viral antigen expression in infected APC had a strong impact on viral T cell epitope presentation and processing. The puzzling issue was the delayed triggering of CTL by late viral proteins.

To follow up on this, different antigen-specific CTL lines were generated that recognize epitopes derived from vaccinia virus (VACV) proteins or model antigens with distinct expression kinetics, so that the presentation of early or late viral antigens can be monitored. As a first result, one CTL line derived from the VACV protein A3, which represents a late gene product according to literature, was found to be activated also at early time points after infection. This finding was verified by qPCR.

More importantly, late antigens, in contrast to early antigens, could not efficiently activate TC by direct (endogenous) presentation. Additionally, they were also unable to activate CTL via the cross (exogenous) presentation pathway (infected MHC-mismatched APC as an antigenic source and MHC-matched DC as cross-presenters).

Furthermore, distinct availability of early and late antigens for MHC I presentation was not due to the impairment of the antigen presentation machinery, but due to different subcellular localizations of early and late antigens. This was demonstrated by late produced recMVA envelope protein (H3) which was visualized during infection as early as viral factories had been established and thereafter was sequestered within these structures up to three hours. In addition, H3 protein produced late was more stable as compared to H3 produced early. In contrast to this, although late produced recombinant GFP or ova was first discovered in viral factories, it was found to be quickly distributed into the cytoplasm. Thus, compartmentalization may be the decisive factor for the delayed MHC class I presentation of viral late antigens. Additionally, the types of APC which we have investigated also displayed distinct presentation patterns for late antigens.

As a result, the timing of viral antigen production and subsequent localization to specific cell compartments plays an important role for recMVA antigen delivery and further antigen processing.

List of Abbreviation

APC	Antigen presenting cells
BFA	Brefeldin A
BMDC	Bone marrow derived dendritic cells
BSA	Bovine serum albumin
CEF	Chicken embryo fibroblasts
CTL	Cytotoxic T lymphocytes
CVA	Chorioallantois vaccinia Ankara
DC	Dendritic cells
dH_2O	Distilled water
DMSO	Dimethylsulfoxide
DNA	Desoxyribonucleic acid
dNTP	Desoxy nucleotide tripohosphate
DTT	1,4- Dithiothreitol
EDTA	Ethylenediaminetetraacetic acid
EEV	Extracellular enveloped virus
EMA	Ethidium monoazide bromide
ER	Endoplasmatic reticulum
FACS	Fluorescence activated cell sorter
FCS	Fetal calf serum
FITC	Fluorescein isothiocyanate
Flt-3	fms-like tyrosine kinase 3
FSC	Forward scatter
GFP	Green fluorescent protein
GM-CSF	Granulocyte macrophage colony-stimulating factor
HA	Hemagglutinin (influenza)
HEPES	N-(2-Hydroxyethyl) piperazine-1-ethanesulfonic acid
HLA	Human leucocyte antigen

h.p.i.	Hours post infection
ICS	Intracellular cytokine staining
IEV	Intracellular enveloped virus
IFNγ	Interferon γ
IL	Interleukin
IMV	Intracellular mature virus
i.p.	Intraperitoneal
kb	Kilo bases
kDa	Kilo dalton
LCL	Lymphoblastoid cell line
LPS	Lipopolysaccharid
M	Mol
M-CSF	Macrophage colony stimulating factor
MHC	Major histocompatibility complex
Min	Minute
mM	Millimolar
mRNA	Messenger ribonucleic acid
MOI	Multiplicity of infection
MVA	Modified vaccinia virus Ankara
NP-40	Nonidet-P40 (octyl phenoxylpolyethoxylethanol)
ORF	Open reading frame
ova	Chicken Ovalbumin
PAGE	Polyacrylamidgel-Electrophoresis
PBS	Phosphate buffered saline
PCR	Polymerase chain reaction
PE	Phycoerythrin
PerCP	Peridinin chlorophyll protein
PFA	Paraformaldehyde
PMSF	Phenylemethylsulfonylfluoride

PO	Peroxidase
Rec	Recombinant
rpm	Rounds per minute
RT	Room temperature
s.c.	Subcutaneous
SDS	Sodium dodecyl sulphate
SSC	Sideward scatter
TAE	Tris-acetate-EDTA buffer
TAP	Transporter associated with Antigen Processing
TBS	Tris buffered saline
TCGF	T cells growth factor
TEMED	N, N, N', N'-Tetramethylethylendiamine
TLR	Toll-like receptor
TNF	Tumor-nekrose-faktor
Tris	Trishydroxymethylaminomethane
Ub	Ubiquitin
UV	Ultraviolet
VACV	Vaccinia virus
wt	Wild type

1. Introduction

1.1 Vaccinia Virus

Vaccinia Virus, a member of the Orthopoxvirus genus from the Poxviridae, is a large enveloped double-stranded DNA virus that replicates in the cytoplasm. It has a large genome ranging from 185 to 200kbp and encoding around 200 proteins, which function in disabling host defenses, enabling virus replication and transcription, and assembling. The two major forms of virions are MV (mature virion) and EV (enveloped virion), which contain a dumbbell-shaped core (20 proteins), lateral bodies (80 proteins) and lipid membranes (20 proteins). EV has an additional outer membrane (6 proteins). (Moss, 2007).

1.1.1 Vaccinia virus replication cycle and gene expression

Vaccinia virus can enter cells by fusion after MV binding to the cell membrane or EV membrane interruption, or via internalization by macropinocytosis for both virus types (Schmidt *et al*., 2012). MV proteins - A26 (binds laminin), H3, A27 (binds heparin) and D8 (binds chondroitin) - are responsible for attachment. A further nine proteins (A16, A21, A28, G3, G9, H2, J5, L5, O3) are components of EFC (entry fusion complex) and required for entry. The ways in which entry is achieved also depends on the viral strains. For MVA, plasma membrane fusion is more likely because of the loss of the A25 and A26 EV genes (Chang *et al*., 2010).

The most recent analysis of VACV WR suggests that there are 118 early (0-1.5h), 53 intermediate (1-3h) and 38 late (>3h) genes, depending on their time of expression (Yang *et al*., 2011). Early gene transcription starts immediately as the core is

released into the cell cytoplasm (entry), which activates viral RNA polymerase and subsequently the early gene transcription factors. Early viral genes encode enzymes and factors are required for DNA replication and intermediate gene transcription and also result in production of immunodulatory proteins that block the innate antiviral defenses (Price *et al*., 2013). Early gene expression also disrupts the virus core (uncoating), leading to DNA replication. Intermediate genes are transcribed and translated to form trans-activating factors for late proteins. Late viral genes, encoding structural, membrane and core proteins, enzymes and early transcription factors, are then transcribed (Fig.1).

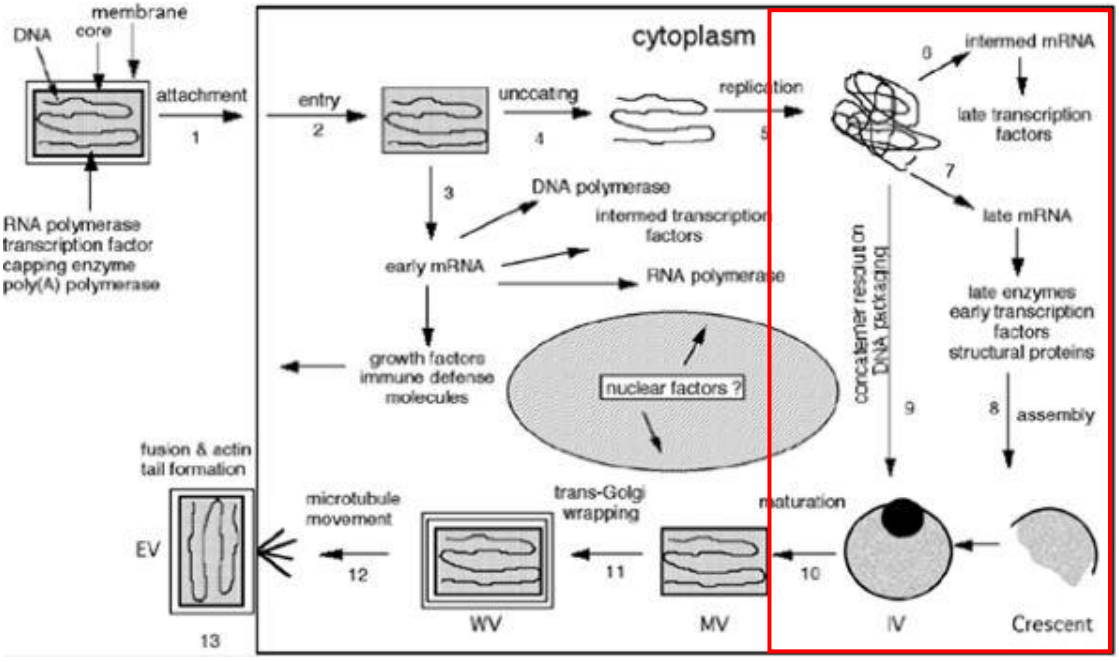

Figure 1: Vaccinia virus replication cycle. Red area shows processes within the viral factory. (Moss, 2007)

Poxvirus is a unique DNA virus because it replicates in the cytoplasm rather than in the nucleus. Additionally, the sites of replication are known to be viral organells

called viral factories. Each viral factory formed from a single genome is the site of transcription and translation as well as DNA replication (Katsafanas *et al*., 2007). Early viral proteins are synthesized at a place distant from the cores. The factories will first appear at two hours post-infection as numerous tiny spots throughout the cytoplasm of the cell (Schramm *et al*., 2006). They grow in size, decrease in number over time and gradually collect besides the nucleus. They are surrounded by ER derived membranes. Factories can be clearly visualized as early as four hours p.i. and disappear later when virus assembly begins (Fig.2 Tolonen *et al*., 2001). Virus assembly is characterized by the forming of crescent viral membranes, i.e., around immature virus particles containing a DNA nucleoid in factories (Fig.3 Condit, 2006). Next, the viral DNA is incorporated into immature virions (IV) (Fig.1:9). In mammalian cells, MVA will stop at this step of replication due to a block in morphogenisis. For other strains, which can replicate in mammalian cells, IV will mature into infectious intracellular mature virions (IMV) (Fig.1:10) being transported out of factories, which requires microtubules and the A27 protein (Sanderson *et al*., 2000).

IMV is wrapped by a double membrane, which is derived from the trans-Golgi network or the endosome to form intracellular enveloped virions (IEV) (Fig.1:11). This requires B5 and F13 proteins. IEV move to the cell surface which requires microtubules and the F12 protein. Its outer membrane fuses with the cell membrane. Respective viruses attached to the cell surface are termed CEV (cell-associated enveloped virus). After release from the cell membrane, free viruses are called EEV (extracellular enveloped virus) which require A33, A34 and B5 proteins.

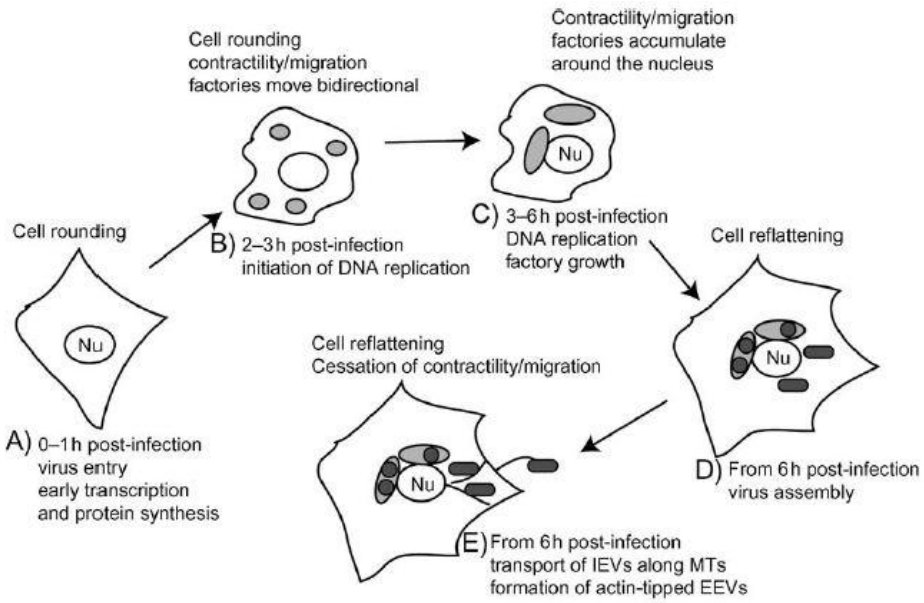

Figure 2: Vaccinia virus replication sites formation. (Schramm *et al*., 2006)

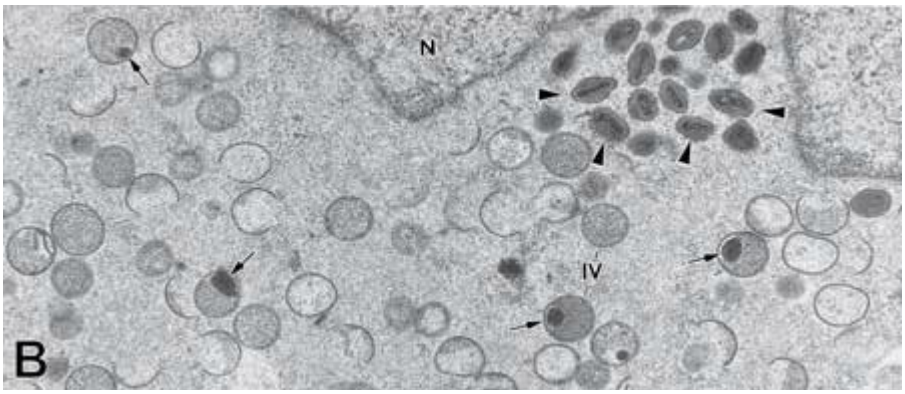

Figure 3: Electron microscopy of a factory at a late stage of infection, showing virus assembly. IV, immature virion; Arrows, IV with nucleoid; Arrowhead, mature virions. (Condit *et al*., 2006)

H2-K^b-restricted	Location	Function	Time	Reference
A19L	Core	Zinc finger	Late	Satheshkumar *et al.*, 2013; Mercer *et al.*, 2006; Tscharke *et al.*, 2005
A3L	Core	p4b precursor of core protein 4b	Early/Late	Oseroff *et al.*, 2008; Moutaftsi *et al.*, 2006; Tao *et al.*, unpublished
B8R	Cytoplasmic	Like IFN γ receptor, virulence	Early	Moutaftsi *et al.*, 2006; Tscharke *et al.*, 2005

H2-D^b-restricted	Location	Function	Time	Reference
A42R	Cytoplasmic	Profilin-like	Late	Moutaftsi *et al.*, 2006; Tscharke *et al.*, 2005
K3L	Cytoplasmic	interferon resistance	Early	Moutaftsi *et al.*, 2006; Tscharke *et al.*, 2005

HLA-A2-restricted	Location	Function	Time	Reference
B22R	Cytoplasmic	serpins	Early	Terajima *et al.*, 2003
A6L	Core	Membrane formation	Late	Oseroff *et al.*, 2005; Pasquetto *et al.*, 2005
H3L	MV membrane	IMV heparin binding surface protein involved in IMV maturation	Late	Pasquetto *et al.*, 2005; Drexler *et al.*, 2003
I1L	Core	DNA binding	Late	Oseroff *et al.*, 2005; Pasquetto *et al.*, 2005

1.1.2 MVA as vaccine

In 1798, Edward Jenner opened the field of vaccination by using cowpox to protect against smallpox. For a safer alternative, Professor Anton Mayr, in the 1950s in Germany, began to attenuate CVA (chorioallantois vaccinia Ankara) to generate MVA (Modified vaccinia virus Ankara), which was used as vaccines for smallpox in the 1970s. This highly attenuated strain lost about 30kb of its genomes in the course of over 570 passages on CEF (chicken embryo fibroblast) cells and experienced multiple deletions compared to its parental strain, CVA. Hence, it is unable to complete its replication cycle in human cells and nearly all other mammalian cells (Drexler *et al*., 2004), as only immature virions are formed (Sutter and Moss, 1992). However, the lack of many immunomodulatory genes, which encode inhibitors or receptors for cytokines and chemokines to subvert the host immune defense (Price *et al*., 2013; Antoine *et al*., 1998), supplies MVA with a high immune-stimulating capacity e.g. by activation of human dendritic cells even in the absence of virus multiplication (Drillien *et al*., 2004).

Furthermore, the large genome with its six major deletion sites together with the late block in replication allow for a large insertion capacity for foreign genes and a high level gene expression beneficial for inducing strong immune responses, e.g. T cell responses, or for other applications such as targeting or visualizing tumor cells. Till now, MVA has been widely used for other infectious diseases (Gilbert *et al*., 2013; Cottingham *et al*., 2013; Volz *et al*., 2013), like HIV (DNA prime/MVA boost vaccine (Hayes *et al*., 2013; Brandler *et al*., 2010), malaria (MVA-ME-TRAP express a linear construct of CD4+ and CD8+ T cell and B cell epitopes) and TB (MVA85A). It has been well used as a

therapeutic immunization agent against cancer, because recombinant MVA have a high ability to induce immunogenicity of tumor-associated antigens (TAAs), such as 5T4, gp100 (Hanwell *et al*., 2013), and other melanoma antigens (combination of 7 epitopes from 5 melanoma antigens into a polyepitope string in MVA-Mel3; Dangoor *et al*., 2010).

MVA also encodes some virulence factors that target innate signal pathways, such as IFN, TLR and inflammatory cytokines (Price *et al*., 2013; Delaloye *et al*., 2009). These innate responses may also initiate stronger adaptive immune responses, as TLR signaling is crucial for CD8+ T cell memory development following vaccinia virus infection (Amiset *et al*., 2012).

VACV is a common model for studying adaptive immune responses, including CD8, CD4 and antibody responses. CD8 responses usually focus on early antigens, while CD4 and antibody responses focus on late and structural proteins (Moutaftsi *et al*. 2010). Dendritic cells are thought to directly present early antigens and present late antigens via antigen uptake. It is still under discussion as to how the CD8+ T cells respond to late antigens and how the CD4+ T cells respond to early antigens e.g. by which antigen presentation pathways. Nonetheless, studies showed that MVA elicits both, antibodies and T cell mediated immune responses in mice (Mullarkey *et al*., 2013; Wyatt *et al*., 2004) and in humans (Sheehy *et al*., 2012).

Our group, for the first time, has performed comparative analysis and monitoring of epitope-specific CD8+ T cell responses elicited against both viral vector-derived and recombinant antigens after immunization (Drexler *et al*., 2003). Using the attenuated VACV-strain MVA, we demonstrated that primary CTL responses against

VACV-produced antigens were dominated by cross-priming *in vivo*, while infected professional antigen-presenting cells (pAPC), such as dendritic cells (DC), failed to induce primary CTL (Kastenmuller *et al*., 2006; Gasteiger *et al*., 2007). In the recall, we found that the immunodominance pattern was shaped by competing CTL (Kastenmuller *et al*., 2007). Thereby, the outcome of T cell competition in secondary responses is strongly depended on the timing of viral antigen expression in infected APC, particularly characterized by poor proliferation of T cells recognizing epitopes derived from late viral proteins. Furthermore, the timing of VACV gene expression after infection has a strong impact on viral T cell epitope presentation and processing (Meyer *et al*., 2008).

1.2 Adaptive Immunity

After two to three days of infection, if the innate immune response can not clear bacterial or viral pathogens by macrophages, granulocytes and NK cells, adaptive immunity will help after transport antigens to lymphoid organs, where they encounter naïve B cells and T cells. The activated B and T cells will proliferate and differentiate into effector cells to kill the infected cells and produce antibodies to neutralize the virus. Protection continues for several weeks, then the immune reponse returns to silence when the activated T cells are eliminated by apoptosis having left the LN to the peripheral tissues. Some immune cells will differentiate into memory cells for longer protection.

1.2.1 Antigen Presenting Cells

Professional APC effectively internalize antigens and present them to T cells which include dendritic cells (DC), macrophages and B cells. They differentiate from bone marrow precursors called hematopoietic stem cells (HSCs), which develop into myeloid and lymphoid precursors (CMP and CLP). CLP further give rise to T cell or B cell precursors. CMP are initially thought to generate DC, macrophages and monocytes from Granulocyte-macrophage precursors by the "myeloid" hormone GM-CSF (granulocyte–macrophage colony-stimulating factor), because DC have many similarities to macrophages. However, it was discovered that myeloid and lymphoid precursors may develop both, cDC and pDC, based on the expression of the receptor Flt-3 (fms-related tyrosine kinase 3, Ricklin *et al*., 2010; Damico *et al*., 2003, Chicha *et al*., 2004). As a result, GM-CSF or Flt-3 ligands are being used to generate DC from bone marrow *in vitro* (Satpathy *et al*., 2012; Naik *et al*., 2005). It is noteworthy, bone marrow derived BMDC, which express CD24, Clec9a and CD127a^{low}, have the same function as CD8a+ cDC in the spleen (Shortman *et al*., 2007). (Fig.4)

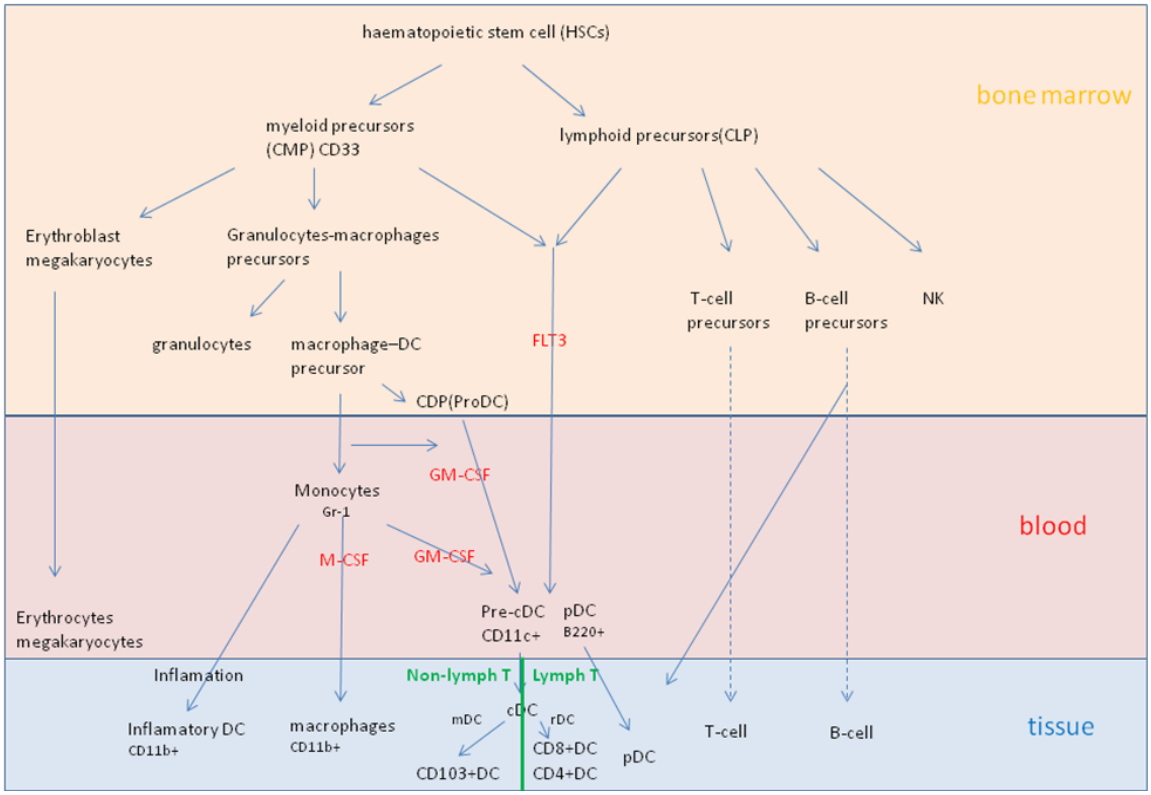

Figure 4: Dendritic cell development. Hematopoietic stem cells (HSCs) give rise to myeloid and lymphoid precursors (CMP and CLP). CLP develop into T-cell or B-cell precursors. CMP generate later granulocytes and Granulocytes-macrophages precursors. The latter can develop *in vitro* into DC by adding "myeloid" hormone GM-CSF (granulocyte–macrophage colony-stimulating factor) or Flt-3 (fms-related tyrosine kinase 3).

Dendritic cells (DC) are unique APC with regard to their ability to initiate primary immune response by activating naïve T cells. The membrane-bound pattern recognition receptors (PRRs) on DC serve to identify pathogen-associated molecular patterns (PAMPs), which are associated with cell damage (development of self tolerance) or foreign pathogens (danger signal). They are derived from endogenous cellular structures or from pathogens. C-type lectin receptors (CLRs) are one type of endocytic PRRs. Upon binding, CLRs internalize antigen for presentation onto MHC class I or II molecules for presentation to T cells (Unger *et al.*, 2011; Gijzen *et al.*, 2006). Different

receptors, including DEC-205, Langerin, Dectin-1 in human; Mannose Receptor (MR), DC-SIGN and Clec9A in both human and mouse DC; internalize antigens via different endosomal pathways. MR (Martinez-Pomares., 2012) in mouse DC delivers antigens into early endosomal compartment specialized in loading MHC I for cross-presentation, while loading of MHC II occurs in late endosomes or lysosomes by scavenger receptors (Burgdorf *et al*., 2007). However, some CLRs also affect signaling by Toll-like receptors (TLRs), which recognize bacterial or viral components, and TLRs are also the mediators for activation and maturation stimuli for DC to promote migration towards lymph nodes. In the presence of TLR signaling, co-stimulatory molecules are upregulated and antigen uptake and presentation through CLRs can initiate immunity through T cell stimulation (Th1, Th2 or Th17) (Szatmary., 2012; Van Vliet *et al*., 2008).

There are distinct DC subtypes in mice, which differ in location, immunological functions and generation stimuli. These subtypes include conventional DC (cDC), plasmacytoid DC (pDC) and inflammatory DC (Ansuman *et al*., 2012; Shortman *et al*., 2007). cDC and pDC are steady-state DC, which means present in healthy conditions, while inflammatory DC develop from monocytes in both periphery and lymphoid organs under conditions of inflammation (Dominguez *et al*., 2010). pDC combat viral infections by producing antiviral cytokines, such as type I interferons (Demoulin *et al*., 2013; Villadangos *et al*., 2008). cDC include resident DC and migratory DC. Resident DC are directly found in the lymphoid organs (splenic DC), while migratory DC enter the circulation and home to peripheral tissues where they reside as immature DC with high phagocytic capacity, awaiting activation by "danger" signals. This danger signal can be

direct infection, cytokines or death signals induced by neighboring cells or viral proteins. Immature DC capture the antigen and become activated/matured, upregulate the chemokine receptor CCR7 (Hwang, 2012; Yoshida *et al*., 1997) and migrate into the draining lymph nodes. Here, mature DC from periphery and local resident DC express high levels of co-stimulatory molecules (CD40, CD80, CD86) and moderate to high surface levels of MHC II (Shortman *et al*., 2002), permitting antigen presentation to T and B cells, or pass on their antigen to lymph nodes-resident DC (Segura *et al*., 2012) for further presentation and initiation of immune responses. The question of whether migratory or resident DC present peripheral antigen to T cells is still controverse. Olivier and co-workers found that migrating CD1b+ lymphatic dendritic cells can present Salmonella antigens to naive T cells (Olivier *et al*., 2012). However, He and co-workers found that skin-derived DC (sDC) can also induce CD8+ T cell responses (He *et al*., 2006) and resident CD141 (BDCA3)+ dendritic cells in human skin can induce regulatory T cells that suppress skin inflammation (Chu *et al*., 2013). (Fig.5)

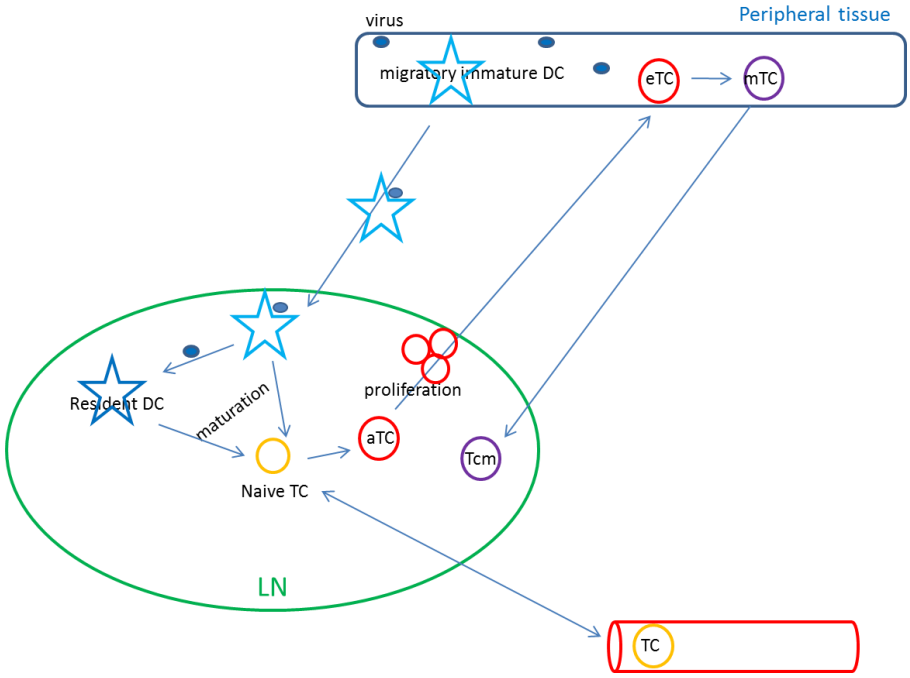

Figure 5: Dendritic cell and T cell activation.

In MVA infection, DC are preferentially targeted by MVA in secondary lymphoid tissues. The infected DC express high levels of viral early Ags, undergo rapid maturation during the first 12 hours post infection, produce a substantial amount of IFN-α, then become apoptotic in the next 24 hours. The infected DC are readily taken up by uninfected bystander DC, with their protein constituents then made available via cross-presentation mechanisms of antigen presentation to elicit virus-specific adaptive immune responses (Guzman *et al*., 2012; Iborra *et al*., 2012; Pascutti *et al*., 2011; Liu *et al*., 2008).

1.2.2 MHC class I antigen presentation

MHC I antigen presentation enables the immune system, mainly CD8+ T cells, to recognize infected or antigen containing cells by a specific peptide processed and presented from foreign pathogens or modified self-proteins. The peptides are mainly

generated from endogenous proteins (direct-presentation); however, peptides can also be derived from exogenous antigens, which is called cross-presentation, as exogenous antigens are traditionally presented to CD4+ T cells. Recently, another indirect antigen presentation pathway has been discussed, called cross-dressing. Cross-dressing decribes a process in which MHC I/peptide complexes are directly translocated to other cells without the requirement for further processing. It has been shown that cross-dressed $CD8\alpha^+/CD103^+$ DC can prime naïve and memory CD8+ T cells (Li *et al*., 2012).

1.2.2.1 Direct-presentation

MHC class I molecules present antigens that have been generated by proteasome-mediated degradation. DRiPs (defective ribosomal products) are misfolded or truncated proteins which are immediately degraded after and allow for much faster antigens presentation than anticipated from their natural half-lives (Yewdell, 2011). The antigens are degraded into small peptides of eight to ten amino acids in the cytosol by the proteasome. The peptides are transported to the ER (endoplasmic reticulum) lumen by TAP (transporter associated with antigen presentation) to be loaded onto MHC I molecules, which contain a polymorphic heavy chain and a light chain β_2m (β_2-microglobulin). Without peptide, MHC I molecules are stabilized by calreticulin, ERp57 and tapasin, known as PLC (peptide loading complex). Tapsin interacts with TAP, so the peptide transported in the ER will obtain easy access to MHC I molecules and can insert into the MHC I peptide-binding groove in order to keep the complex stable. The complex is then released from the PLC and ER and translocates to the cell surface membrane via the Golgi apparatus. (Fig.6) (Blum *et al*., 2013; Neefjes *et al*., 2011)

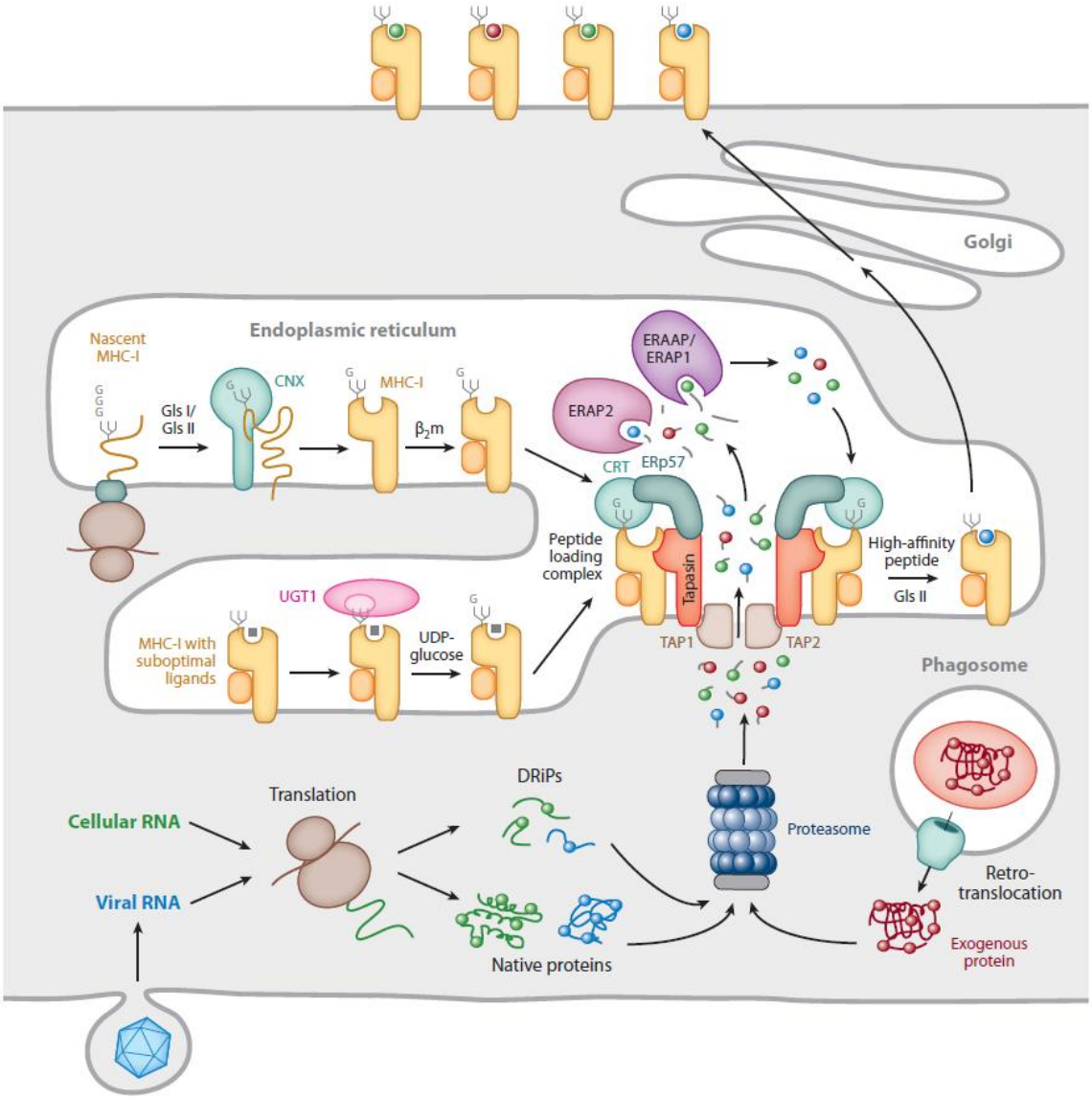

Figure 6: MHC I presentation pathways. (Blum *et al*., 2013).

1.2.2.2 Cross-presentation

When APC are not directly infected, they need to catch up exogenous antigens and present them via MHC I molecules, a process defined as cross-presentation. The main cross-presenters are dendritic cells *in vivo* (Joffre *et al*., 2012; Hopkins *et al*., 2012), though other APC can also do the job *in vitro*. However, which subtype of DC has the

ability is still not entirely clear. In mice, lymphoid organ-resident CD8α+ DC (Segura *et al*., 2013; Shortman *et al*., 2010), non-lymphoid tissue CD103+ DC, which migrate to lymph nodes (Desch *et al*., 2011), and inflammatory DC (Segura *et al*., 2009) are specialized at cross-presentation and have developed specific adaptations concerning their endocytic pathways (neutral pH, low degradation, and high export to the cytosol). These DC can cross-present cell-associated (Tel *et al*., 2013; Iborra *et al*., 2012; Sancho *et al*., 2009) and soluble antigens (Tel *et al*., 2013; Zhao *et al*., 2012). In humans, CD141(BDCA3)+ DC (recently shown to be the homologue to mouse lymphoid organ-resident CD8α^+ DC) and mouse non-lymphoid tissue CD103+ DC (Haniffa *et al.,* 2013; Segura *et al*., 2013; Poulin *et al*., 2010), Langerhan cells (Klechevsky *et al*., 2008) and CD1a+ DC (Segura *et al*., 2012) display high intrinsic cross-presentation capacity.

After phagocytosis, exogenous antigens can be degrad either by proteasomes or phagosomes. The former is known as cytosolic pathway and is the dominant pathway for cross-presentation; the latter is known as vacuolar pathway independent from proteasomes and TAP and may be inhibited by chloroquine (Joffre *et al*., 2012; Segura *et al*., 2011). (Fig.7)

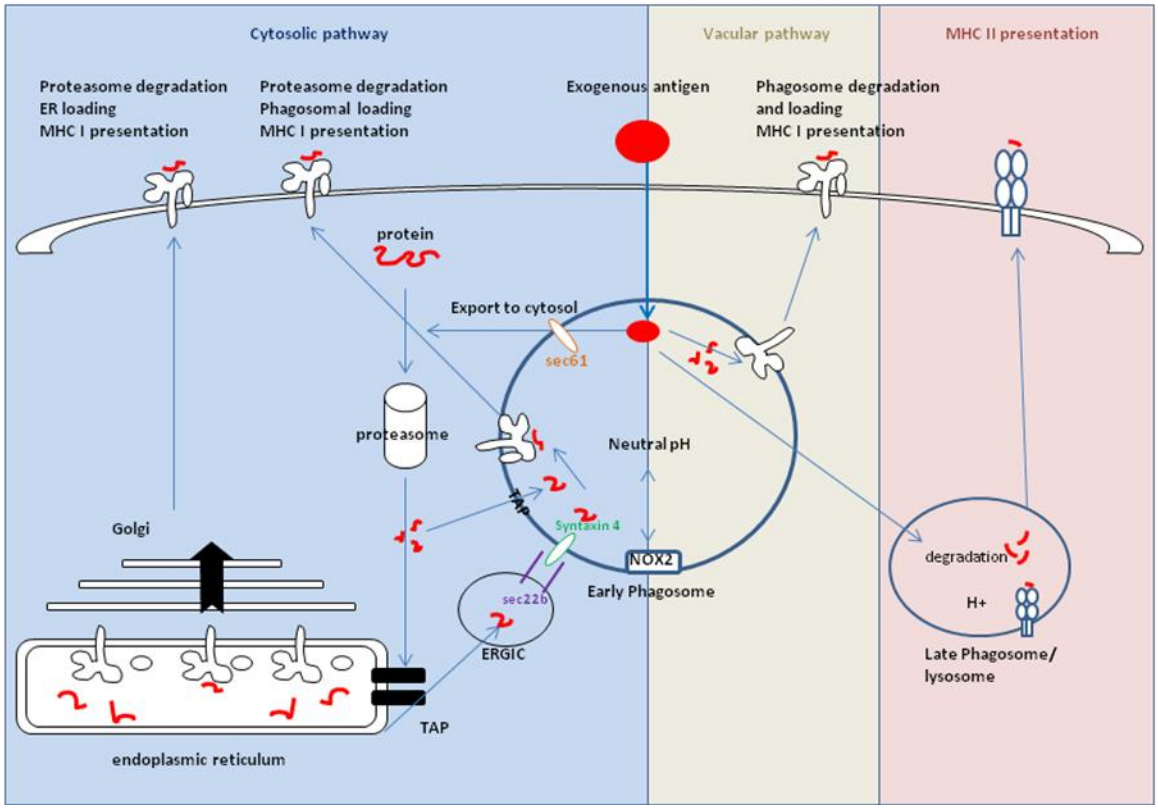

Figure 7: Intracellular ways of cross-presentation. Modified from Joffre *et al*., 2012 and Mantegazza *et al*., 2013.

The former route by which antigens are delivered to early endocytic compartments, is important for multiple DC populations and highly effective in presenting exogenous antigens to CD8+ T cells (Cohn *et al*., 2013; Compeer *et al*., 2012). Antigens in the endosome or phagosome can then be exported to cytosol via ERAD (ER associated protein degradation) protein sec61, which is also found on phagosomal membranes (Houde *et al*., 2003) or poly-ubiquitylation of the MR recruits p97 toward the endosomal membrane (Zehner *et al*., 2013). Furthermore, another frequently described route is the translocation of the exogenous antigens from ER to cytosol. The SNARE Sec22b, which localizes in the ER Golgi intermediate compartment (ERGIC), interacts with syntaxin4 on the phagosomes and recruits exogenous ER proteins to phagosomes

for cross-presentation (Cebrian *et al*., 2011). Thereby, cytosolic proteins can be processed by proteasomes. (Mantegazza *et al*., 2013)

After degradation, the peptides follow the traditional MHC I presentation pathway (the cytosolic translocation pathway with ER loading) or maybe re-transported to the phagosome for further MHC I loading (the cytosolic translocation pathway with phagosomal loading). It has also been shown that CD74 in the ER of DC can mediate the trafficking of newly synthesized MHC class I to endolysosomal compartments for loading with peptides (Basha *et al*., 2012). Thus, the peptide loading on MHC I molecules can occur independently in ER or endocytic compartments (Cebrian *et al*., 2011, Burgdorf *et al*., 2008), as well as by TAP (Merzougui *et al*., 2011). Antigens are delivered into early endocytic compartments which are less degradative and this leads to more efficient cross-presention (Burgdorf *et al*., 2007). Delivering to late endocytic compartments with high acidification is more efficient for MHC II presentation. Therefore, the pH in phagosomes for cross-presentation is also controlled or regulated by sustained reactive oxygen species (ROS) (Savina *et al*., 2006). (Mantegazza *et al*., 2013)

Cross-presentation has been studied in human monocyte-derived DC (MoDC), mouse spleen and BMDC (Nierkens *et al*., 2013). GM-CSF induced BMDC *in vitro* can use both pathways for cross-presentation (Dresch *et al*., 2012; Saveanu *et al*., 2009, Segura *et al*., 2009). However, whether DC catch dead cell material or living/cell associated protein is still under debate. Yet, it is clear that the splenic CD8α^+ DC family is efficient in capturing material from dead or dying cells, as well as processing exogenous antigens for cross-presentation on MHC class I (Nierkens *et al*., 2013; Nopora *et al*., 2012; Schulz *et*

al., 2002). These cells use only cytosolic pathways for cross-presentation (Segura *et al*., 2009). In mice, besides these lymphoid-tissue-resident CD8α+ DC, the migratory CD103+ DC have also been shown to be especially efficient at cross-presentation (Shortman *et al*., 2010; Desch *et al*., 2011). DNGR-1 (Clec9a: C-type lectin domain family 9, member a) is selectively expressed at high levels by both, mouse CD8α^+ DC (Poulin *et al*., 2010) and CD103$^+$ DC (Poulin *et al*., 2012), and by their human equivalents (Poulin *et al*., 2010). DNGR-1 has been identified as a receptor for necrotic cells favoring cross-priming of CTL to dead cell–associated antigens in mice (Sancho *et al*., 2009). It is essential for cross-presentation of dying vaccinia virus-infected cells to CD8+ T cells *in vitro* (Iborra *et al*., 2012).

In MVA-infected DC cultures, the leading role with respect to functionality and maturation characteristics is hold by bystander DC (Pascutti *et al*., 2011). Uninfected immature DC can achiev complete maturation by uptake of MVA-infected leukocytes and this may be the basis for cross-presentation of MVA-encoded antigens (Flechsig *et al*., 2011). CTL responses against MVA-produced antigens were shown to be dominated by cross-priming *in vivo*, despite the ability of the virus to efficiently infect professional antigen-presenting cells, such as dendritic cells. Moreover, stable mature protein is preferred to processed antigens as the substrate for cross-priming (Gasteiger *et al*., 2007).

1.2.3 CD8+ T cell response

Naive T cells circulate between blood and secondary lymphoid organs and accumulate in the latter, such as the spleen and lymph nodes. In the spleen, they first home to the white pulp, and then move to red pulp after a few hours. T cells home to LN

using the receptors CD62L and CCR7. If a naïve T cell is triggered via antigen-specific MHC I/TCR interaction by an APC (signal 1), CD28 on the naïve T cell will interact with B7-1/2 on the APC. These activated T cells express CD40L, which can interact with CD40 on APC (signal 2). Then, the antigen-specific T cells will proliferate and produce anti-viral cytokines, like IFN-γ (signal 3), over the course of five to eight days. This proliferation phase is accompanied by differentiation into effector CD8+ T cells that down regulate CCR7 and CD62L, leave the spleen or LN and finally migrate into peripheral tissues to fight against the infected cells (Fig.5) (Zhang *et al*., 2011). The effector T cell division and survival seems to be regulated by local signals, but not LN-priming (Geurtsvan Kessel *et al*., 2008; McGill *et al*., 2008).

After finishing the acute effector response, the activated T cells will move from LN to periphery and experience AICD (activation-induced cell death). At last, they turn into a silencing phase. Some of the T cells will differentiate into memory T cells which up-regulate the marker CD44. Since they are undergoing both expansion and silencing, they also express CD62L and lymph node–homing chemokine receptor CCR7 (Zhang *et al*., 2011). The terms "central memory" and "effector memory" have been used to distinguish $CD62L^{hi}$ $CCR7^{hi}$ from $CD62L^{lo}$ $CCR7^{lo}$ T cell populations, respectively, in humans and mice (Sallusto *et al*., 1999; 2000). Memory T cells can quickly move to peripheral tissues and display an immediate effector function. Tcm have little or no effector function, but readily proliferate and differentiate to effector cells in response to antigenic stimulation. Memory CD8+ T cells decline faster than CD4+ T cells. The

stability in CD8+ T cell memory is achieved by continuous low-level division (Razvi *et al*., 1995) dependent on IL-15 (Rubinstein *et al*., 2006; Stoklasek *et al*., 2006).

Memory CD8+ T cells also localize in different places in the body for fast recall responses. Some reside in peripheral tissues conferring direct protection; others stay in lymphoid organs and after antigen re-encounter may differentiate into effector cells and migrate into peripheral tissues to mediate their effector functions (van der Most *et al*., 2003). Upon antigen exposure, despite existing memory T cell responses, peripheral DC will still migrate to LN to activate a second round of response. Interestingly, migratory DC only stimulate naïve CD8+ T cells (Belz *et al*., 2007), while CD8+ DC resident in LN can activate both, naïve and memory CD8+ T cells (Khanna *et al*., 2008).

MVA induces high, broad, polyfunctional and long-term effector memory T cell responses in mice (Gómez *et al*., 2013; Sánchez-Sampedro *et al*., 2012). For MVA, CD8+ T cell epitops are dominantly found in early, non-structural genes and transcription factors (Terajima *et al*., 2008).

2. Materials

2.1 Chemicals

Chemicals	**Manufacturer**
100% Acetic Acid	Merck
2-Mercaptoethanol	Sigma
Ammonium persulfate (APS)	Roth
Arabinosid C	Sigma
Brefeldin A	Sigma
ß2-Microglobulin	Sigma
Chromium-51	MP Biomedicals
DMSO	Merck
DNase I	Roche
DTT	Serva
EDTA	Serva
Epoxomicin	Sigma
FCS	Biochrom KG
Film	Kodak
Glycerol	Merck
Guanadinium Thiocyanate	Sigma
HEPES	Roth
Iodacetamid	Calbiochem
Lactacystin	Sigma
LPS	Sigma
Methanol	Merck
Methionine, L-35S	PerkinElmer
Mercapto	Sigma
MG132	Sigma
NP40/Igepal	Sigma
Paraformaldehyd (PFA)	Sigma
Pen-Strep	Cambrex, Bio Whittaker
Phenol	Sigma
PMSF	Roth
Psoralen (4`-aminomethyl-trioxsalen)	Calbiochem (La Jolla, CA, USA)
Prestained Protein Ladder	NEB BioLabs / Themo
Protein G-Sepharose	GE Healthcare

Protein Kinase Inhibitor Cocktail	Roche
RNasin	Promega
Sarcosyl	Sigma
Sodium Citrate	Sigma
Sucrose	Roth
TEMED	Roth
Triton X-100	Sigma
Trypan Blue	Biochrom KG
Trypsin	Biochrom KG
Rotiphorese Gel 30	Roth
RNAsin	Pro mega
RPMI 1640	Biochrom KG
RPMI 1640 without L-Cystein, L-Methionin	BioWhittaker

2.2 Buffers and Solutions

Name	**Composition**
FACS Buffer	1% BSA 0.02% NaN_3 In PBS
PFA	2% Paraformaldehyde In PBS
PBS	0.14M NaCl 2.7mM KCl 3.2mM Na_2HPO_4 1.5mM KH_2PO_4
SDS-PAGE fixing buffer	50% Methanol 40% H_2O 10% acetic acid
SDS-PAGE buffer pH 8,3 (10x)	25 mM Tris 192 mM Glycine 0,1% SDS (w/v)
SDS-PAGE loading buffer pH 6,8 (2x)	50 mM Tris 2 % SDS (w/v) 0,04% Bromphenol blue (w/v) 84 mM 2-Mercaptoethanol 20% Glycerol (v/v)
Solution D	4M Guanadinium Thiocyanate 25mM Sodium Citrate 0,5% Sarcosyl

	0,1M 2-mercaptoethanol (add freshly) RNAse-free water to 100ml
TAC buffer	90% NH_4Cl from 0.16M stock 10% Tris pH7.65 from 0.17M stock
TBS buffer pH 7,6	50 mM Tris 150 mM NaCl
TBS-T buffer	TBS buffer pH 7,6 0,1 % Tween 20

2.3 Kits

Name	**Manufacturer**
BD Cytofix/Cytoperm Kit	BD Pharmingen
Annexin V : FITC Fluorescence Microscopy Kit	BD Pharmingen
PKH26 mini kit	Sigma
LightCycler DNA Master SYBR green I kit	Roche
Superscript III RNase H reverse transcriptase	Invitrogen

2.4 Cell lines

Name	**Description**	**Reference**
B16-GMCSF	GM-CSF producing B16 murine melanoma cells	Kind gift from Georg Häcker, Freiburg, Germany
Cloudman	Melanoma from DBA mice (H2-D)	ATCC Nr. CCL-53.1
DC2.4	Murine dendritic cell	Kind gift from Kenneth L. Rock, University of Massachusetts, USA (Shen *et al.*, 1997)
EL4	Mouse ascites lymphoma lymphoblast	ATCC Nr. TIB-39
LCL	lymphoblastoid B cells	Our lab (Kastenmuller *et al.*, 2007)
J774	murine macrophages cell line established from a tumor that arose in a female BALB/c mouse	Kind gift from Georg Häcker , Freiburg, Germany
RMA	Murine Thymoma cell line	Kind gift from Dr.F.Lemmonier
A375	Human HLA-A*0201 positive malignant melanoma cells	ATCC CRL-1619
HeLa	Human epithelioid carcinoma	ATCC CCL-2
RAW264.7	Murine leukemia virus transformed macrophage-like cell line from BALB/C mice	ATCC TIB-71

P815	mouse lymphoblast-like mastocytoma DBA/2 (H2-D)	ATCC TIB-64

2.5 Cell Culture Medium

Name	Composition
Freezing Medium	90% FBS 10% DMSO
M2 Medium	RPMI 1640 10% FCS 1% Pen-Strep 50 μM 2-β-Mercaptoethanol

2.6 Synthetic Peptides

All peptides were purchased from Biosynthan. Peptides were diluted in DMSO (1mg/ml) and stored in -80°C Freezer. For peptide loading, they were used in concentration of 1μg/ml.

Peptides	MHC restriction	Aminoacid sequence	Origin	Reference
$A19L_{47-55}$	$H2\text{-}K^b$	VSLDYINTM	130L-A19L	Tscharke *et al*., 2004
$A3L_{270}$	$H2\text{-}K^b$	KSYNYMLL	122L-A3L	Moutaftsi *et al*., 2006
$B8R_{20}$	$H2\text{-}K^b$	TSYKFESV	176R-B8R	Tscharke *et al*., 2005
$Ova_{257-264}$	$H2\text{-}K^b$	SIINFEKL	Chicken Ovalbumin	Rotzschke *et al*., 1991
$fluNP_{20-27}$ PR/8	$H2\text{-}K^b$	ASNENMDAM	Influenza nuclear protein	Freer *et al*., 1993
$A42R_{88}$	$H2\text{-}D^b$	YAPVSPIV	154R-A42R	Tscharke *et al*., 2005
$K3L_6$	$H2\text{-}D^b$	YSLPNAGDVI	024L-K3L	Tscharke *et al*., 2005
$A6L_6$	HLA-A*0201	VLYDEFVTI	117L-A6L	Oseroff *et al*., 2005
$B22R_{79}$	HLA-A*0201	CLTEYILWV	189R-B22R	Terajima *et al*., 2003
$I1L_{211}$	HLA-A*0201	RLYDYFTRV	062L-I1L	Pasquetto *et al*., 2005
$H3L_{184}$	HLA-A*0201	SLSAYIIRV	093L-H3L	Drexler *et al*., 2003
Tyr_{369}	HLA-A*0201	YMDGTMSQV	Human Tyrosinase	Skipper *et al*., 1996

2.7 Antibodies

2.7.1 FACS (Dilution is all 1:200)

Specificity	Clone	Isotype	Conjugate	Manufacturer
CD8a	5H10	Rat IgG2b	APC	Caltag
CD11c	HL3	Ar Ham IgG1, λ2	APC-Cy7	BD Pharmingen
CD16/32 Fc Block	2.4G2	Rat IgG2b, κ	-	BD Pharmingen
CD86	GL1	Rat IgG2a, κ	APC	BD Pharmingen
F4/80	BM8	Rat IgG2a, κ	PB	eBiocience
H2-K^b	AF6-88.5.5.3	Mouse IgG2a	PB	eBiocience
IFN-γ	XMG1.2	Rat IgG1	FITC	BD Pharmingen
SIINKEFL/K^b	eBio25-D1.16	Mouse IgG1, κ	APC	eBiocience
MHC II(I-A/I-E)	M5/114.15.2	Rat IgG2b, κ	PB	eBioscience
Clec9a	-	Rat IgG2a	AF 488	R&D

2.7.2 Confocal Microscopy

Specificity	Dilution	Isotype	Conjugate	Manufacturer
ER (anti-Calnexin)	1:300	Rabbit polyclonal	-	Sigma
ERGIC-53	1:200	mouse monoclonal IgG2a	-	Santa Cruz
GFP	1:400	Goat polyclonal, IgG	-	Abcam
GOLPH4	1:400	Rabbit polyclonal, IgG	-	Abcam
cis-Golgi (GM130)	1:400	Mouse IgG1, κ	-	BD Pharmingen
H2-K^b	1:400	Mouse monoclonal, IgG	-	ebiocience
mCherry	1:400	Rabbit polyclonal, IgG	-	Biovision
TGN46	1:400	Mouse monoclonal, IgG1	-	Abcam
ova	1:200 (10μg/ml)	mouse	AF594	Invitrogen
Proteasome	500nM	Murine and human	Probe 488	BostonBiochem
Anti-mouse	1:700	goat	AF647	Invitrogen
Anti-goat	1:700	donkey	AF488	Invitrogen
Anti-rabbit	1:700	chicken	AF594	Invitrogen

2.7.3 Western Blot

Specificity	Dilution	Isotype	Conjugate	Manufacturer
GFP	1:1000	Mouse monoclonal, IgG1 κ	-	Roche
ova	1:10000	Rabbit polyclonal, IgG	-	Abcam
H3	1:250	Rabbit polyclonal	-	genesis
Tyrosinase (T311)	1:250	Mouse polyclonal, IgG2a	-	Dako
Cox4	1:1000	rabbit	-	Abcam
HA	1:1000	rabbit	-	Sigma
Anti-mouse	1:3000	IgG	Peroxidase	Dianova
Anit-rabbit	1:3000	IgG	Peroxidase	Dianova
Anti-goat	1:3000	IgG	Peroxidase	Dianova

2.8 Fluorescent Dyes

Dye	Stock Concentration	Final Concentration	Manufacturer
DAPI	According to the manufacturer description		Invitrogen
Hoechest	According to the manufacturer description		Invitrogen
PI	10mg/ml	1μg/ml	Invitrogen
EMA	2mg/ml	1μg/ml	Invitrogen

2.9 Primers

All primers used for q-PCR were HPLC grade and were purchased from eurofins mwg operon.

18s rRNA Forward: 5′-AAACGGCTACCACATCCAAG-3′;
Reverse: 5′-CCTCCAATGGATCCTCGTTA-3′
A3L-MVA Forward: 5′-ATGGAAGC GTGGTCAATAG-3′;
Reverse: 5′-CCTGCACGTTTAGGTTTGGT-3′
B8R-MVA Forward: 5′-ATCCGCATTTC AAAGAATG-3′;
Reverse: 5′-ACATGTCACCGCGTTTGTAA-3′
H3L-MVA Forward: 5′-GTCTTGAAGGCAATGCATGA-3′;
Reverse: 5′-TCCCGATGATAGACCTCCAG-3′
B5R-MVA Forward: 5′-TGTCCTAATGCGGAATGTCA-3′;
Reverse: 5′-AACGCCACCGATAGAAAATG-3′
G8R-MVA Forward: 5′-ATCGATAAACTGCGCCAAAT-3′;
Reverse: 5′-CTCCGCGGTAGAACACTGAT-3′

2.10 Virus

Modified vaccinia virus Ankara (MVA, cloned isolate F6) at 582nd passage on CEF and recombinant MVA (recMVA) were generated by homologous recombination as described previously (Staib *et al.,* 2004).

MVA-NP-SIIN-eGFP-PK1L/P7.5/P11 expresses a fusion gene encoding nucleoprotein (NP) from influenza A virus (type Puerto Rico 68), the peptide siinfekl ($ova_{257-264}$) derived from the protein ovalbumin (ova) and an enhanced form of the green fluorescent protein (eGFP). The targeted gene is under the control of either early (PK1L) or early/late (P7.5) or late (P11) promoters.

MVA-ova-PK1L/P7.5/P11 expresses the full length ova gene under the 3 different promoters.

MVA-mH3L-eGFP-PK1L/P11 expresses a mutant form of envelope protein H3 (327bp sequence ttttttt into tttcttt) fused with eGFP under early or late promoter.

MVA-ova-mCherry-PK1L/P11-H2K^b-eGFP-PK1L/P11 simultaneously expresses an mcherry fusion ova protein and an eGFP fusion MHC I ($H2K^b$). Both fusion genes are separately controlled by different promoters (early or late active).

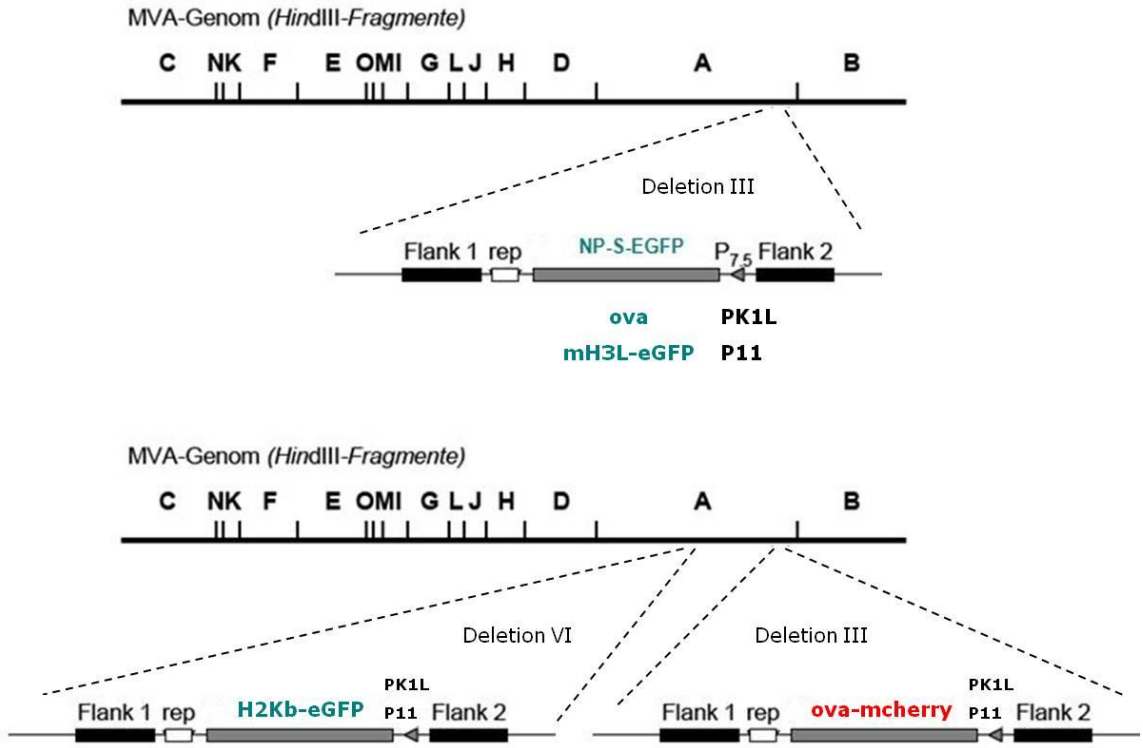

2.11 Mice

Strain	MHC restriction	Reference
C57BL/6	H2-K^b/H2-D^b	http://jaxmice.jax.org/strain/000664.html
HHD	HLA-A*0201	Pascolo *et al.*, 1997

All mice were derived from in-house breeding under specific pathogen-free conditions at the Helmholtz Zentrum München animal facility in Neuherberg or the TVA at the Uni-Klinikum Düsseldorf following institutional guidelines.

HLA-A2 (Human leukocyte antigen A2) transgenic mice (HHD) express modified MHC class I molecules combining the human alpha-1 and alpha-2 domains of HLA-A*0201 with the alpha-3 domain of mice H2-K^b covalently linked to human β_2m (Fig.7). This animal model allows the study of CTL response dependents on HLA-A2.1 restricted antigen presentation in mice (Pascolo *et al.*, 1997).

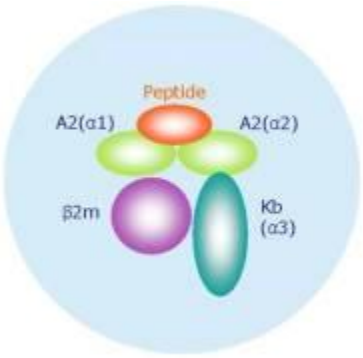

Figure 7: A2-K^b tetramers. (Choi *et al*., 2002)

2.12 Consumables

Product	**Manufacturer**
Cell chamber	Mo Bi Tec
Cell culture flask (T75, T185)	Greiner / Corning / Nunc
Cell culture plate (6-,12-,24-,96-well)	Corning
Cell culture dish (10cm)	Corning
Cell culture petridish (5cm)	Nunc
FACS tubes	BD Pharmingen
Falcon(15ml, 50ml)	BD Pharmingen
Glass bottom dish, P35G-1.5-14-C	MatTek
Imaging dish CG 1.5, 35mm	Bo Bi Tec
ART Pipette tips	Molecular Bioproducts
Pipettes 'Cellstar' (1-25 ml) Greiner	Corning
Sterile filters (Minisart 0.2-0.45 μm)	Sartorius AG
Whatman 3MM Chr Papier	Whatman
Whatman Protran Nitrocellulose Memb	Whatman

2.13 Laboratory Equipment

Name	**Type**	**Manufacturer**
Centrifuge	Megafuge 1.0R	Heraeus
CO_2 Incubator	Function line Hera cell 150 Cellstar	Heraeus Nunc
Confocal Microscopy	Olympus FV10i-W LSM 780	Olympus Carl Zeiss
Crosslinker	Bio-Link BLX 365	Peqlab
Electro-blotting System	Fastblot B33/B34	Biometra
Film processor	CAWOMAT 2000 IR	CAWO
Flow cytometer	FACS Canto I/II	BD
Fujifilm	FLA-3000	raytest
Freezer (-20°C)	Excellence	Bauknecht
Freezer (-80°C)	Hera freeze Ult 2090	Heraeus Revco
Fridge (4°C)	UT6-K	Bauknecht
Gel dryer	Gel dryer 583	Biorad
Ice machine	AF 200	Scotsman (Milan, Italy)
Laminar flow	HERAsafe HS 12	Heraeus
LightCycler	1.5	Roche
Micropipette	Pipetman P10-1000	Gilson
Microscope	Kolleg SHB 45 Axiovert 25	Eschenbach Carl Zeiss
Multi channel pipette	Transferpette-12 (20-200µl) Calibra 852	Brand Socorex
Nitrogen container	Cryo 200	Forma Scientific
Pipettor	Easy jet pipetman	Eppendorf Gilson
Sonicator	Sonopuls HD200/UW200	Bandelin
Vortexer	VF2 Vortex Genie 2	IKA Werke Scientific Industries
Waterbath	Assistant VTE Var 3185	Hecht

2.14 Software

Name	Manufacturer
Aida Image Analyzer v.3.24	raytest
BASReader 3.14	raytest
FacsDIVA	Becton Dickinson
FlowJo 6.4.2	Treestar, Ashland
LightCycler Workstation	Roche
MS Office	Microsoft, Redmond
ZEN 2011	Carl Zeiss

3. Methods

3.1 Cell Culture

3.1.1 Mammalian cell culture

Mammalian cells were cultured and handled under sterile conditions. The cells were cultured in a 37°C incubator, which provided a 5% CO_2 atmosphere and 95% humidity.

All the cell lines were grown in M2 medium, which is RPMI 1640 medium supplemented with 1 % penicillin streptomycin, 10% fetal calf serum (FCS) and 0.05M 2-Mercaptoethanol. Cell lines were either grown in suspension or in monolayers in T185 or T75 cell culture flasks or cell culture dishes. Cells were split at a ratio of 1:2 to 1:10 (depending on their growth kinetics and usage) when growth reached approximately 90 % confluence.

For adherent cell lines, the medium was first removed, subjected to two rounds of PBS washing, covered with 3ml trypsin and incubated at 37°C for approximately three minutes. When the cells were detached from the flask, 7ml of fresh M2 medium were added to the cells. Resuspended and required fractions were transferred into new flasks or dishes with fresh medium, or cell culture plates for further experiments.

3.1.2 Cryo conservation of eukaryotic cells

Cells in good condition and in a phase of growth were subjected to freeze storage. Adherent cells cultivated in a T185 cell culture flask were harvested by trypsination. Cells were centrifuged for 5 min at 4°C and 1500 rpm. The cell pellet was resuspended in a cold freezing medium ($1x10^7$cells/ml) and transferred into sterile

cryopreservation tubes in 1ml aliquots. The cells were slowly frozen by storing them over night in slow-cooling containers at – 80°C freezer. Thereafter, the tubes were transferred into liquid nitrogen (-196°C) for long term storage.

T cells after four days of restimulation were directly resuspended in the 24-well-plate, pooled and centrifuged for five minutes at 4°C and 1500 rpm. Next, cells were resuspended with a freezing medium (two wells of T cells in 1 ml of freezing medium per vial). Cells were then processed as described above.

3.1.3 Thawing of cryo conserved eukaryotic cells

To re-cultivate deep frozen cells, the cell suspension was quickly thawed to room temperature and washed with 10 ml of M2 medium. After centrifugation, cell pellets were resuspended with fresh medium and transferred into a T185 cell culture flask or a cell culture dish and cultivated in an incubator.

One cryopreservation tube of T cells was plated in four wells of 24-well-plate for further cultivation.

3.2 Virological Methods

3.2.1 Virus Titration ($TCID_{50}$)

Virus stocks were frozen thawed three times and sonicated for one minute in ice water in a cup-sonicator. Virus stocks were diluted in RPMI 2% medium to obtain dilutions from 10^{-1} to 10^{-10}. Primary CEF cells in 96-well culture plates were infected in duplicates with different virus dilutions (100µl per well).

The infected cells were incubated for 5-7 days in an incubator. The wells with plaque formations were counted as positive.

Titer = % (10*a + 0,5 + (xa/8) + (xb/8) + (xc/8)) * 10

a is the last dilution number of every infected well (10-a); xa refers to the positive wells in a+1 dilution (10-xa); xb denotes positive wells in a+2 dilution (10-xb); xc signifies positive wells in a+3 dilution (10-xc).

stock	10^{-1}	10^{-2}	10^{-3}	10^{-4}	10^{-5}(a)
+ +	+ +	+ +	+ +	+ +	+ +
+ +	+ +	+ +	+ +	+ +	+ +
+ +	+ +	+ +	+ +	+ +	+ +
+ +	+ +	+ +	+ +	+ +	+ +
+ +	+ +	+ +	+ +	+ +	+ +
+ +	+ +	+ +	+ +	+ +	+ +
+ +	+ +	+ +	+ +	+ +	+ +
+ +	+ +	+ +	+ +	+ +	+ +

10^{-6}(xa)	10^{-7}(xb)	10^{-8}(xc)	10^{-9}	10^{-10}	unifected
+ + +	+ + +	+ + +		+	
+	+	+ +	+	+ +	
+ + +	+		+		
+ + +		+ +	+		
+ + +	+	+	+	+	
+ + +	+	+	+		
+	+	+ +	+		
+ + +	+		+	+	

3.2.2 MVA Infection

Cells were adjusted in a flask or dish the day before to a maximum density of $5x10^5$ cells / ml in order to achieve exponential growth for the next day. Cells were collected and centrifuged in 15 ml falcom tubes to obtain a cell pellet. Viruses (stored at –80°C) were thawed on ice, sonicated in ice water for one minute and then vortexed in order to singularize viral particles. Cells were then infected at the desired MOI at a low volume. Infected cells were incubated at 37°C and resuspended every 10 minutes. After one hour of infection, 1ml of fresh media was added into the falcon tube. One hour later, cells were transferred into a plate initially seeded with $1x10^6$ cells/ml. For exact infection time kinetics, cells infected with virus were first incubated on ice for 40min up to 1h, in order to assure that virus particles attached, but did not enter into the cells. Viruses were

then washed away twice with cold medium. Cells were then transferred onto a plate seeded with $1x10^6$ cells / ml and placed in an incubator to allow infection.

Infection occurred in a 6-well-plate and $1x10^6$ cells were plated per well. After cells adhered, left small volume of medium, viruses with proper MOI were added to the well. Cells were then incubated in an incubator. For exact infection time kinetics, the plate was incubated first on ice for 10min, the proper amount of virus for different MOI on ice was added, incubated for another 40min to 1h, then replaced twice with the cold medium. Cells were then transferred into the incubator and so began the infection time count.

3.2.3 PUVA induced MVA inactivation

For MVA virus only, the desired amount of MVA was suspended in PBS and incubated with 10 μg/ml psoralen (4`- aminomethyl-trioxsalen) at room temperature for 10min in a 6-well plate. Subsequently, the mix was irradiated for 5 min in a Stratalinker 1800 UV crosslinking unit untill the mixture was used for further experiments.

For MVA infected cells, infected cells were first incubated with 0.3μg/ml psoralen for 10min in a 6-well–plate. The mixture was irradiated for 15min in a 365 nm UV-Crosslinker (Bio-Link BLX 365, Peqlab) to get rid of the infective viruses that possibly stuck on the cell surface. Cells were collected, washed with medium and then plated out into a new plate.

3.3 Immunological Methods

3.3.1 Preparation of Splenocytes

The spleen was removed and homogenated with a syringe plunger over a cell strainer into M2 medium. After centrifuging (5', 1500rpm) the erythrocytes were lysed with 3ml TAC buffer (2', 37°C) and washed with 50ml M2. The cells were again filtered over a Nylon filter and counted.

3.3.2 Cell counting

Splenocytes were counted at a 1:40 dilution. 50µl of cell suspension was mixed with 450µl PRMI 1640 medium. From this 1:10 dilution, 50µl were mixed with 50µl of Trypan blue solution (0.4%, Sigma) and 100µl 4% acetic acid, resulting in a 1:40 dilution (total). Others were counted in appropriate dilutions. Cells were counted in a Neubauer counting device. Two quadrates were counted and the cell number was calculated using the following formula: n (cells/ml) = mean of two quadrates x dilution factor x 10^4

3.3.3 Generation of antigen-specific CD8+ T cell lines

3.3.3.1 LipoPolySaccharid-Blasts

Splenocytes from naïve C57BL/6 mice were prepared as described in 3.3.1. Total volume was caculated by $1x10^6$ cells/ml splenocytes, 25µg/ml LPS and 7µg/ml Dextran-SO_4. Calculated amounts of compounds were added into the mixture and filled up to the total amount with M2 medium. The cells were cultured in a T75 flask of 40ml in standing position at 37°C, 5% CO_2 and 90% humidity for three days.

3.3.3.2 Primary culture

The LPS treated cells from 3.3.3.1 were harvested and irradiated with 3000 rad (30Gray). The cells were separated into falcon tubes for different peptides. They were washed with 20ml RPMI 1640 medium and added to the resuspended cells with 1ml RPMI 1640 medium and 5µg ß2-microglobulin (10µl) and 250ng peptide (2.5µl from 100µg/ml). After being incubated for 30min at 37°C, they were washed twice with 10ml of M2 medium. The cells were adjusted to $3x10^6$cells/ml with fresh M2 medium.

Peptide stocks (1mg/ml) were sonicated for 30sec and diluted with DMSO to the desired concentration.

Splenocytes from MVA vaccinated C57BL/6 mice (1 week) were prepared as previously described. After washing, splenocytes were adjusted to $7x10^6$ cells/ml with fresh M2 medium and 1 ml added into one well of a 24-well-plate containing 1ml of LPS treated cells. Cultures were further incubated for eight days.

3.3.3.3 T cell Restimulation

For maintenance, T cells were restimulated every seven days for the first three weeks according to the following scheme.

EL4 cells were irradiated with 10000rad (100Gray). The cells were separated into falcon tubes for different peptides. They were washed with 20ml of RPMI 1640 medium. Resuspended cells with 1ml RPMI 1640 medium received an additional 10µl of ß2-microglobulin and 1µl peptide from 1µg/ml (final 1ng/ml). Next, they were incubated in the breeder for 30min and washed twice with 10ml of M2 medium. Cells were adjusted to $1x10^6$ cells/ml with fresh M2 medium.

Splenocytes from naïve mice were irradiated with 3000 rad (30Gray). After washing, splenocytes were adjusted to $12x10^6$ cells/ml with fresh M2 medium.

T cells from the primary culture were collected and media were replaced with fresh M2 medium.

In one well of a 24-well-plate, 0.5ml of peptide loaded EL4 cells, 0.5ml of splenocytes, 0.5ml of 5% TCGF (conditioned medium as supernatant from rat splenocytes stimulated with 5µg/ml Concanavalin A as previously described Beeton *et al*., 2007) and 0.5ml of T cells were added. The culture was incubated in the breeder for eight days.

T cells were frozen after three days of restimulation if desired.

For HHD CTL generated from HHD mice, JA2.1 cells instead of EL4 cells were used for restimulation.

3.3.4 Preparation of BMDC

Both hind legs of the mouse were amputated and the tissues around the bones were removed. Bones were sterilized with 70% Ethanol and then put into M2 medium. The ends of the bones were cut away, 1ml injection with M2 was used to flush the bone marrow into the dish and the inside of the bone was then washed three times from each end. The mixture was collected into a falcon, resuspended and centrifuged (1500rpm, 5min). Erythrocytes were lysed in 5ml TAC buffer (0.144M NH_4Cl and 0.017M Tris PH 7.65) in a 37°C water bath for 2min while being shaken. Thereafter, cells were washed once with PBS (1500rpm, 5min) and filtered through a 100µm cell strainer. Within 94x16 mm petri dished, $5x10^6$ cells were seeded in and cultivated with 10ml RPMI1640

containing 10% FCS, 1% Pen-Strep, 50 μM 2-Mercaptoethanol and 10% GM-CSF (conditioned medium obtained as supernatant from B16 cells expressing GM-CSF - cells were a gift from Georg Häcker, Freiburg, Germany). Cultures were incubated at 37°C in a humidified atmosphere containing 5% CO_2 in air. On day three, additional fresh 10ml containing 10% GM-CSF were added to the dish. On day six, 10ml medium was replaced with fresh medium containing 10% GM-CSF. The cells were collected and used for the experiments on day seven.

GM-CSF was produced by the B16-GMCSF cell line. About $5x10^5$ cells were cultured in a T175 flask. The supernatant from the cells was collected from day three till day five and centrifuged to remove the cells. The supernatant was filtered sterile.

BMDC were stained with antibodies specific for CD11c, CD80, CD86 and I-Ab (all BD Pharmingen). Propidium iodide (Molecular Probes) was added immediately before FACS analysis for live/dead-discrimination.

3.3.5 Preparation of BMM

The bone marrows were prepared the same way as described in 3.3.4. Cells at $5x10^6$ were added into one 10 cm cell culture dish, supplied with M2 containing 20% M-CSF. M-CSF was produced from L929 cells, which were grown for one week, and then supernatants were collected. On day four, supernatants were removed and non-adherent cells in the suspension were washed away. Next, M2 medium with 10% M-CSF was added to the adherent cells. On day seven, cells were rested without M-CSF for one day and plated out on a 6-well-plate for further experiments ($2x10^6$ cells per well). On day eight, adherent cells could be used for assays.

3.3.6 Direct-presentation assays

BMDC at day seven were infected for 2h at MOI 1 and then washed with cell culture medium. In the presence of 1µg/ml BFA (Sigma) for 4h in 96-well-plate in the breeder, $4x10^5$ BMDC per well were co-cultured with $2x10^5$ antigen-specific CTL. Additionally, uninfected BMDC were plated at the same density as negative controls or pulsed with peptide (1ng) as positive controls to assess the background activity of T-cells. Staining and analysis for intracellular IFN-γ production was carried out as described in 3.3.7.

Other cell lines, DC2.4 or J774 were infected at MOI 10. To detect K^b-SIINFEKL-complexes, infected cells were stained with the SIIN-APC K^b antibody (eBioscience).

3.3.7 Cross-presentation assays

Cloudman cells were infected with MVA at MOI 1 for two hours and then washed twice with M2 and incubated in the breeder for an additional 10 hours. PUVA inactivation was carried out as described in 3.2.3. Infected Cloudman cells were added to BMDC with a ratio of 1:1 and incubated for another 12 hours. They were co-cultured at a 2:1 ratio with antigen-specific CTL lines in the presence of 1µg/ml BFA (Sigma) for four hours. Staining and analysis for intracellular IFN-γ production was carried out as described in 3.3.8.

3.3.8 Intracellular cytokine staining (ICS)

3.3.8.1 Peptide stimulation of T cells

For peptide stimulation, 100µl M2 medium containing 4×10^5 APC were transferred to flat-bottom 96-well plates (one well per sample). For each peptide, a 100µl

mastermix was added to APC, which contained vortexed and sonicated peptide (1µl 1µg/ml peptide + 1ml M2). Cells were incubated with the peptides for 30min in the incubator. Cells were then washed twice with M2 with a final 100µl volume. Next, 100µl CTL ($2x10^6$cells/ml) with brefeldin A (stock 1mg/ml to final 1µg/ml) were added for four hours in the breeder. For titration, peptides were diluted into 10^{-8} (1µg/ml), 10^{-9}, 10^{-10}, 10^{-11}, 10^{-12} M. The control peptides were used 10^{-8} M.

3.3.8.2 EMA-staining

Cells were transferred into a 96 well V-bottom plate, washed with FACS buffer and then incubated with 1µg/ml EMA (1:2000) for 20min and illuminated with bright light to stain dead cells. Cells were then washed twice with the FACS buffer in a total volume of 180µl for 2min, with 1400rpm at 4°C. EMA staining is used for live/dead discrimination, since this photo-activated molecule can enter only dead or damaged cells that no longer have intact membranes. Upon entering these cells, EMA can form stable links to nucleic acids present in the cell. This reaction requires the presence of visible light and is irreversible.

3.3.8.3 Surface markers and intracellular cytokine staining

After EMA staining, washed cells were stained in the dark on ice with 50µl/well surface markers CD8a-APC (Caltag Laboratories GmbH 1:250 dilution) for 30min. Then, the cells were fixed and permeabilized with BD Cytofix/Cytoperm™ Fixation / Permeabilization Kit according to the manufactures protocol (BD Pharmingen™, Heidelberg, Germany). Thereafter, the cells were washed again and incubated with 50µl/well of intracellular anti-IFNγ FITC-labeled antibodies (BD 1:300 dilution) in Perm-

Wash buffer for 30min in the dark on ice. Finally, cells were washed again and fixed with 1% PFA and stored until used for analysis.

3.3.9 FACS Flow

Single-suspended stained cells or other particles pass through the focused laser beam and scatter the laser light and fluorescence. They can be distinguished by their physical parameters (size, density by forward light scatter or FSC and sideward light scatter or SSC) and combined fluorochrome-conjugated antibodies or with the use of dyes (FITC/APC…). The dyes can absorb high energy photons and emit a lower energy light known as fluorescence. These differences between excitation and emission allow the laser to excite many fluorochromes. Their emitted lights can be detected by specific PMTs (photomultiplier tube) through placement of LP dichroic mirrors (reflects lower wavelengths on to the next PMT) and BP filters (admits specific light range). However, as fluorochromes emit light over a range of wave lengths, a signal from one fluorochrome can appear in a detector used for another fluorochrome. This spillover must be corrected, or compensated.

Normally, the protocol of the author from the present study was to first find the cell population by FSC and SSC scatter. Next, living cells by EMA or PI negative staining were gated, which is detected by PerCP and PE channels. Then respective surface markers or intracellular cytokines were gated by their respective fluorescence labeling (CD8-APC/ IFNγ-FITC) (Fig.8).

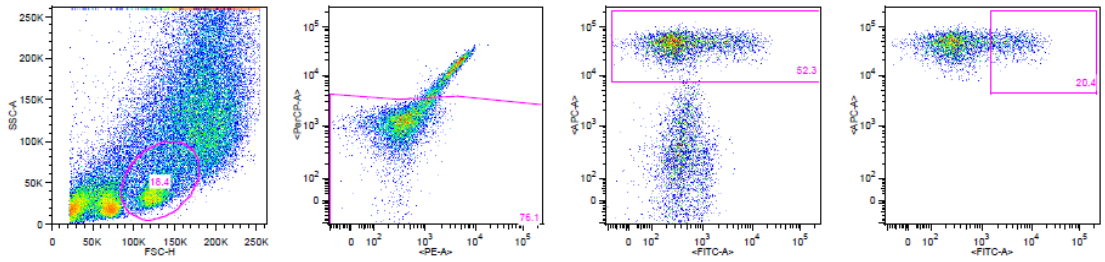

Figure 8: FACS gates for CTL. Cell populations (FSC+SSC), living cells (PE+PerCP), CD8+ TC (CD8-APC), CD8+IFNγ+ TC (IFNγ-FITC).

3.3.10 ^{51}Cr release assays

Specific lysis by H2-K^b-restricted murine CTL reactive against defined peptides was determined in a four hours standard ^{51}Cr-release assay. H2-K^b-positive DC2.4 cells were infected for two hours at MOI 10 or 2µl peptides (100µg/ml)-pulsed, washed and labeled for 1.5 hours at 37°C with 150µl ^{51}Cr per sample, and then washed four times. Labeled target cells were plated in U-bottom 96-well plates at 1 x 10^4 cells/well and incubated with effector cells at various E:T ratios. After four hours of co-incubation, supernatants were taken into scinti counter-plates. Plates were dried overnight. Then the specific ^{51}Cr release was counted by using a top-count scintillation counter. (Drexler *et al*., 1999)

3.3.11 Phagocytosis Assays

For proteins, 10µg/ml AF594 labeled ova proteins (Invitrogen) were used to feed with BMDC for 30min, 1h, 2h or 3h. BMDC were then analyzed by confocal microscopy (CLSM) or FACS for red fluorescence. Controls were pretreated with 5µM CytD one hour before phagocytosis.

For infected cells, MVA infected Cloudman cells were labeled with PKH26 (kit from Sigma), then co-incubated with BMDC for four hours with a ratio of 1:4 (Cloudman

: BMDC). Controls were co-incubated on ice without infection or pretreated with CtyD 5μM for one hour.

3.3.12 Immunofluorescence staining

Immunofluorescence is a technique used for fluorescence microscopy. This technique uses the specificity of antibodies to their antigen to target fluorescent dyes to specific biomolecule targets within a cell, and therefore allows visualization of the distribution of the target molecule in a given sample.

Adherent cells were grown and infected in the microscopy dish or chamber. Cells were washed three times with PBS and then fixed in cold 4% PFA for 15min at room temperature in the dark. The cells were washed with PBS for three times. If intracellular staining was needed, the cells were permeabilized with 0.25%Triton X-100 for 3min. Cells were washed in PBS three times for 5min. 5% BSA or FCS in PBS solution was used for blocking of the unspecific binding for one hour at room temperature. Primary Abs, which detected special proteins or cell compartments, were diluted in 5% FCS, then added to the cells and incubated overnight in 4°C or at room temperature for 1h. Cells were washed three times with 1% FCS for 5min. Second Abs, which detected the primary Abs (labeled with fluorochromes) were diluted in 5% FCS and then added to the cells for 1h at the room temperature in the dark. Cells were washed three times with 1% FCS for 5min in the dark. Cells could then be kept in PBS at 4°C. Before analysis, in order to label the nuclear cellular DNA, DAPI (one drop/1ml, Invitrogen) was added to the cells for 10min in the dark.

3.4 Protein Analysis

3.4.1 Western Blot

Western Blotting is an antibody-based method that can be used to detect and quantify proteins that have been separated by sodium dodecyl sulphate polyacrylamide gel electrophoresis (SDS-PAGE) according to their molecular weight.

3.4.1.1 Preparation of cell lysates

To isolate proteins, cell monolayers were removed from 6-well-plates using a cell scraper and transferred into pre-cooled 1.5 ml Eppendorf tubes. The tubes were centrifuged at 2000 rpm for three minutes at 4°C. Supernatants were removed and the cells were washed three times with 1ml cold PBS. The pellets were resuspended in 1ml 150mM NaCl lysis buffer, rotated for 30min at 4°C and centrifuged for 30min at 14000rpm and at 4°C. Then, supernatants, which contain proteins, were kept for analysis.

Lysis buffer contains pH regulators (HERPES, NaCl to raise ionic strength), detergent (dissolves the cell membrane: Glycerol, NP40), chelating agents (EDTA binds to Mg^{2+}/Ca^{2+}, which is needed by DNAses and proteases; DTT reduces disulfide bonds to maintain the protein of interest isolate, as proteins can form intermolecular -S-S- bridges with themselves or other proteins) and protease inhibitors (PMSF, pepstatin, Tablets).

Lysis Buffer 2x stock (without NaCl)	Volume (50ml)
EDTA	20µl
KCL	1ml
$MgCl_2$	1ml
HEPES PH7.4 (with KOH)	2ml
Na_3VO_4	50µl
Gylcerol	10ml
NP-40/ IGEPAL	500µl
PMSF	100µl
DTT	1ml
Pepstatin	100µl
Tablette (Roche)	1
dH_2O	34.23ml
PH	7.4

150mM NaCl = ½ stock + totalx150/5000 5M NaCl + dH_2O
250mM NaCl = ½ stock + totalx250/5000 5M NaCl + dH2O
500mM NaCl = ½ stock + totalx500/5000 5M NaCl + dH2O

3.4.1.2 SDS-Page

Up to 50µl of cell lysates were mixed with 12.5µl 5x protein loading buffer and heated for 5 min at 95°C to denature proteins and break disulfide bonds. After a short centrifugation to clear condensed fluid from the top of the reaction vessels, samples were applied to the pockets of the stacking gel. The same procedure was applied to the protein molecular weight marker adding 6µl per sample (Prestained Pro Lader). The gel was run at 150V 12mA for 14h over night or 300V 40mA for 3h in a vertical electrophoresis chamber.

Resolving gel 10%	**Big gel**
Bis/Acrylamide 30%	12ml
2M Tris pH 8.8	7.6ml
SDS 20%	180µl
TEMED	72µl
H2O milliQ	15.9ml
APS 10%	432µl

Stacking gel	**Big gel**
Bis/Acrylamide 30%	3ml
0.5M Tris pH 6.8	2.4ml
SDS 20%	90µl
60% Saccharose	4.2ml
TEMED	24µl
H2O milliQ	8.4ml
APS 10%	240µl

Separation was stopped when the visible loading buffer front had nearly reached the lower edge of the gel. The gel was removed from the electrophoresis chamber and transferred into blotting buffer after the stacking gel had been cut off. The gel and a nitrocellulose membrane (0.45µl pore size) of the same size as the gel were equilibrated in a blotting buffer. The gel and membrane were placed between six layers of whatman paper. Blotting was run at 16V 1000mA for 90min.

After blocking the membrane with 5% milk powder in TBS-T for 40min, it was washed three times for 10 minutes in TBS-T and then incubated with the diluted primary antibody in 5% milk powder overnight at 4°C on a shaking device. The unbound antibody was removed by washing with TBS-T 3 times. The membrane was then incubated for 1h with the secondary PO labeled antibody (1:3000) in 5% milk powder and subsequently washed again as described previously.

Depending on the size of the membrane, 5-10ml substrate solution (1:1 mix of Lumi-Light solution A and B) were used to cover the membrane for 2min. The membrane was dried using whatman paper and put between the plastic. Protein-specific signals were detected by exposure to a photographic film.

For further usage e.g. for detecting other proteins, the membrane was washed 3 times with TBST and dH_2O. It was then incubated with re-blotting solution (1:10 in dH_2O) for not more than 30min to wash the former antibodies away. Then the same procedure was carried out like before for other antibody detections.

3.4.2 Immunoprecipitation and metabolic labeling

To monitor the half life of proteins within infected cells, pulse-chase experiments using radio-active sulphur (^{35}S) labeled methionine were conducted.

For each time point, $1x10^6$ HeLa cells were seeded in a 6-well-plate in 1 ml M2. Before infection, cell culture plates were placed on ice for 20min before the addition of the cold medium. Cells were infected at MOI 10 for 1h and thereafter, remaining viruses were washed away. A synchronized infection was initiated by placing the cell culture plate at 37°C. 12h post infection, cells were washed twice and L-Met/L-Cys starved for 1h in pre-warmed L-Methionin-/L-Cystein-free DMEM. Both contained (ultra)glutamine and pyruvate 1% (w/v) (RIPA starvation medium). Subsequently, 12µl of (methionine-^{35}S) EasyTag Express ^{35}S protein labeling mix (PerkinElmer) were added into the starving medium of each well. Cells were incubated/labeled for 1h. To stop the pulse, the ^{35}S-containing medium was removed by washing with Met/Cys-free chase Medium (M2 medium with 1.5 mg/ml methionine/cysteine) twice. Afterwards, cells were kept in 1ml chase medium per well and incubated for different time points at 37°C. During the pulse, *de-novo* protein synthesis leads to incorporation of radioactively labeled methionine/cysteine into newly synthesized proteins. At the indicated chase times, the cells were washed with ice-cold PBS 3 times and lysed with the western-blot lysis buffer,

as described previously in 3.4.1.1, and then subsequently frozen in liquid nitrogen. After collecting all samples, lysates were thawed and subjected to immune-precipitation using 2µg of anti-GFP mouse Ab. The lysates were incubated with the Ab overnight with continuous rotation at 4°C. Added in every sample was 40µl Protein-G-Sepharose (using tips) to precipitate the GFP Ab together with the bound antigen (in this case the H3-GFP fusion protein). Lysates were incubated for 2h at 4°C and then centrifuged for 1min at 1000rpm at 4°C. The pellet was washed consecutively with lysis buffers containing 150mM, 250mM, 500mM, 500mM, 250mM and 150mM NaCl. Precipitates were boiled at 95°C for 5min in 40µl 2.5x loading buffer and the supernatant was separated by 10% SDS-PAGE. Gels were fixed for 1h in a fixation buffer (40% (v/v) methanol and 10% (v/v) acetic acid) and then dried (using a gel dryer (Biorad)). Analysis of radioactivity was visualized on a phosphor imager plate, scanned by Fujifilm FLA-3000 and read by BASReader 3.14 software. The intensity of the bands was calculated by using Aida Image Analyzer v.3.24 software.

3.5 qRT-PCR

BMDC were used for infections of 0h, 1h, 2h, 3h, 4h, 5h, 7h and 9h. Total RNA was extracted from approximately 1×10^6 cells by Solution D, collected in 2 ml tubes for 15 min on ice, and then stored at -20°C. Guanidinium thiocyanate, Sarcosyl and 2-mercaptoethanol in the Solution D were used for denaturing proteins, including RNases, and separates rRNA from ribosomal proteins.

Total RNA was isolated by using acid guanidinium thiocyanate-phenol-chloroform as described previously (Chomczynski *et al.*, 1987). In this method, RNA was

separated from DNA and protein by using an acidic solution of phenol (mastermix 1) and chloroform/IAA (100µl/sample) mixed with guanidinium thiocyanate (from Solution D) and sodium acetate. Samples were vortexed and incubated on ice for 15 min. After centrifugation (10,000rpm, 20min, 4°C), 3 phases were separated: aqueous phase (RNA), inter phase and organic phase (most of DNA and protein). The upper phase was carefully transferred to fresh 1,5ml tubes. Next, RNA was recovered from the aqueous phase by precipitation with 400µl Isopropanol for 4h or overnight at 4°C. After centrifugation, RNA is localized at the bottom of the tube. The liquid was carefully removed with tip. The RNA pellet was washed two times with 200µl 70% ethanol. The liquid was carefully removed after centrifugation and allowed pellet to air-dry for 5min. The pellet was resuspended in 10µl DMDC-H_2O (RNAse-free water) by slow pipetting with a filter tip. After 5min of incubation on ice, the samples were stored in -80°C.

The amount of RNA was measured by NanoDrop ND1000. For reverse transcription (RT), 3µg RNA with RNAse-free water 9µl and 1µl DNase (10U, Roche) were used for each sample to digest genomic DNA. The 5µl DNA-free RNA was incubated at 37°C for 20min at room temperature for 40min. 8.5 µl Mastermix2 was added with 5µl DNA-free RNA for 5min at 65°C to denaturate the RNA and RNA samples were shortly placed on ice to avoid refolding. The mixture together with Mastermix3 was added into PCR tube to synthesize cDNA. cDNA synthesis was performed for 60min at 50°C and 15min at 72°C by using 200U Superscript III RNase H reverse transcriptase (Invitrogen), 7.5 pmol oligo$(dT)_{12\text{-}18}$ (Invitrogen), 20 U of RNasin

(Promega), and 10mM each deoxynucleoside triphosphate (Qiagen). Samples can then be stored then at -20°C.

The qRT-PCR was performed twice and repeated in at least two separate experiments using the following conditions. 10nmol/µl each of forward and reverse primers were used for each reaction. Reaction mixtures at 18µl and 10 times diluted cDNA at 2µl were added into a capillary vessel. The qRT-PCR controls were performed with 2 µl RNAse-free water which did not show any amplification. Lightcycler Roche qPCR included initial denaturation at 95°C (15s), followed by 36 cycles at 54°C (15s) and 72°C (9s). Fluorescent data were acquired during each extension phase. After 36 cycles, a melting curve was generated by slowly increasing the temperature from 63°C to 95°C, while the fluorescence was measured. Primers targeting 18s rRNAs transcripts (ribosomal RNAs) and A3L, H3L, B8R, G8R, B5R transcript genes were designed using clone manager 9 software and are shown in 2.9. dsDNA are recognized by dsDNA dye-SYBR Green (Roche).

The melting curves were used to verify primer specificities. Standard curves were generated by plotting the threshold cycle (Ct) vs. the fluorescence expression of puridied PCR products. The threshold is set in the linear range of the amplification curve. Ct was calculated by determining the cycle number at which the change in the fluorescence of the reporter gene crossed the threshold.

$\Delta Ct = Ct(18s) - Ct(gene)$

$\Delta\Delta Ct = \Delta Ct(xh) - \Delta Ct(0h)$

Incresed fold of DNA copy numbers = $2^{\Delta\Delta Ct}$

Since the primers chosen were all tested for reaction efficiency (all close to 100%), the value of two can be used for the copy number calculation.

Mastermix1: 7.2µl Mercapto, 50µl Na Acetate (pH 4), 500µl Phenol

Mastermix2: 3.5µl RNAse-free water, 4µl dNTP, 1µl Oligo dT primer (7.5µM)

Mastermix3: 4µl 5xFSB, 1µl DTT, 1µl RNAsin, 1µl Superscript III

Reaction mixtures: LightCycler DNA Master SYBR green I kit (Roche):

SYBR Green I dye (dNTP, reaction buffer, DNA polymerase) + MgCl2 + FWD and REV primer (100 µM, to obtain final concentration of 500 nM in 20 µL reaction volume).

4. Results

4.1 Generation of MVA antigen-specific CTL

Cytotoxic CD8+ T cells (CTL) have an important role in clearing acute viral infections. Our group has previously shown for MVA that antigen presentation of late viral gene products to CTL is substantially delayed and dramatically shapes the CTL repertoire in secondary expansion due to T cell competition (Kastenmuller *et al*., 2007; Meyer *et al*., 2008). Thereby, the timing of viral antigen expression in infected APC has a strong impact on viral T cell epitope presentation and processing.

As introduced before, the vaccinia virus (VACV) life cycle can be divided into early, intermediate and late phase and a set of antigen-specific CTL lines have been generated from C57BL/6 mice vaccinated with recMVA viruses (See methods 3.3.3 and Fig.1). These CTL recognize epitopes derived from vaccinia virus (VACV) proteins (A19-late, A3-late and B8-early) or model antigens (ova/NP) that are produced early or late during the viral life cycle (Fig.2).

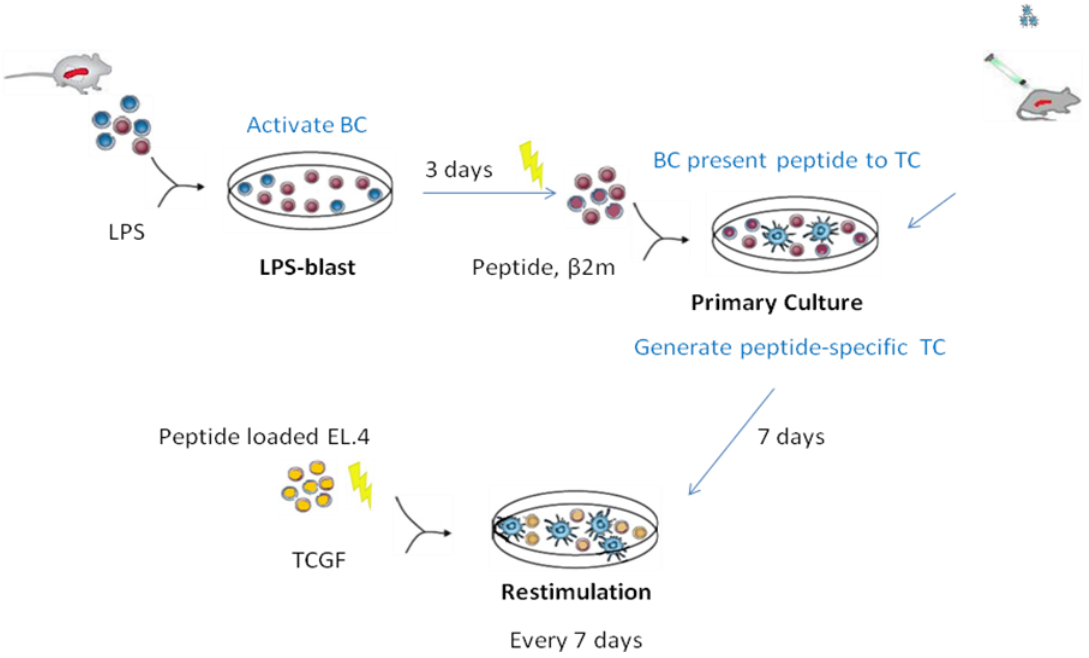

Figure 1: Generation of epitope-specific CTL. Splenocytes from naïve C57BL/6 mice were mixed with LPS for 3 days, loaded with specific peptides and ß$_2$m, and added to splenocytes from MVA vaccinated mice. Every week they were restimulated again by peptide-pulsed EL4 cells with additional TCGF.

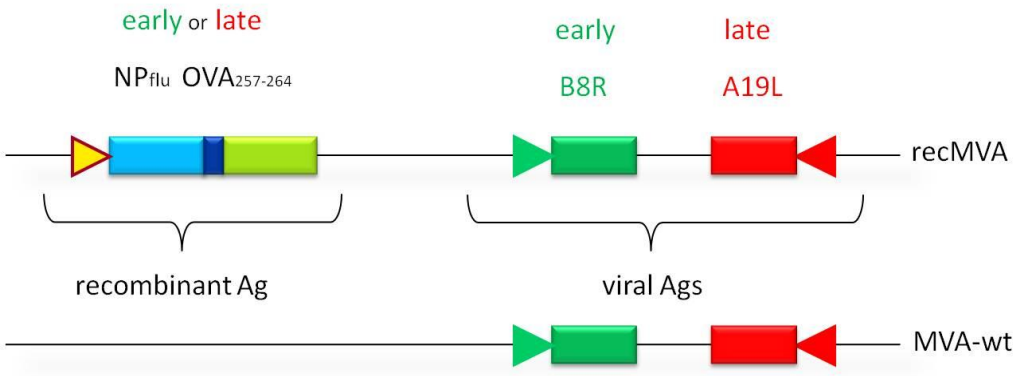

Figure 2: Antigens encoded by recMVA or MVA-wt (C57BL/6). A19-late, A3-late, B8-early, NP/ova-early or -late.

4.1.1 CTL could be activated by endogenous antigens or exogenous peptides

CTL were tested for activation by exogenous (peptide-pulsed) antigen presenting cells (DC2.4 cell line) by measuring the IFN-γ production by intracellular cytokine staining (ICS) (see methods 3.3.8.1). All CTL lines showed a dose-dependent activation using high to low concentrated peptides for stimulation. The control peptides yield no activation indicating CTL had no background activity or reacted unspecifically (Fig.3). All CTL had comparable avidity for their cognate peptide.

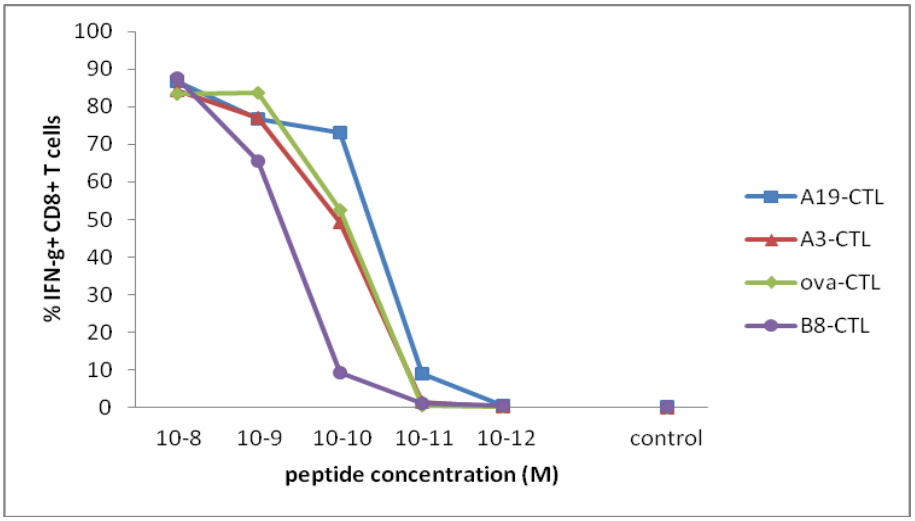

Figure 3: Comparable avidity of T cell lines for peptide-pulsed target cells. DC2.4 cells were loaded with specific peptides at concentrations ranging from 10^{-8} M to 10^{-12} M. ICS for IFN-γ production.

CTL were also tested for endogenous antigen presentation by infected cells, in which different recMVA were used that control their target gene expression with early and/or late promoters. The CTL were also be specifically activated by the infected APC (Fig.4). The peptide control showed good activation by the specific peptide or no activation by the irrelevant control peptide. The infection with recMVA or WT for 12h

resulted in a strong activation by all the early antigens (ova/B8), while one late antigen (A19) elicited very poor activation, the other late antigen (A3) resulted in a medium activation.

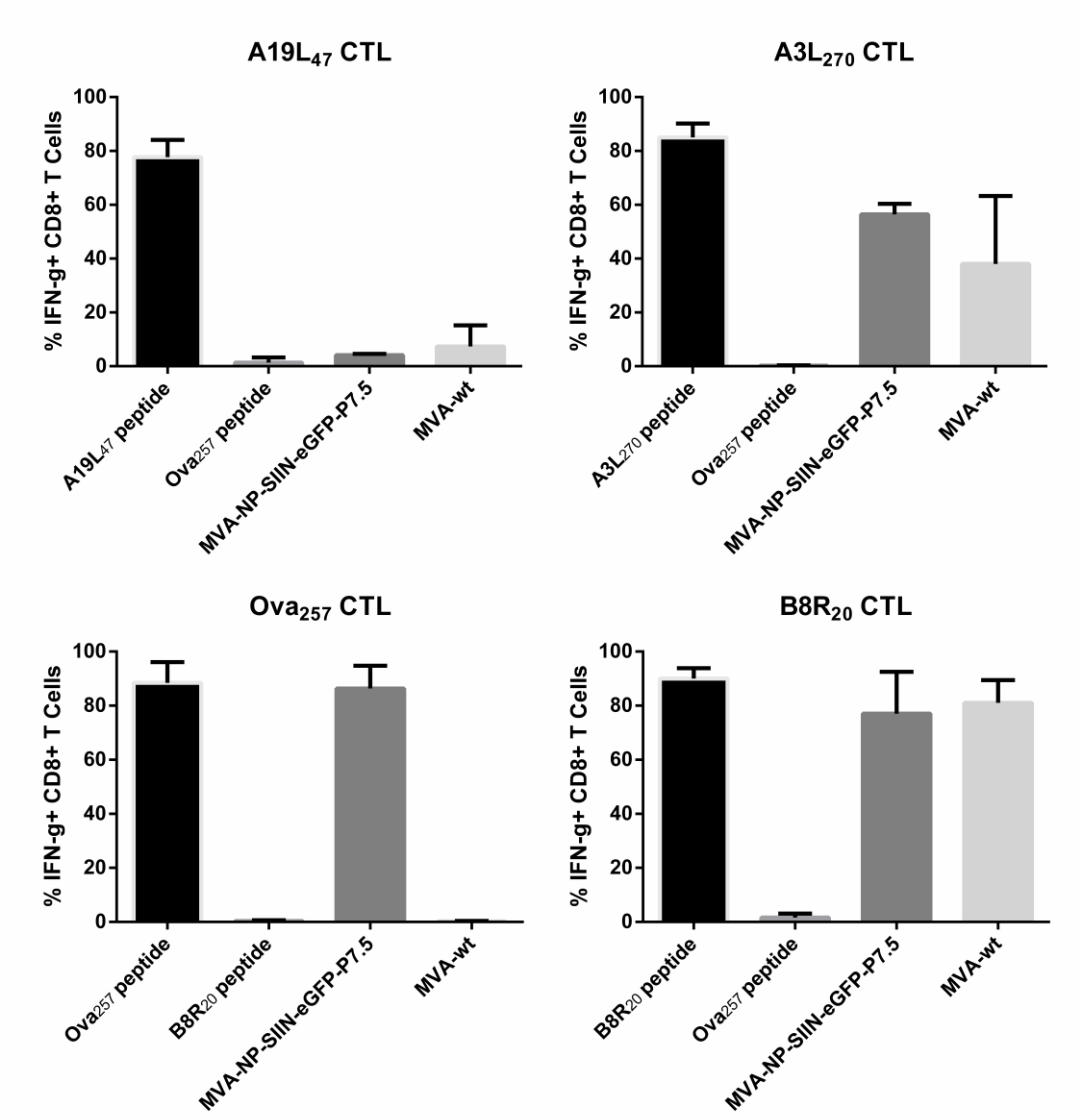

Figure 4: Exogenous (peptide) and endogenous (infection) TC activation (IFN-γ %). DC2.4 cells were infected with MVA-P7.5-NP-SIIN-eGFP and MVA-wt at MOI 10 for 12h and cocultured with T cells for 4h. ICS for IFN-γ production. Peptides were used at 10^{-8} M.

4.1.2 CTL showed ability for killing target cells in ^{51}Cr release assays

It is also important that cytotoxic T cells are not only able to secret cytokines, but also kill target cells. Hence, CTL were tested in chromium release assays for their killing ability (see methods 3.3.10). They could sufficiently lyse target cells, which were infected by MVA (Fig.5). NP and ova CTL could additionally kill recMVA infected target cells, while B8 A19 and A3-specific CTL could only kill wt infected target cells. A19 peptide stimulation worked as a positive control for A19-specific CTL. Target cells, which were not infected, worked as negative controls for the whole setting.

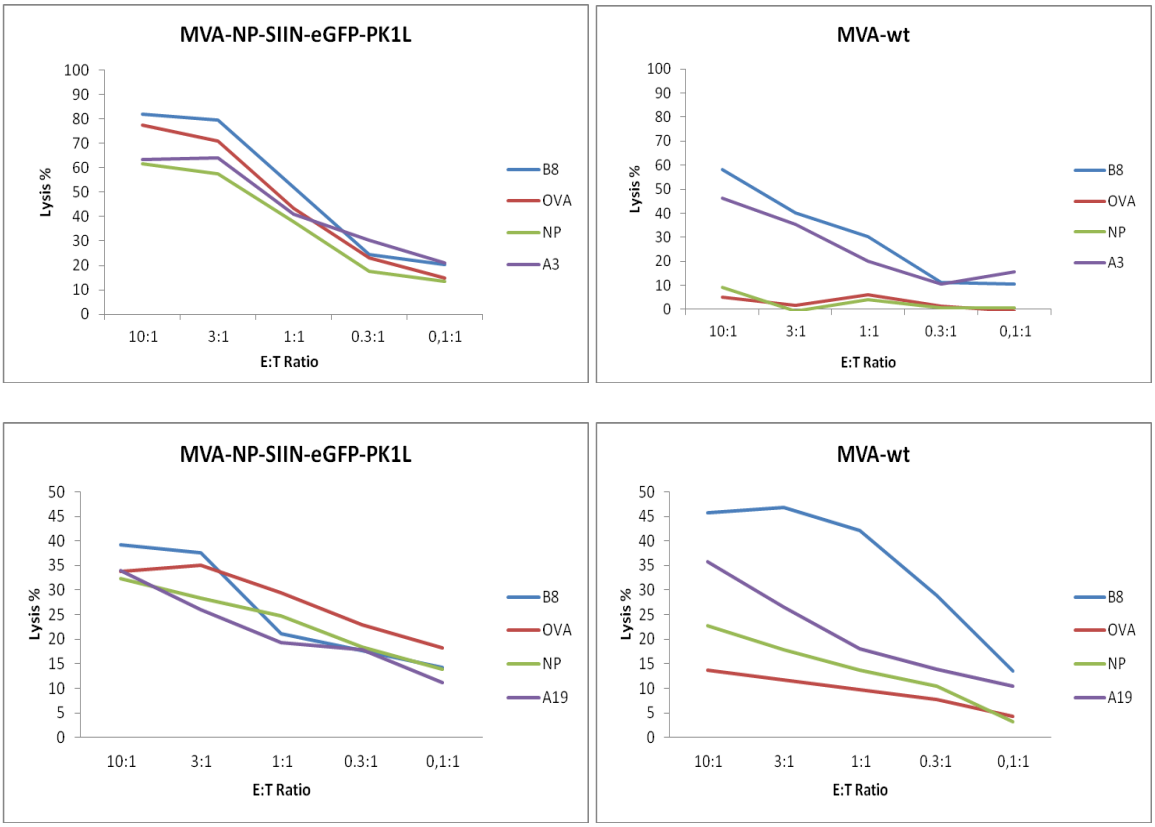

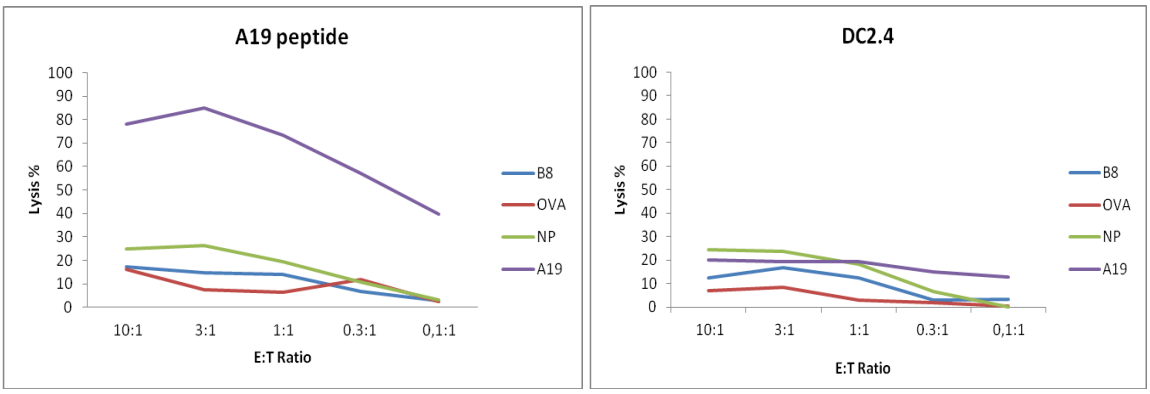

Figure 5: CTL-mediated cytoxicity by ^{51}Cr release assay. First panel shows B8, ova, NP and A3-specific CTL. E:T show the ratio of effector cells (CTL) to target cells (DC2.4). DC2.4 were infected by MVA-NP-SIIN-eGFP-PK1L or WT for 2h at MOI 10, labeled with ^{51}Cr for 1.5h and incubated with TC at various E:T ratios for 4h. The supernatants were taken to scinti counter for analysis. **Second and third panels show B8, ova, NP and A19-specific CTL.** DC2.4 were either infected by MVA-NP-SIIN-eGFP-PK1L or WT at MOI 10 or A19 peptide loaded or uninfected (DC2.4).

As a result, all CTL showed efficient activation and killing ability.

4.2 Direct-presentation to CTL

4.2.1 A3L is an early and late gene

One CTL epitope was derived from the VACV protein A3, the major viral core particle component. According to literature, A3 represents a late gene product (Oseroff *et al*., 2008; Moutaftsi *et al*., 2006). Interestingly, we found that MVA-infected target cells also activated CTL specific for A3 at early time points (2h) after infection (Fig.6). Other viral antigens such as early B8 could activate CTL at 2h p.i., while late A19 could activate CTL not before 12h p.i.

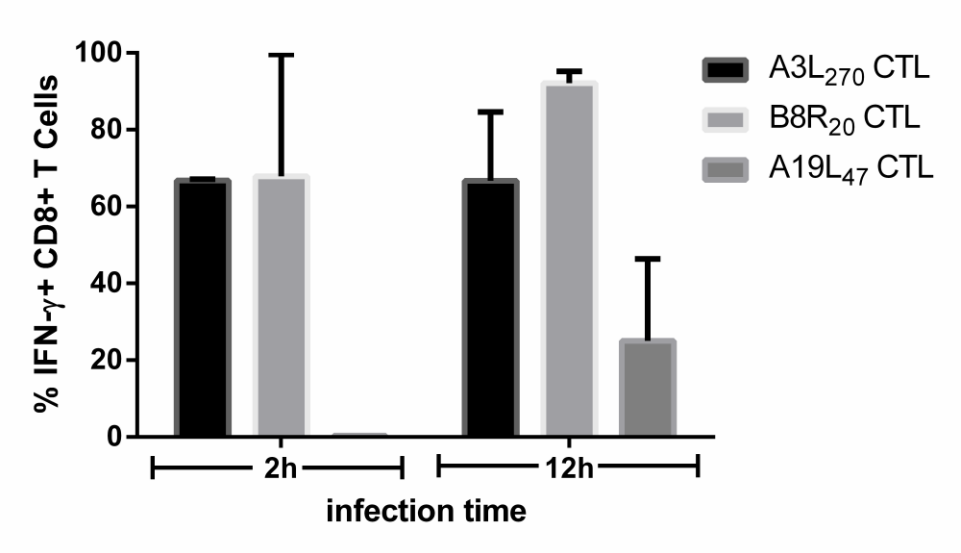

Figure 6: A3-specific CTL can be activated at both, early and late time points. DC2.4 cells were infected with MVA-wt for 2h or 12h and cocultivated with TC for 4h. IFN-γ production (ICS).

In order to confirm that A3 was also expressed early, Arabinosid C (AraC), an inhibitor of VACV late gene expression, was used at 40µg/ml through all steps of the experiments. AraC could not block the A3-specific CTL activation, while it could block the T cell activation by other late antigens (A19 and ova-P11). This was also found for other vaccinia virus strains: Chorioallantois vaccinia Ankara (CVA) and Western Reserve (WR) (Fig.7). Importantly, macrophages were used in the same setting as APC for comparison since they do not allow for late gene expression. Again, A3 as B8 had high CTL activation capacity, while A19-specific CTL activation was nearly missing (data not shown).

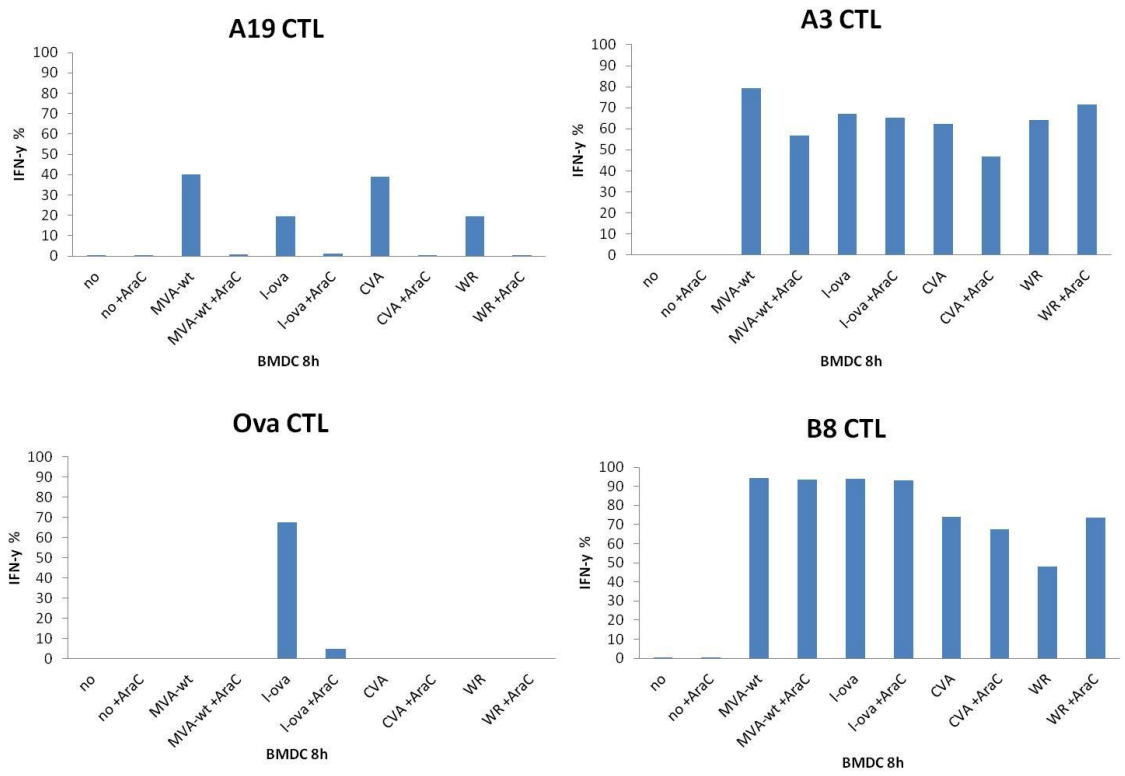

Figure 7: A3-specific CTL activation can not be blocked by AraC after infection with various VACV strains: MVA, CVA and WR. BMDC from C57BL/6 mice were treated with or without AraC at 40µg/ml before being infected with MVA, CVA or WR at MOI 1 for 8h.

A3 expression was also tested at mRNA level by real time PCR which is one of the most sensitive methods and can discriminate closely related mRNAs even in small amounts. BMDC were infected with strains MVA, CVA, WR or Lister for 0h, 1h, 2h, 3h, 4h, 5h, 7h or 9h. Total RNA was extracted from approximately 1×10^6 cells by Solution D. High-quality RNA can be isolated by the Phenol–chloroform extraction method (see method 3.5). 18s rRNAs (ribosomal RNAs) were used as internal standard (loading control) or as reference genes. 18s does not change significantly in expression during the course of infection. A3 showed early and late expression for MVA, CVA and WR, but

only late expression for Lister (Fig.8). Early expressed B8, late expressed H3 and intermediate expressed G8 were expressed as described in literature (data not shown).

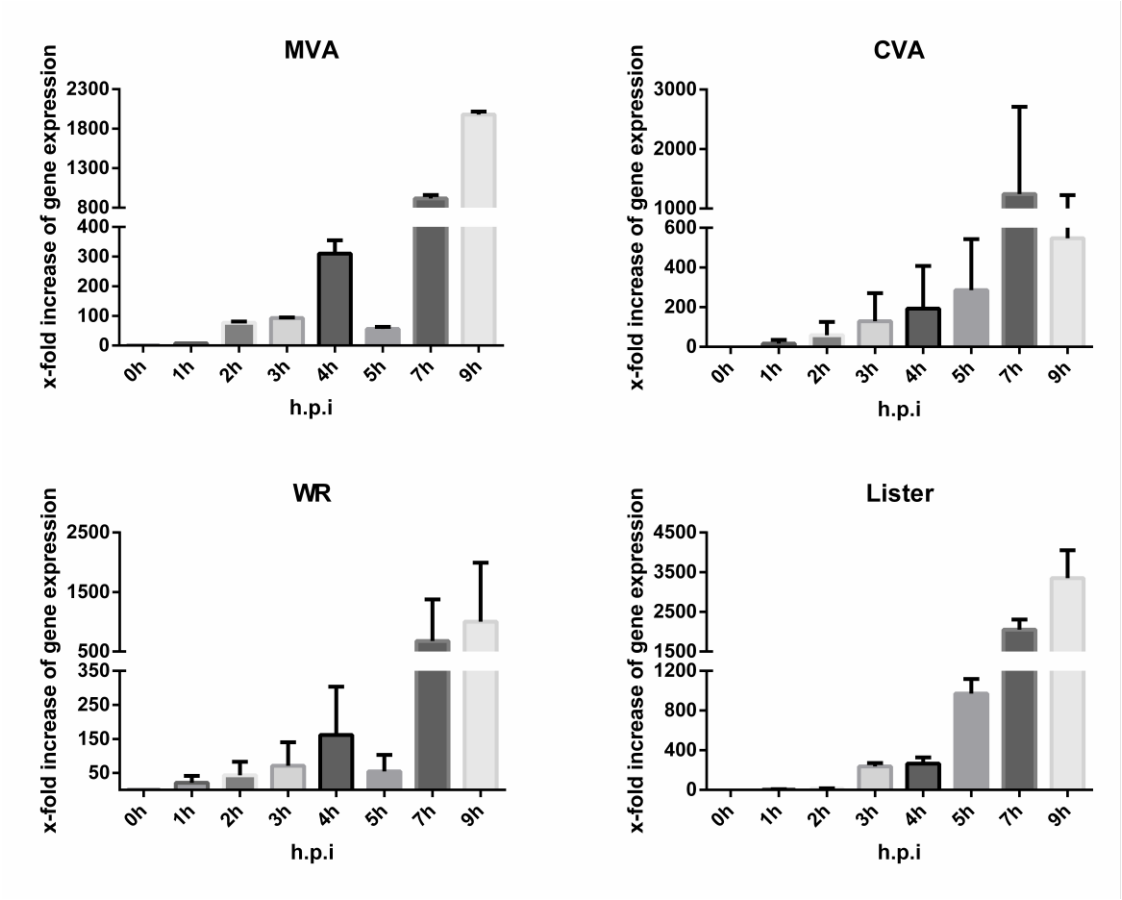

Figure 8: A3 expression on mRNA level. BMDC were infected with strains MVA, CVA, WR and Lister for 0h, 1h, 2h, 3h, 4h, 5h, 7h and 9h. Shown is the increased fold of gene expression.

On the other hand, early activation of CTL may possibly come from the viral input. Therefore, UV-inactivated viruses were used to infect APC and tested for CTL stimulating capacity. Importantly, A3-specific CTL were not activated at all, which indicates the requirement of *de novo* protein synthesis and excludes the possibility of using preformed proteins contained in the viral input (Fig.9).

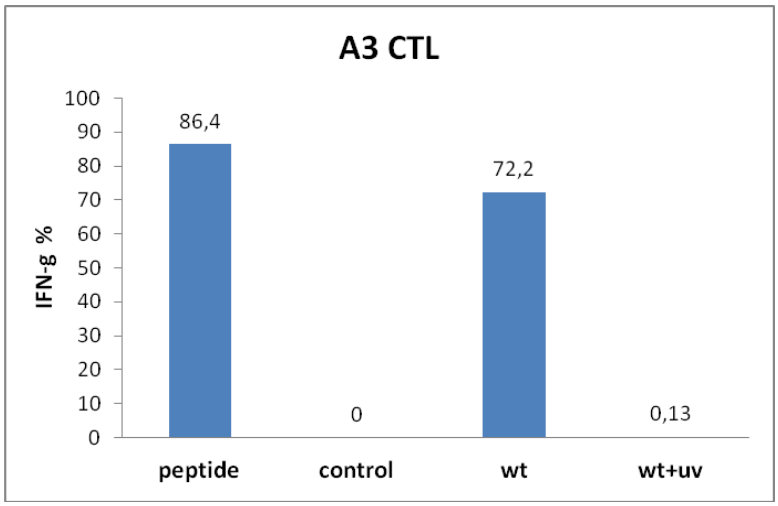

Figure 9: A3-specific CTL activation requires *de novo* protein synthesis. MVA-wt was PUVA treated for 10min (0.15 J/cm²) (wt+uv) or left untreated (wt) before infecting DC2.4 cells for 2h. Left side shows peptide control (A3 peptide or ova control). TC activation was measured by IFN-γ production (ICS).

4.2.2 Direct-presentation of early and late antigens

There are basically three phases of viral gene expression in the vaccinia viral life cycle: early, intermediate and late. The interval time between each phase is only one hour at the transcriptional level (Moss, 2007), which means late antigens will start to be expressed after 3 hours of infection. However, our group has shown before that some late antigens could not activate CTL even after 8h of infection using infected LCL cell lines as stimulators, which are human lymphoblastoid B cells (Kastenmuller *et al*., 2007). In this setting, HLA-A2 restricted CTL specific for early antigen B22 and late antigen A6, I1, H3 were used. All antigens were contained in the backbone of the virus (Fig.10).

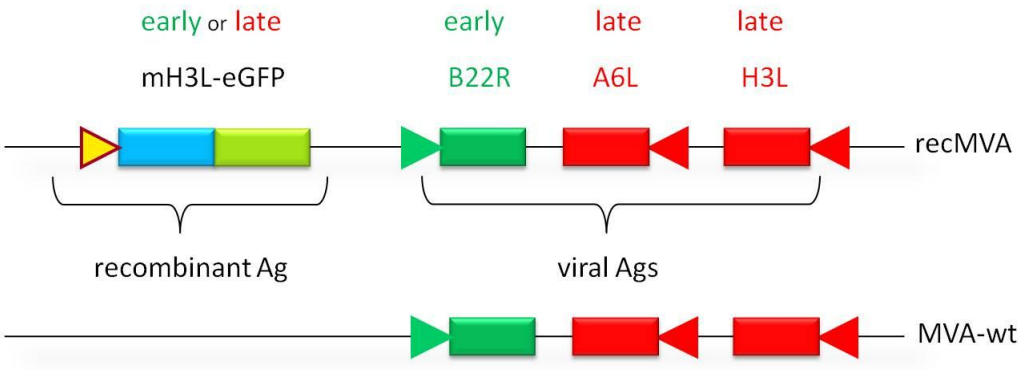

Figure 10: Murine epitope-specific CTL lines recognize antigens from recMVA or MVA-wt in an HHD-restricted manner. B22R-early, A6L-late, I1L-late, H3L-late genes are all at the backbone of the virus.

To confirm result and to extend the above findings, professional APC (BMDC from HHD mice) were used to test antigen presentation by MVA-wt infection for an extended period of time (0/4/6/8/12h p.i.). Again, delayed late antigen presentation was demonstrated and A6 specific CTL were activated around 8h p.i.; I1 and H3-specific CTL around 12h p.i. (Fig.11).

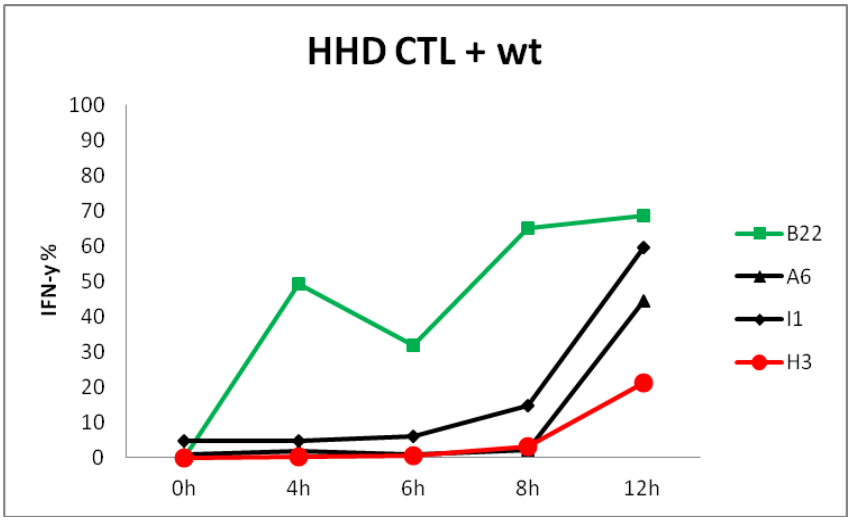

Figure 11: HHD BMDC direct presentation kinetics. BMDC were infected with MVA-wt at MOI 1 for 0/4/6/8/12h. TC activation was measured by IFN-γ production (ICS).

However, antigen presentation can differ in other experimental mouse systems. To find out if delayed late antigen presentation is independent of the mouse strain, early and late antigen activation of CTL in the C57BL/6 model was tested. BMDC were used to be infected with MVA-ova-PK1L or MVA-ova-P11 at MOI 1 or 10. BMDC could present SIIN-K^b complexes derived from early expressed ova protein as early as 2h p.i. and from late expressed ova protein around 9h p.i. (Fig.12A). For CTL activation, BMDC infected with MVA-wt and incubated for a distinct period of time were used. B8 and A3 could activate CTL as early as 4h p.i., but A19 could not activate specific CTL even after 6h of infection (Fig.12B). When infected with MVA-ova-PK1L or -P11, early-ova could activate CTL before 4h p.i., while late-ova could activate ova-specific CTL around 6h p.i. Thus, foreign late-ova antigen could activate CTL earlier than viral late antigen A19. Furthermore, late-A19 also had lower activation of CTL when compared to late-ova (dat not shown). Even after 12h of infection, late antigens (A19, P11-ova, P11-NP) had a very low activation capacity for TC as compared to the early antigens (B8, PK1L-ova, PK1L-NP) (Fig.12C).

Both epitope presentation as well as T cell activation showed a delay of the late antigen's presentation. Also, the late antigen presentation was not as efficient as early antigen presentation.

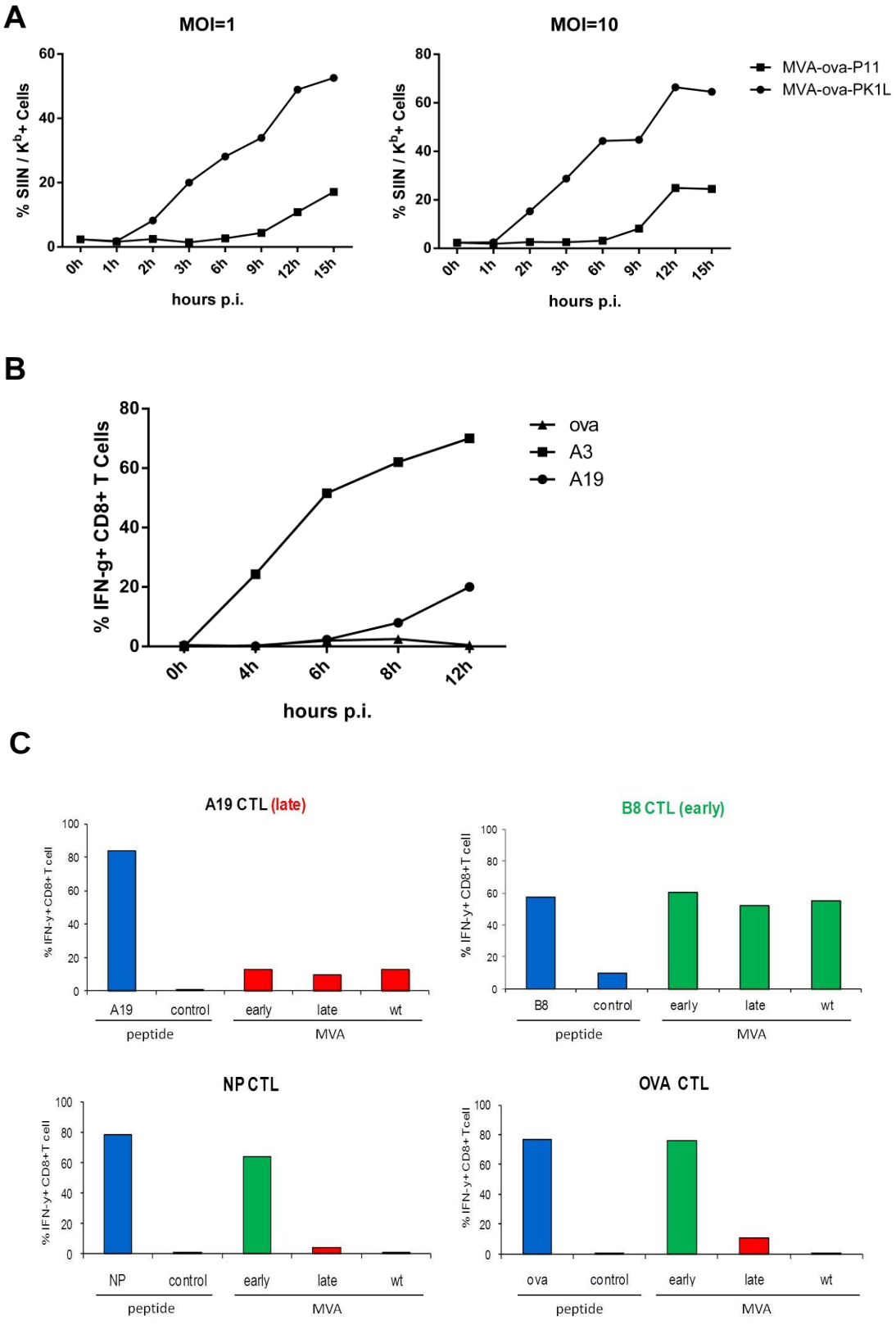
A
MOI=1
MOI=10
% SIIN / Kb+ Cells
hours p.i.
0h
1h
2h
3h
6h
9h
12h
15h
MVA-ova-P11
MVA-ova-PK1L
B
% IFN-g+ CD8+ T Cells
ova
A3
A19
0h
4h
6h
8h
12h
hours p.i.
C
A19 CTL (late)
B8 CTL (early)
NP CTL
OVA CTL
% IFN-γ+ CD8+T cell
A19
B8
NP
ova
control
early
late
wt
peptide
MVA

Figure 12: A. Delayed presentation of SIIN-K^b complexes on the cell surface by BMDC infected with recMVA (e/l-ova) at MOI 1 or 10. SIIN-K^b positive cells stained for SIIN-K^b APC Ab 1:200 are shown. **B. Late antigen shows delayed activation of CTL**. C57BL/6 BMDC infected with MVA-wt at MOI 1 for different time points, were incubated with CD8+ TC and used for ICS (IFN-γ production by FACS analysis). **C. Late viral antigens fail to activate epitope-specific CTL.** DC2.4 cells infected with MVA-NP-SIIN-eGFP-PK1L (early) / -P11 (late) or MVA-wt (wt) for 12h (ICS).

4.3 Cross-presentation to CTL

4.3.1 Establishment of cross-presentation assays

Even if late antigens were not efficiently processed or early enough presented to activate T cells in time, there is still another pathway available for antigen presentation: cross-presentation (Shortman *et al*., 2010). This pathway is executed by noninfected APC (mainly dendritic cells), catching up the antigen from infected cells and processing and presenting it to CTL. According to the literature, GM-CSF induced BMDC should be able to cross-present exogenous antigen (Saveanu *et al*., 2009; Segura *et al*., 2009). Therefore, bone marrow from C57BL/6 mice was prepared and GM-CSF 1:10 added to the culture at day 3 and day 6 as a maturation stimulus. On day 7 to 10, BMDC could be used for assays (see methods 3.3.4).

4.3.1.1 BMDC phenotype and maturation state

BMDC have been tested by surface markers (CD11c for cDC, MHC-II and CD86 for maturation) and were found to be mostly immature conventional DC (CD11c+ CD86- MHC II low or medium DC) which could be further matured by adding LPS (500ng-20μg/ml) (CD11c+ CD86+ and MHC II+ high DC) (Fig.13). Moreover, MVA infection

could induce fast maturation of infected (around 2h p.i) and noninfected (around 4h p.i) BMDC (Fig.14).

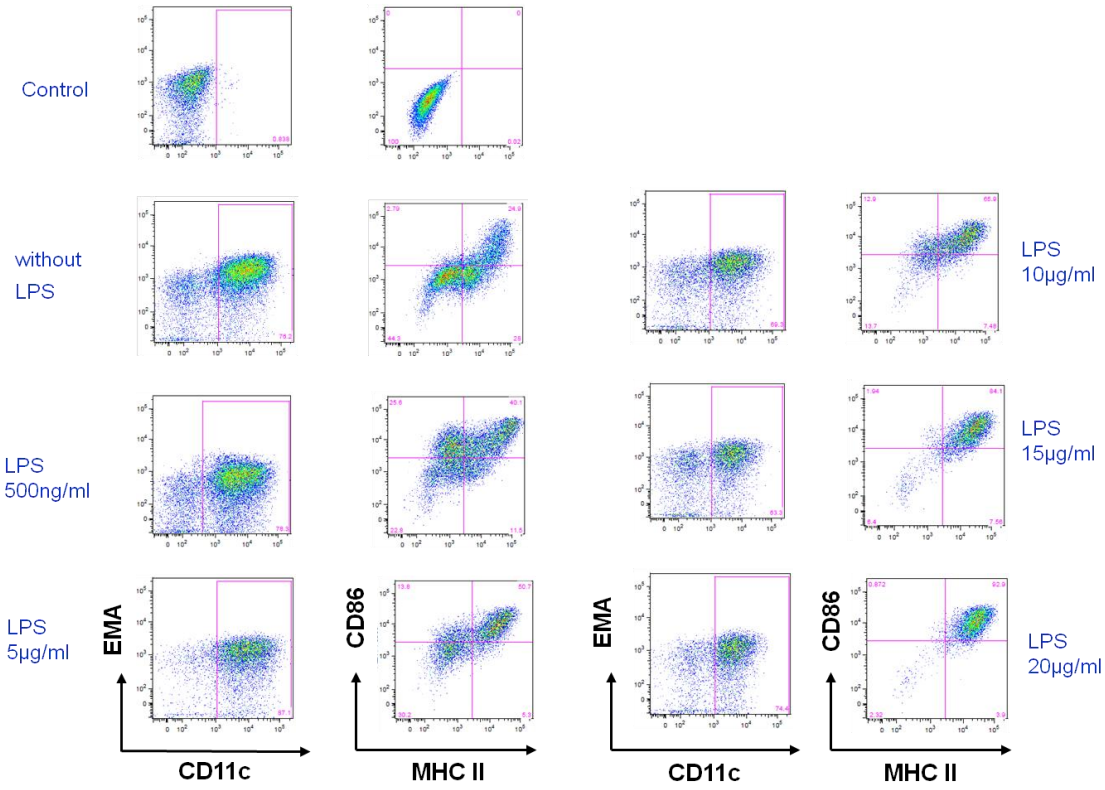

Figure 13: Maturation of immature BMDC by LPS. BMDC were treated with or without LPS in different concentrations (500ng-20µg/ml) for 24h. The cells were stained for PI (to separate living cells), CD11c-APC, CD86-FITC and MHC II-PB Ab analyzed by FACS.

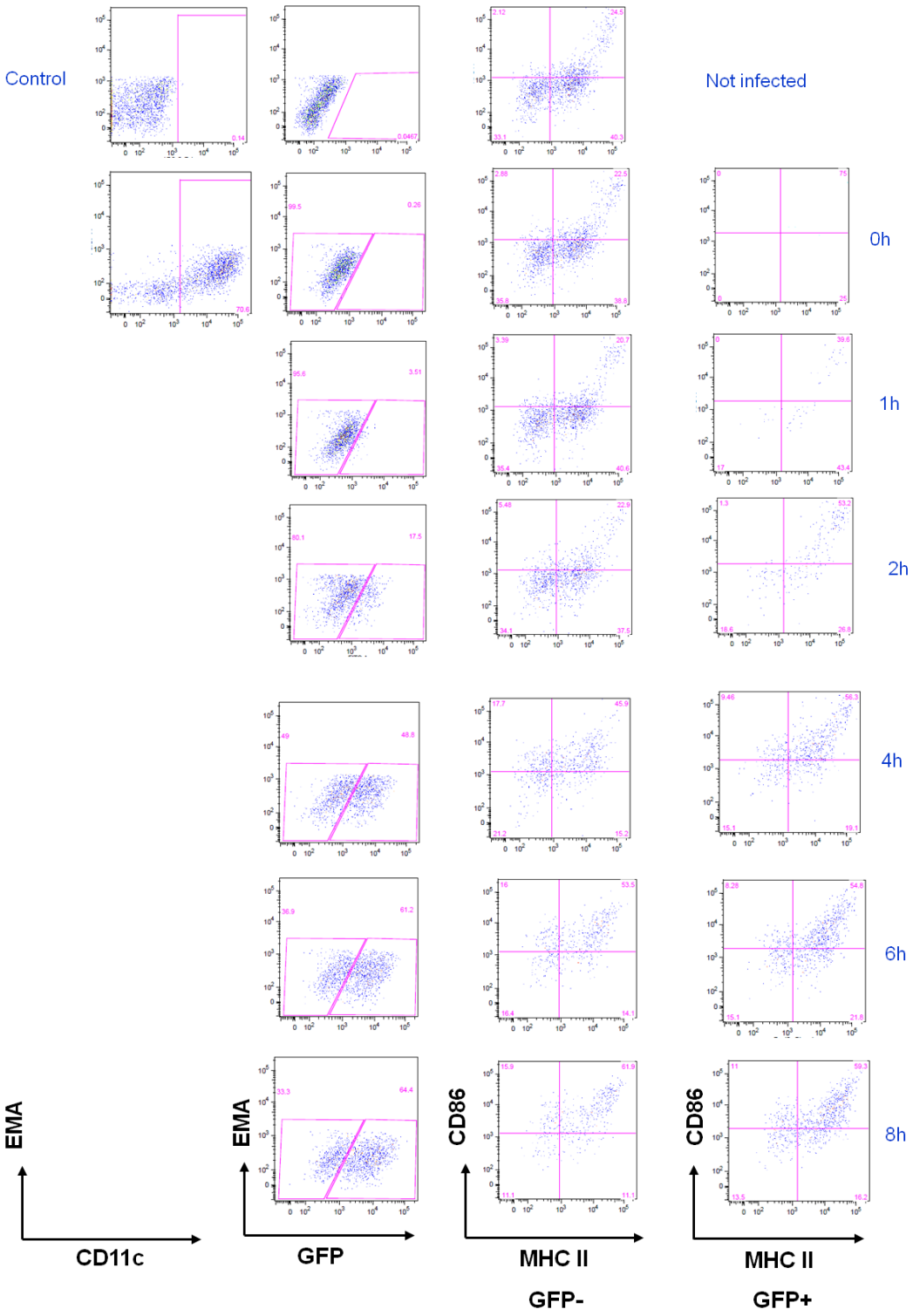

Figure 14: MVA infection induces fast maturation of BMDC. BMDC were infected with MVA-GFP for 0-8h and stained for different surface markers. Cells were gated on GFP+ (infected) and GFP- cells (uninfected bystander) and gated for surface markers.

4.3.1.2 BMDC were able to phagocytose antigens

In order to prove that BMDC could cross present antigens, they were first tested for phagocytosis of exogenous antigens. It has been shown that DC pulsed with 10μg/ml soluble ova protein stimulated ova peptide-specific CD8+ T cells (OT-I) after ova was translocated to the cytosol by an endocytosis-mediated mechanism (Ikeuchi *et al*., 2010; Burgdorf *et al*., 2007). Thus, BMDC were pulsed with 10μg/ml AF594 labeled ova protein for different periods of time. BMDC caught up efficiently ova protein after 30min's co-incubation. Therefore, BMDC should be able to cross-present this exogenous Ag (Fig.15). DC2.4 could not phagocytose ova protein as efficiently as BMDC (Fig.16L). Cytochalasin D (CytD) has been reported to block the finger-like projections formed by actin polymerization in order to inhibit phagocytosis (Schliwa, 1982). However, treatment of BMDC with CytD could not totally block phagocytosis (Fig.16R).

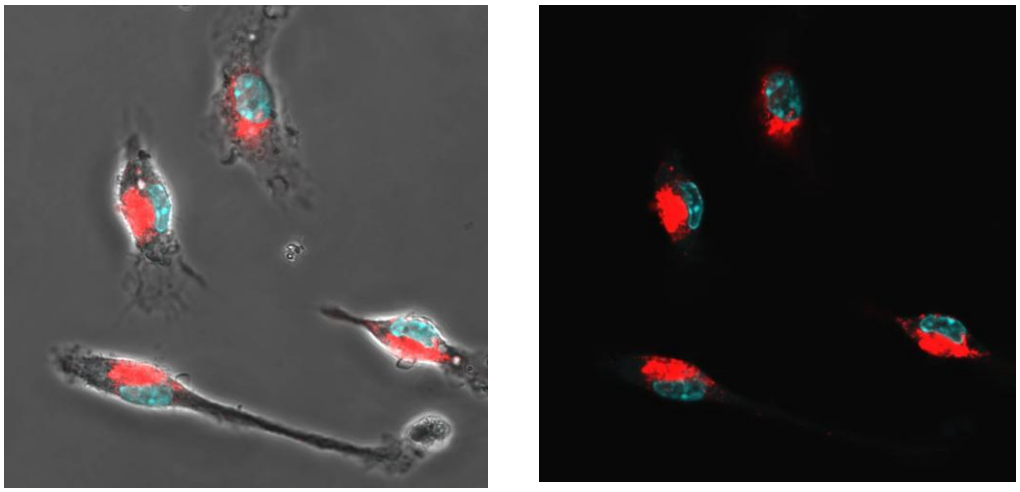

Figure 15: BMDC phagocytose ova protein. BMDC were co-incubated with ova-AF594 (10μg/ml) for 30min. Ova protein (red). Nucleus (DAPI; blue).

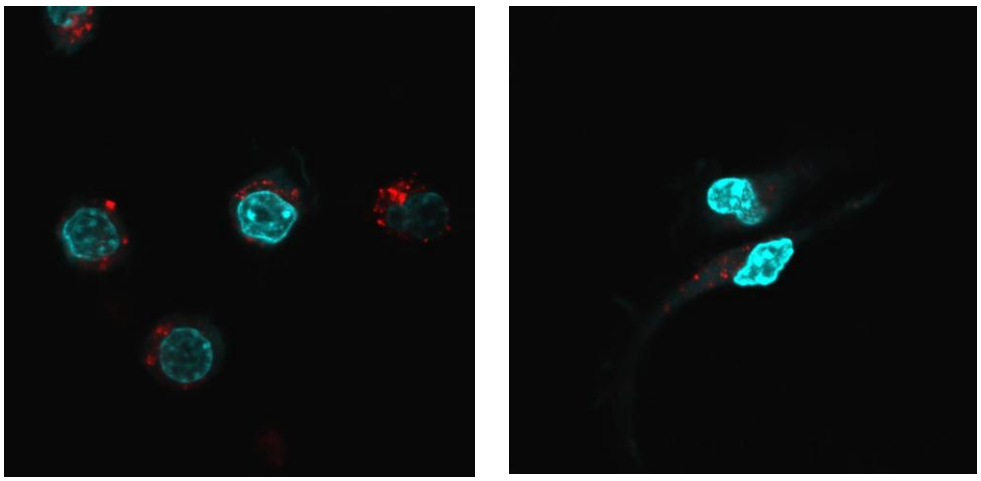

Figure 16: Left: DC2.4 cells phagocytose ova protein less efficient as BMDC. Right: CytD partially blocks phagocytosis. 5µM CytD for 1h before adding ova protein.

Furthermore, it was important that BMDC can not only take up soluble proteins but also infected cellular materials. Wagner and coworker have shown that DC can phagocytose apoptotic bodies from HSV-infected HeLa cells, which were labeled with fluorescent membrane dye PKH26 for 4h co-incubation time (Wagner *et al*., 2012). Here, Cloudman cells infected with MVA-NP-SIIN-eGFP-PK1L were used infected for 15h (MOI=10), followed by UV inactivation. As a last step, cells were labeled on membranes by PKH26. After washing, cells were co-incubated with BMDC which were previously labeled with Hoechest for 20min. Co-incubation of infected Cloudman and BMDC was 4h with a ratio of 1:4 (Cloudman : BMDC). BMDC (Hoechst positive) were analyzed by FACS or were imaged by confocal (BMDC; nuclear blue) to monitor for uptake of red material from infected Cloudman cells (nuclear green). (See methods 3.3.11)

FACS data for BMDC controls showed no GFP or PKH26 background. BMDC coincubated with infected Cloudman showed a high percentage of positive cells for GFP

and PKH26. Co-incubation on ice or BMDC pre-treated with CtyD showed reduced GFP and PKH26 uptake. A hundred percent of Cloudman cells were infected and labeled with PKH26. (Fig.17)

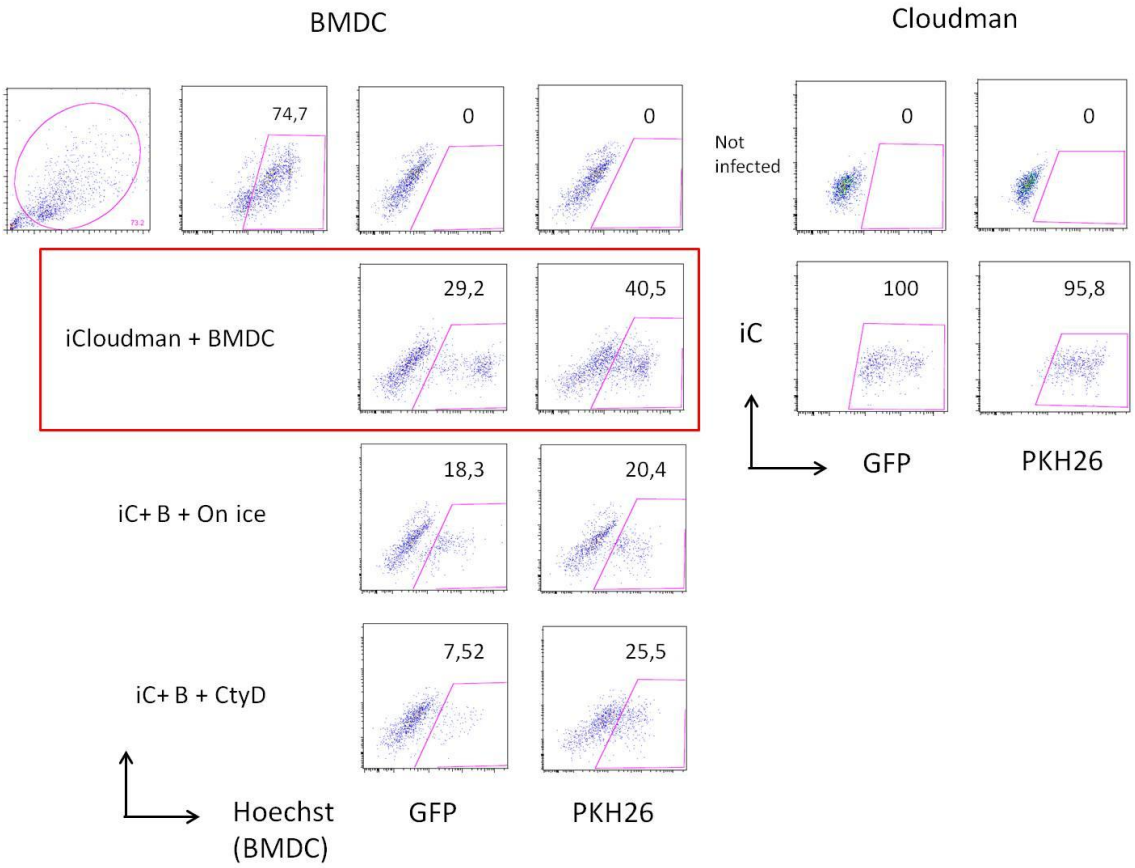

Figure 17: BMDC phagocytose MVA-infected cell material. Cloudman cells (Cloudman) were uninfected or infected with MVA-NP-SIIN-eGFP-P7.5 for 15h (iC), PUVA inactivated and labeled with PKH26 for 5min. BMDC were stained with Hoechst for 20min. Both cell types were co-incubated together for 4h. **C**o-incubation on ice (iC+B+on ice) or BMDC pretreated with CtyD (iC+B+CtyD) worked as controls. BMDC were first gated on Hoechst-positive cells and then gated on GFP- or PKH26-positive cells.

Using confocal microscopy, nucleus green and cytosol red showed infected Cloudman cells. BMDC were stained by Hoechst (smaller nucleus as compared to Cloudman cells). BMDC could catch up red and green material from infected Cloudman

cells (Fig.18). BMDC were pre-treated with CtyD 5µM for 20min (Fig.19 upper) or co-incubated on ice (Fig.19 lower) and used for negative controls. Controls showed disabled phagocytosis of BMDC.

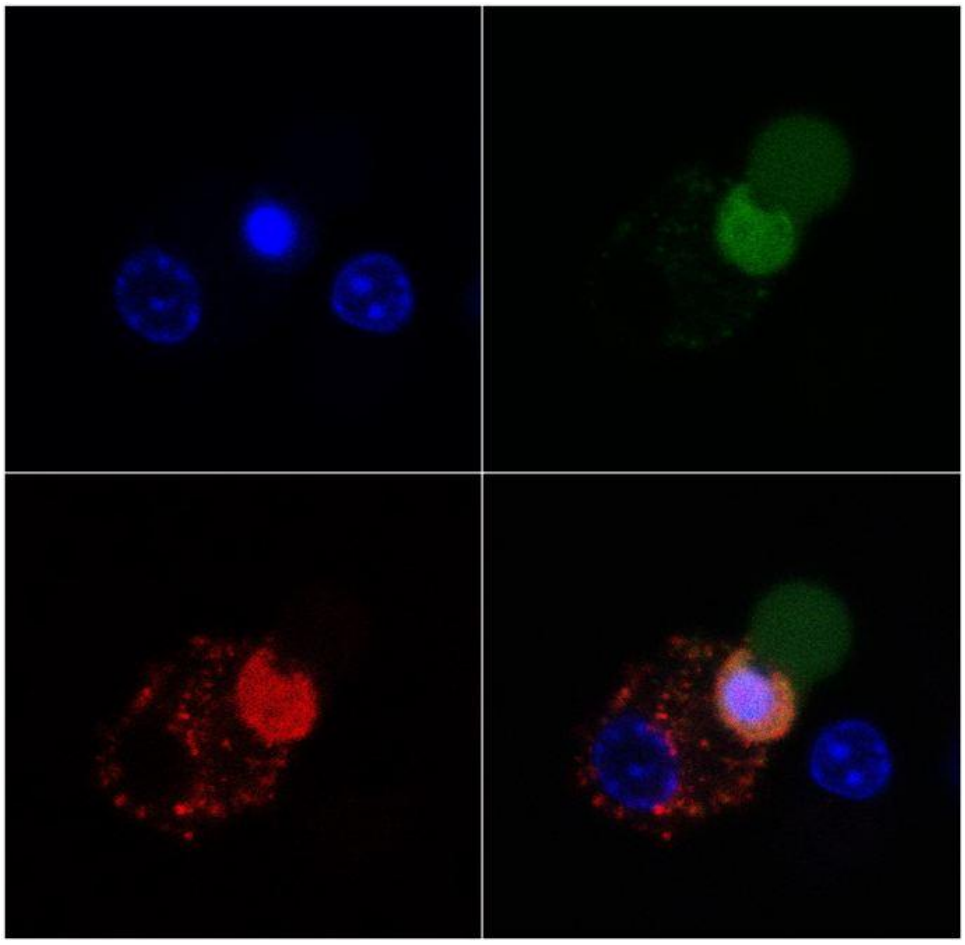

Figure 18: BMDC phagocytose MVA-infected cell material. Cloudman cells were infected with MVA-NP-SIIN-eGFP-P7.5 for 15h, virus inactivated by PUVA and labeled with PKH26. BMDC were stained with Hoechst for 20min. Cells were co-incubated for 4h. Infected Cloudman cells had a green nucleus. PKH26 (AF555; in red) corresponds to infected Cloudman cell material. BMDC nucleus was stained by Hoechst (in blue).

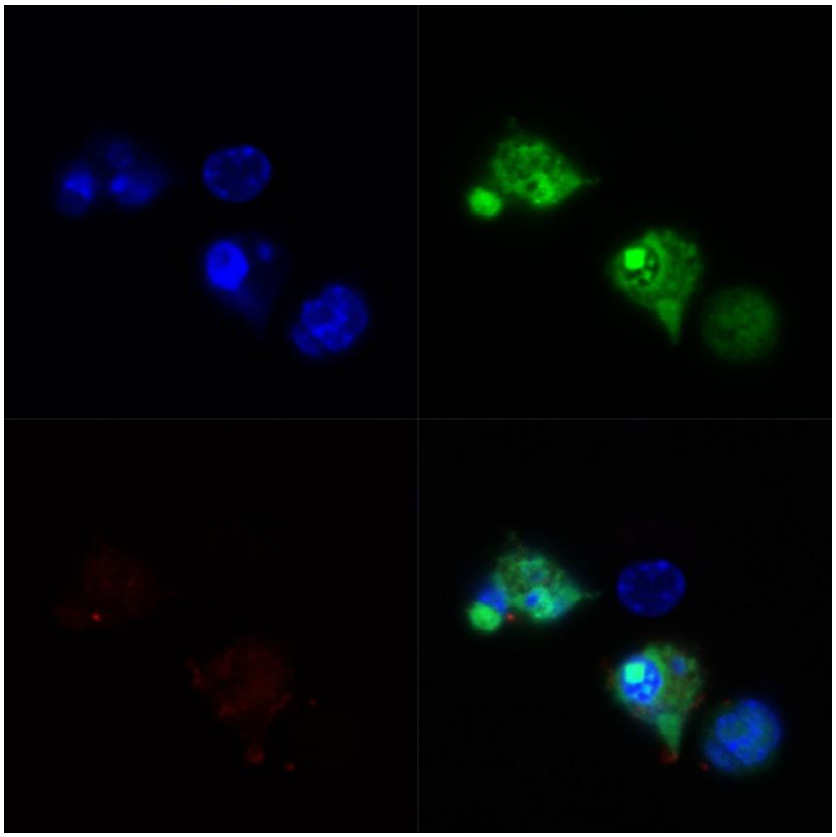

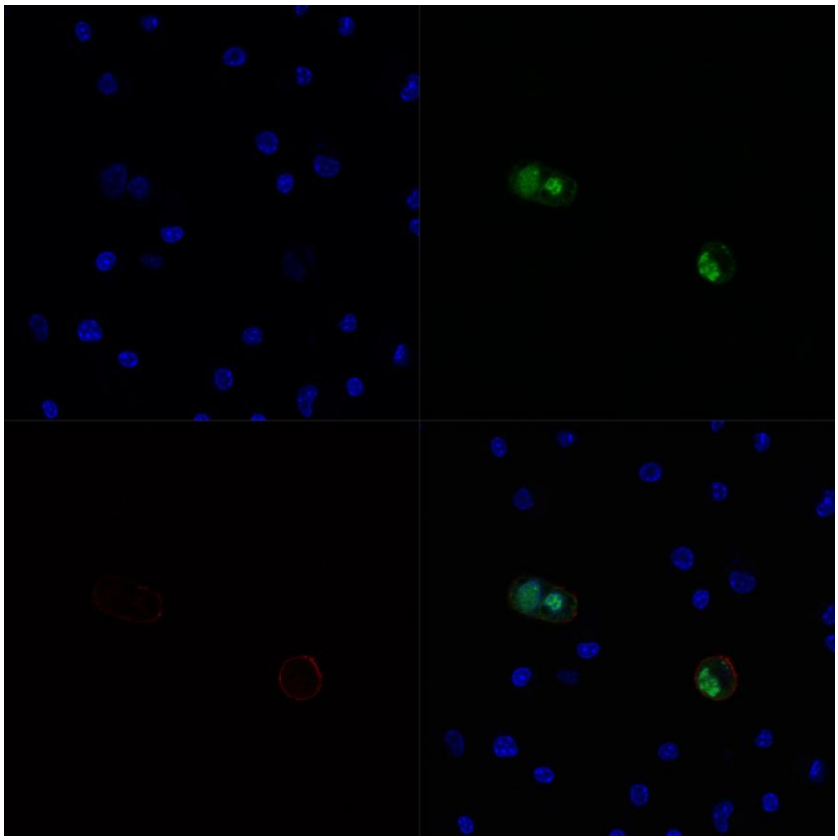

Figure 19: Upper: CtyD inhibits phagocytosis by BMDC. BMDC were pretreated with CtyD for 20min. **Lower: Phagocytosis by BMDC is inhibited on ice.** Co-incubation was on ice for 4h. Infected Cloudman cells (nucleus green). PKH26 (in red) represents membraneous material derived from infected Cloudman cells. BMDC Nuclei (Hoechst; in blue).

To test if MVA infection has an impact on the the ability of BMDC to phagocytosee exogenous antigens, ova protein only or ova protein combined with MVA (J774 infected by MVA-wt) were added to BMDC or DC2.4 for 30min, 1h, 2h or 3h. TC activation (ova/B8-specific CTL) was measured by FACS (ICS for IFNγ). Uninfected BMDC pulsed with ova protein could activate ova-specific CTL as expected. Furthermore, MVA infected BMDC induced an even higher ova-specific CTL activation. This indicates that MVA infection had an enhancing effect on phagocytosis activity and cross-presentation capacity of BMDC. Samples without ova protein worked as negative controls (Fig.20). All samples infected wit MVA had B8-specific CTL activation used as positive controls for infection. DC2.4 had comparably low phagocytosis ability (as shown before in Fig.16) and led to lower ova-specific CTL activation when pulsed with ova proteins with or without MVA infection.

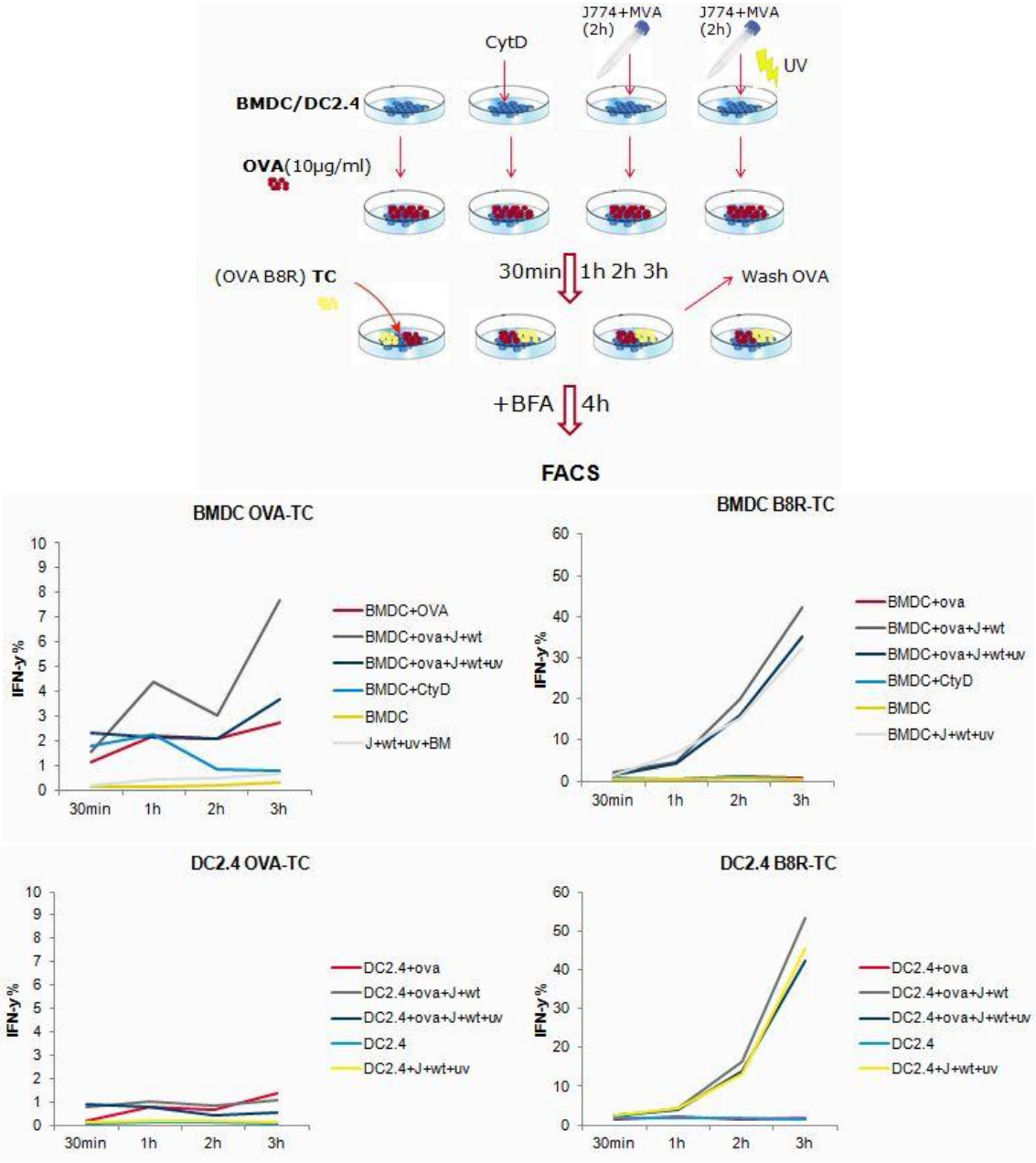

Figure 20: Activation of ova or B8-specific TC from ova pulsed BMDC with or without MVA infection. Ova protein only or ova protein with MVA infection (J774 infected by MVA-wt) were incubated with BMDC or DC2.4 for 30min, 1h, 2h or 3h. An activation of ova / B8-specific CTL was measured by FACS (ICS).

4.3.1.3 PUVA-mediated inactivation of MVA in infected cells

In order to assure that there was no residual virus, which derived from infected K^b negative feeder cells, which could infect BMDC, virus titers were tested after infection of J774 cells for 2h. After washing, cell pellets were used for virus titration on CEF cells (see methods 3.2.1). Interestingly, even after several washing steps after MVA infection, viruses were still present. Virus titers ranged up to 2.4 x 10^5 (Fig.21).

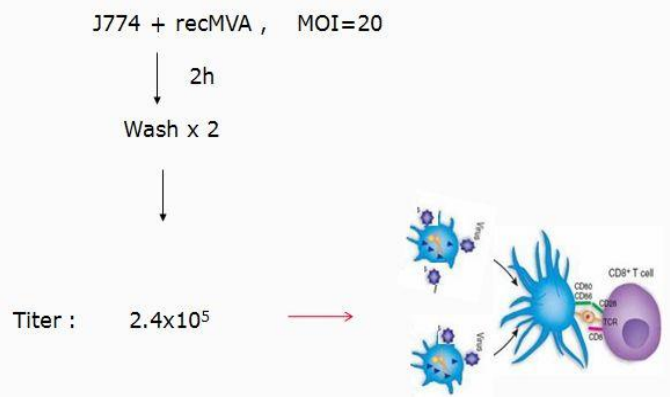

Figure 21: Virus titers after washing MVA infected cells. J774 cells were infected with MVA. After 2h infection, cells were washed twice. The cell pelletes were used for titration.

To get rid of these viruses, PUVA (Psoralen+ UVA) treatment of infected cells was performed (Tsung *et al*., 1996). Upon exposure to UVA light, psoralen can induce DNA interstrand cross-links (ICLs), which will block viral DNA replication and transcription (Fig.22A). In order to confirm that PUVA damages the virus DNA and blocks intermediate and late gene expression, the activity of early and late promoters (P7.5) was tested for the respective viruses after PUVA treatment. The infection rate for MVA-P7.5-NP-SIIN-eGFP without PUVA treatment was nearly 65%. MVA was effectively inactivated by only 5min of PUVA treatment and no infected cell (GFP expression) was detected in PUVA (5min, 10µg/ml Psoralen) treated cultures (Fig.22B).

A

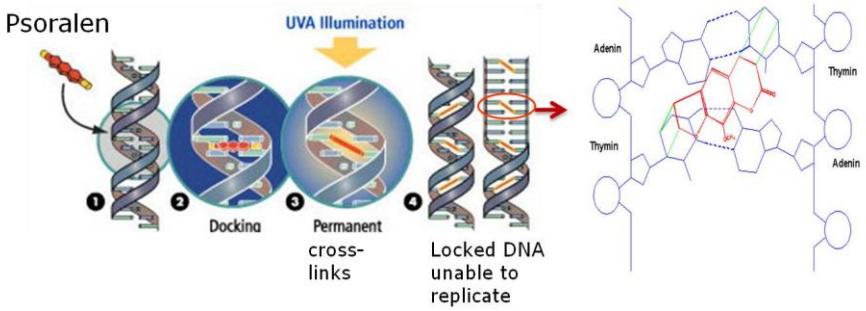

B

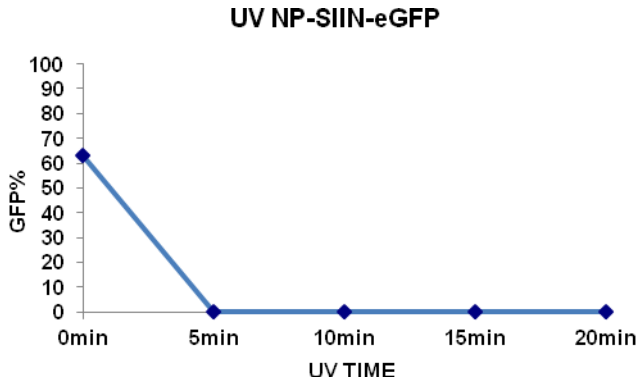

Figure 22: A. PUVA (Psoralen+ UVA) inactivation. Upon exposure to UVA light, psoralen can induce DNA interstrand cross-links (ICLs). **B. Viruses were efficiently inactivated by PUVA.** MVA-NP-SIIN-eGFP-P7.5 inactivated by PUVA for 0, 5, 10, 15 or 20min with 10µg/ml Prosolen before infection of J774 cells. Transcriptionally active viruses were measured by GFP expression in infected cells.

Smaller genes (SIINFEKL 24 bp) will be harder to be inactivated by PUVA than larger genes (ova 1160 bp or NP-SIIN-eGFP 2262 bp). To determine the effective dosage for virus inactivation, J774 were infected with MVA-SIIN-P7.5 or MVA-ova-P7.5 for 2h, washed twice with media and further incubated for additional 10h. Next, infected cells were incubated with 10, 1, 0.3 or 0.1µg/ml psoralen for 10min at 37°C (less psoralen has shown to be more effective [Tsung *et al*., 1996]) and UV irradiated for 0, 5, 10, 15 or 20min (1.125, 2.25, 3.375 or 4.5 Joules/cm^2). Irradiated J774 cells were added to DC2.4 cells for another 12h. If there were active viruses left, they would infect DC2.4 and induce SIIN presentation. SIIN presentation from MVA-ova or MVA-SIIN is shown in

Fig.23. It took 10min to inactivate MVA-ova, but 15min for MVA-SIIN, because the ova gene is more easily damaged than the small SIINFEKL peptide encoding DNA fragment. The lowest but most effective concentration of psoralen (15min PUVA treatment) was 0.3μg/ml.

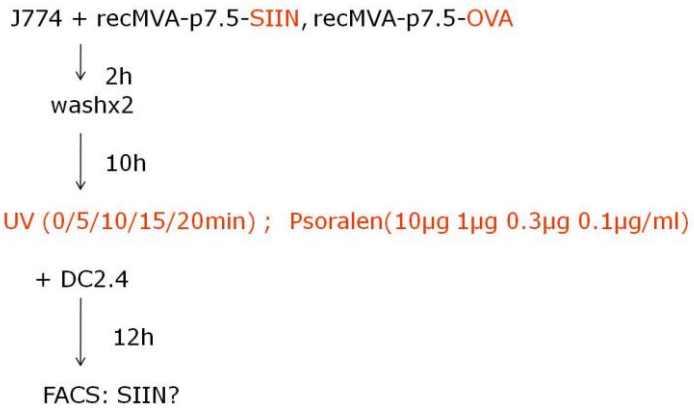

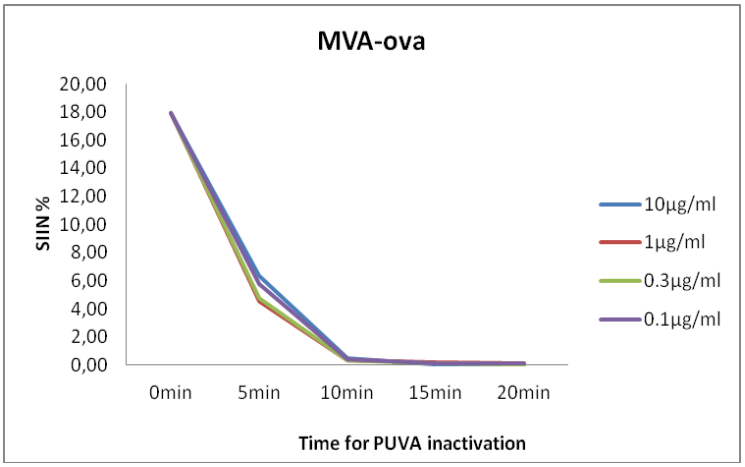

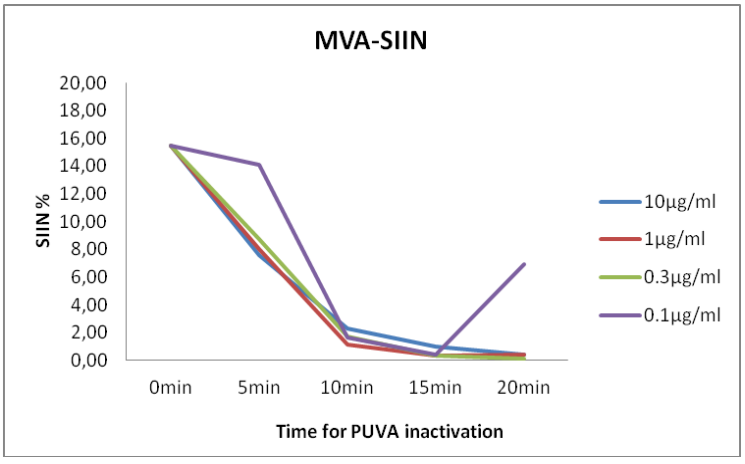

Figure 23: Inactivation capacity of PUVA depends on the length of genes, irradiation time and dosage. J774 cells were first infected with MVA-ova-P7.5 or MVA-SIIN-P7.5 for 2h, washed twice and incubated for an additional 10h. Cells were treated with different doses of psoralen and UV-irradiated for various periods of time (PUVA). Irradiated and infected J774 cells were then added to DC2.4 cells for 12h. The efficiency of PUVA inactivation is shown by SIINFEKL presentation (%) in DC2.4 cells.

4.3.1.4 Protocol for cross-presentation assay

Cloudman cells were used as the antigenic source (feeder cells). It is a H2-K^b negative melanoma cell line derived from Balb/C mice. BMDC from C57BL/6 mice were used as cross-presenters. Cloudman cells were able to strongly express recombinant antigens after MVA infection (Fig.24), but could not present peptide-K^b complexes to the cell surface (Fig.25). Thus, these cells only transfer the antigen to BMDC, which as H2-K^b positive cells could present SIIN-K^b (Fig.12A).

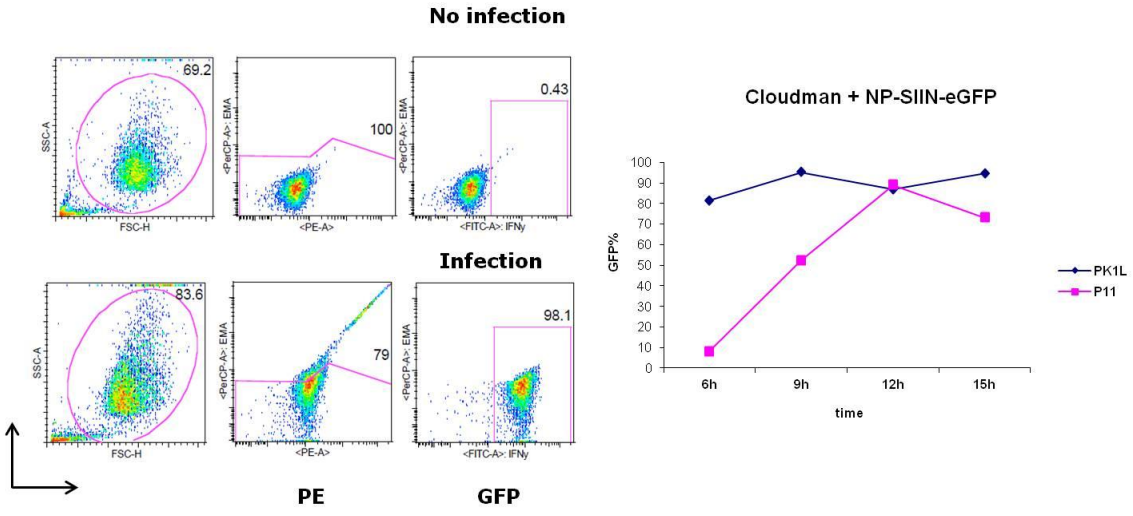

Figure 24: Cloudman has a high early and late gene expression profile. Left figure shows GFP expression in noninfected or infected Cloudman cells. Right figure shows GFP expression after infection with MVA-NP-SIIN-eGFP-PK1L/P11 at MOI 1 for 6h, 9h, 12h or 15h p.i.

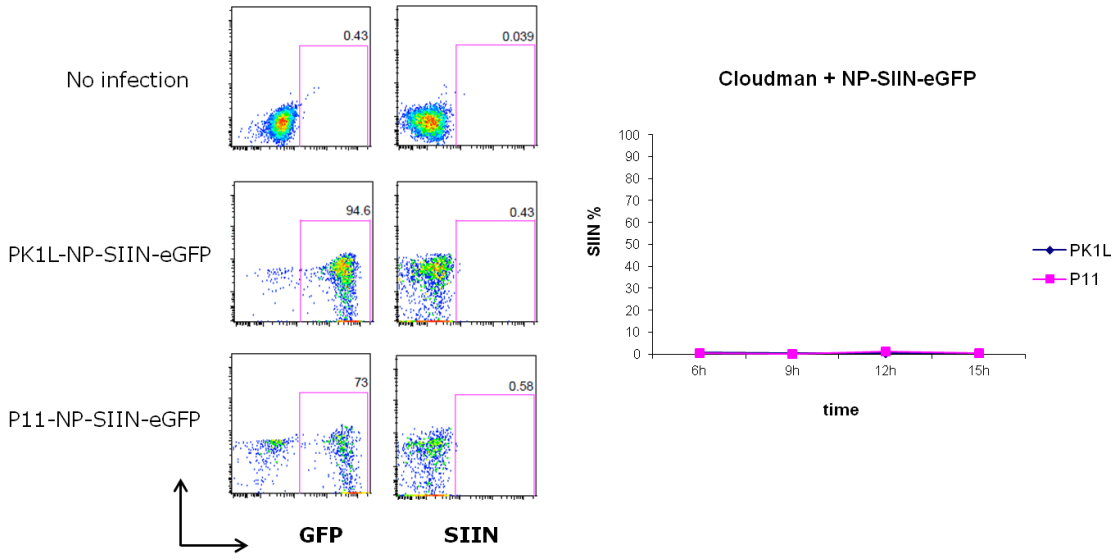

Figure 25: H2-K^b negtive Cloudman were unable to present K^b to the cell surface. Cloudman cells were infected with MVA-NP-SIIN-eGFP-PK1L/P11 for 6h, 9h, 12h or 15h p.i. SIIN-K^b complexes were detected by SIIN-APC Ab.

The final steps for the cross-presentation assay were settled as follows: H2-K^b negative Cloudman cells were infected with MVA at MOI 1 for 2h. After washing twice, infected cells were incubated for additional 10h to allow for efficient early and late gene expression. After PUVA inactivation with 0.3 μg/ml Psoralen for 15min, cells were washed again before coculturing with BMDC at a ratio of 1:1 and incubated for another 12h, so that BMDC could take up antigens from Cloudman cells. For comparison, BMDC were directly infected with MVA. Finally, cells were co-cultured with antigen-specific CTL lines at 2:1 ratios in the presence of 1μg/ml BFA for 4h. ICS and FACS analysis for intracellular IFN-γ production was carried out as described in methods 3.3.8. (Fig.26)

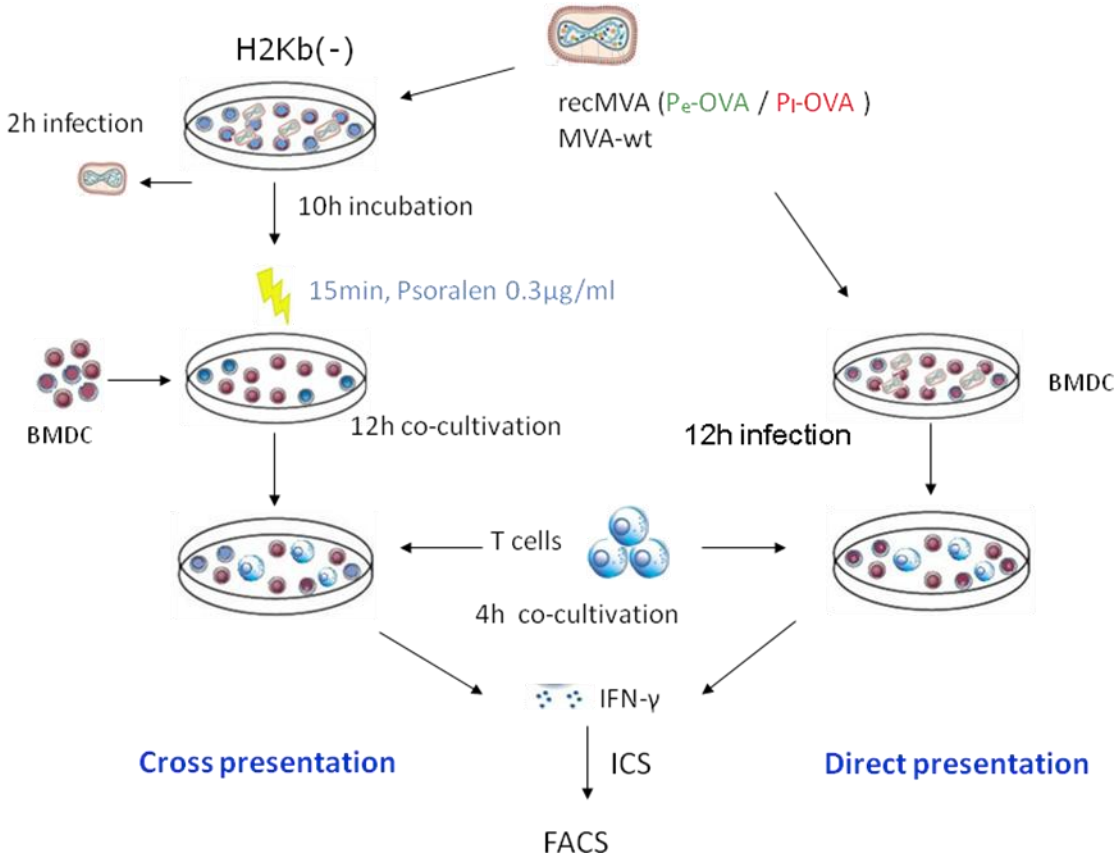

Figure 26: Protocols for direct and cross presentation assays. K^b negative Cloudman cells were infected with MVA at MOI 1 for 2h. After washing twice, they were incubated for additional 10h. Viruses were inactivated by PUVA using 0.3 µg/ml Psoralen for 15min. Cells were washed again before coculturing with BMDC at a ratio of 1:1 and incubated for another 12h. BMDC were also directly infected with MVA. Infected cells were co-cultured with antigen-specific CTL lines at a 2:1 ratio in the presence of 1µg/ml BFA for 4h, followed by ICS (IFN-γ) and FACS analysis.

4.3.2 Cross-presentation of early and late antigens

MVA-ova-PK1L or -P11 or wt infected Cloudman cells were used as an antigenic source. After 12h of infection, cells were PUVA inactivated as described earlier. C57BL/6 BMDC were used as presenter cells and co-incubated with infected Cloudman cells for additional 12h. Finally, H2-K^b restricted T cells (A19, ova, B8) were added for 4h in the presence of BFA. The IFN-γ production of CTL was analyzed by FACS after ICS.

The results show that late antigens (A19) were unable to activate TC as efficient via direct presentation as early antigens (B8, PK1L-ova), as was shown earlier for DC2.4 cells (see Fig.12C). However, late antigens were also not processed via cross-presentation, because late A19 and P11-ova did not activate CTL by this pathway. Early B8 could efficiently activate CTL by this route (Fig.27).

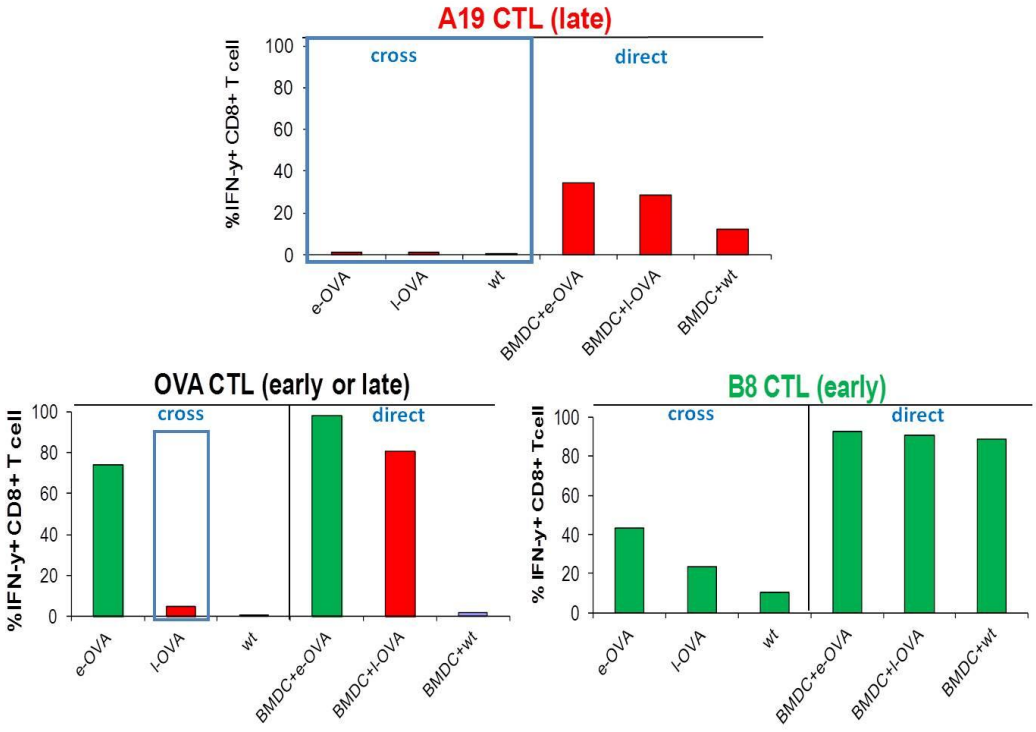

Figure 27: Cross-presentation of late antigens is impaired in the C57BL/6 model. MVA-ova-PK1L (e-OVA) or -P11 (l-OVA) or wt infected Cloudman cells were infected for 12h followed by PUVA inactivation. C57BL/6 BMDC were used as presenter cells and co-incubated with infected Cloudman cells for an additional 12h. Then CTL (A19, ova, B8) were added and cocultured for 4h in the presence of BFA. IFN-γ production of CTL was analyzed by FACS after ICS. The left part of the figure shows cross-presentation (cross), the right part shows direct-presentation (direct) within the same experiment.

Interstingly, another recombinant antigen NP, the nuclear protein from influenza virus, showed different activation capacities as compared to ova antigen (Fig.28). Late-NP antigen allowed for less CTL activation via direct-presentation than late-ova.

Cytoplasmic early-ova antigen could enter the cross-presentation pathway, but early-NP could not as it was located in the nucleus and hence may not easily to be endocytosed by BMDC. All late antigens did not enter the cross-presentation pathway. Yet, early-ova was activating CTL more efficiently by cross-presentation than early-NP-SIIN-eGFP, possibly because ova was secreted, while SIIN (part of the fusion protein) was targeted to the nucleus by nuclear targeting signal contained in the NP.

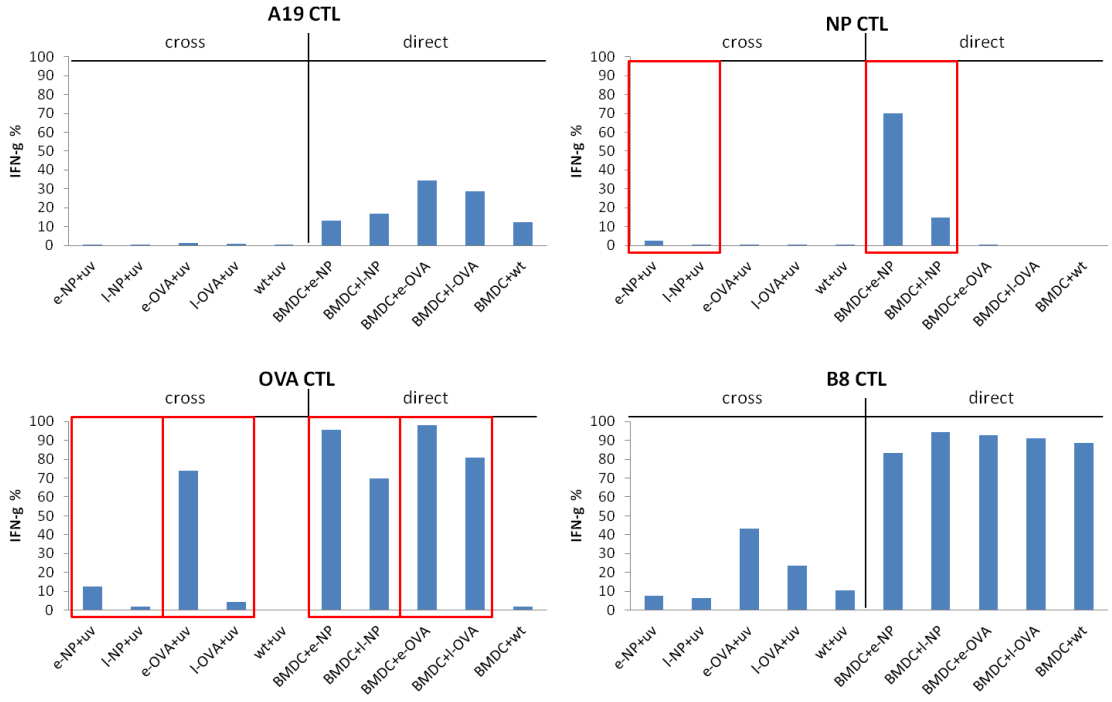

Figure 28: NP- and ova-specific TC show different activation by direct and cross-presentation of NP-SIIN-eGFP and ova antigens. Left part (cross) of each of the graphs shows results from cross-presentation for which Cloudman cells were infected with MVA-NP-SIIN-eGFP-PK1L (e-NP) or -P11 (l-NP) or MVA-ova-PK1L (e-OVA) or -P11 (l-ova) or wt for 12h. Thereafter, infected cells were UV-treated (+UV) and added to BMDC for additional 12h. Right part (direct) shows direct-presentation for which BMDC were infected with the indicated viruses for 12h. For both, cross- and direct-presentation, CTL were added and cocultured for 4h in the presence of BFA. IFN-γ production of CTL was analyzed by FACS after ICS.

Importantly, when other K^b negative cells (HeLa, A375, J774 or Balb/C BMDC) were used as feeder cells instead of Cloudman cells in this experimental setting, they showed similar impairment of late antigen's cross-presentation (data not shown).

Was this finding special for H2-K^b restricted antigen presentation? Or is it reproducible for other MHC I restrictions? Again, Cloudman cells were used as feeder cells infected with MVA-mH3L-eGFP-PK1L/P11 or wt for 12h. After PUVA inactivation, cells were co-incubated with HHD BMDC for additional 12h and then cocultivated with HHD-derived T cells (H3, B22, A6, I1-specific) for 4h. AraC or LPS were used to block late gene expression in infected APC.

The data show that late antigens (A6, I1, P11-H3) can activate TC by direct presentation as early antigens (B22, PK1L-H3), but with considerable delay at 12h p.i. However, late antigens did not enter the cross presentation pathway in contrast to early antigens (Fig.29). AraC and LPS could block A6 and late H3, but surprisingly not I1 presentation, which is also described as late antigen. Tyr-specific CTL worked as control.

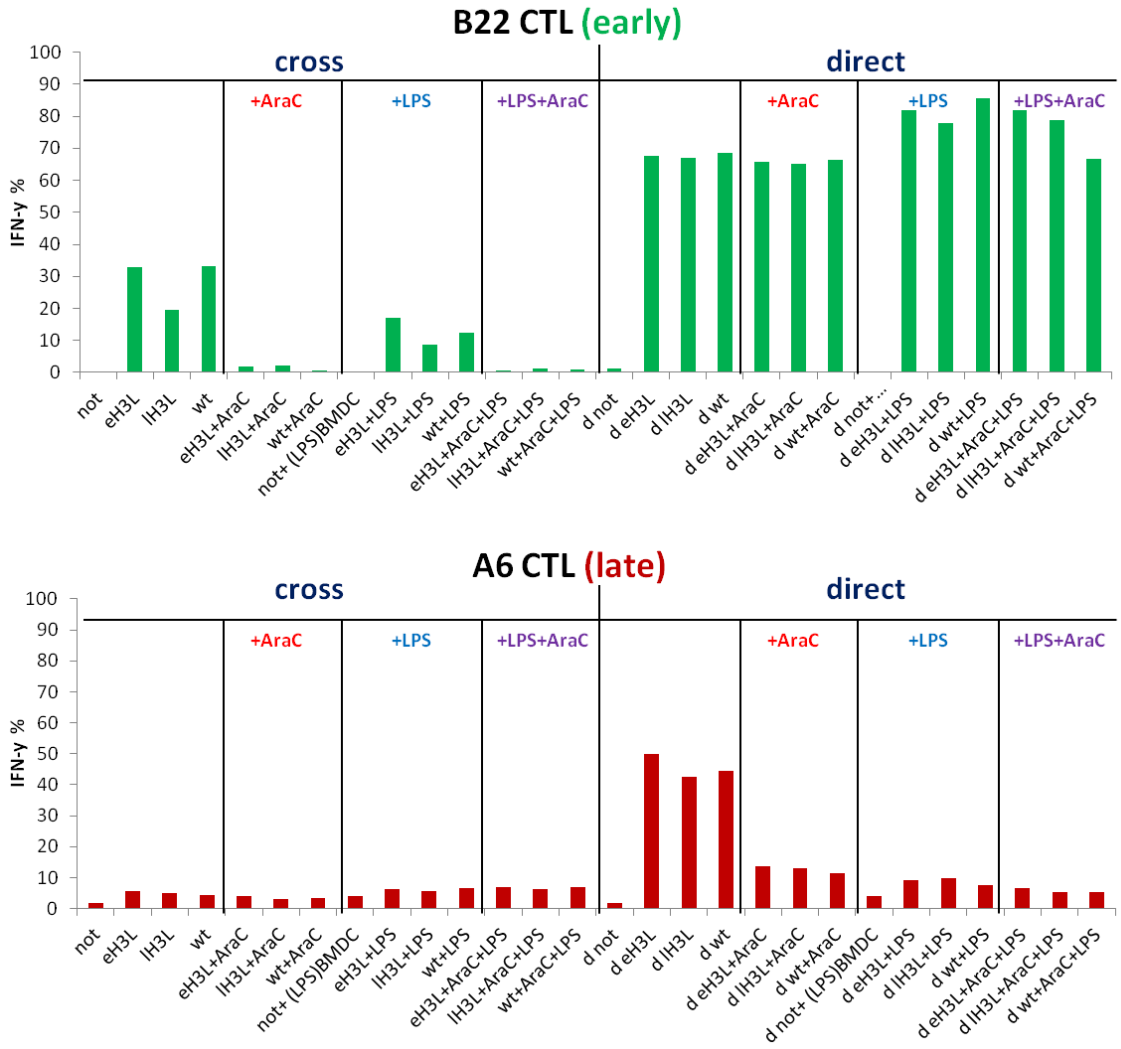
B22 CTL (early)
cross
direct
+AraC
+LPS
+LPS+AraC
+AraC
+LPS
+LPS+AraC
IFN-γ %
100
90
80
70
60
50
40
30
20
10
0
not
eH3L
IH3L
wt
eH3L+AraC
IH3L+AraC
wt+AraC
not+ (LPS)BMDC
eH3L+LPS
IH3L+LPS
wt+LPS
eH3L+AraC+LPS
IH3L+AraC+LPS
wt+AraC+LPS
d not
d eH3L
d IH3L
d wt
d eH3L+AraC
d IH3L+AraC
d wt+AraC
d not+ ...
d eH3L+LPS
d IH3L+LPS
d wt+LPS
d eH3L+AraC+LPS
d IH3L+AraC+LPS
d wt+AraC+LPS

A6 CTL (late)
cross
direct
+AraC
+LPS
+LPS+AraC
+AraC
+LPS
+LPS+AraC
IFN-γ %
100
90
80
70
60
50
40
30
20
10
0
not
eH3L
IH3L
wt
eH3L+AraC
IH3L+AraC
wt+AraC
not+ (LPS)BMDC
eH3L+LPS
IH3L+LPS
wt+LPS
eH3L+AraC+LPS
IH3L+AraC+LPS
wt+AraC+LPS
d not
d eH3L
d IH3L
d wt
d eH3L+AraC
d IH3L+AraC
d wt+AraC
d not+ (LPS)BMDC
d eH3L+LPS
d IH3L+LPS
d wt+LPS
d eH3L+AraC+LPS
d IH3L+AraC+LPS
d wt+AraC+LPS

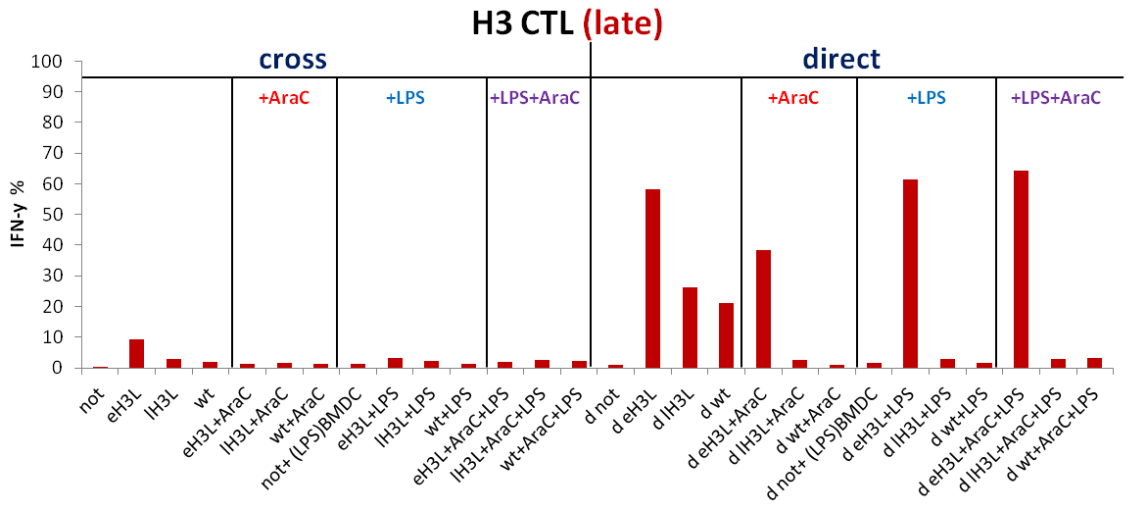
H3 CTL (late)
cross
direct
+AraC
+LPS
+LPS+AraC
IFN-γ %
not
eH3L
lH3L
wt
eH3L+AraC
lH3L+AraC
wt+AraC
not+ (LPS)BMDC
eH3L+LPS
lH3L+LPS
wt+LPS
eH3L+AraC+LPS
lH3L+AraC+LPS
wt+AraC+LPS
d not
d eH3L
d lH3L
d wt
d eH3L+AraC
d lH3L+AraC
d wt+AraC
d not+ (LPS)BMDC
d eH3L+LPS
d lH3L+LPS
d wt+LPS
d eH3L+AraC+LPS
d lH3L+AraC+LPS
d wt+AraC+LPS

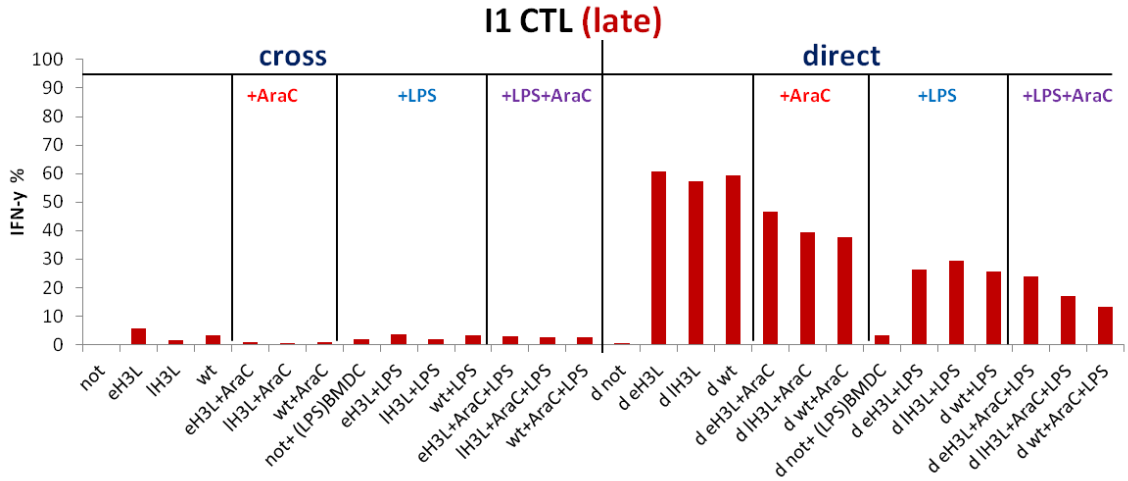
I1 CTL (late)
cross
direct
+AraC
+LPS
+LPS+AraC
IFN-γ %
not
eH3L
lH3L
wt
eH3L+AraC
lH3L+AraC
wt+AraC
not+ (LPS)BMDC
eH3L+LPS
lH3L+LPS
wt+LPS
eH3L+AraC+LPS
lH3L+AraC+LPS
wt+AraC+LPS
d not
d eH3L
d lH3L
d wt
d eH3L+AraC
d lH3L+AraC
d wt+AraC
d not+ (LPS)BMDC
d eH3L+LPS
d lH3L+LPS
d wt+LPS
d eH3L+AraC+LPS
d lH3L+AraC+LPS
d wt+AraC+LPS

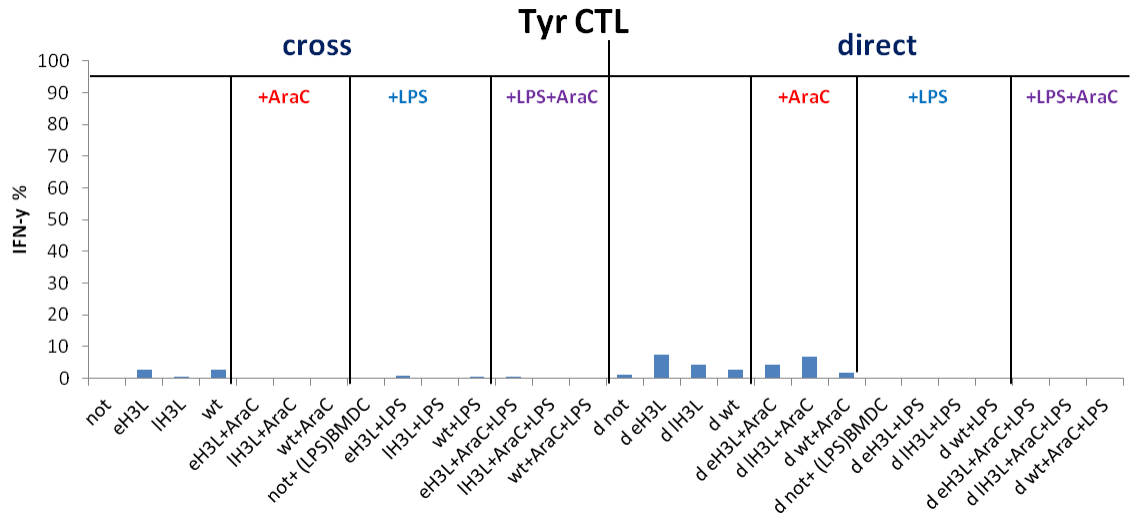
Tyr CTL
cross
direct
+AraC
+LPS
+LPS+AraC
IFN-γ %
not
eH3L
lH3L
wt
eH3L+AraC
lH3L+AraC
wt+AraC
not+ (LPS)BMDC
eH3L+LPS
lH3L+LPS
wt+LPS
eH3L+AraC+LPS
lH3L+AraC+LPS
wt+AraC+LPS
d not
d eH3L
d lH3L
d wt
d eH3L+AraC
d lH3L+AraC
d wt+AraC
d not+ (LPS)BMDC
d eH3L+LPS
d lH3L+LPS
d wt+LPS
d eH3L+AraC+LPS
d lH3L+AraC+LPS
d wt+AraC+LPS

Figure 29: Cross-presentation of late antigen is impaired (HHD). Cross-presentation (cross): Cloudman cells infected with MVA-mH3L/eGFP-PK1L (eH3L) or -P11 (lH3L) or wt for 12h or left uninfected (not). After PUVA inactivation, cells were co-incubated with HHD BMDC for an additional 12h. Direct-presentation (direct): BMDC were infected with the indicated viruses for 12h. For both, cross- and direct-presentation, HHD-derived T cells (H3, B22, A6, I1) were added and co-cultured for 4h. Pre-treatment of cells with AraC (40µg/ml) and/or LPS (5µg/ml) for 24h was performed to block late gene expression.

In order to confirm the data obtained for cross-presentation, it was attempted to inhibit cross presentation by using chemical compounds/inhibitors. According to the literature, immature BMDC have the ability to cross present antigens (Hotta *et al*, 2006). Thus, 5µg/ml LPS for 36 hours was used to mature BMDC before co-incubation in order to block their cross presentation ability due to a diminished abiltiy to phagocytose exogenous antigens after maturation.

The data show that LPS successfully blocked late gene expression for both, direct and cross-presentation (A19, P11-ova). This was because LPS matured BMDC could no longer uptake exogenous antigens on the one side and, on the other side, late gene expression was impaired in these cells (Fig.30).

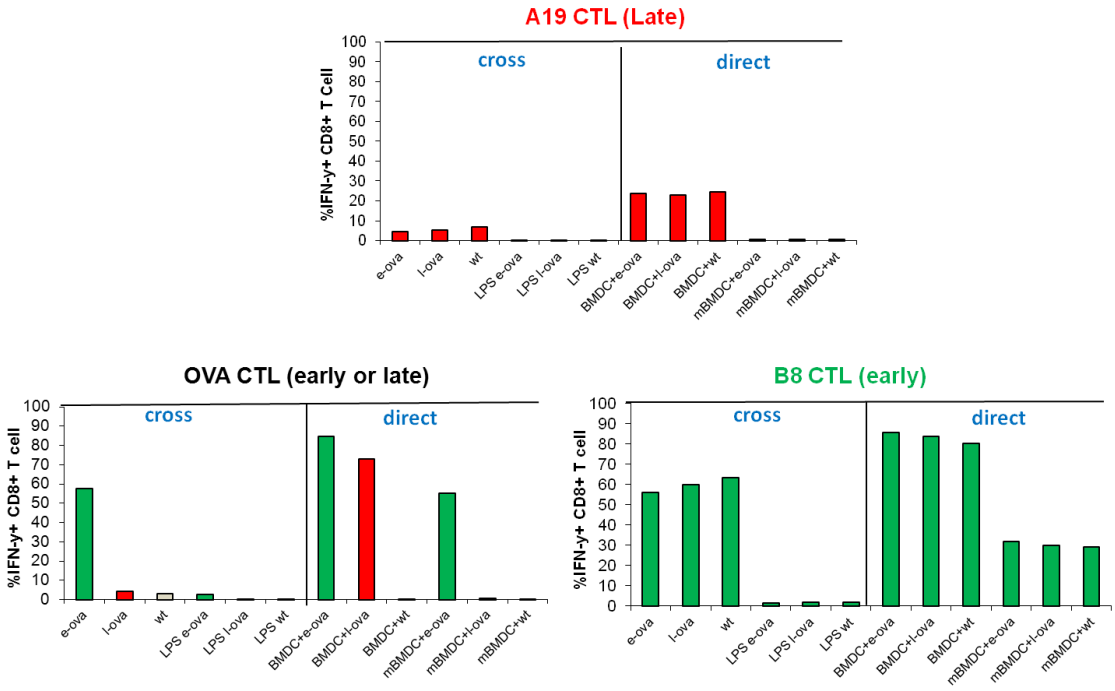

Figure 30: Cross presentation and late gene expression is inhibited by LPS (C57BL/6). Cross- or direct-presentation was performed as described above. Pretreatment of BMDC with 5µg/ml LPS for 36h was used (LPS or mBMDC).

Peptidoglycan (PGN) is a component existing in LPS preparations. It has been shown that DC matured with 2µg/ml PGN completely lost the ability for cross-presentation (Wagner *et al*., 2012). Further, PGN may shut down cross-presentation, while pure LPS enhance cross-presentation. Since LPS could not totally block cross-presentation in our assay system, the decision was made to use PGN instead. First, BMDC maturation was determined by screening surface markers in FACS analysis after incubation with or without PGN (2µg/ml) / pure LPS (1µg/ml) / LPS (5µg/ml) for 32h with the same setting as described in the paper by Wagner *et al*. PGN treated BMDC had

nearly the same maturation state as non-treated BMDC. Pure LPS or less pure LPS activated BMDC maturation (Fig.31).

Additionally, after similar treatment, BMDC were used for direct- and cross-presentation assays. Pure LPS showed the same inhibitory effect as LPS, but PGN could not block any presentation pathway as was to be expected according to the BMDC maturation state obtained with this compound. Another interesting point was that PGN treatment resulted in a slightly higher TC stimulation via direct-presentation of antigens (Fig.32).

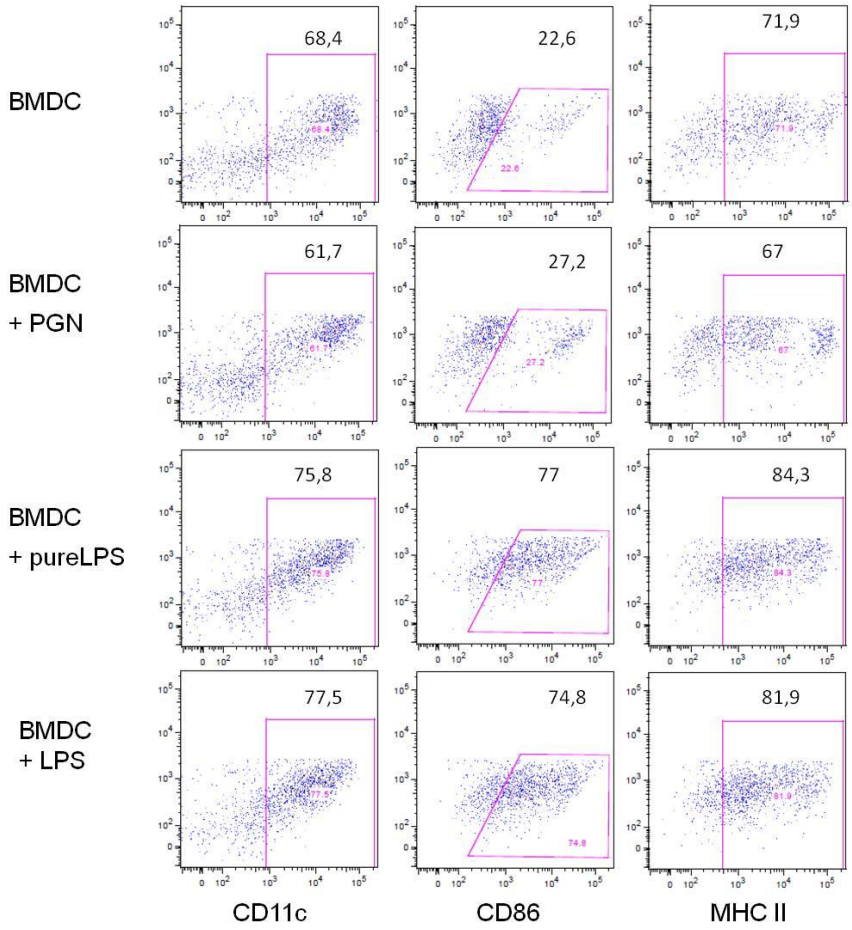

Figure 31: PGN treatment could not induce maturation of BMDC. BMDC were stained for PI, CD11c, CD86 and MHC II (living CD11c+DC are gated additional for CD86+ and MHCII+ cells) after treatment with PGN, pure LPS or LPS or no treatment (BMDC).

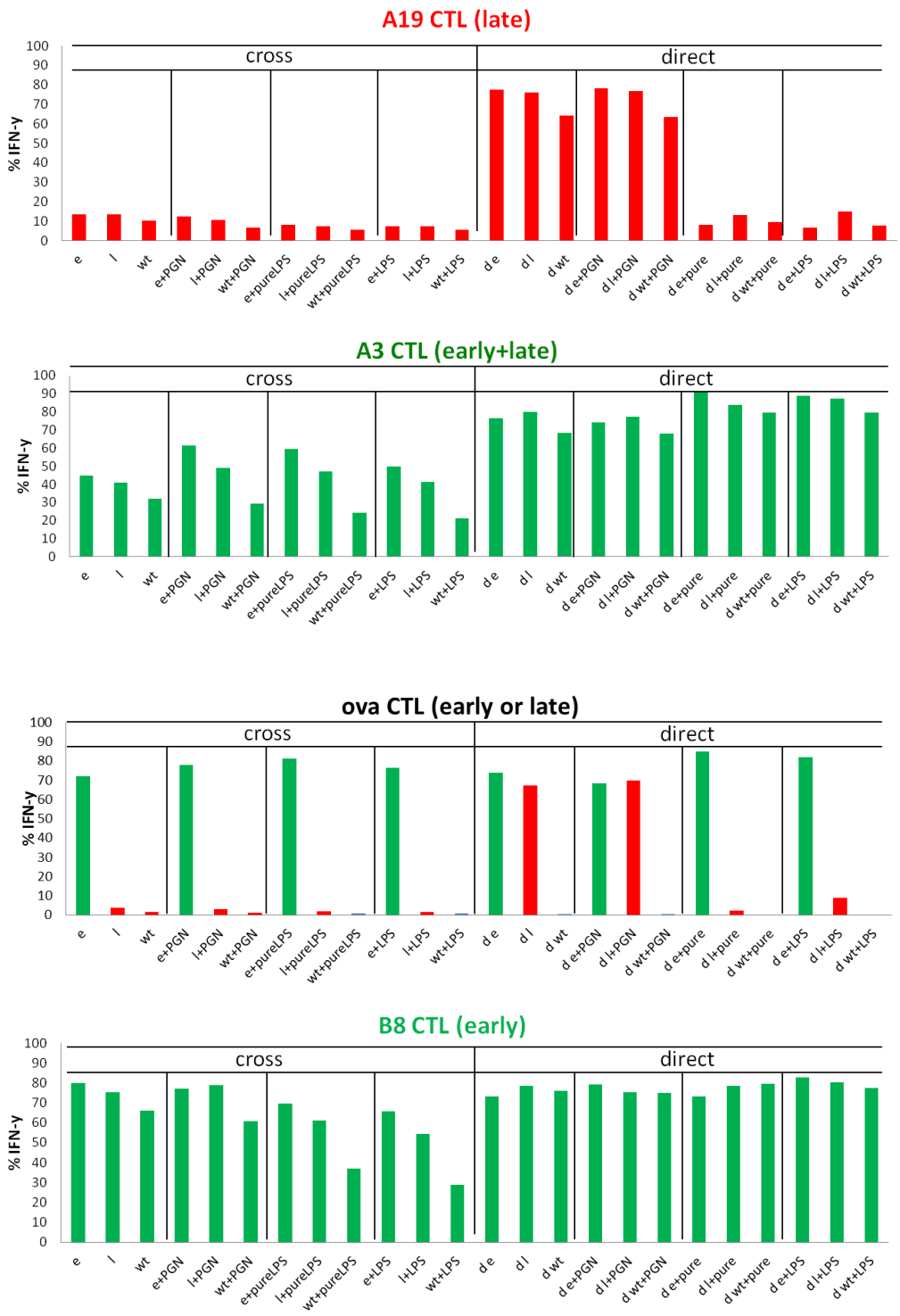

Figure 32: Cross-presentation and late gene expression was not inhibited by PGN. Cross- or direct-presentation assays were performed as described above. Cells were infected with MVA-ova-PK1L (e) or -P11 (l) or wt. Where indicated, BMDC were pretreated with PGN (2µg/ml), pure LPS (1µg/ml) or LPS (5µg/ml) for 32h.

Furthermore, AraC (40µg/ml) was used to inhibit late gene expression in both direct- and cross-presentation assays. Notably, it was found that AraC had a strong influence on cross-presentation. AraC can bind to DNA. Since MVA DNA replication is a prerequisite to initiate viral intermediate transcription and translation, AraC blocks intermediate and late gene expression. As expected, this was the case for direct presentation, but surprisingly, this compound blocked cross-presentation of all gene products including early proteins (Fig.33).

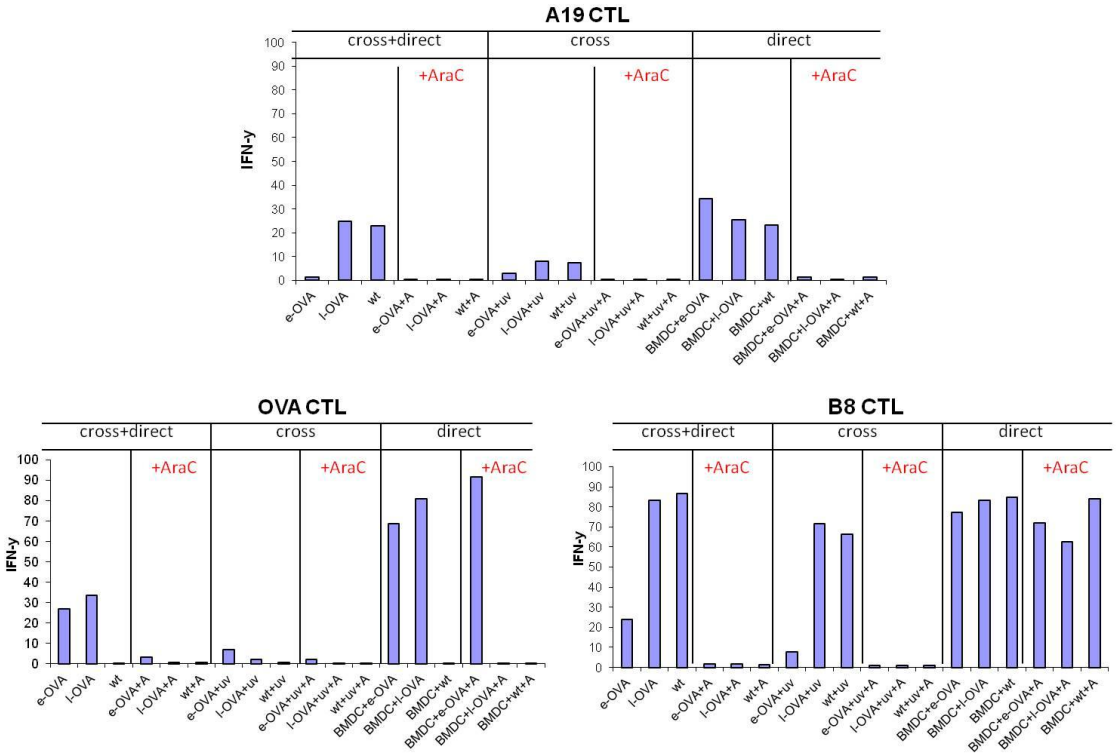

Figure 33: AraC inhibits cross-presentation of early and late gene products. Cross-presentation: Cloudman cells were infected with MVA-ova-PK1L (e-OVA) or -P11 (l-OVA) or wt for 12h with (+AraC) or without AraC (40µg/ml). Cells were then treated by PUVA (cross) or left untreated (cross+direct) and co-incubated with BMDC for an additional 12h. Direct-presentation (direct): BMDC were infected with the indicated viruses and treated with (+AraC) or without AraC for 12h. For both, cross- and direct-presentation, CTL were added and co-cultured for 4h. IFN-γ production of CD8+ TC was analyzed by FACS (ICS).

In order to exclude that AraC was toxic to the cells used (Cloudman or BMDC), cell viability was checked for apoptosis or necrosis by staining for Annexin V (AnnexinV-FITC Ab) or Propidium Iodide (PI), respectively. However, Cloudman cells or BMDC treated with or without AraC for different hours (3, 6, 9, 12 or 15h) did not show significantly increased signs of cell death (Fig.34).

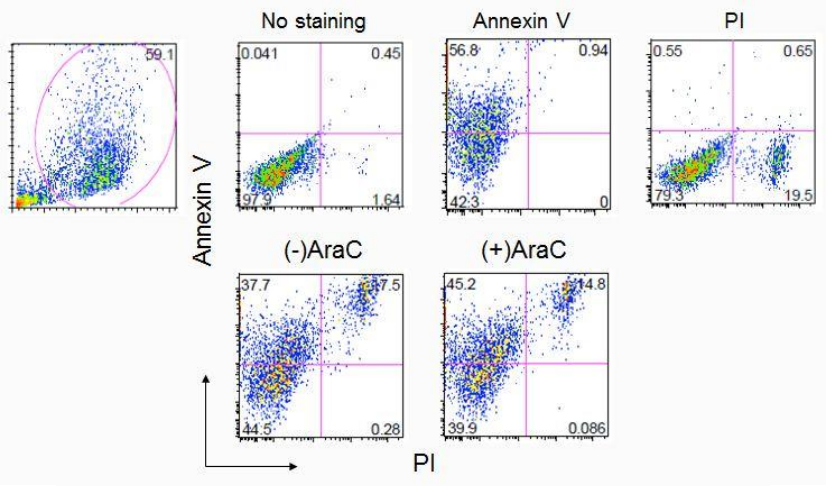

BMDC	AraC		(-)	
	Annexin V	AV+PI	Annexin V	AV+PI
3h	41,8	12,9		
6h	41,5	14,5		
9h	45,2	14,8	37,7	17,5
12h	40,6	19,6		
15h	41,8	23,4	38,4	19,2

Cloudman	AraC		(-)	
	Annexin V	AV+PI	Annexin V	AV+PI
3h	13,5	8,37		
6h	14,4	8,13		
9h	15,2	6,59	12,8	9,91
12h	24,2	5,32		
15h	23,7	9,22	20,6	6,17

Figure 34: AraC did not induce significant cell death. BMDC or Cloudman cells treated with or without AraC for 3, 6, 9, 12 or 15h and stained for Annexin V (apoptotic cells) and PI (necrotic cells). **Upper**: Gating strategy and controls for no staining, AnnexinV or PI only, with or without AraC treatment. **Lower:** Percentages of apoptotic and/or necrotic cells from total cells are shown.

The next question was whether AraC exerted the inhibitory effect on the feeder cell population (Cloudman) or the APC (BMDC). Therefore, AraC was added to either the two cell populations present in the cross-presentation setting. The result showed that, interestingly, AraC interfered excusively on the side of the infected cells (Cloudman) with cross-presentation of MVA early antigens (Fig.35). It may be anticipated that AraC inhibits activating stimuli for the phagocytosis or antigen processing/presentation capability of BMDC. Next, it was examined if AraC had a toxic effect on MVA infected Cloudman cells. Cloudman cells treated with or without AraC were infected with MVA-NP-SIIN-eGFP-PK1L or MVA-eGFP-PK1L for 8h. In general, AraC treated Cloudman cells appeared rounded and not healthy (Fig.36).

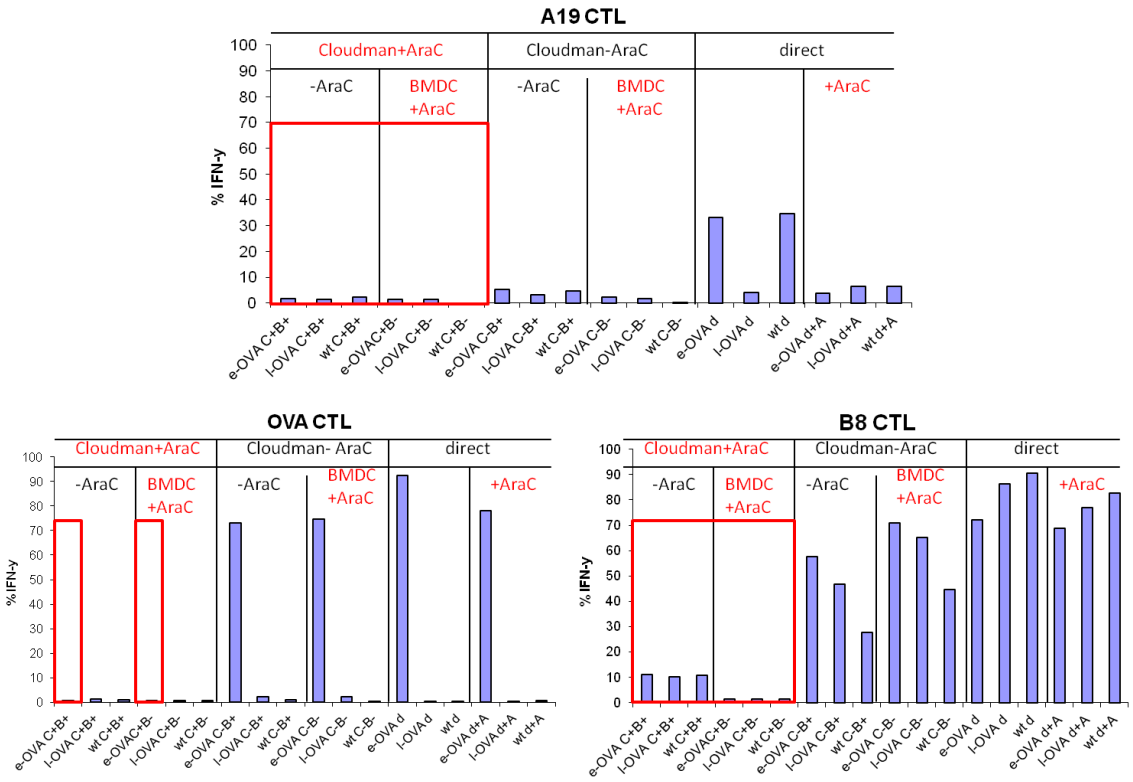

Figure 35: AraC affects feeder cells when inhibiting cross presentation of MVA early antigens. Cloudman cells were treated with (+AraC) or without AraC (40µg/ml) and infected with MVA-ova-PK1L (e-OVA) or -P11 (l-OVA) or wt for 12h and added to BMDC which were also treated with (+AraC) or without AraC. Directly infected BMDC were also treated with (+AraC) or without AraC. After 12h co-incubation with CTL. IFN-γ production of CD8+ TC was analyzed by FACS (ICS).

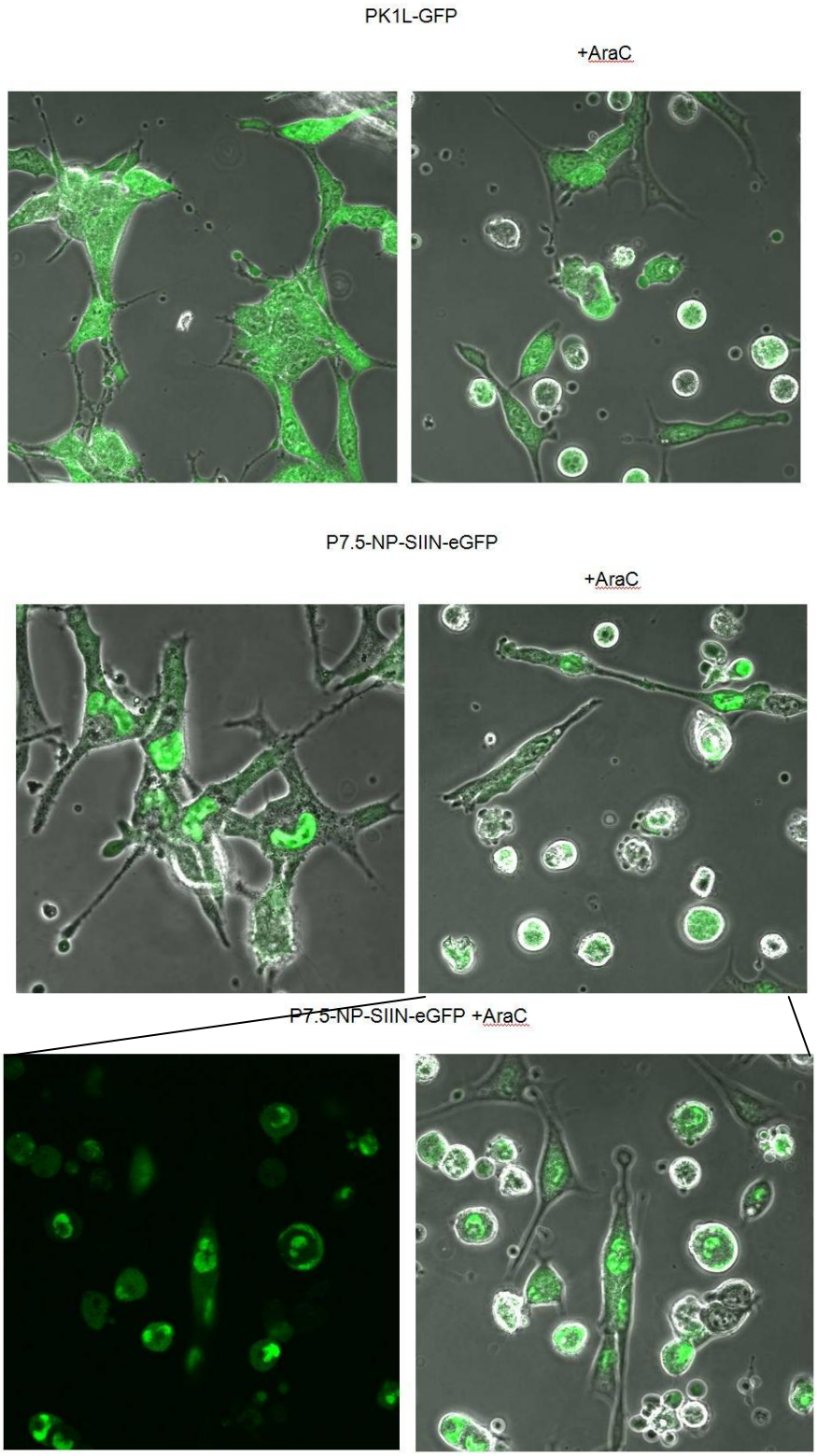

Figure 36: Morphology of MVA infected cells treated +/-AraC. Cloudman cells treated with or without AraC were infected with MVA-eGFP-PK1L or MVA-NP-SIIN-eGFP-PK1L for 8h. Infected cells are green.

4.4 Reasons for the impairment of both presentation pathways for late viral antigens

4.4.1 Antigen presentation machinery

4.4.1.1 Early or late K^b can be successfully presented

To achieve successful antigen presentation, the MHC class I antigen presentation machinery of the APC must be fully functional. Thus, H2-K^b negative J774 cells have been infected by recMVA, which express recombinant antigen (ova) early and late (P7.5 promoter). Simultanously eGFP fused to H2-K^b was produced by these viruses, but was separately controlled by PK1L or P11 promoters. Thus, the MHC I presentation route could be easily followed by monitoring for fluorescent GFP. Cells were stained using antibodies specific for MHC I containing compartments ER (anti-Calnexin) and Golgi (cis-Golgi), respectively, to visualize the localization of MHC I molecules (Fig.37).

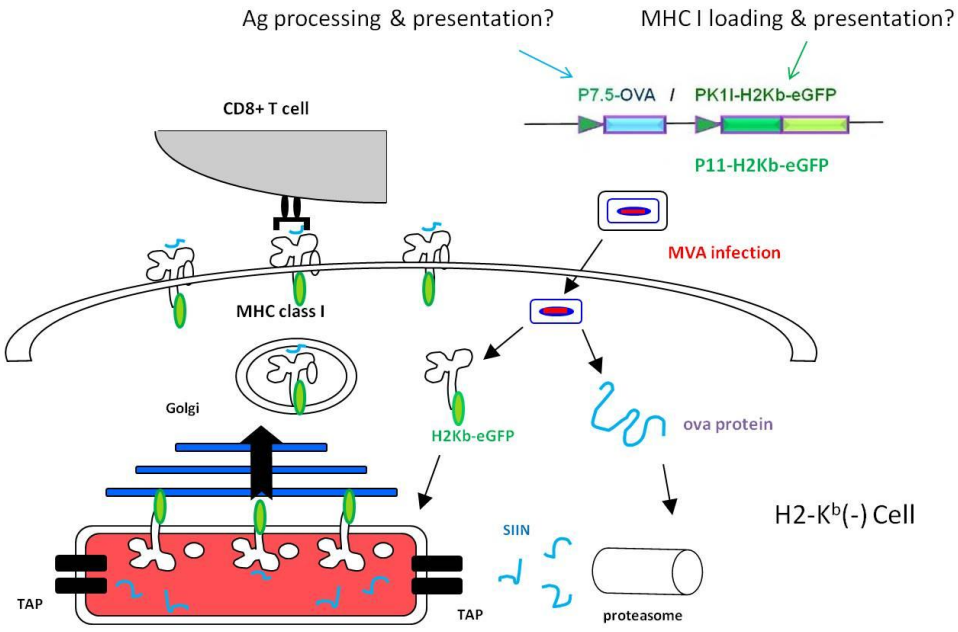

Figure 37: Strategy to test the MHC I antigen presentation machinery. H2-K^b negative cells were infected by recMVA, which express ova early or late and simultaneously H2-K^b (fused to eGFP) early or late. Cells were stained for ER (red) and Golgi (blue) to visualize the localization of MHC I molecules (green).

MVA-encoded eGFP-tagged H2-K^b is localized to the ER (red) and Golgi (blue) after 5h infection (Fig.38) and translocates to the cell surface after 12h of infection. This applies for both, early (Fig.39 upper) and late (Fig.39 lower) produced K^b molecules in infected APC (J774). Importantly, the MHC I complexes (H2-K^b/eGFP) at the cell surface are functional and enogenously loaded with the ova-derived SIINFEKL peptide (SIIN-K^b/GFP) as shown by confocal microscopy (Fig.40) and FACS (Fig.41). Other professional APC (BMDC from Balb/C mice) gave similar results (Fig.42). Therefore, we excluded a general impairment of the antigen presenting machinery.

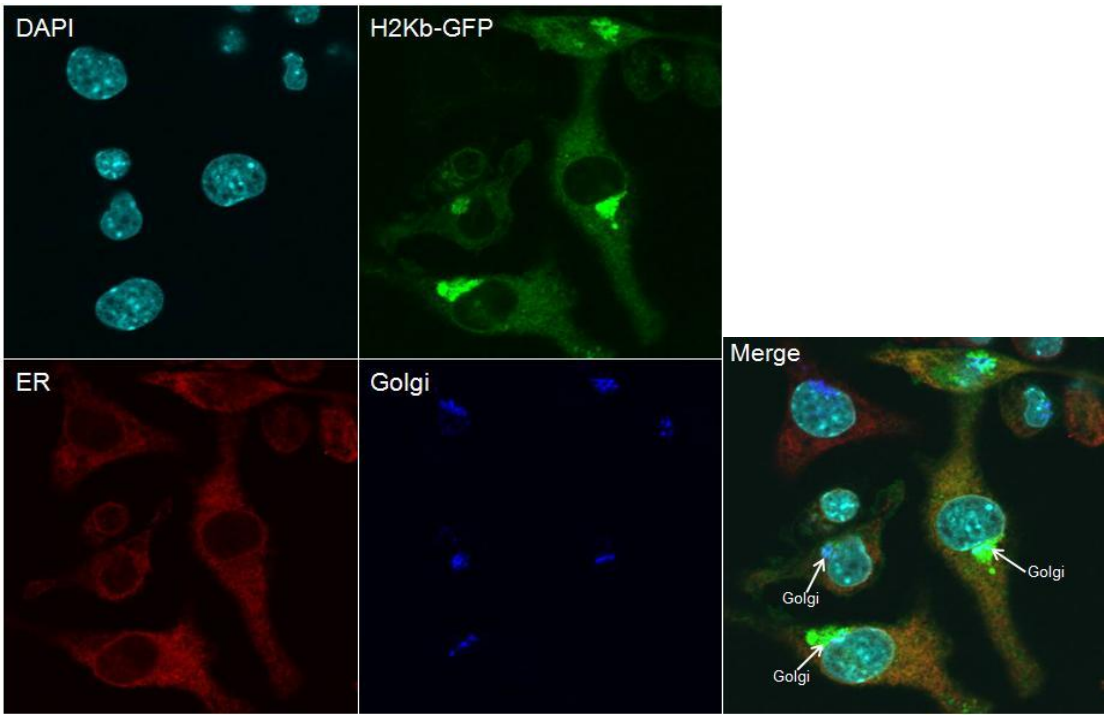

Figure 38: MVA encoded early expressed MHC I localized to ER and Golgi at 5h p.i. J774 cells were infected with MVA-ova-P7.5-H2K^b-eGFP-PK1L (green) and fixed with PFA. The nucleus was stained by DAPI (light blue) and ER (red) was stained by anti-Calnexin rabbit antibody, followed by anti-rabbit AF594 second antibody. Golgi (dark blue) was stained by anti GM130 mouse antibody, followed by anti-mouse AF647 second antibody. White arrows indicate the Golgi.

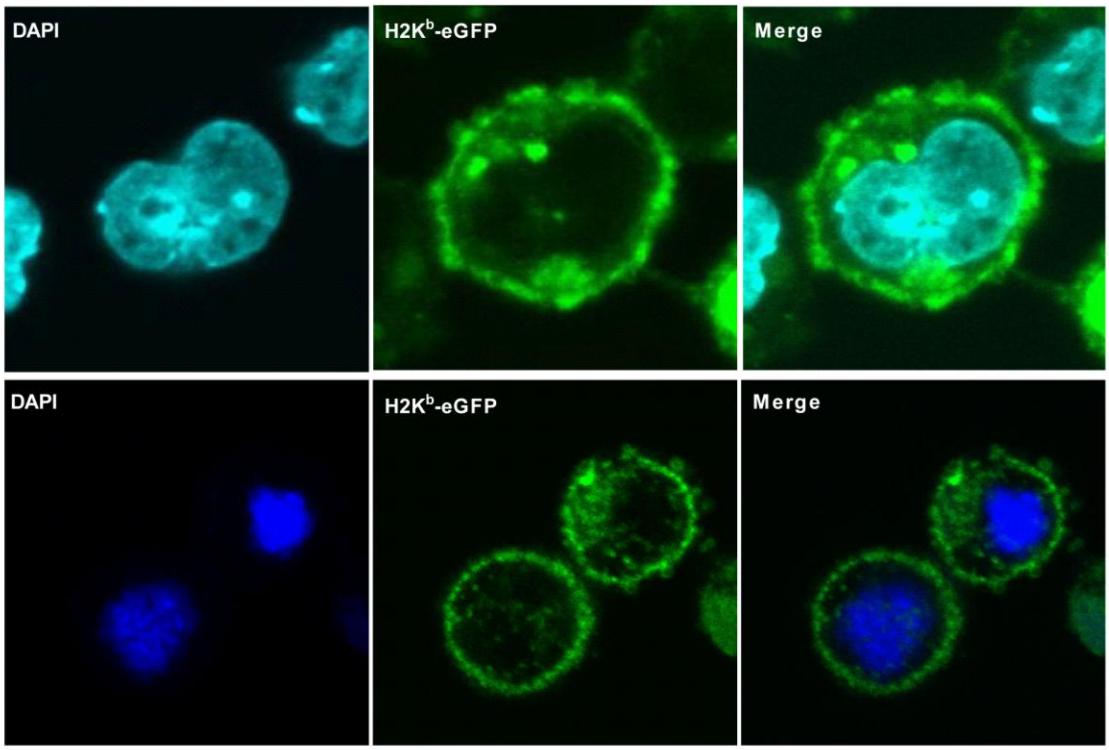

Figure 39: MVA encoded MHC I expressed early or late can translocate to the cell surface (12h p.i.). Upper: J774 cells infected with MVA-ova-P7.5-H2K^b-eGFP-PK1L (green). Lower: J774 cells infected with MVA-ova-P7.5-H2K^b-eGFP-P11 (green). Cells were fixed with PFA. DAPI stained cell nucleus (blue).

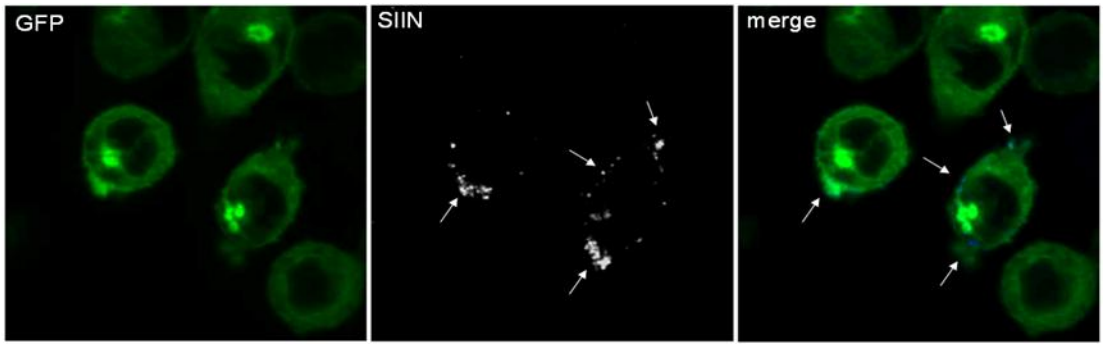

Figure 40: Peptide-loaded MHC I (SIIN-K^b complexes) translocate to the surface. J774 cells were infected with MVA-ova-P7.5-H2K^b-eGFP-PK1L for 6h and stained by SIIN-Kb Ab (1st Ab), followed by anti-mouse AF647 Ab (2nd Ab). The white arrows indicate SIIN-K^b complexes.

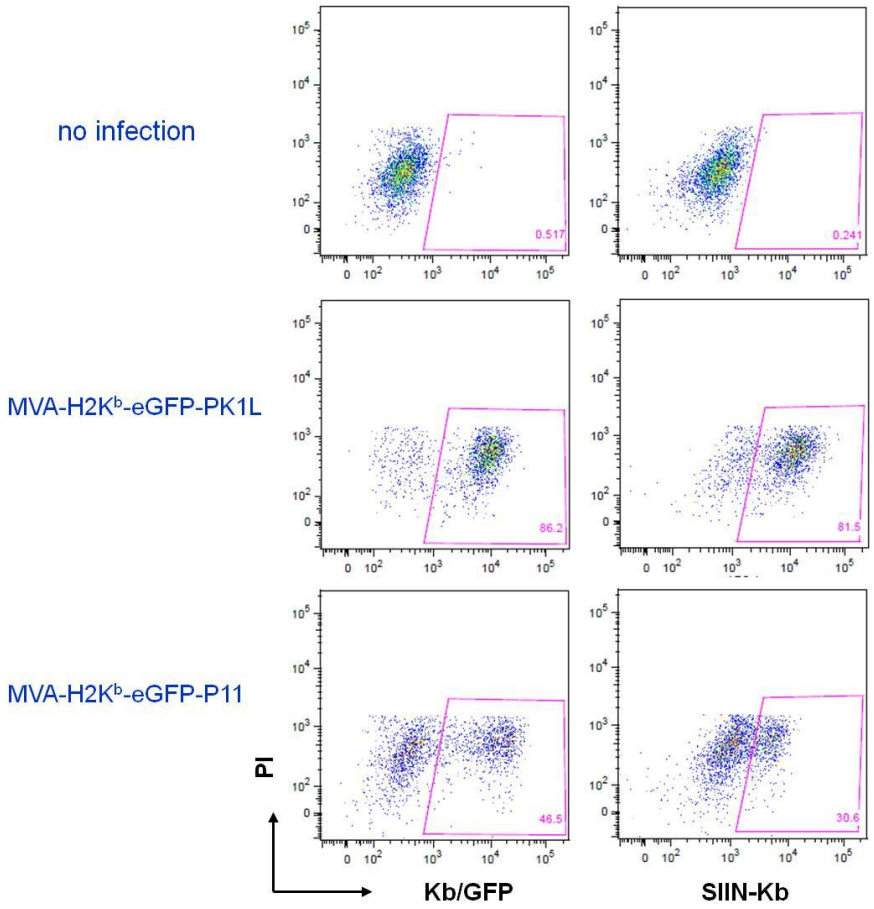

Figure 41: Efficient presentation of MHC I/peptide complexes (SIIN-K^b/GFP). J774 cells were infected with MVA-ova-P7.5-H2K^b-eGFP-PK1L (MVA-H2K^b-eGFP-PK1L) or -P11 (MVA-H2K^b-eGFP-P11) for 8h or left uninfected (no infection). Cells were stained with SIIN-K^b APC Ab. FACS analysis of infected cells (gated on living cells). GFP+ (infected) or SIIN-K^b+ cells (infected + Ag-presenting).

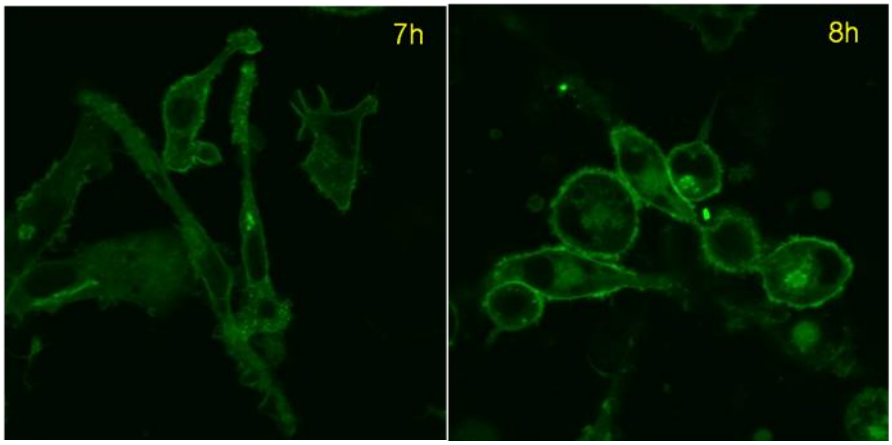

Figure 42: BMDC from Balb/C mice translocate GFP/MHC I to the cell surface. BMDC infected with MVA-ova-P7.5-H2K^b-eGFP-PK1L for 7h or 8h.

4.4.1.2 Early or late antigens for peptide/K^b presentation in infected cells

Antigens and MHC I are two important parts of MHC I/peptide complex formation. Early or late expressed K^b was translocated to the cell surface and presented peptides when the antigen was expressed continously (ova-P7.5). The next question was whether an antigen which expressed only early or late could still be presented on MVA produced K^b. Thus, we generated a set of four recMVA which simultaneously produce the recombinant antigen (ova) and the fluorescent protein-fused MHC I ($H2K^b$-eGFP), but expression was separately controlled by distinct promoters (early or late active). They were valuable tools to detect relevant antigen processing and presentation pathways in dependence on the availability of the antigen and the respective processing machinery at early and/or late time points of viral gene expression (PK1L- or P11-ova plus PK1L- or P11-$H2K^b$-eGFP).

MVA-ova-PK1L or -P11//$H2K^b$-eGFP-PK1L or -P11 were used to infect J774 (macrophage like) and Balb/C BMDC. GFP+ or K^b+ or SIIN-K^b+ cells were gated as shown in Fig.43.

GFP and K^b were expressed under control of the same promoter as a fusion gene. When expressed early (e-e or l-e), GFP was detectable quite early (2h p.i) while K^b needed some time to be visulalized (4h p.i). When expressed late (e-l or l-l), GFP was seen around 4h p.i. as was K^b. For SIIN/K^b detection, both, ova-derived peptide SIIN and K^b molecules were needed. Interestingly, with all four expression profiles obtained with the respective recMVA viruses, SIIN-K^b was found to be presented. Therefore, it may be

concluded that the antigen presentation machinery is in principle functional for early or late expressed antigens.

Which part will be more important for peptide/MHC I presentation, antigen or K^b? According to the data, SIIN-K^b complexes can be more efficiently generated and presented with late-ova (l-e). However, when K^b was brought in late (e-l), it showed a similar presentation efficacy irrespective from the expression time of ova (l-l). Therefore, the K^b molecule seems more important for MHC I-peptide (SIIN-K^b) complex formation. In contrast, in Balb/C BMDC antigen expression kinetics had a slightly more importance as compared to K^b molecules indicating a cell type dependent effect. C57BL/6 BMDC were used as K^b positive controls, because SIIN-K^b complex formation was independed from the virally mediated K^b expression and relied only on the antigen ova. (Fig.43)

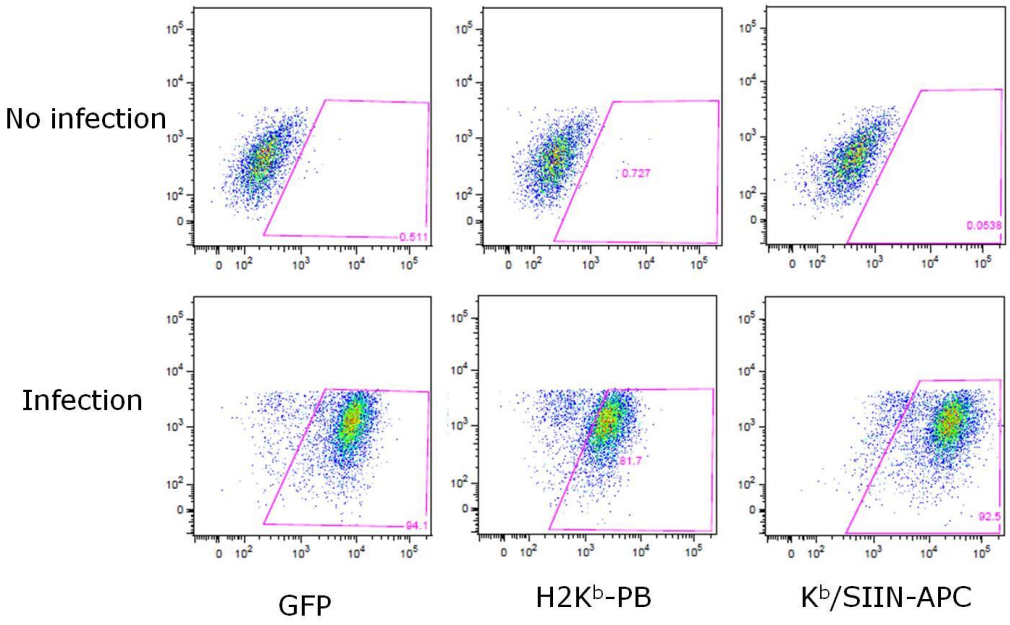


J774 GFP
% GFP+ cells
100
90
80
70
60
50
40
30
20
10
0
2h
4h
8h
12h


J774 SIIN
% SIIN+ cells
100
90
80
70
60
50
40
30
20
10
0
2h
4h
8h
12h
e-e
e-l
l-e
l-l

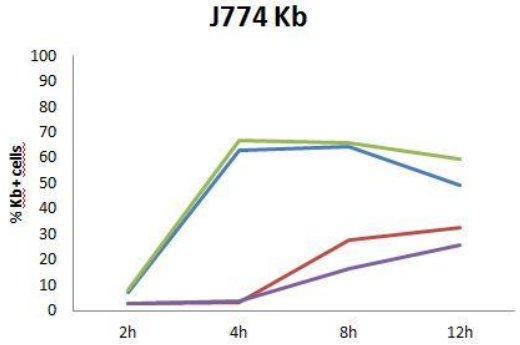
J774 Kb
% Kb+ cells
100
90
80
70
60
50
40
30
20
10
0
2h
4h
8h
12h

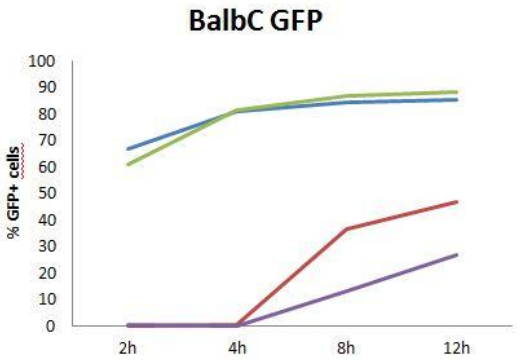
BalbC GFP
% GFP+ cells
100
90
80
70
60
50
40
30
20
10
0
2h
4h
8h
12h

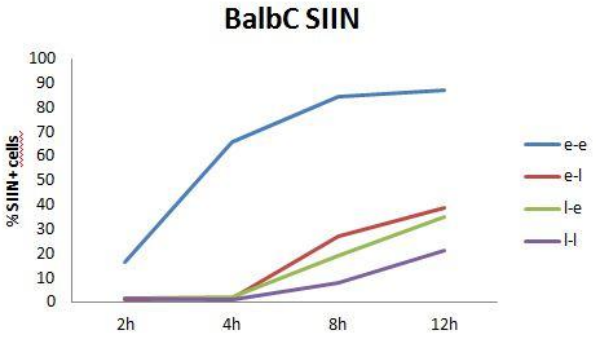
BalbC SIIN
% SIIN+ cells
100
90
80
70
60
50
40
30
20
10
0
2h
4h
8h
12h
e-e
e-l
l-e
l-l

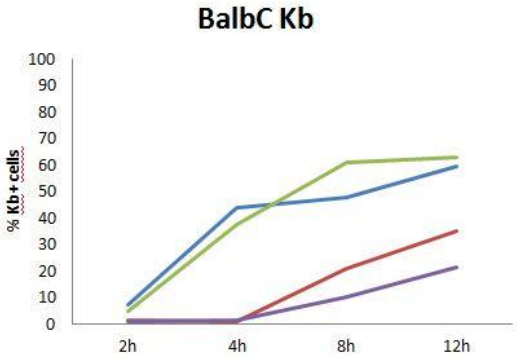
BalbC Kb
% Kb+ cells
100
90
80
70
60
50
40
30
20
10
0
2h
4h
8h
12h

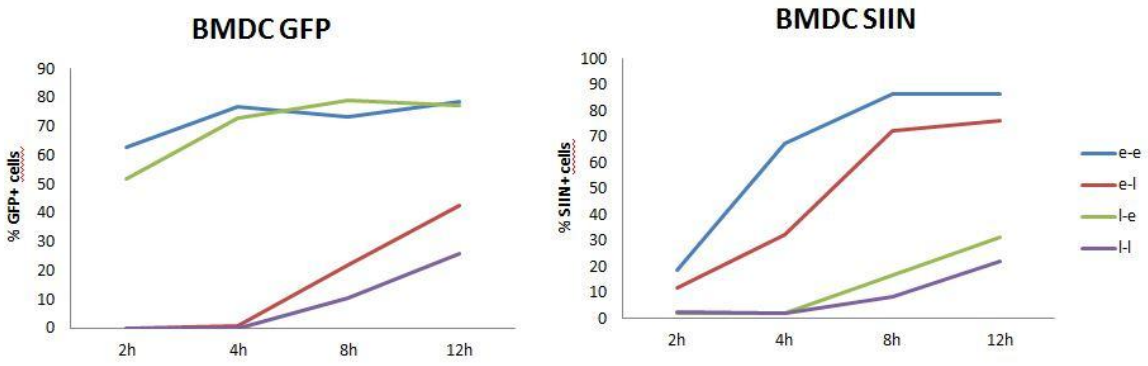

Figure 43: SIIN-K^b presentation kinetics obtained with recMVA. J774 cells (J774), Balb/C BMDC (BalbC) or C57BL/6 BMDC (BMDC) as target cells infected with either MVA-ova-PK1L or -P11// H2K^b-eGFP-PK1L or -P11 for 2, 4, 8 or 12h, and stained for H2K^b-PB and K^b/SIIN-APC Abs. Living cells (PI negative).

4.4.1.3 Viral antigen for peptide/K^b presentation

Antigen and K^b molecules were kinetically monitored at different expression times. However, could viral antigens still be presented by K^b, if K^b was expressed early or late? In this case, K^b negative cell line J774 was infected with either MVA-K^b-ova-P7.5 or MVA-ova-P7.5-H2K^b-eGFP-PK1L or -P11 or MVA-ova-P7.5 or wt. In these viruses, K^b was expressed early or late. Viral early (A3) or late (A19) antigen presentation was detected by specific CTL. At 4h, 6h or 8h's post infection, APC were co-incubated with respective CTL for 4h and IFN- γ production determined by ICS and FACS.

After 6h of infection, viral late antigens (A19) could be presented and activate CTL whenever K^b was expressed either early (MVA-K^b-ova-P7.5 , MVA-ova-P7.5-H2K^b-eGFP-PK1L) or late (MVA-ova-P7.5-H2K^b-eGFP-P11). Addionally, all early antigens had high CTL activation for viruses containing K^b early or late. There was no activation using MVA-ova-P7.5 (data not shown) or wt missing K^b expression (Fig.44). Balb/C BMDC showed comparable results (data not shown).

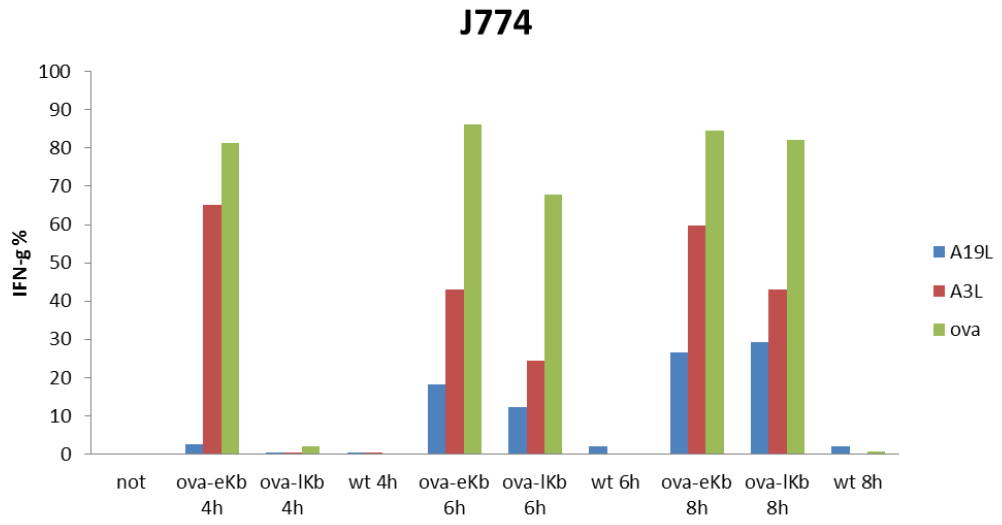

Figure 44: CTL activation by viral antigens in K^b negative cells. J774 were infected with MVA viruses expressing K^b early (eKb) or late (lK^b) and ova or MVA-wt for different periods of time or were uninfected (not). MOI=10.

4.4.1.4 K^b positive cells for peptide/K^b presentation

When K^b positive C57BL/6 BMDC were infected by MVA-wt or MVA-ova-P11, there was no CTL activation for viral A19 at 6h p.i, but there was SIIN presentation from late-ova (Fig.45). Thus, viral late antigens had a disadvantage to be presented by K^b positive cells, while foreign late antigen could be easily presented. However, when K^b was produced by the virus, viral late antigens were presented faster, too: A19-specific CTL activation at 6h p.i. (Fig.44). Here, vaccines which already contain MHC I molecules may have an advantage being able to present (viral) late antigens faster or at all.

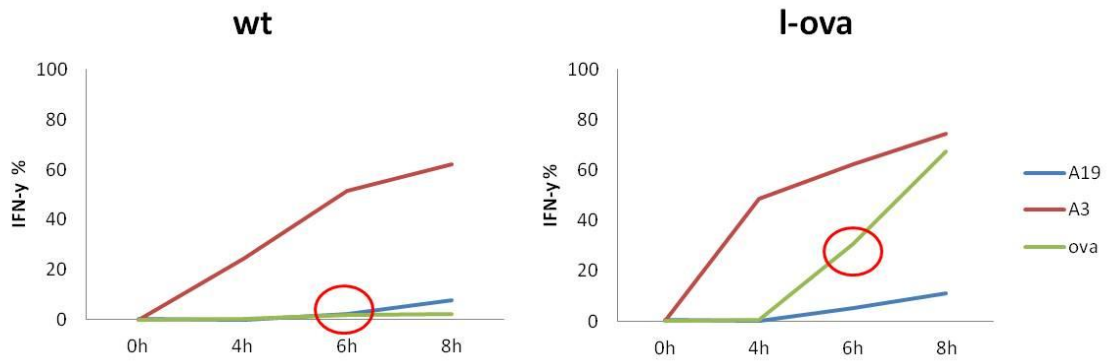

Figure 45: Viral late antigens (A19) were presented by K^b positive cells with a strong delay. C57BL/6 BMDC were infected with MVA-wt or MVA-ova-P11 (l-ova) for different periods of time and added to T cells. IFN- γ production of CD8+ TC was analyzed by FACS (ICS).

4.4.2 Different subcellular localization of early or late antigens

In order to study how the host cell processes and presents the different viral antigen subsets under early or late promoters, we first determined the localization of viral antigen H3 and foreign antigen GFP. H3 is an envelope protein and expressed late. To be able to study the different characteristics of the same antigen when expressed early or late, recMVA were made which encoded an additional copy of a mutant H3L gene expressed under early or late promoters. Since H3L posesses an early stop sequence which interupts transcription when expressed early, the gene was mutated for this sequence at position 327 (from ttt**t**ttt to ttt**c**ttt) to allow for undisturbed early gene expression. To track the protein location, H3 was fused with eGFP (MVA-eGFP/mH3L-PK1L or -P11).

4.4.2.1 H3

recMVA were used for kinetic infection experiments in HeLa cells and monitored for the intracellular localization of the protein by CLSM. When H3 was

expressed under control of the early promoter, the protein was localized to ER at 5h p.i. (Fig.46); while H3 synthesized late was located in the viral factories (virus DNA replication place, Katsafanas *et al*., 2007) at 5 to 7h p.i. (Fig.47). Recombinant late H3-GFP escaped from viral factories after 8h p.i. (Fig.48). Moreover, viral H3 encoded in the backbone of recMVA as well, should be integrated into the viral IMV membrane because of its membrane targeting signal. However, the H3-GFP fusion protein seemed too big to be packaged into the virion and, therefore, did not reach the cell surface. Late expressed H3-GFP was retained in the cell and did not make its way to the cell surface even after 15h p.i. (Fig.49).

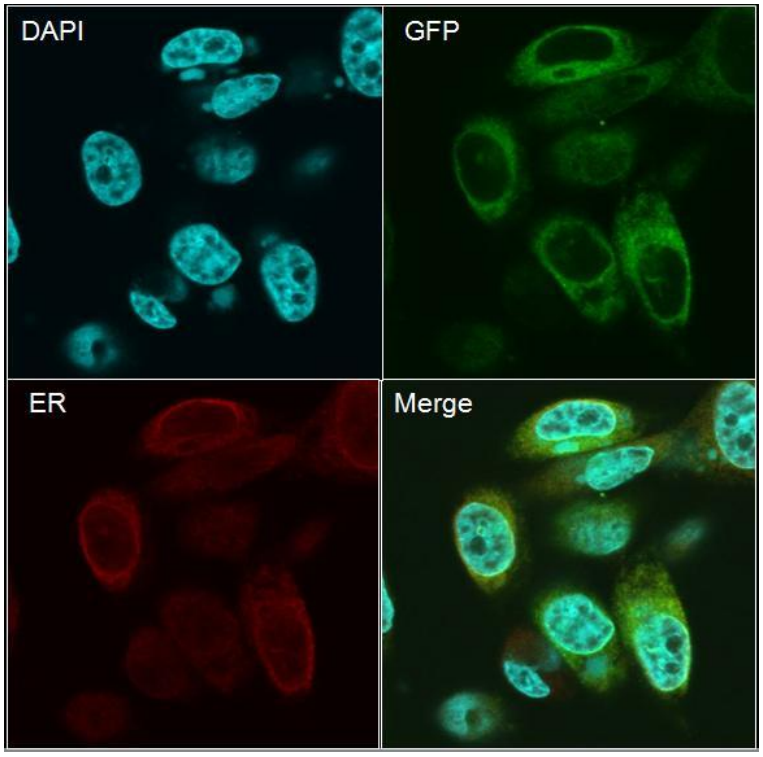

Figure 46: Early produced H3-GFP colocalized with ER at 5h p.i. HeLa cells infected with MVA-eGFP/mH3L-PK1L were fixed and stained with DAPI (nucleus; blue) and anti-ER Ab (red). GFP (green) indicates location of early-H3.

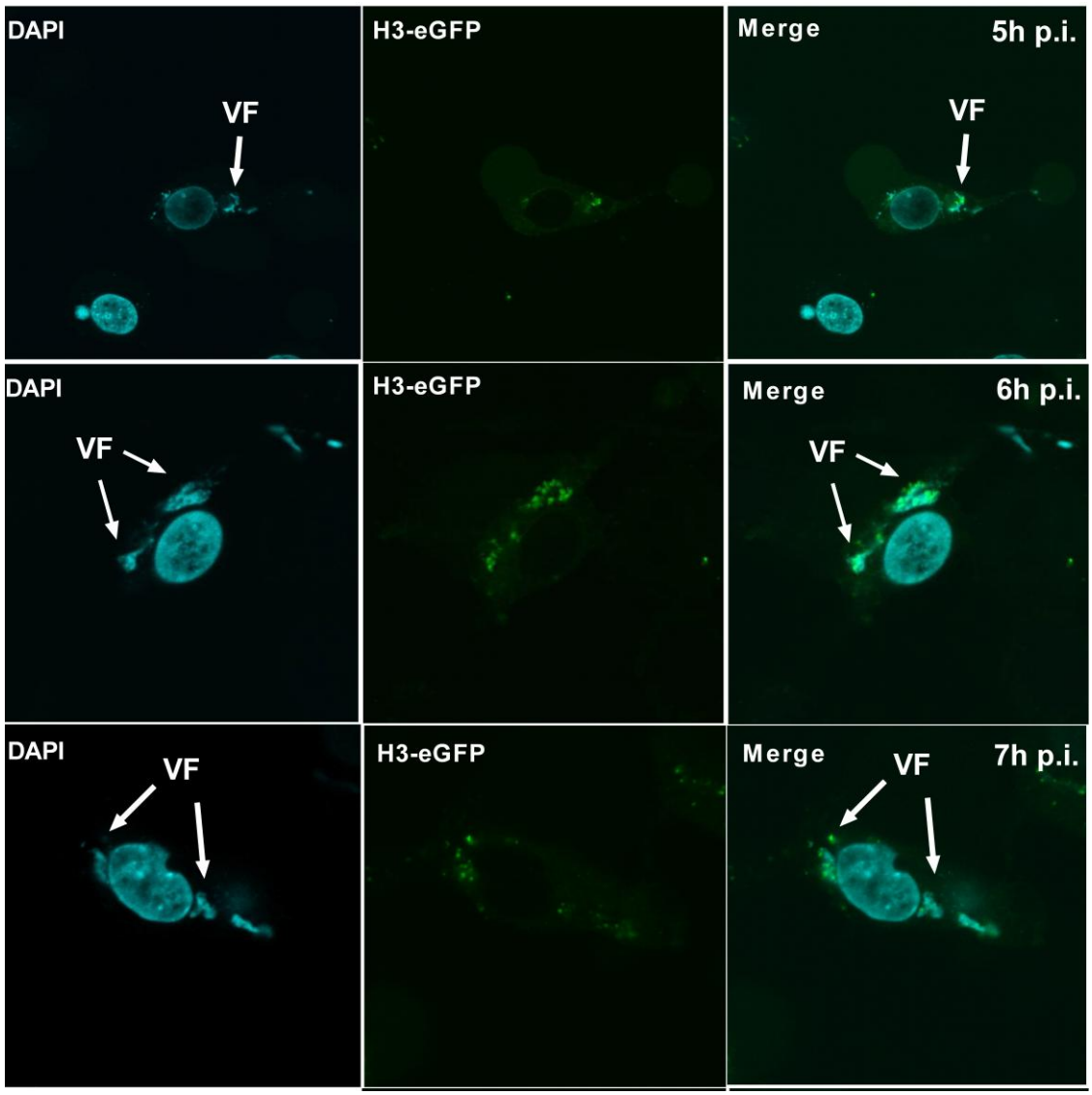

Figure 47: Late H3-GFP is produced and localized in viral factories (5-7h p.i). HeLa cells infected with MVA-eGFP/mH3L-P11 were fixed and stained with DAPI (blue). DAPI indicates nucleus and viral factories. GFP (green) shows late-H3 location. White arrows point to viral factories.

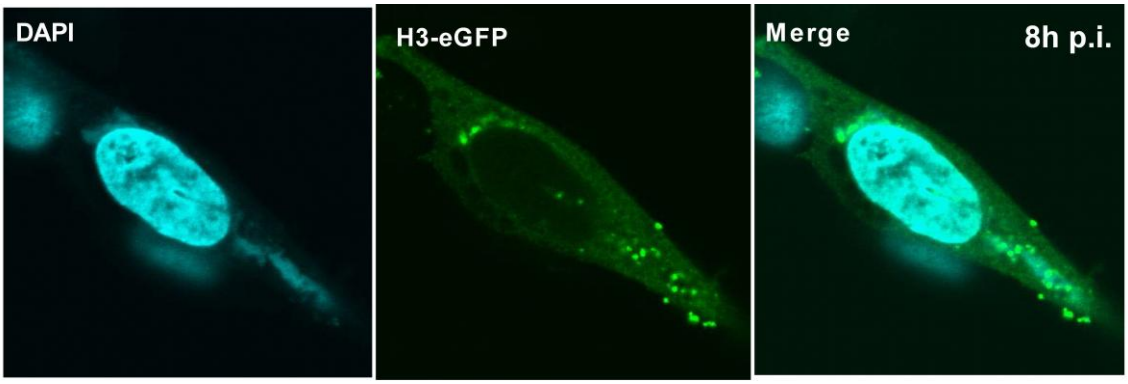

Figure 48: Late H3-GFP escapes from viral factories after 8h p.i. HeLa cells were infected by MVA-eGFP/mH3L-P11. GFP (green) indicates late-H3 location.

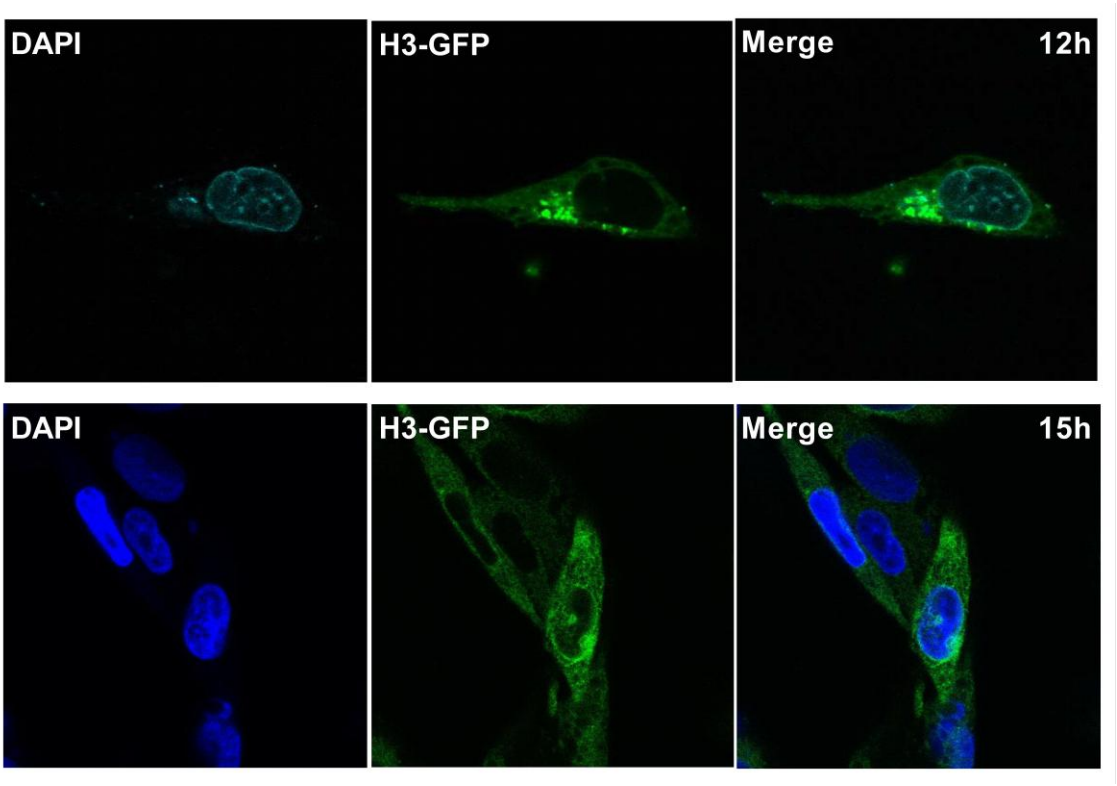

Figure 49: H3-GFP is retained within the cell. Upper: HeLa cells infected with MVA-eGFP/mH3L-P11 for 12h. **Lower:** HeLa cells infected with MVA-eGFP/mH3L-P11 for 15h. GFP (green) indicates late-H3 location. DAPI (blue) stained nucleus.

4.4.2.2 GFP

In contrast to viral protein H3, foreign protein GFP distributed all over the cell when expressed under the early promoter (Fig.50). In addition, it was first localized in viral factories when expressed under control of the late promoter at 6h p.i. (Fig.51), but could quickly leave this compartment and distribute into the cytoplasm of the cell (Fig.52). Thus, the foreign cytoplasmatic antigen GFP had distinct characteristics as compared to the viral antigen H3.

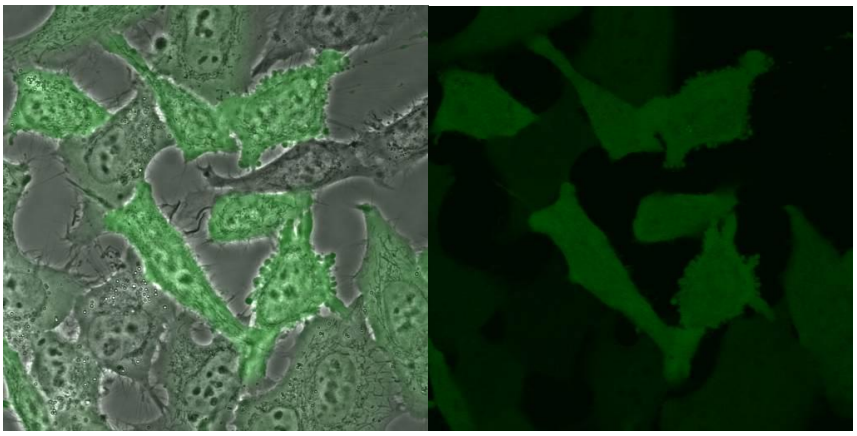

Figure 50: Early GFP expression at 6h p.i. HeLa cells infected with MVA-GFP-PK1L.

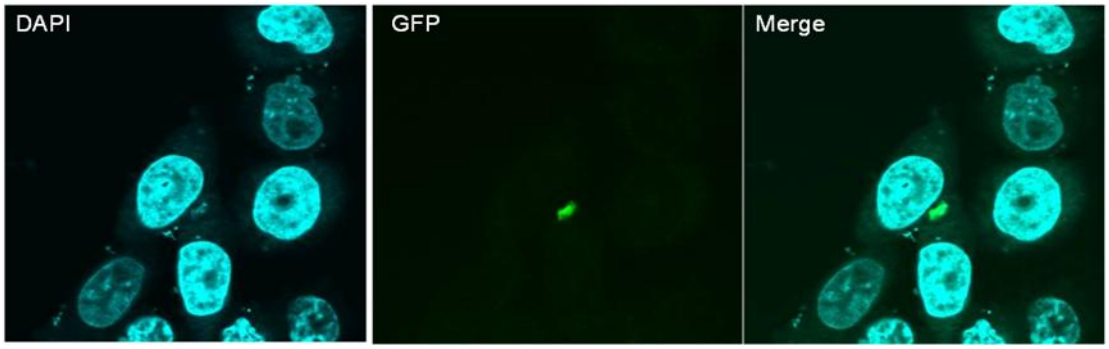

Figure 51: Late-GFP localized in the viral factories at 6h p.i. HeLa cells infected with MVA-GFP-P11. DAPI (blue) stained nuclei and viral factories.

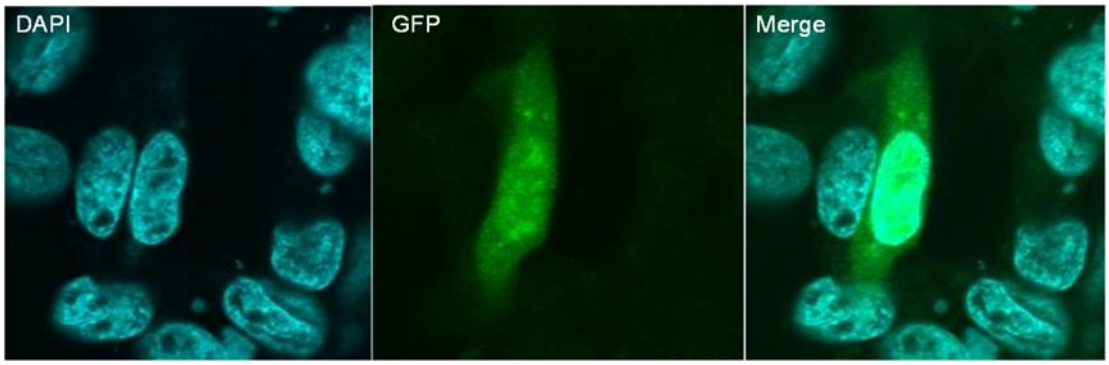

Figure 52: Late-GFP present outside of viral factories at 7h p.i. HeLa cells infected with MVA-GFP-P11. DAPI (blue) stained nuclei and viral factories.

4.4.2.3 Other antigens

To determine if a different quality of the antigen might additionally result in localisation to distinct processing and presentation pathways, MVA-ova-mcherry-PK1L

or -P11// H2K^b-eGFP-PK1L or -P11 viruses were generated and used to visualize ova- (cytoplasmic antigen) and H2K^b–specific (ER-targeted antigen) localization (Fig.53).

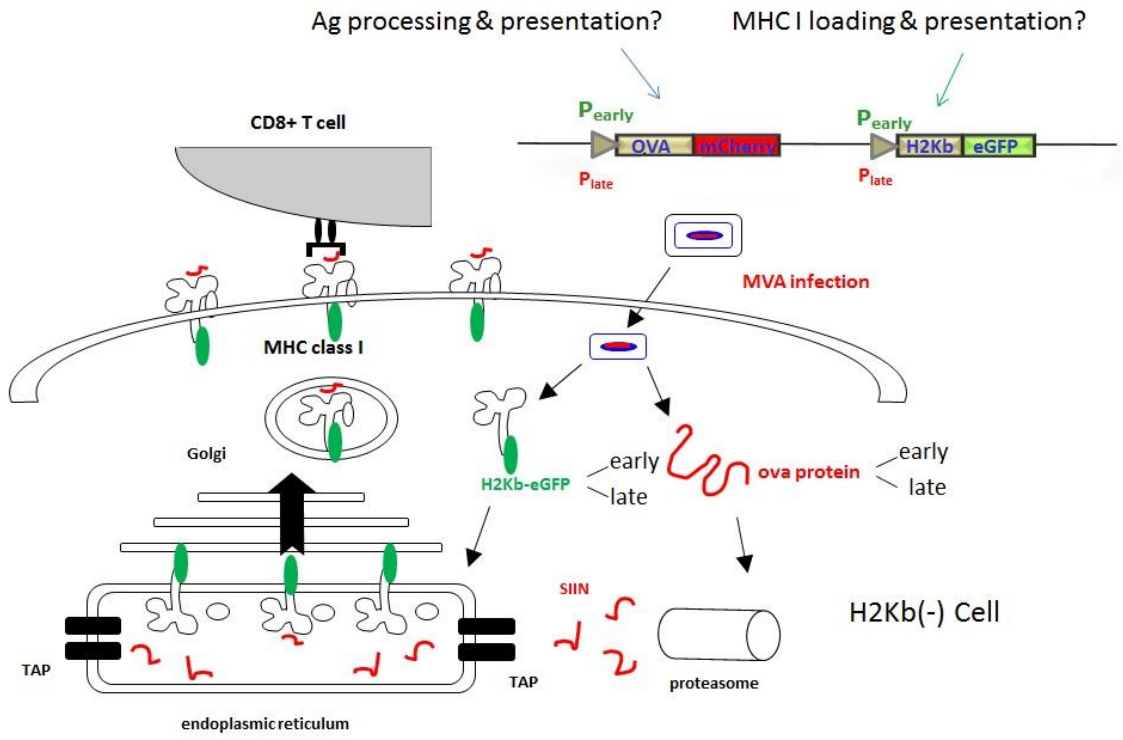

Figure 53: Schematic of MVA-ova-mcherry-PK1L or -P11 // H2K^b-eGFP-PK1L or -P11 and strategy to demonstrate processing/presentation pathways. recMVA simultaneously expressed recombinant fluorescent fusion genes as i) antigen to be processed (ova-mcherry) and ii) presenting MHC I (H2K^b-eGFP). Fusion gene expression was separately controlled by distinct promoters active early (P_{early}) or late (P_{late}). After infection of K^b negative cells, K^b and SIIN-K^b complexes may be presented at the cell surface. K^b and ova localization may be monitored due to their different fluorescent labelling.

K^b negative HeLa cells were infected MVA constructs. When ova and K^b were produced early, they were both present in the cytoplasm (Fig.54). When these proteins were produced late, they were present outside of viral factories (vf) at earlier time points as compared to H3, presumably because they represent non viral proteins. H2-K^b as an ER-targeted molecules had left viral factories very fast (around 5.5h p.i.) and were exclusively visible in vf for only 30 min (Fig.55). Ova behaved similar to GFP. It stayed in

the viral factory for 1h and then translocated to the cytoplasm (Fig.56). When ova and K^b were produced late, K^b could be observed out of vf at 6h p.i., while ova was still localized in vf at 6h p.i. and left vf at 7h p.i. (Fig.57). In Balb/C BMDC comparable results were obtained as in HeLa cells (Fig.58).

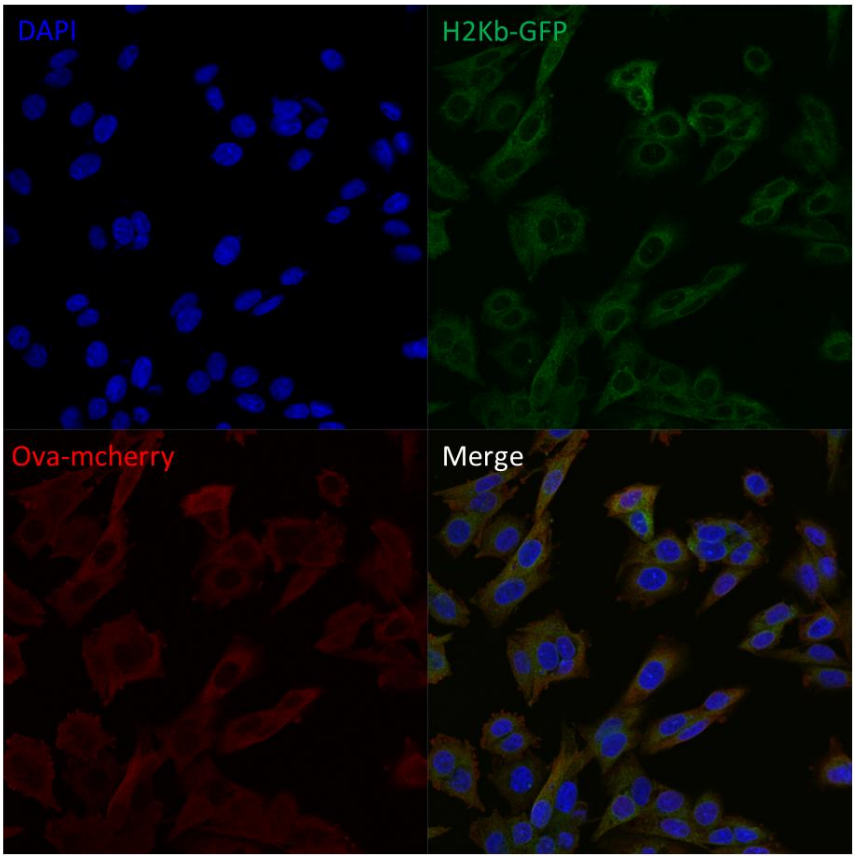

Figure 54: Localization of antigen and MHC I in HeLa cells infected with MVA-PK1L-ova-mCherry-PK1L-H2K^b-eGFP for 5h. DAPI (blue) stained nucleus and vf. ova location (red). GFP (green) indicates H2-K^b location.

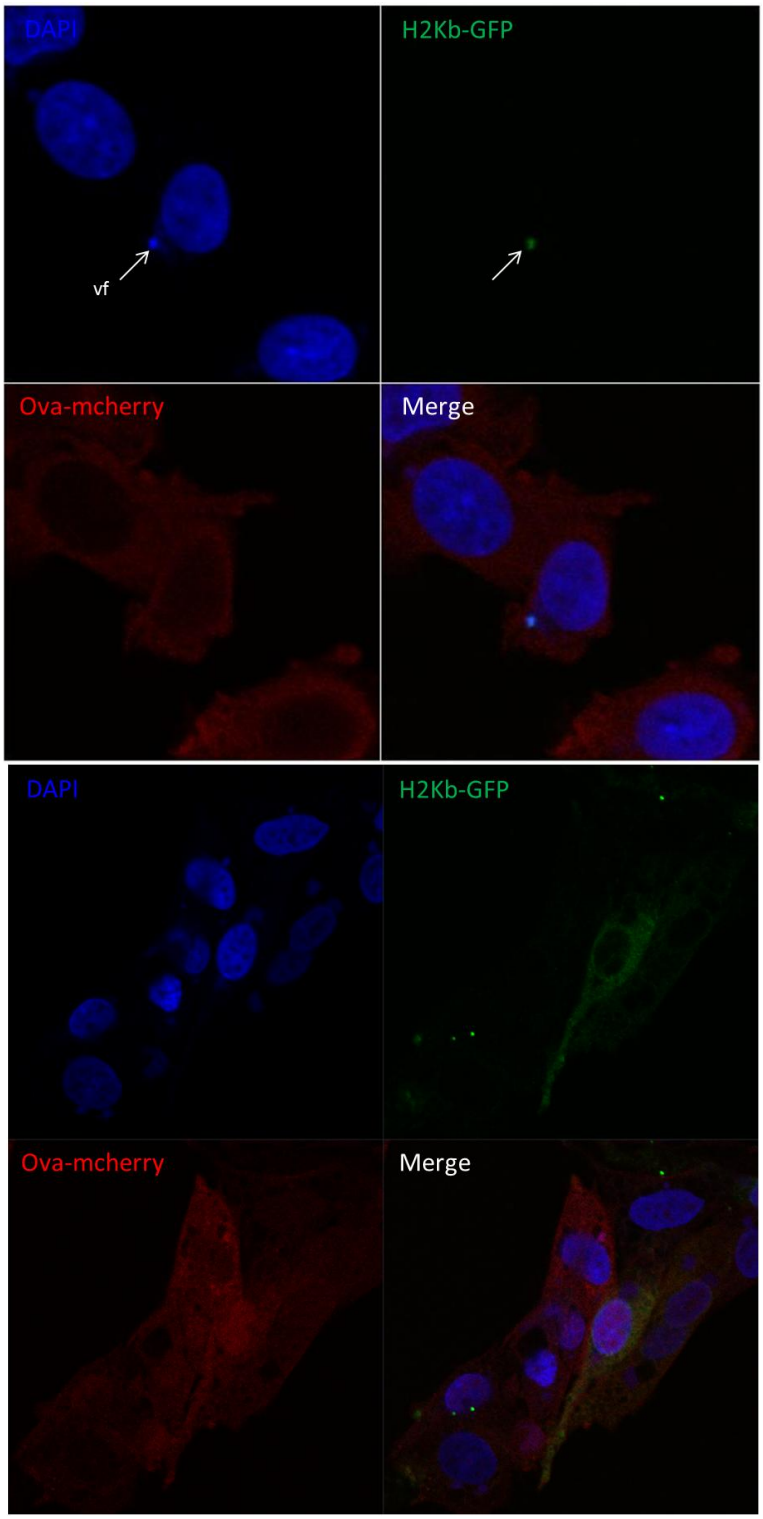

Figure 55: Localization of antigen and MHC I in HeLa cells infected with MVA-PK1L-ova-mCherry-P11-H2K^b-eGFP. Upper: at 5h p.i. Lower: at 5.5h p.i. DAPI (blue) stained nucleus and vf. ova location (red). GFP (green) indicates H2-K^b location. White arrow points to vf.

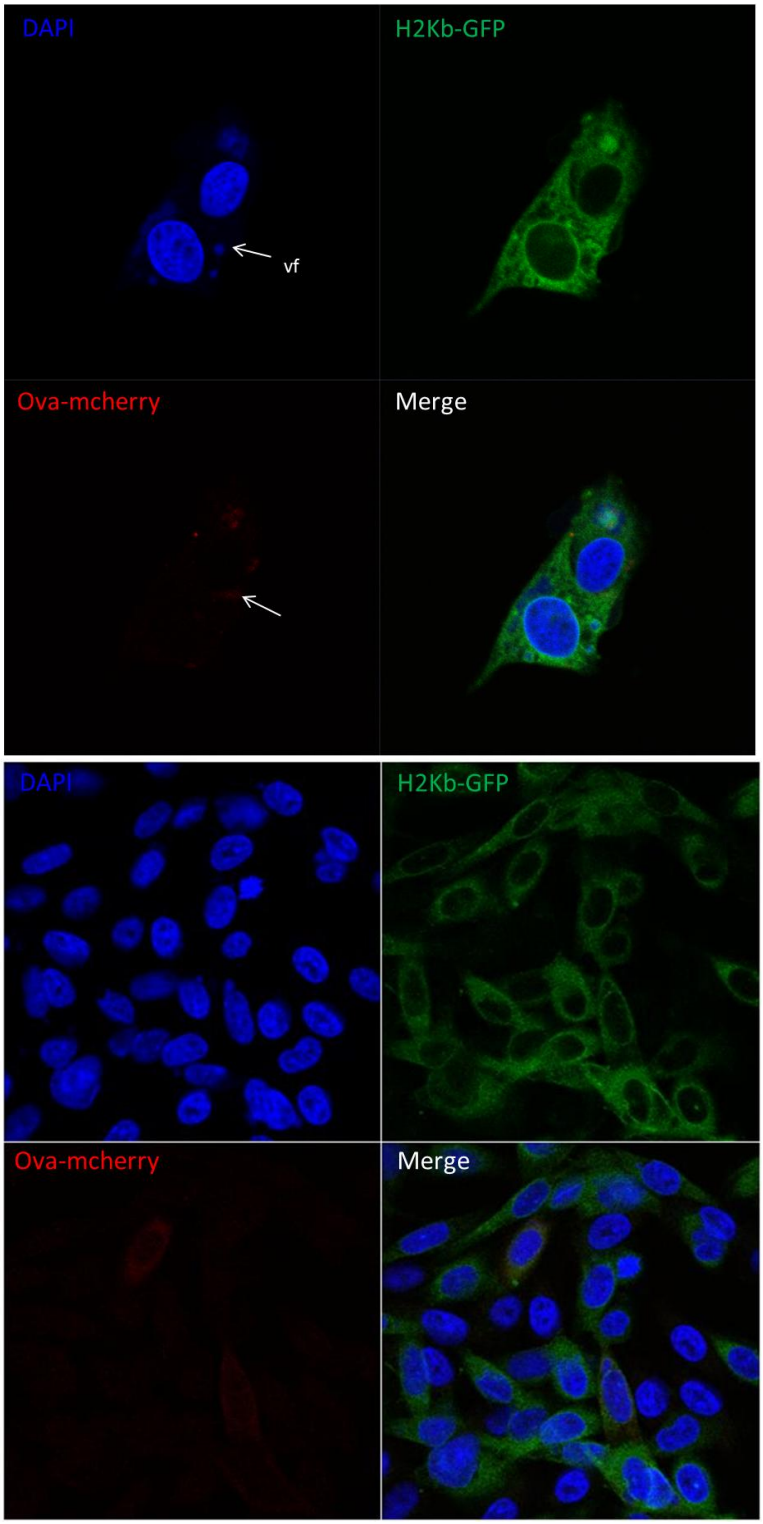

Figure 56: Localization of antigen and MHC I in HeLa cells infected with MVA-P11-ova-mCherry-PK1L-H2K^{b}-eGFP. Upper: at 5.5h p.i. Lower: at 6.5h p.i. DAPI (blue) stained nucleus and vf. ova location (red). GFP (green) indicates H2K^{b} location. White arrow points to vf.

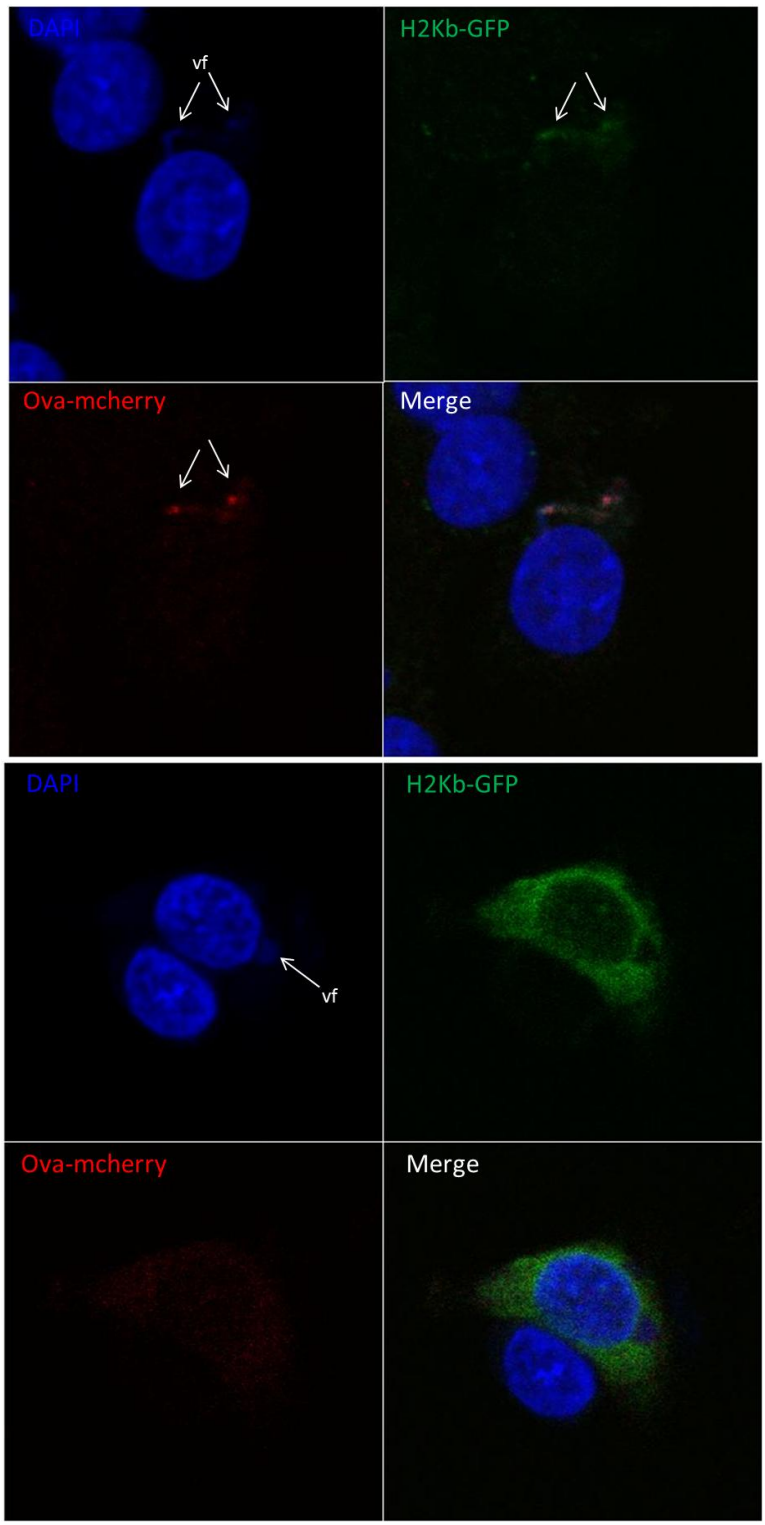

Figure 57: Localization of antigen and MHC I in HeLa cells infected with MVA-P11-ova-mCherry-P11-H2K^b-eGFP. Uper: 6h p.i. Lower: 7h p.i. DAPI (blue) stained nucleus and vf. ova location (red). GFP (green) indicates H2K^b location. White arrows point to vf.

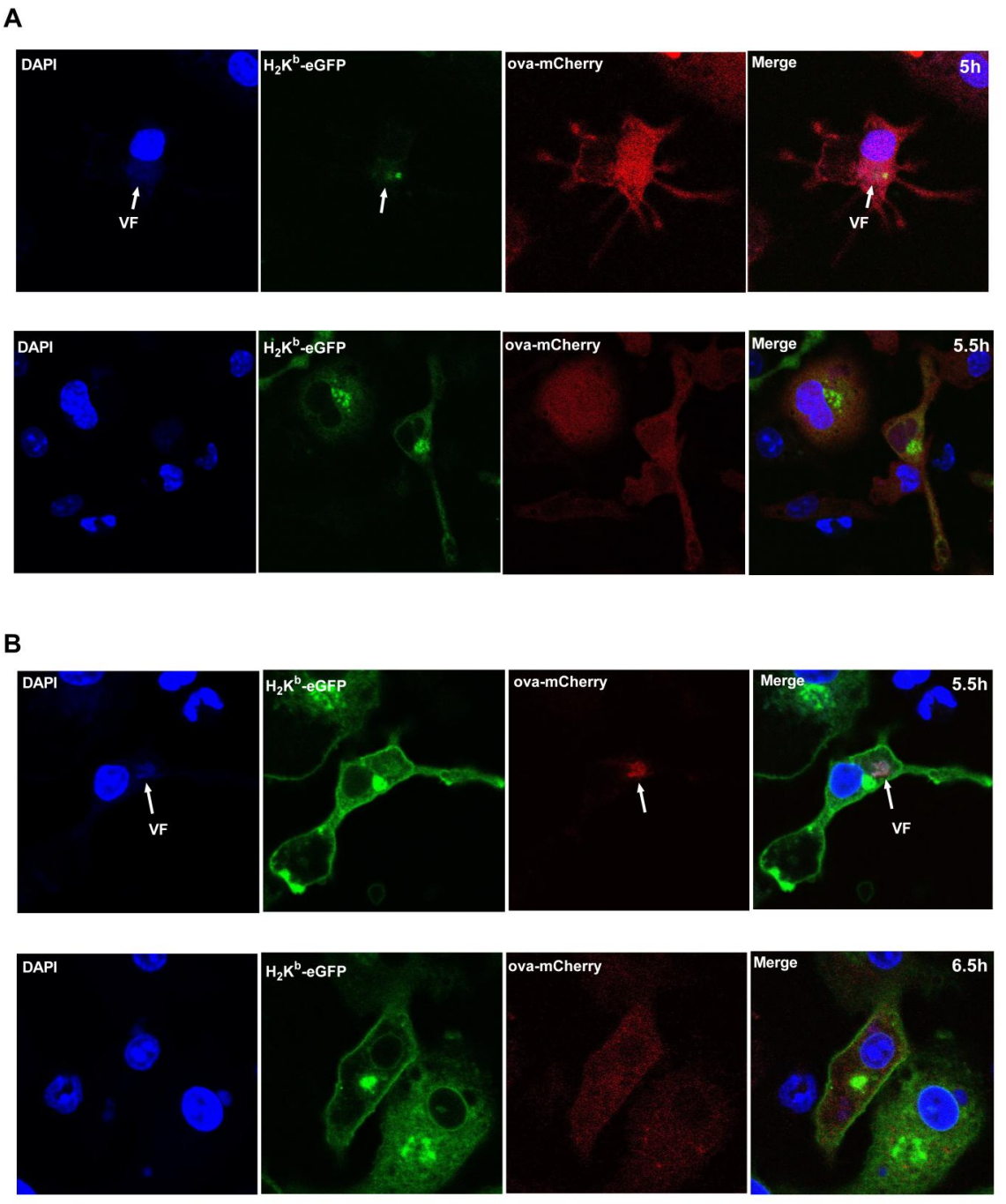

Figure 58. Localization of virus-derived antigen (ova) and MHC I (H2Kb) in infected BMDC. (A) Balb/CBMDC infected with MVA-PK1L-ova-mCherry-P11-H2Kb-eGFP (MHC I: H2Kb-GFP expressed late) for 5h and 5.5h. (B) BMDC infected with MVA-P11-ova-mCherry-PK1L-H2Kb-eGFP (antigen: ova-mCherry expressed late) for 5.5h and 6.5h. DAPI (blue) stained nucleus and viral factories (VFs). Ova (red). GFP indicates localization of H2Kb. White arrows point to VFs.

4.4.3 Distinct stability of early and late antigens with H3 as a model

As shown before, late expressed H3-GFP fusion proteins (H3-GFP) were localized in viral factories at 5h p.i., but left viral factories around 8h p.i. (Fig.47-48). Additionally, H3-derived peptides were presented to CTL with strongly delayed kinetics starting to activate specific T cells around 8h p.i. (Fig.59). Therefore, we hypothesize that H3 is sequestered in viral factories, which causes the delay of late antigen presentation. Since the proteasome is crucial for the generation of most peptides for subsequent MHC I presentation, the question was raised if H3 was protected from proteasomal degradation within the viral factory, thereby escaping the immune system. To its end, immune-precipitations (IP) were performed to test the stability of H3 and to determine ubiquitylation of H3 under early or late gene expression conditions (Fig.60).

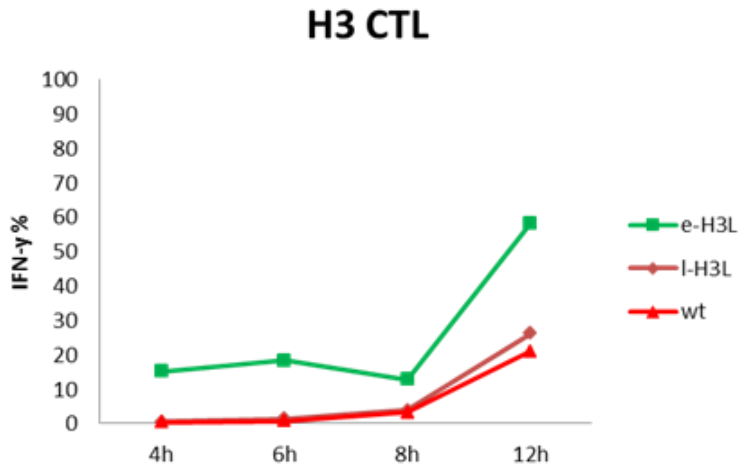

Figure 59: H3 expressed late results in delayed activation of H3-specific CTL (8h p.i.). BMDC infected with MVA-mH3L/eGFP-PK1L (e-H3L) or -P11 (l-H3L) or wt for different time periods. APC were co-cultured with CTL for 4h. IFN-γ production (ICS) was analyzed by FACS.

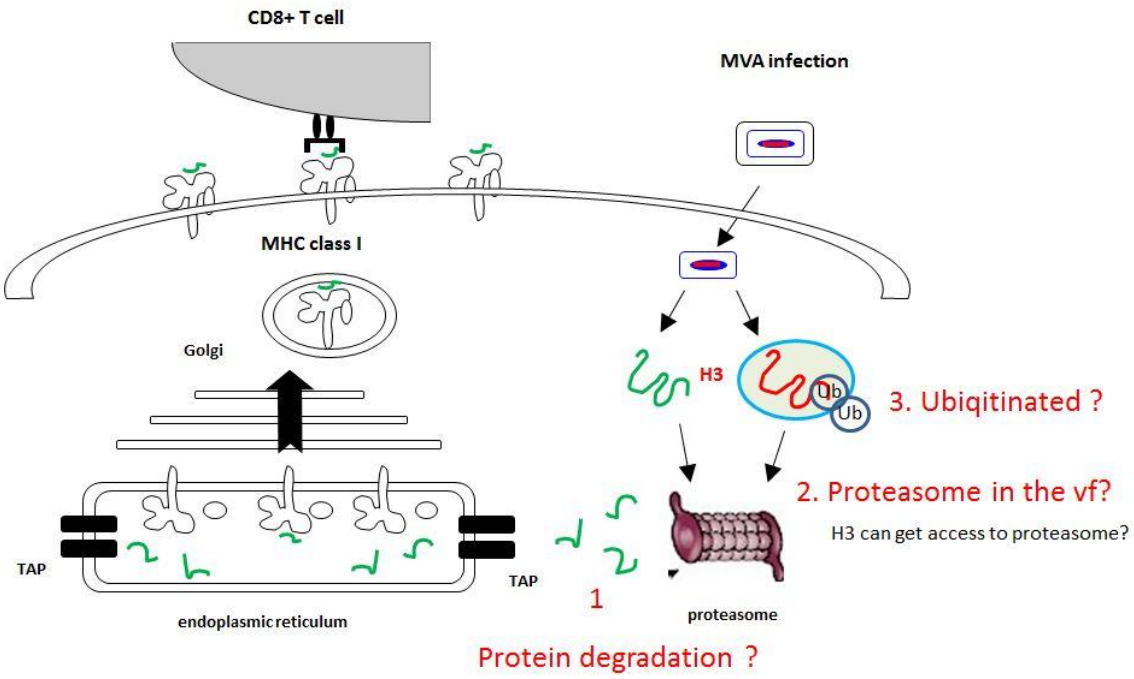

Figure 60: Differential H3 ubiquitylation status in dependence on localization (cytoplasmic vs. viral factory).

4.4.3.1 IP Antibody

First, the IP (immunoprecipitation) conditions for cold-IP were determined. HeLa cells were infected with MVA-mH3L-eGFP-PK1L or -P11 for 15h or left uninfected. H3-specific rabbit Abs (1mg/ml) at 2µg or GFP-specific mouse Abs (0.4mg/ml) at 2µg were comparatively applied for IP. To retrieve the antibodies and to precipitate H3-eGFP (66kDa) 40µl Protein-G-Sepharose per sample were used. For WB, 10% SDS-PAGE gels were run. H3 Ab (1mg/ml) 1:1000 (v/v) or GFP Ab (0.4mg/ml) 1:1000 (v/v) was used for detection. H3-eGFP had been precipitated by H3 or GFP IP antibodies, followed by H3 or GFP WB Abs (Fig.61). For cell lysates, anti-H3 or -GFP Abs were used for WB (Fig.62).

	1	2	3	4	5	6
MVA	uninfected	e-H3-GFP	e-H3-GFP	l-H3-GFP	e-H3-GFP	l-H3-GFP
IP Ab	ova (rabbit)	No Ab	GFP (mouse)	GFP (mouse)	H3 (rabbit)	H3 (rabbit)
WB Ab	H3 (rabbit) 1:1000					
	GFP (mouse) 1:1000					

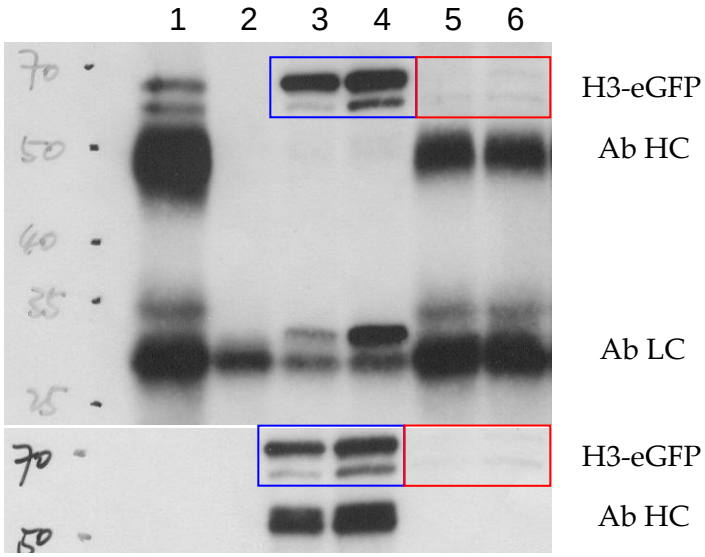

Figure 61: H3-eGFP may be precipitated by using anti-GFP Abs. 1-6 indicate samples described in the table above. H3L-eGFP was expressed early (e-H3-GFP) or late (l-H3-GFP). GFP (blue rectangle) or H3 (red rectangle) Abs were used for cold-IP to precipitate H3-GFP proteins. Upper WB: H3 rabbit Ab 1:1000 (1st Ab), anti-rabbit PO 1:3000 (2nd Ab). Lower WB: GFP mouse Ab 1:1000 (1st Ab), anti-mouse PO 1:3000 (2nd Ab).

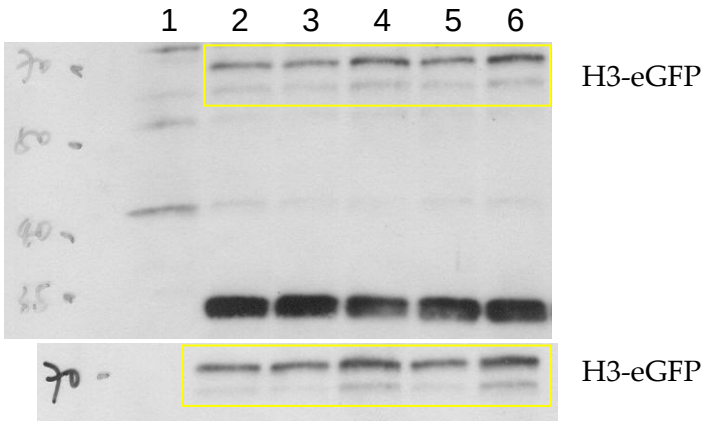

Figure 62: Cell lysates for detection of H3-eGFP by western blot. 1-6 indicate samples described in the table above. Yellow rectangles show H3-eGFP proteins. Upper WB: H3 rabbit Ab 1:1000 (1st Ab), anti-rabbit PO 1:3000 (2nd Ab). Lower WB: GFP mouse Ab1:1000 (1st Ab), anti-mouse PO 1:3000 (2nd Ab).

The results showed that GFP Abs performed better than H3 Abs in IP experiments for H3-eGFP detection. For WB, H3 Ab could be used at a low dilution ranging from 1:500 to 1:800 (v/v); GFP Ab could be used at 1:1000 (v/v) dilution.

4.4.3.2 H3 protein degradation (^{35}S labeled protein half life)

Since late antigens showed delayed presentation, late proteins should be more stable and may have a longer half life than the early proteins, if proteasomal degradation is a correlate for this phenomenon. Thus, the half life of H3 proteins within infected cells was monitored by pulse-chase experiments using radio-active sulphur (^{35}S) labeled L-cycteine and L-methionine.

HeLa cells were either infected with MVA-mH3L-eGFP-PK1L or -P11 for 15h or left uninfected. Cells were starved for 1h and labeled with ^{35}S for 1h. Protein degradation was chased for 0h, 6h, 24h or 48h, respectively. GFP Ab (2µg) was used for IP. The procedure was carried out as described before in methods 3.4.2. Indeed, late-H3 was found to be more stable than early H3. The intensity of protein bands was quantified. Early encoded H3 declined faster than late H3 (Fig.63).

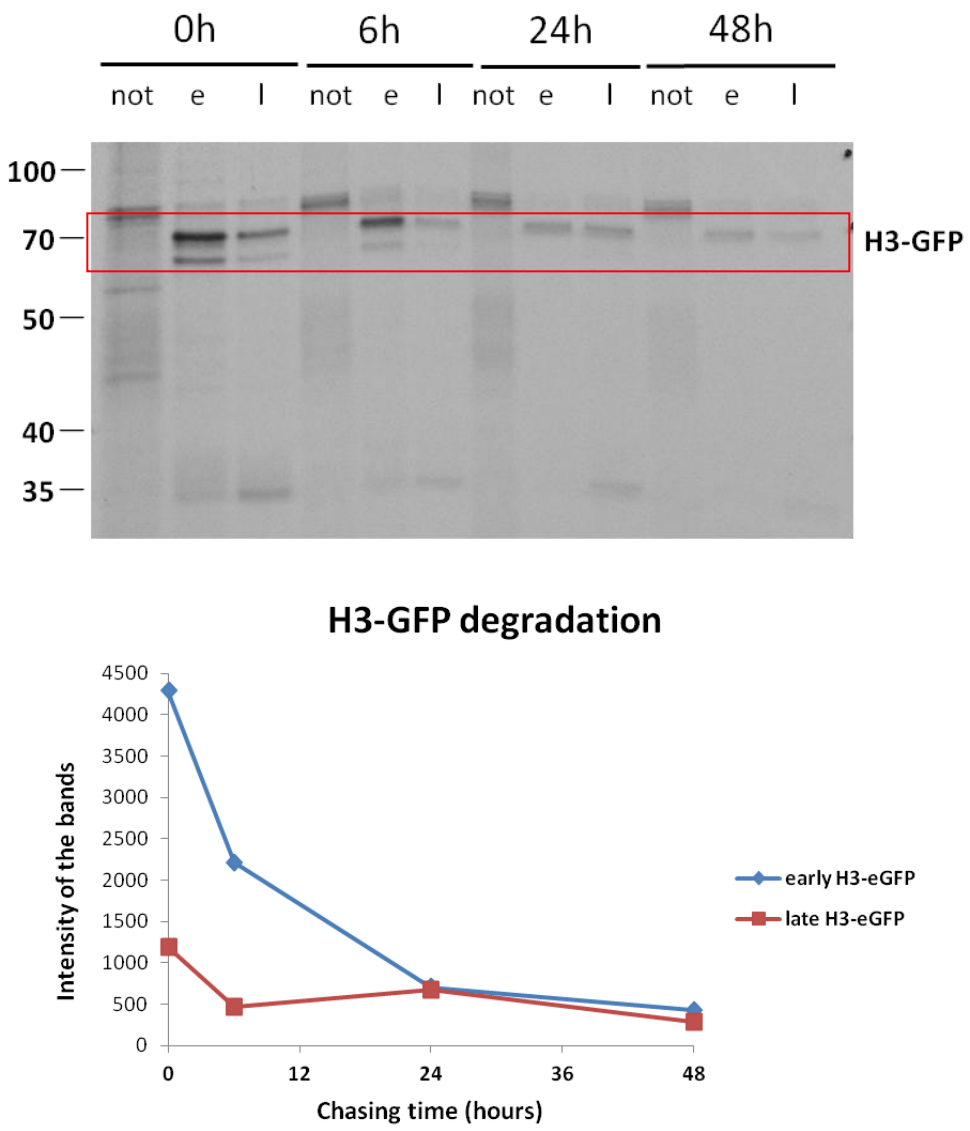

Figure 63: Late H3-GFP was more stable than early H3-GFP. Upper: H3-GFP protein detected by hot-IP. HeLa cells either infected with MVA-mH3L-eGFP-PK1L (e) or -P11 (l) for 15h or left uninfected (not). Cells were starved for 1h and labeled with ^{35}S for 1h. Protein degradation was chased for 0h, 6h, 24h or 48h. 2µg GFP Ab was used for IP. Red rectangle indicates H3-GFP protein. **Lower: Degradation of H3-GFP according to radioactive decay.** The radioactive intensity of the protein bands was calculated by Aida Image Analyzer v.3.24 software.

Since 12h p.i. may not present the ideal/suitable time to assess early gene expression, HeLa cells were infected with MVA-mH3L-eGFP-PK1L for only 2h or

infected with MVA-mH3L-eGFP-P11 for 4h. ^{35}S labeling was performed for 1h and the chase for 0h, 4h, 8h, 18h or 24h. 2µg GFP Abs were used for IP. However, at these conditions, there was no obvious difference concerning the stability of early or late expressed H3-GFP (Fig.64 A H3-GFP protein band in the red rectangle with a closed arrow). In contrast, the faster migrating smaller H3-GFP isoform (Fig.64 A H3-GFP protein band in the red rectangle with an open arrow) seemed to be more stable under late gene expression conditions as compared to early gene expression conditions. To get a more precise estimation, the intensity of the bands was calculated as shown in Fig.64B. From the statistics, the main upper bands of H3-GFP (after 5h chase), late-H3-GFP was not more stable than early-H3-GFP. However, before 5h of chasing, late-H3-GFP degraded faster as compared to early-H3-GFP. For the smaller H3 isoforms (blue rectangle), the statistic did not prove a significant difference between early- and late-H3. Furthermore, non-recombinant viral H3 was quite stable.

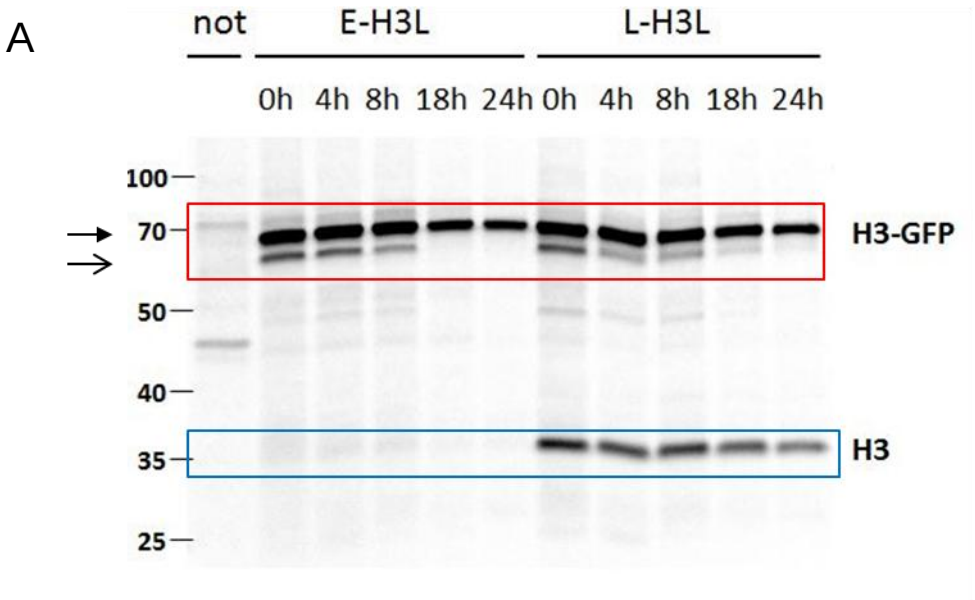

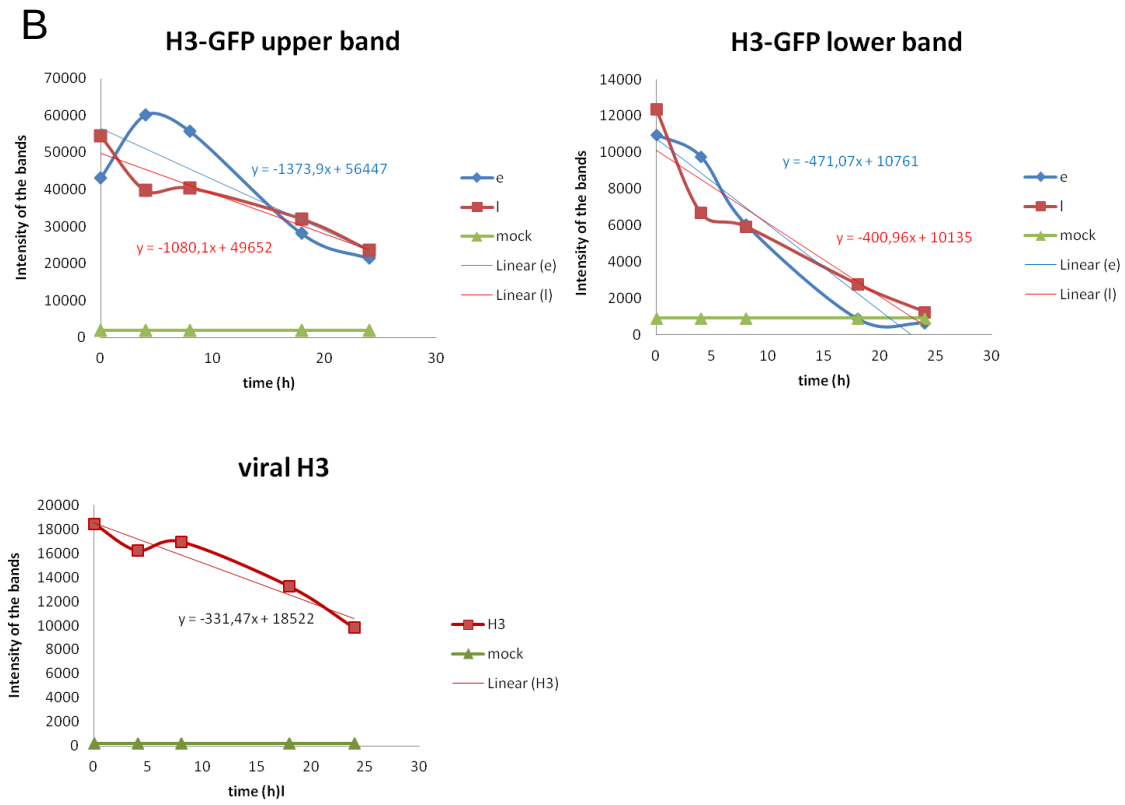

Figure 64: H3 produced late is more stable than H3 produced early. A: H3-GFP protein precipitates from the hot-IP. HeLa cells infected with MVA-mH3L-eGFP-PK1L for 2h (E-H3L) or infected with MVA-mH3L-eGFP-P11 (L-H3L) for 4h or uninfected (not). ^{35}S labeling for 1h, chasing for 0h, 4h, 8h, 18h or 24h. 2µg GFP Ab for IP. Red rectangle indicates H3-GFP proteins, blue rectangle highlights viral H3 protein. Closed arrow indicates main H3-GFP protein, open arrow points to smaller isoforms of H3-GFP protein. **B: Statistics for early- or late-H3-GFP protein degradation**. H3-GFP upper band as indicated by a closed arrow in A. H3-GFP lower band as indicated by an open arrow in A. The bands intensity was calculated by Aida Image Analyzer v.3.24 software.

4.4.3.3 Proteasomal activity in viral factories

The late-H3 protein was trapped in viral factories. Vaccinia virus cores are opened by proteasomal degradation of associated viral core proteins which have been ubiquitylated before infection (Mercer *et al*., 2012). The present study followed the hypothesis that, if late proteins such as H3 were ubiquitylated in the vf, access to proteasomes or proteasomal activity must be prevented in this compartment in order to

avoid premature degradation until cores will be finally protected by the membraneous envelope. Thus, HeLa cells were infected with MVA-NP-SIIN-eGFP. The proteasomes in infected cells were stained by using a Proteasome Activity Probe (Me4BodipyFL-Ahx3Leu3VS, 500nM), which is a cell permeable fluorescent substance that allows for accurate profiling of proteasomal activity in cell lysates or intact cells with high sensitivity (Berkers *et al*., 2007) (Fig.65A). Interestingly, active proteasomes were not detectable within viral factories, but accumulated around this compartment (Fig.65B).

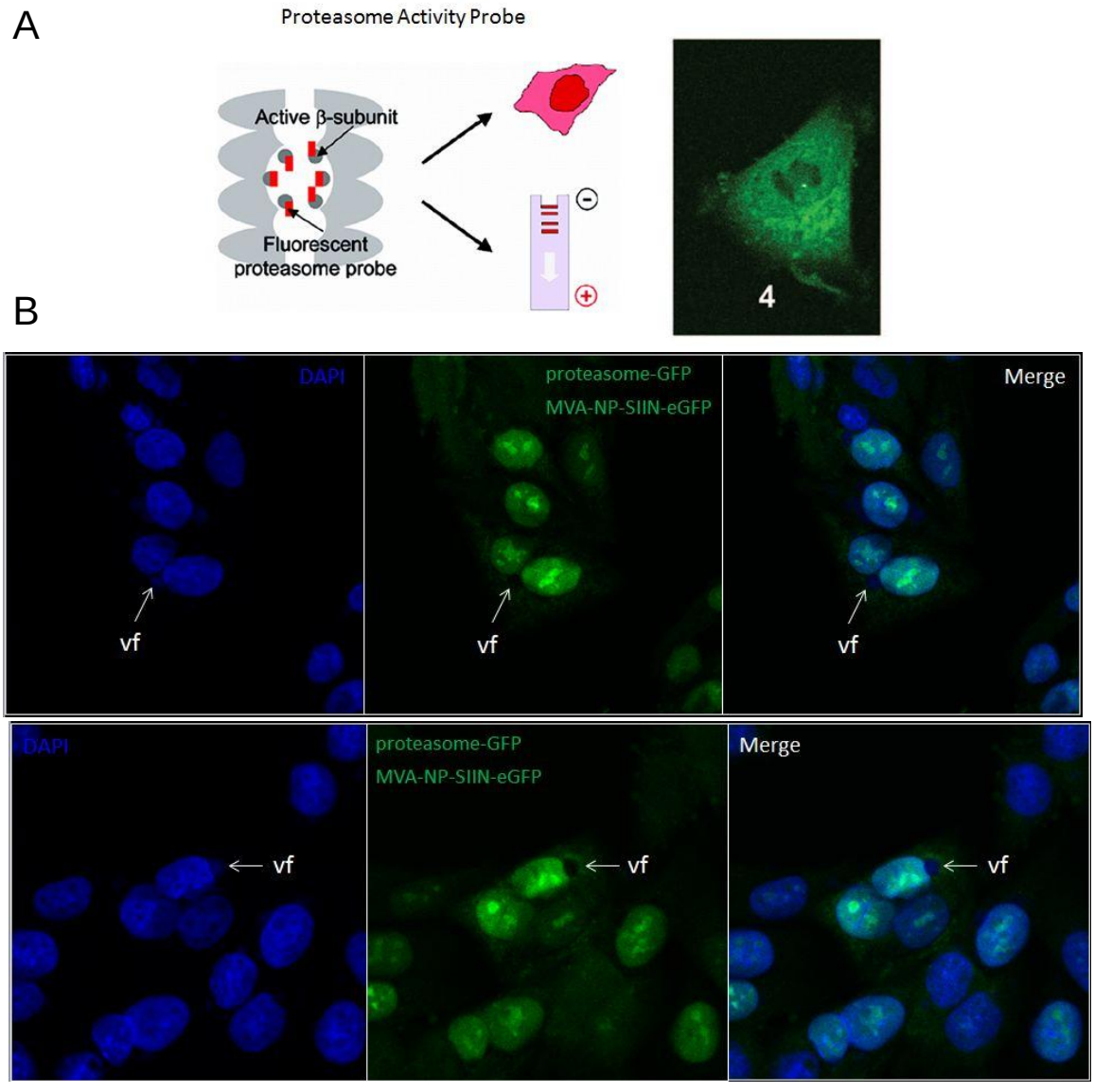

Figure 65: Active proteasomes were excluded from viral factories in MVA infected cells (6h p.i.). A. Proteasome Activity Probe (low green). B. CLSM: HeLa cells were infected with MVA-NP-SIIN-eGFP (high green), DAPI (blue) stained nuclei and vf. Arrows indicate vf. Infected cells display a green nuleus due to the targeting signal of NP.

4.4.3.4 Ubiqitiylation and degradation of H3

Since active proteasomes were not present in viral factories, other proteins preferentially or exclusively located within vf should have a longer half life although potentially conjugated with ubiquitin (Ub).

HeLa cells, which stably expressed an influenza hemagglutinin (HA)-tagged form of ubiquitin (Ub) (HeLa-HA/Ub) were used to investigate the ubiquitylation status of proteins in infected cells. The HA-Tag (YPYDVPDYA, 1,47 kDa) was derived from a part of the HA molecule corresponding to amino acids 98-106. It has been extensively used as a general epitope tag in expression vectors. HeLa-HA/Ub cells were infected with MVA-mH3L/eGFP-PK1L or -P11 or wt for 15h. The lysis buffer contained the proteasome inhibitor MG132 (5μM) or 5μM of the deubiqitylation inhibitor iodoacetamide (IAA) and 20μM N-ethylmaleimide (NEM). Protein accumulation by treatment with MG132 should indicate absence of protein degradation by proteasomes. As we know from the previous results that active proteasomes did not co-localize with vf, MG132 should exhibit no (or limited) effects on the stability of viral late proteins which are expressed in vf. If the protein is affected by IAA and NEM treatment, this indicates that the protein is subjected to the de-ubiquitiylating activity of the Ub-specific protease.

Ub was detected via its HA-tag by using HA-specific Ab. However, there was no Ub conjugation of the H3-GFP protein detectable (Fig.66). A global analysis of Ub-conjugated proteins (by performing a WB with HA-specific Abs recognizing Ub-HA) revealed that MG132 and IAA-NEM treatment increased the formation of high molecular weight forms containing Ub by inhibiting the proteasome or un-specific proteases, respectively (Fig.67).

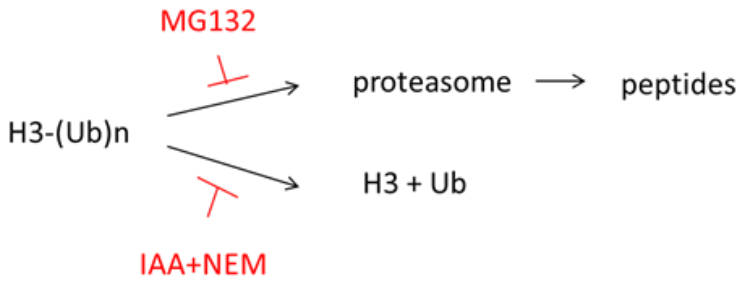

IP Ab	GFP(2µg) + ProG
WB	HA (rabbit) 1:5000
	GFP (mouse) 1:1000
	H3 (rabbit) 1:800
	Cox4 (rabbit) 1:3000

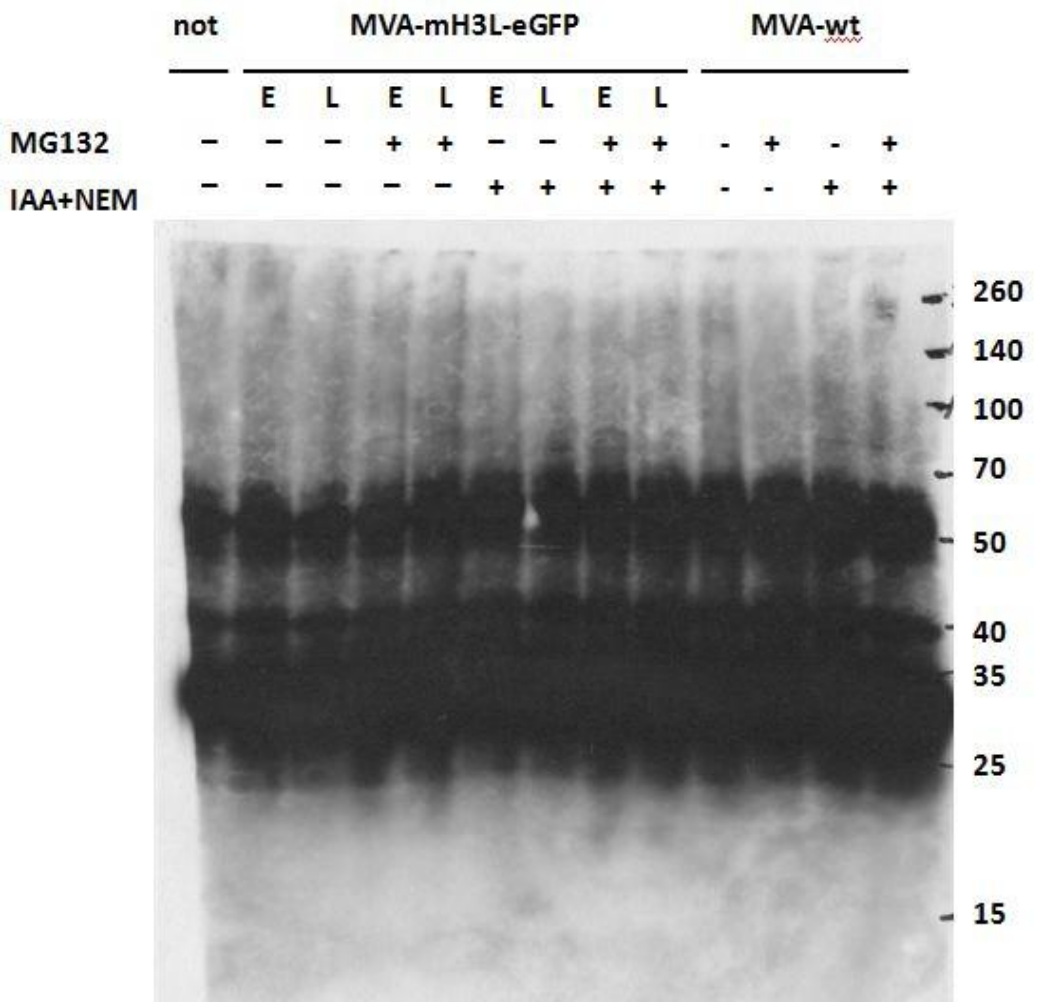

Figure 66: Ubiquitylation of H3-GFP (Cold-IP). HeLa-HA/Ub cells infected with MVA-mH3L/eGFP-PK1L (E) or-P11 (L) or wt for 15h or left uninfected (not). Proteasome inhibitor 5µM MG132 or 5µM IAA plus 20µM NEM were contained in lysisbuffers. Anti-GFP Abs were used for IP and HA rabbit Ab 1:5000 (1st Ab) and anti-rabbit PO 1:3000 (2nd Ab) were used for WB.

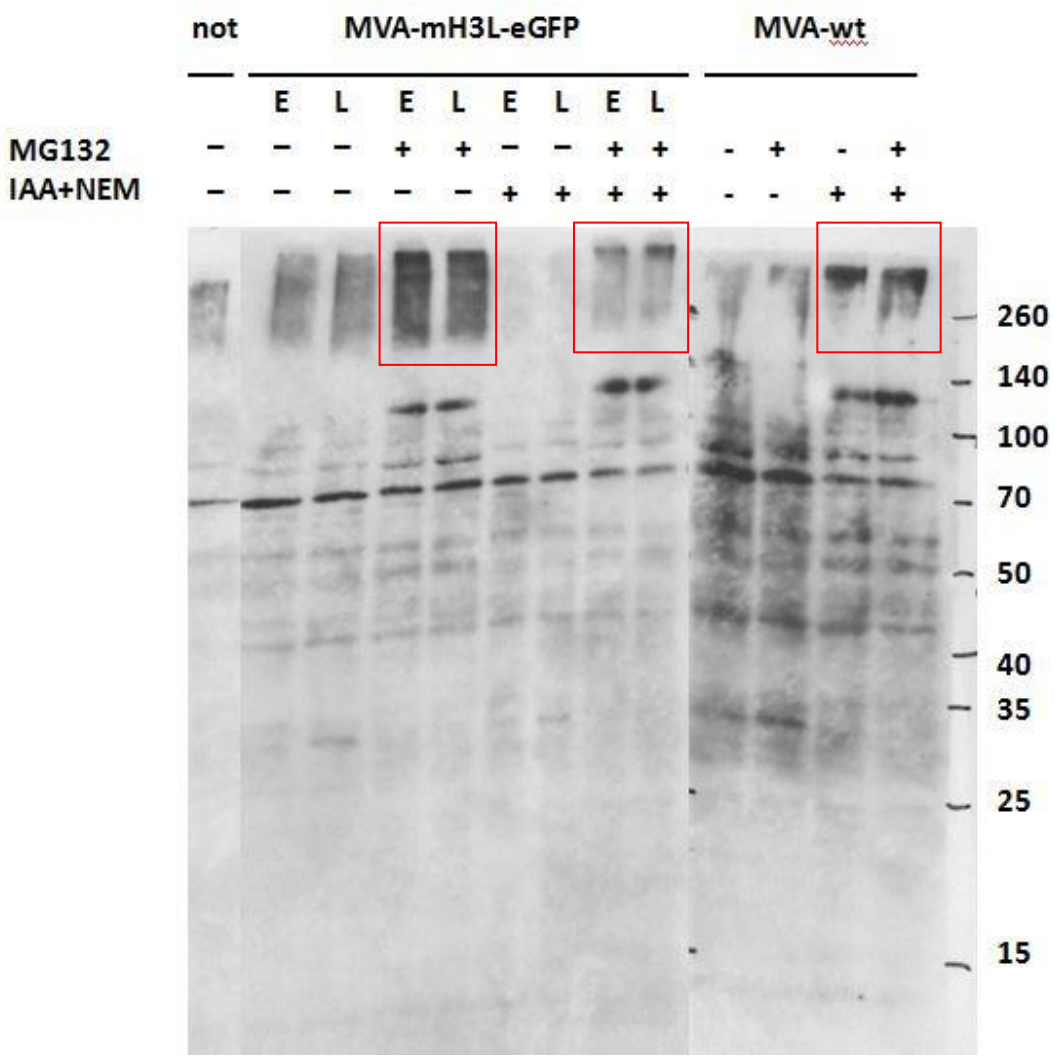

Figure 67: Detection of Ub in cell lysates. WB from cell lysates. HA rabbit Ab 1:5000 (1st Ab), anti-rabbit PO 1:3000 (2nd Ab). Red squares show Ub-proteins.

H3L-eGFP precipitated by using anti-GFP Abs was affected by the presence of IAA+NEM (Fig.68). Cox4 as a house-keeping protein served as loading control.

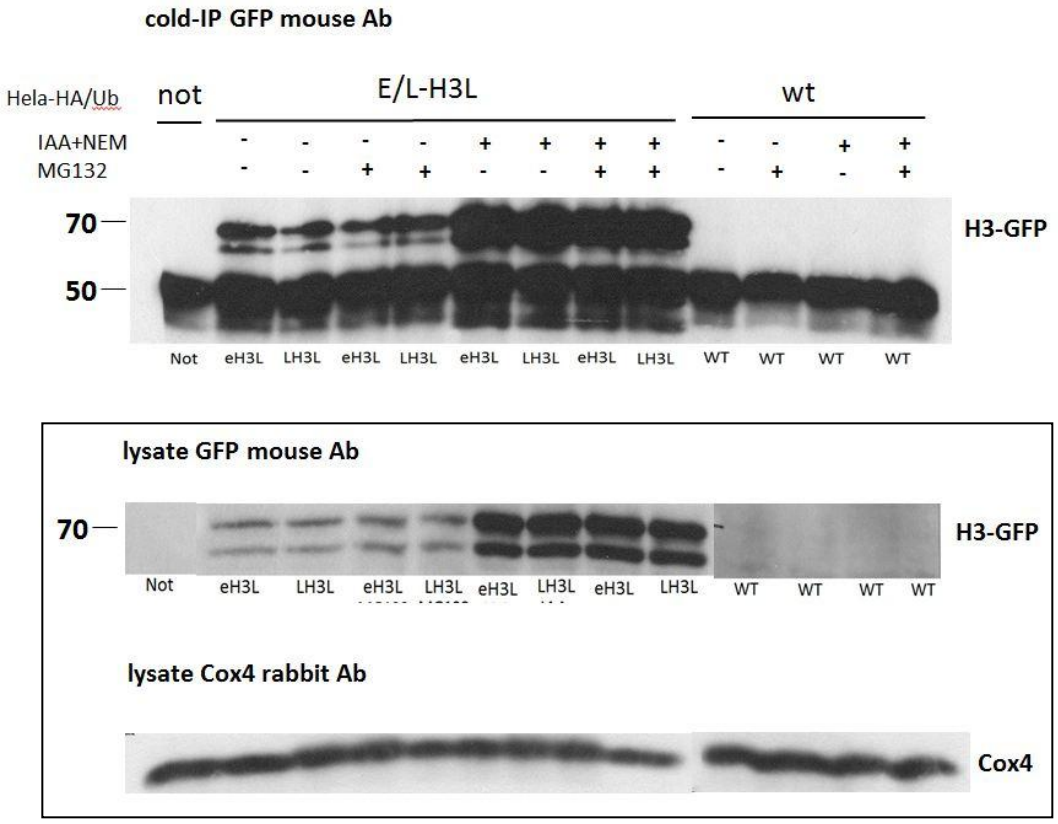

Figure 68: Determination of protein amounts of H3-GFP with or without inhibitors. For cold-IP (upper panel): Anti-GFP Abs were used for IP. Anti-GFP mouse Ab 1:1000 (1st Ab) and anti-mouse PO 1:3000 (2nd Ab) were used for WB. For cell lysates (blots framed black), anti-GFP mouse Ab 1:1000 (1st Ab) and anti-mouse PO 1:3000 (2nd Ab) or anti-cox4 rabbit 1:3000 (1st Ab) and anti-rabbit PO 1:3000 (2nd Ab) were used for WB.

4.4.4 Distinct APC types for presentation

4.4.4.1 APC present native MHC I

We have demonstrated the different localization for early and the late antigens localizations. However, could distinct APC subsets infected by the MVA have different antigen presentation abilities for late proteins? To answer this question, BMDC from HHD mice and LCL (human B lymphoblastoid cells), which present HLA-A2-restricted epitopes were infected with MVA and then tested for TC activation determined at different time points post infection. Both LCL and BMDC resulted in strong early B22-

specific T cell activation. Yet, in contrast to LCL, only BMDC were able to stimulate H3-, A6- and I1-specific T cells (Fig.69A). This difference hold also true for the C57BL/6 mouse systems. BMDC from C57BL/6 mice could present both, early and late antigen-derived MHC I/peptide complexes. In contrast, H2-K^b positive RMA cells (T cell lymphoma) present late antigen-derived peptide/MHC I complexes to the cell surface (Fig.69B) even at higher MOI (data not shown).

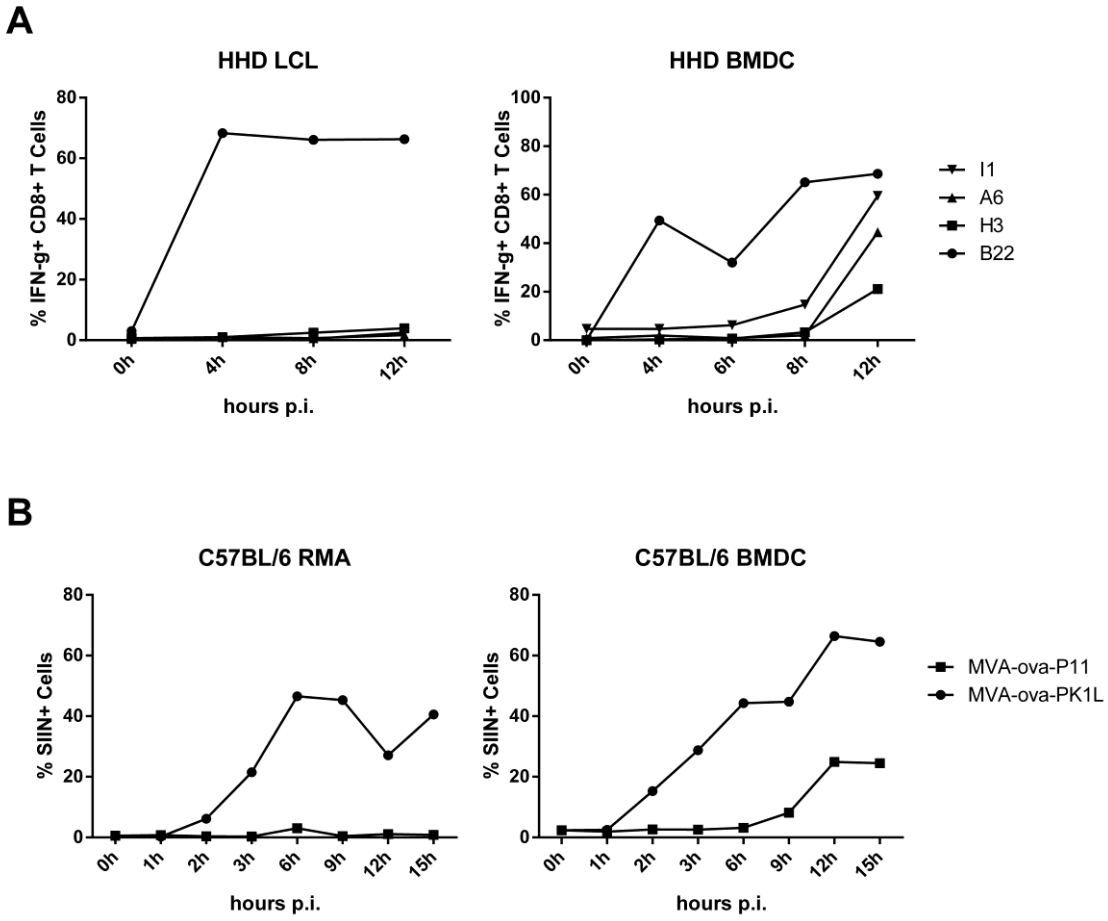

Figure 69: Antigen presentation ability of different APC subtypes. A. TC activation was impaired using LCL cells. Cells were infected with MVA-wt for different periods of time. LCL infected with MOI=5, BMDC with MOI=1. Coculture with CTL for 4h. IFN-γ production (ICS) was determined by FACS analysis**. B. SIIN presentation was impaired in K^b+ RMA cells.** C57BL/6 BMDC or RMA cells infected with MVA-ova-PK1L or -P11

for different time periods. MOI=10. Cells were stained with anti- K^b/SIIN-APC Abs and measured by FACS. Percentage of K^b/SIIN+ cells (% SIIN+ Cells) is shown.

Treatment of LCL with 10ng/ml human IFN-γ for 16h prior to infection could not enhance specific T cell activation against late antigens (Fig.70), which indicates that late antigens were not degraded or properly processed and peptide epitopes were not available for MHC I peptide loading since IFN-γ should only upregulate MHC I, but not affect the processing machinery.

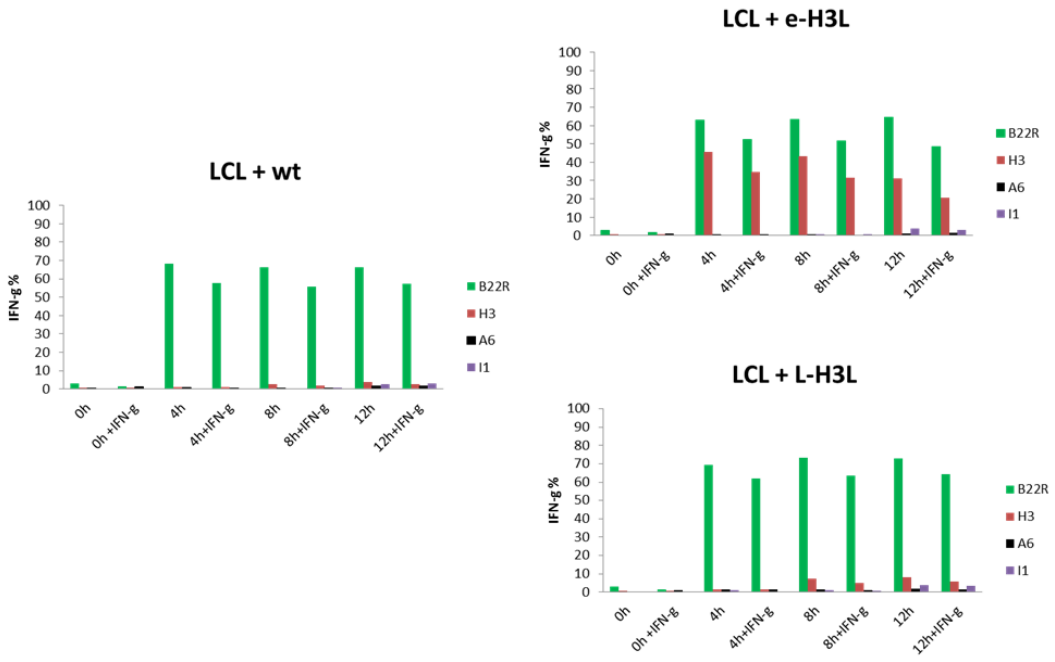

Figure 70: IFN-γ treated LCL cells could not improve late epitope-specific T cell activation. Cells treated with IFN-γ for 16h, followed by infection with MVA-mH3L/eGFP-PK1L or -P11 or wt for different periods of time. Co-incubation with CTL for 4h.

4.4.4.2 Cells present foreign MHC I

When MHC I originated from a recombinant virus, different cells types also showed variable presentation abilities. As shown before, K^b negtive cells J774 translocate K^b to the cell surface (Fig.39-41). However, in some non-professional APC, like

Cloudman cells (melanoma), GFP-tagged MHC I molecules were retained within the cell (Fig.71) and could not be detected at the surface of infected cells (Fig.72). This indicates that viral and/or host factors modulating the antigen presenting capacity. Other non-professional APC (HeLa) showed the same deficient ability (data not shown).

However, pretreatment with mouse IFN-γ (1, 5 or 10ng/ml for 24h) resulted in upregulation of MHC I surface expression. Cloudman cells could gain the ability of presenting K^b to the surface as demonstrated by FACS (Fig.73) or by confocal microscopy (Fig.74).

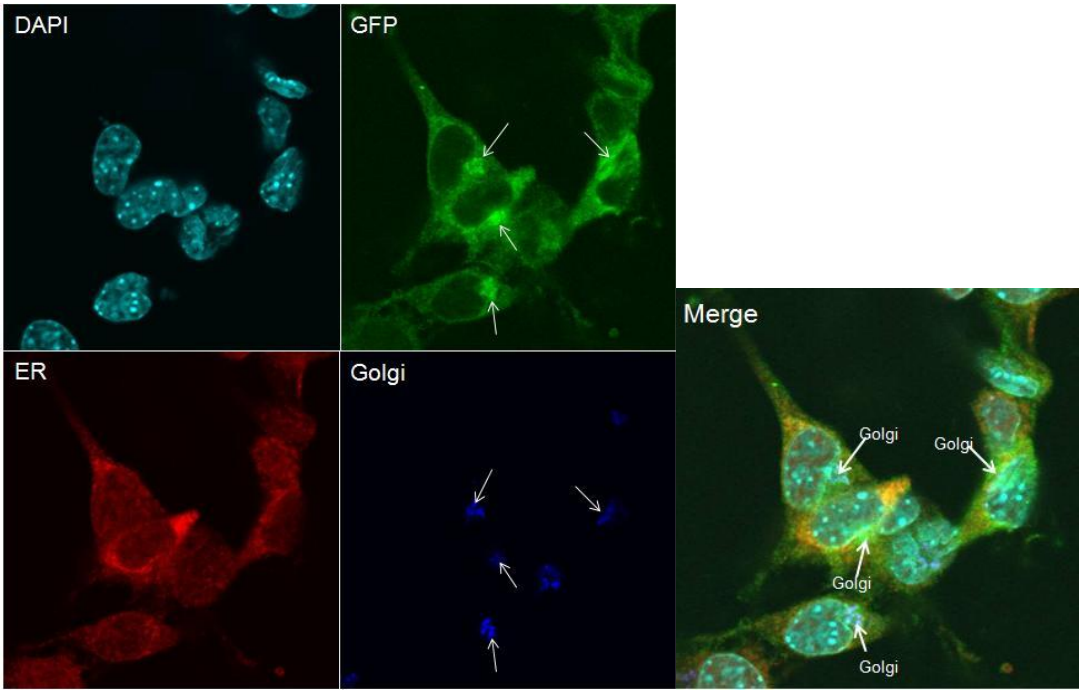

Figure 71: Infected Cloudman cells intracelluarly retain MHC I encoded by MVA (12h p.i.). Cells infected with MVA-ova-H2K^b-eGFP-PK1L (green). ER (red) and Golgi (dark blue) were stained as described before. White arrows indicate the Golgi.

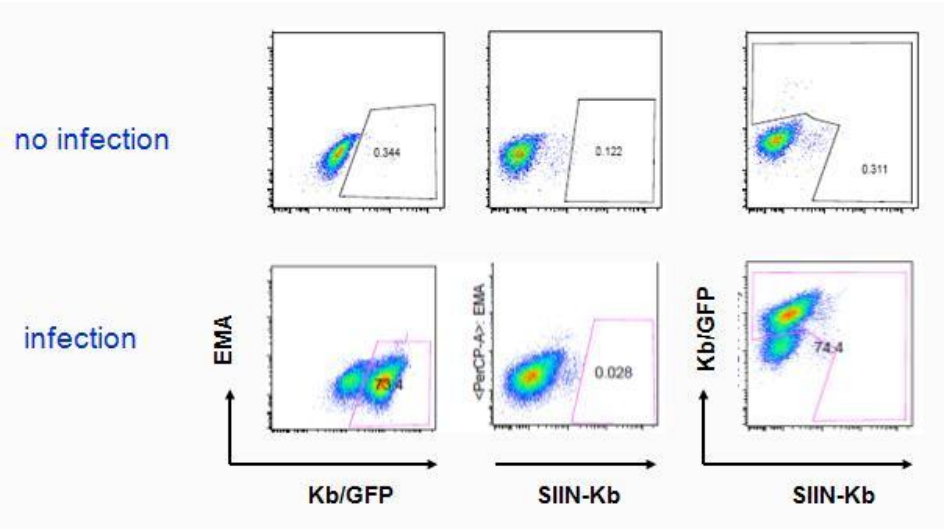

Figure 72: Infected Cloudman cells intracelluarly retain MHC I encoded by MVA. Infected cells (gated on living cells) discriminated for GFP+ (K^b/GFP) or SIIN-K^b+ (SIIN-K^b) cells. Right panel illustrates GFP and SIIN double positive cells.

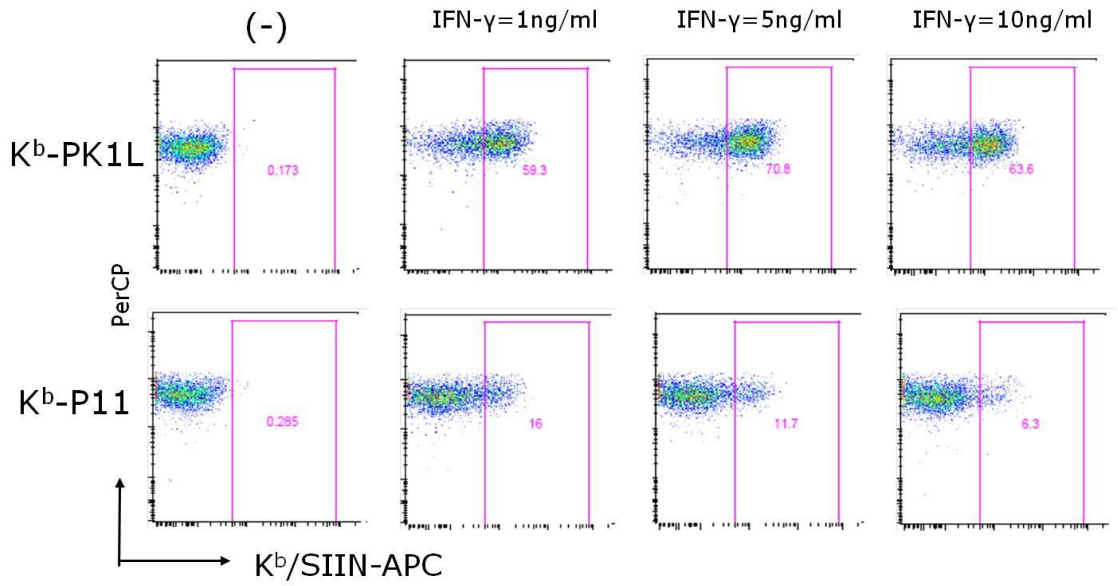

Figure 73: IFN-γ upregulates MHC I and peptide-loaded K^b/SIIN-complexes at the cell surface. Cloudman cells not treated or treated with 1, 5 or 10ng/ml IFN-γ for 24h, and infected with MVA-ova-H2K^b-eGFP-PK1L (K^b-PK1L) or -P11 (K^b-P11) for 8h. Cells were stained with K^b/SIIN-APC Abs. K^b/SIIN+ cells are shown.

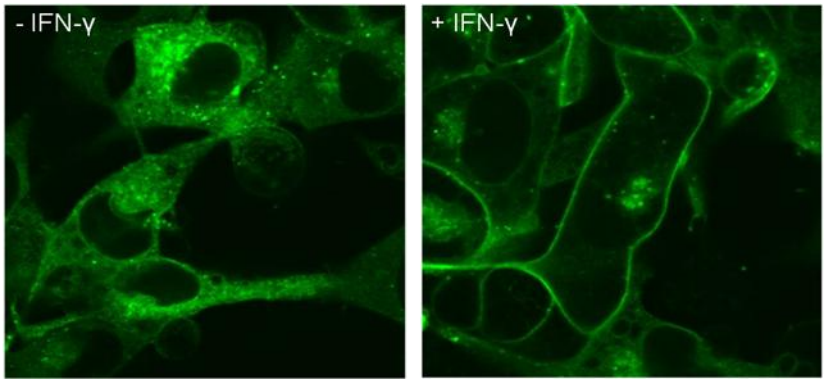

Figure 74: Translocation of MHC I to the cell surface after IFN-γ treatment. Cloudman cells treated or non-treated with 5ng/ml IFN-γ for 24h and infected with MVA-ova-H2K^{b}-eGFP-PK1L for 8h. GFP (green) represents the localization of H2-K^{b}.

5. Discussion

The cytotoxic CD8+ T cell (CTL) response plays an important role in antiviral immunity for its fast clearing of acute virally infected cells and its release of cytokines. This release is achieved by recognition of the peptides processed and presented from foreign pathogens as well as from modified self-proteins on the surface of infected or antigen transferred cells. Indeed, virus-specific antibodies can neutralize viruses by recognizing the surface structural components; on the other hand, CD8+ T cell responses can essentially be directed against any intracellular protein and many viral proteins made inside of an infected cell contain epitopes presented by the MHC class I pathway.

The CTL response is essential for clearing most viral infections, especially due to the following aspects: First, some viruses are resistant to antibody neutralization, like human immunodeficiency virus (HIV). Qualitative aspects of the HIV-specific CD8 T-cell response play a critical role in the efficacy of antiviral control (Kitchen *et al*., 2012; Betts *et al*. 2006). Second, virus-specific CTL also contribute to viruses with antigenic drift variants, which are difficult to target by antibodies. It has been shown for decades that Influenza A virus infections induce CTL directed against most viral components, although majority is specific for the virus nucleoprotein (NP) and the matrix 1 protein (M1) (Budimir *et al*., 2012; Yewdell, 1985). Third, some chronic viruses' infections, like HBV, rely on T cell responses for clearing the virus. CD8+ T cells are the main cellular subset responsible for viral clearance (Lambe *et al*., 2013; Depla *et al*., 2008) and the CTL response persists decades after clinical recovery from acute infection (Rehermann *et al*.,

1996a) in that it can be further observed after resolution of chronicity (Rehermann *et al*., 1996b).

Thus, there is an increasing interest in developing vaccines that can raise efficient antiviral CD8+ T cell responses. The first recombinant viral vectors used to elicit CD8+ T cell responses against inserted target genes were based on vaccinia virus which has become a common vector used for antigen delivery since then (Bennink *et al*., 1990). Recombinant modified vaccinia virus Ankara (recMVA), despite lacking various immunomodulatory genes (Antoine *et al*., 1998), shows high immune-stimulatory capacity (Zimmerling *et al*., 2013) and strong activation of human dendritic cells even in the absence of virus replication (Drexler *et al*., 2004; Drillien *et al*., 2004).

5.1 MVA late viral antigen is delayed in presentation to CTL

As mentioned in the introduction (1.1.1), the vaccinia viral gene expression can be divided into early, intermediate and late phases. The time between each period is only about one hour at the transcriptional level (Moss, 2007). One way to study CTL responses to vaccines is to analyze and monitor epitope-specific CD8+ T cell responses after immunization elicited against both, viral vector and recombinant antigens (Lambe *et al*., 2013; Gómez *et al*., 2013; Drexler, 2003). Our group has generated MVA epitope-specific CTL lines in HHD background, which were used as tools to analyze early or late antigen presentation. We have generated CTL specific for antigens, produced at different times in the MVA life cycle. By using CTL lines specific to vaccinia virus early or late proteins, we have found that presentation of viral late gene products to CTL was substantially delayed (Kastenmuller *et al*., 2007). The early B22-CTL could be stimulated

to produce IFNγ after two hours of infection, while the late A6- or I1-specific CTL did not receive any activation even after eight hours infection. Nevertheless, this was only the case for HLA-A2 restricted antigens and it has not been possible to further elucidate the delayed late antigen presentation in this methods. To obtain more informations as to if and when late antigens would be presented, the kinetics analysis had been extended up to 12 hours. Interestingly, H3, A6 and I1 received CTL activation at 12 hours p.i. by BMDC, but not by BC (LCL) (Fig.68A). Nonetheless, the earliest time for late antigen specific T cell activation was eight and 12 hours p.i. for H3 and other late antigens, respectively. To confirm that this was a general phenomenon and not particular for the HHD system, CTL lines which recognize the epitopes derived from the C57BL/6 background, have been generated. The results showed a similar kinetic with delayed late antigen presentation. Late antigen A19 could activate specific CTL around eight hours p.i. (Fig.12B). The results demonstrate that viral late antigens have a postponed presentation to CTL in at least two different strains of mice (HHD and C57BL/6), indicating that the time point of viral antigen expression in infected APC has a strong impact on viral T cell epitope processing and presentation.

There are many studies that have dealt with MHC I presentation for VACV epitopes restricted to mice (Siciliano *et al*., 2013; Lu *et al*., 2012; Moutaftsi *et al*., 2006; Liu *et al*., 2008; Tewalt *et al*., 2009) or humans (Flechsig *et al*., 2011; Brandler *et al*., 2010; Drexler *et al*., 2003; Jing *et al*., 2005; Oseroff *et al*., 2005; Pasquetto *et al*., 2005). CD8+ T cell responses to vaccinia virus are broad and diverse, rather than focused on a few antigenic targets (Moutaftsi *et al*., 2010). However, the recognition pattern indicates a nonrandom

distribution of all epitopes. Some antigens can be regarded as dominant or, commonly across different MHC types, some are recognized rather infrequently or not at all (Oseroff *et al*., 2008). The most effective CD8+ T cells are often those specific to proteins made early in the viral life cycle (Moutaftsi *et al*., 2006, 2010; Oseroff *et al*., 2005; Coupar *et al*., 1986), such as non-structural genes and transcription factors (Terajima *et al*., 2008; Moutaftsi *et al*. 2010). Other viruses also display a dominant immune response to early antigens. The major CTL response to human cytomegalovirus (HCMV) is directed against a protein expressed immediately upon infection (Hesse *et al*., 2013; Martin *et al*., 2008); Similar findings have been reported for Listeria monocytogenes infection (a bacterial intracellular pathogen) (Zaiss *et al*., 2008) or for HSV-1 infection in which proteins were favored targets of CD8+ T cells that were expressed before viral DNA synthesis begins (St Leger *et al*., 2011).

By contrast, late antigens are poorly immunogenic for CD8+ T cells (Tewalt *et al*., 2009; Kauffmann *et al*., 2006; Coupar *et al*., 1986), but correspond to CD4+ T cell recognition and Ab (Moutaftsi *et al*., 2007, 2010). Thus, dendritic cells are thought to directly present early antigens while late antigens are recognized via antigen uptake and presentation by non-infected APC (Liu *et al*., 2008). However, it is still under discussion how CD8+ T cells respond to the late antigens.

5.2 Late viral antigens are impaired in cross-presentation

Our group has previously demonstrated that CTL responses against MVA produced antigens were dominated by cross-priming *in vivo* (Gasteiger *et al*., 2007). Furthermore, vaccinia virus gene products may be presented by both direct-priming and

cross-priming (Schliehe *et al*., 2012; Basta *et al*., 2002). The question of whether late antigens could be presented by cross-presentation *in vitro* was considered in this research work. Surprisingly, late viral antigens could not activate CTL in cross-presentation as demonstrated in two mouse models, HHD and C57BL/6.

Various publications have shown that antigens can be cross presented *in vivo* by various viruses. For instance, lung migratory CD103+ DC are not productively infected by influenza virus and thus were able to only induce virus-specific CD8+ T cells through cross-presentation of antigens from virally infected cells (Helft *et al*., 2012). Priming of CD8+ T cells against cytomegalovirus-encoded antigens is dominated by cross-presentation (Busche *et al*., 2013). Measles virus vaccine infects tumor cells and induces tumor antigen cross-presentation by human plasmacytoid dendritic cells (Guillerme *et al*., 2013). Vaccinia virus antigens have been shown that they could be cross-presented by DC (Iborra *et al*., 2012) and cross-presentation happens soon after infection (Ramirez *et al*., 2002) and requires the occurrence of early antigen transfer (Serna *et al*., 2003). However, for vaccinia virus, most of the studies focused on the early stage after infection demonstrating that early antigens can be cross-presented and did not specifically address this issue for late antigens. Our research group also showed previously that cross-priming was dominant for MVA (Gasteiger *et al*., 2007). The current results proved that early antigens can enter a cross-presentation pathway (Fig.27-29). However, when we talk about late antigens, one publication from Tewalt *et al* showed that VACV late antigen did not enter cross-presentation pathways (Tewalt *et al*., 2009), which concurs with the results of this study.

There are also studies comparing direct- and cross-presentation for vaccinia virus induced CD8+ T cell responses. Schliehe *et al* showed that a stable antigen was most effective for eliciting CD8+ T cell responses after DNA vaccination and infection with recombinant vaccinia virus *in vivo* (Schliehe *et al*., 2012). NY-ESO-1 is expressed by various cancers and is highly immunogenic. NY-ESO-1(88-96) was much more efficiently cross-presented by the soluble form as compared to NY-ESO-1(157-165) (Zhao *et al*., 2012). HSV-specific CTL responses entirely depended on the CD8α+ DC subset which may present via direct- or cross-presentation depending on the immune evasion equipment of the respective viruses (Nopora *et al*., 2012). Incubation of MVA-infected leukocytes with uninfected immature DC led to complete maturation of the DC and might be the basis for cross-presentation of MVA-encoded antigens (Flechsig *et al*., 2011). By disrupting cross-presentation, additional research has shown that direct-presentation is sufficient for an efficient anti-viral CD8+ T cell response for vaccinia virus (Xu *et al*., 2010). Taken together, these findings indicate that special features are required for cross-presentation.

Recent researches which detected cross-presentation are carried out mostly *in vivo* for CMV (Busche *et al*., 2013), HBV (Moffat *et al*., 2013) and VACV (Xu *et al*., 2010; Serna *et al*., 2003), using model proteins, such as chicken ovalbumin (ova) and transgenic OT I mice (Moffat *et al*., 2013; Nierkens *et al*., 2013; Henry *et al*., 2013; Xu *et al*., 2010) and other deficient mice models, such as Batf3-/- mice (Bachem *et al*., 2012) and Serpinb9(Spi6)-/- mice (Rizzitelli *et al*., 2012). It is difficult to clearly separate direct or cross presentation *in vivo* and only few studies investigate cross-presentation *in vitro*.

Therefore, this research has set up an *in vitro* assay for cross-presentation, which is based on functional gene expression in feeder cells (Fig.24-25), phagocytosis ability (Fig.15;17-18) and efficient presentation capacity by the APC (Fig.12A) and also includes PUVA treatment, which inhibits virus transfer (Fig.23). MVA infection also had an enhancing effect on the phagocytosis and cross-presentation activity of BMDC (Fig.14). The current study has compared direct-presentation and cross-presentation in parallel to one another demonstrating that early antigens can enter both pathways, while late antigens do not enter cross-presentation and are delayed when being presented by direct-presentation (Fig.27-29). Importantly, different APC (BMDC/DC2.4) (Fig.27/12C) and different feeder cells (Cloudman/HeLa/A375) gave similar results (data not shown).

Cross-presentation and MHC II presentation share many components. They both need the antigen to be translocated into the cytosol for further processing, but the loading of the MHC occurs in a different cell compartment. Published data showed that antigens for cross-presentation are the most commonly released from endosomes or phagosomes to the cytosol (Houde *et al*., 2003), or from the ER into the cytosol (Cebrian *et al*., 2011). However, there is less data showing that an antigen can escape from viral factories, which are specific cell compartments formed after vaccinia virus infection. Husain *et al* showed that ER membrane component COP II could select some viral proteins and transport them out of viral factories. Earlier membrane proteins (MV) A9/L1/A17 were negatively selected and fused with viral crescent membranes, while some later membrane proteins (EV) B5/A36 were positively selected to be translocated to

Golgi (Husain *et al*., 2007). From the current results, it was shown that late H3 (an MV membrane protein) was present in viral factories but later also localized to the cytoplasm. However, we have not tested whether H3 is localized to the viral crescent membrane by electronic microscopy. Nonetheless, after H3 has translocated from viral factories, it was also available for presentation to CD8+ TC or possibly for more dominant CD4+ TC reponses or antibody recognition. For the late expressed protein B5, an EV membrane protein, we have seen early CD4+ T cell activation. Perhaps it localized much earlier to the Golgi and for internalization into the membrane or B5 used a competely different pathway for presentation. As such, we have not yet checked B5 activation for CD8+ T cells. However, these are late structural proteins, which are usually more dominantly recognized by CD4+ T cells or antibody than by CD8+ T cells (Moutaftsi *et al*., 2007).

Since a late antigen can translocate from the viral factory to the cytosol, it should be able to be presented by cross-presentation. Therefore, it is interesting that late antigens did not follow a cross-presentation pathway. Aleyas *et al* showed that impaired cross-presentation of CD8α+ CD11c+ dendritic cells by the Japanese encephalitis virus in a TLR2/MyD88 signal pathway dependent manner (Aleyas *et al*., 2012). Zhao *et al* elicited an important role for MyD88 in initial anti-VACV CD8+ T cell responses (Zhao *et al*., 2009). Helft *et al* showed that cross-priming by migratory lung DC was coupled with the acquisition of an anti-viral status, which was dependent on the type I IFN signaling pathway (Helft *et al*., 2012). It was also shown that MVA infection gives functional maturation to bystander DC, which was important for cross-presentation (Pascutti *et al*.,

2011; Flechsig *et al*., 2011). All these findings give a hint that innate immunity can influence cross-presentation.

VACV and MVA are recognized via multiple host-sensing pathways, including TLRs and RIG-I like receptors (RLR) (Delaloye *et al*., 2009). MVA is unique when compared to other VACV strains, since many immune evasion genes are inactivated or lost in the MVA genome (Antoine *et al*., 1998). As a result, activation of immune responses by MVA may strongly rely on the proper induction of innate immunity (Price *et al*., 2013). Flechsig *et al* showed that monocytes, DC and BC were most susceptible to MVA infection. Expression of chemokine ligand (CXCL10), tumor necrosis factor (TNF)-α, interleukin (IL)-6 and IL-12p70 was enhanced by MVA infection, but IL-1β and IL-10 were stable or even downregulated (Flechsig *et al*., 2011). Zimmerling *et al* also described that viral IL-1ß receptor expressed by MVA interferes with interleukin-1β activity produced by various virus-infected antigen-presenting cells (Zimmerling *et al*., 2013). Chemokines are especially important in developing CD8+ T cell responses. CCL2 could attract leucocytes to the site of infection (Lehmann *et al*., 2009). CXCL9 optimized the memory CD8+ T cell response in lymph nodes (Kastenmuller *et al*., 2013). As a result, cytokines and chemokines induced from MVA infection can bridge the innate responses and to adaptive immunity. Therefore, by recognition of MVA by innate receptors is essential for developing adaptive immunity.

MVA infection also induces pro-inflammatory cytokines, such as type I interferons (Eitz Ferrer *et al*., 2011; Delaloye *et al*., 2009; Waibler *et al*., 2007). It has been shown that MVA induced T-cell expansion was IFNAR-signalling dependent (Frenz *et*

al., 2010). There is an important, but not essential role for type I IFN in MVA-induced immunity (Paran *et al*., 2009). Due to the innate immune sensing of MVA, IFN I may play a role in the MVA mediate cross-presentation. Late antigens may not be able to trigger these innate signals, resulting in a block regarding the activation of cross-presentation. In addition to the current data, the presence of AraC in the feeder cell culture also resulted a total block of cross-presentation (Fig.33/35), which was not a result of toxicity to the cells (Fig.34). AraC is usually used for inhibiting DNA replication. This may imply that a DNA sensing signal may influence or regulate MVA mediated cross-presentation. Nevertheless, there is evidence that other innate recognition pathways e.g. mediated by TLRs or RLRs may also contribute to initiate adaptive responses to MVA (Price *et al*., 2013; Delaloye *et al*., 2009).

5.3 Reasons for delayed late viral antigen presentation

There are various factors which contribute to the epitope specificities of VACV induced T cell responses during infection, such as MHC binding affinity, efficiency of cellular antigen processing to generat the relevant peptides and TCR recognition, which also shapes the immunodominance pattern (Sette *et al*., 2009). Both antigen and MHC I molecules are important components for antigen presentation, as well as the APC itself. Therefore, three aspects have to be considered: 1) the antigen presentation machinery may not work; 2) different subcellular localization of early or late antigens may play a role or 3) distinct APC types may also influence the presentation ability.

To answer the first issue, K^b negative cells have been infected by MVA which itself encoded K^b. The peptide/K^b complex was successfully presented whenever K^b was expressed early or late (Fig.39). Even when the antigen was expressed late (l-ova or A19), it still could be visualized at the cell surface or activate the specific T cells (Fig.43). An interesting point is that in contrast to late expressed ova, the viral late antigen A19 could not be presented by K^b positive cells at six hours p.i. (Fig.45). However, when K^b came from a virus (J774 cells infected by MVA-H2K^b virus), the viral late antigen (A19) could be presented even faster and already activated CTL at four hours p.i. (Fig.44). This result indicates new options for the design of vaccines by using vectors that encode the MHC I molecules to activate late antigen specific immune responses.

Since the antigen presentation machinery is not impaired, a second possibility needs to be discussed: the location of different classes of antigens. Current models working on antigen presentation and T cell activation are based mostly on *in vivo* experiments and recombinant antigens, but very few publications have investigated viral antigens or compared viral antigens to recombinant antigens. Furthermore, there is still the open question of why antigens follow different pathways and why some antigens are impaired in direct- or cross-presentation.

A former study has shown that VACV expressing the foreign antigen ß-gal did not enter cross-presentation pathway when it is expressed late (Tewalt *et al*., 2009). The study was entirely based on only one antigen, ß-gal and therefore may not be representative for all late expressed vaccinia viral or recombinant genes. Additionally,

the BMDC maturation state was unknown, because they have shown no late gene expression of BMDC, which could account for the low antigen presentation *in vitro* experiments. However, they showed *in vivo* low ß-gal specific T cell activation from the VACV-late- ß-gal when compared to the VACV-early- ß-gal. The late ß-gal, which localized in the viral factory five hours p.i., was impaired for cross-presentation. The paper gives evidence, but is still not convincing in searching a final conclusion that all late antigens are impaired for cross-presentation, because they only showed one foreign antigen (ß-gal) and one time point. Other papers has demonstrated that the cellular location of antigens could impact direct-presentation (Gregg *et al*., 2011) and cross-presentation (Shen *et al*., 2004), but again, only stable ova antigens were used as the monitor. Besides, the quality of antigens can also influence the efficiency of direct-presentation (Kratzer *et al*., 2010) and cross-presentation (Schliehe *et al*., 2012).

According to the data presented here, all late viral antigens tested were delayed for presentation to CTL, such as A19 from C57BL/6 and H3, A6, I1 from HHD background (Fig.11/12). The foreign late antigen ova mediated higher activation than the viral antigen A19 (Fig.27). Not only have the different viral (A19/H3) and recombinant antigens (GFP/ova) been compared, but the kinetics for antigen direct-presentation in different genetic backgrounds of mice also been investigated (C57BL/6 or HHD). In addition, the present results demonstrate that 1) foreign and viral antigens behave differently with respect to antigen presentation: late ova could be presented earlier than late viral antigen, and 2) each recombinant antigen showed difference in presentation: late NP mediated less CTL activation than late ova (Fig.28). Thus, the quality of the

antigen itself determines its presentation capavity. Hence, it seems not to be justified for other publications to simply extend own results obtained from one specific late antigen to the whole class of late antigens. This study included the quality of antigens, such as ER-targeted antigen (K^b) or cytoplamatic antigen (ova). As a result, the data showed new aspects in antigen presentation not seen in former publications.

This study was the first attempt to find explanations for the phenomenon that presentation of late antigens to T cells is delayed. First, impairment of the MHC I antigen presentation machinery has been ruled out by using MVA-H2K^b-eGFP and ER Golgi staining. Second, late viral antigen H3 has been shown to be exclusively in viral factories from five hours to eight hours p.i. (Fig.47-48) and to activate the CTL earliest after eight hours infection (Fig.58). This demonstrated a major reason for the delayed antigen presentation of late viral antigens. Recombinant late antigens GFP or ova were visible in the viral factories for a shorter period compared to H3 (Fig.51-52/ 56), probably because they were not virus functional genes and also activated the CTL rather early after infection (Fig.45 l-ova). Recombinant K^b directly translocated from the viral factories because of its target signal to the ER and was transported to the cell surface (Fig.55). The present study gives a detailed analysis of the kinetics of MVA-expressed gene products in specific subcellular compartsments which was a key element to give an explanation for the delayed antigen presentation to CTL.

Vaccinia virus is characterized by its replication in the cytoplasm for which it forms special organells called viral factories close to the nucleus. Early viral proteins are synthesized at a place distant from the cores. The intermediate and late phase of the

replication cycle will occur in viral factories, which are known to be the site of transcription, translation as well as DNA replication (Katsafanas *et al*., 2007). As factories gradually will be collected besides the nucleus, new synthesized ER membranes are recruited to the replication sites; these will eventually form an almost completely sealed ER envelope around the site (Tolonen *et al*., 2001) (Fig.1). Some viral membrane proteins synthesized within viral factories are selected to be fused with viral crescent membranes or to translocate to the Golgi (Husain *et al*., 2007) (Fig.2).

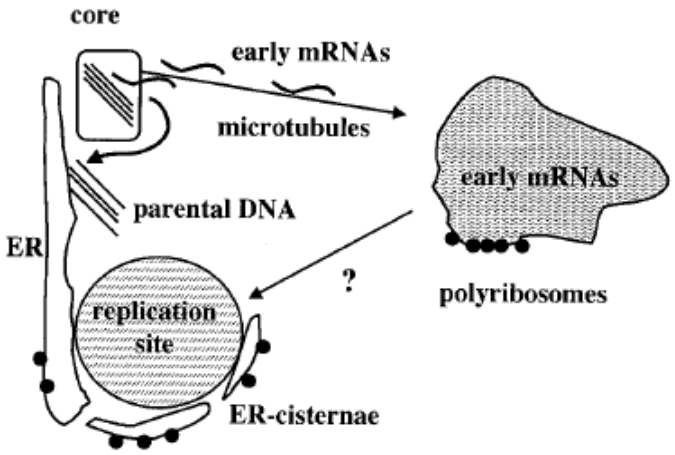

Figure 1: Cytoplasmic organization of the early stages of vaccinia virus infection. (Mallardo *et al*., 2002) As factories are gradually collected besides the nucleus, new synthesized ER membranes are recruited to the replication sites; these will eventually form an almost completely sealed ER envelope around the site.

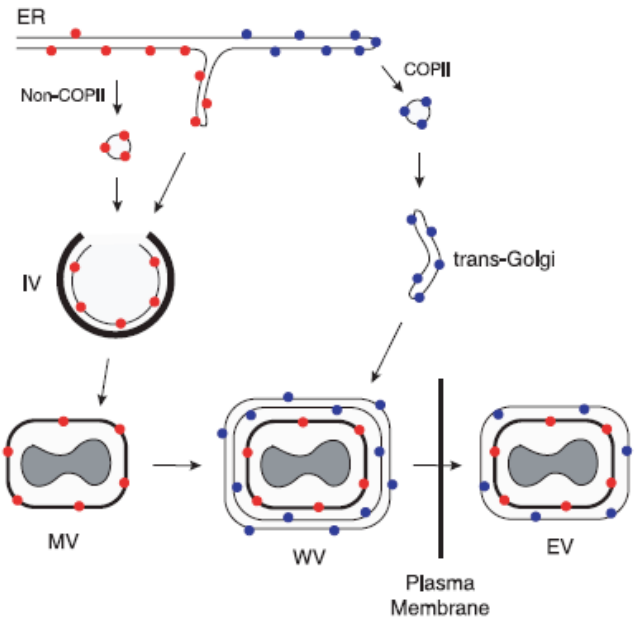

Figure 2: Sorting of proteins to MV and EV membranes. (Husain *et al*., 2007) ER membrane component COP II could select some viral proteins and move them out of viral factories. Some viral membrane proteins synthesized within viral factories are selected to be fused with viral crescent membranes or to translocate to the Golgi.

In the current study, early antigens were localized in the ER or cytosol so that antigen presentation was supposed to be easy, while late antigens were localized in viral factories, causing delayed presentation. Vaccinia virus infection did not result in presentation of late viral proteins, which might even be regarded as an immune evasive step to be protected from the host immune response. Therefore, the data also point out a new evasion mechanism affecting adaptive immunity, since alteration of the antigen location, may alter the presentation efficiency. Cowpox virus can also prevent MHC I presentation by trapping MHC class I molecules in the ER (Dasgupta *et al*., 2007; Byun *et al*., 2007). Therefore, targeting non-presented antigens to other compartments allowing for presentation could be one way to enhance the immunogenicity. Although H3 own a membrane targeting signal as well, it is present in the viral factories for an extended

time. Studies from others have shown that some viral proteins associate with others to home or leave the viral factories. For instance, when A6 expression was repressed, MV membrane proteins A13, A14, D8, and H3 did not localize to viral factories, but instead accumulated in the secretary compartments, including the endoplasmic reticulum (Meng *et al*., 2012). A10 and A4 proteins both first localized within the cytoplasm and later accumulated inside viral factories (Risco *et al*., 1999). So, the rules or the signals for being retained within or recruited to or leaving viral factories still need to be further characterized. Third, it was found that active proteasomes were excluded from viral factories and early H3 was less stable than late H3 which was not degradated. This finding is in line with the delay in late antigen presentation. Since most if not all direct-presentation is dependent on proteasome degradation, one could also speculate to provide late antigen access to the proteasome in order to achieve faster processing and presentation. Proteasome function has been implicated in the regulation of viral trafficking, replication, egress, and immune evasion (Banks *et al*., 2003). Mercer *et al* have also shown recently that vaccinia viral core proteins were already ubiquitylated during virus assembly. After entering the cytosol of an uninfected cell, the viral DNA was released from the core through proteasomal activity. Further, a Cullin3-based ubiquitin ligase mediated a further round of ubiquitylation and proteasomal action. This was needed to initiate viral DNA replication (Mercer *et al*., 2012). Thus, proteasome and ubiquitylation both play an important role in vaccinia virus replication. In this respect, one may anticipate already marked by ubiquitins in the viral factories, must be protected from the proteasome. Other researcher has observed the accumulation of ubiquitins in

colocalization with other proteins within poxvirus replication sites (Nerenberg *et al*., 2005), while the present study was not able to detect late H3 with ubiquitin by IP. However, we do not know if at the time the IP was performed, late H3 was still present in viral factories. Furthermore, we used different methods to detect ubiquitylation and the ubiquitins in viral factories detected by microscope may also be attached to other late antigens.

Third, the sequestration of late antigens to viral factories is not the only reason for delayed presentation. Different APC types, whether from human or mouse, additionally play a role. HLA-A2 or K^b positive cells showed different abilities for peptide/MHC I presentation (Fig.68), while K^b negative cells also showed different behaviors for peptide/K^b presentation when K^b was expressed by the virus (Fig.51-52/ 70-71). As shown recently by Duluc *et al*, antigens may need to be targeted to the proper APC subsets to elicite T cell responses (Duluc *et al*., 2012). However, with the treatment of IFN-γ MHC I expression and other components of the antigen presentation machinery can be upregulated. Here, Cloudman cells were able to regain the ability to present K^b at the cell surface (Fig.72-73). The difference between LCL (MHC I-positive (HLA-A2)) and Cloudman cells (MHC I-negative (K^b), but infected with a K^b producing MVA) could be that in Cloudman cells, antigens are close to the MHC I molecules, because they were localized in the same compartment namely the viral factories, and therefore may have early access to MHC I.

6. Conclusion

In the current thesis, a first set of antigen-specific CTL lines were generated from C57BL/6 mice vaccinated with recMVA viruses. These CTL recognized epitopes derived from VACV proteins (A19-late, A3-late, B8-early) or model antigens (ova/NP) that were produced either early or late during the viral life cycle. The CTL were tested for specific activation against endogenous (infected) and exogenous (peptide-pulsed) antigen presenting cells by measuring the IFN-γ production via intracellular cytokine staining (ICS). All the CTL had comparable avidity and were also specifically activated by the antigen presenting infected cells. They could also sufficiently lyse target cells as measured by chromium release.

One CTL line specific for the VACV protein A3, which according to literature represents a late gene product and is the major viral core particle component was surprisingly found to be activated by MVA-infected target cells at early stages after infection. The hypothesis that A3 seemed to be expressed early after infection was further confirmed by experiments using the inhibitory compound Arabinosid C (AraC, an inhibitor of VACV late gene expression). AraC blocked activation of all late antigen specific CTL lines apart from A3-specific CTL which was not inhibited. The failure of UV-inactivated viruses to induce CTL stimulation indicated the requirement of *de novo* protein synthesis and excluded the possibility of antigen sources derived from the viral input (virions). A3 was also expressed early in other vaccinia virus strains (CVA and WR), which was also confirmed at the mRNA level.

To fully test antigen presentation, a new assay for cross-presentation was set up. Cloudman cells (H2-K^b negative melanoma cell from Balb/C mice) were used as an antigenic source; BMDC from C57BL/6 mice were used as cross-presenters. Both showed good early and late gene expression and BMDC showed the ability for phagocytosing antigens and epitope presentation. PUVA was used to clear the virus, which left on infected Cloudman cells, to avoid further infection of BMDC.

By using both the direct- and cross-presentation assays, it was demonstrated that late antigens were not able to activate CTL by direct (endogenous) presentation as efficiently as early antigens and were unable to be stimulated via cross (exogenous) presentation pathways. These have been provn by different presenters (BMDC / DC2.4) for direct-presentation and different feeder cells (Cloudman / HeLa / A375) for cross-presentation. Nevertheless, CTL were tested in different background (C57BL/6 / HHD) as well.

This distinct availability of MHC I presentation and CTL activation was not due to an impairment of the antigen presenting machinery during infection. Thus, whenever K^b was expressed early or late by the virus, it still could be presented independent of antigen source (early/late or viral/foreign). However, when K^b was brought in by the virus, the viral late antigen could also be presented faster than the K^b positive cells. Hence, there is an advantage for the vaccine's design, which already contain the MHC I molecules to present late antigens at an earlier time.

The study revealed that the delay of late antigen presentation was dependent on different subcellular localization of early and late antigens and therefore by the antigenic

origin in infected cells. The recombinant antigen GFP produced late in infection was detected primarily in viral factories at six hours p.i, but translocated to the cytoplasm within one hour. In contrast, viral late envelope protein H3 was first visualized in viral factories at five hours p.i. and exclusively remained there for up to eight hours p.i. Early antigens localized to the ER or cytosol which suggested easy access to presentation pathways, while late antigens were sequestered in viral factories. The distinct compartimental localization was likely responsible for the delayed MHC-class I presentation of late antigens. Furthermore, late H3 protein was also more stable than early H3. In addition, active proteasomes were not visualized in viral factories, so the proteins inside this compartment may not be efficiently degraded and processed to achieve a measurable presentation. The data indicate a new evasion mechanism from adaptive immunity. By trapping viral late proteins in the factories, VACV most likely hides immunogenic components and evades from the host immune reponses. Additionally, the quality of the antigens had an impact on subcellular location and further processing and presentation, since the ER-targeted H2-K^b could translocate from the viral factories much faster than cytoplasmatic ova or GFP which was retained in viral factories for hours. This also indicates that targeting signals in recombinant proteins may circumvent viral immune evasion and enhance immunogenicity. Taken together, the timing of viral antigen production and the subsequent subcellular localization had a strong impact on the immunogenicity of MVA-delivered antigens.

In addition, distinct APC types also displayed a specific antigen presentation pattern. In HHD background, murine BMDC could present both, early and late antigens,

while human HLA-A2 positive LCL were unable to present late antigens. Some K^b negative cells lines, like J774, could present recombinant K^b expressed by MVA, while Cloudman cells could not. When presentation disabled cells were treated with IFN-γ, which upregulated MHC I, Cloudman cells regained the ability to present.

Above all, the timing of viral antigen expression and subsequent localization to specific cell compartments appears to be crucial for recMVA antigen processing and presentation. This research work offers new possibilities for improved vaccine design to overcome viral immune evasion and enhance immunogenicity by targeting recombinant proteins to specific compartments or by coexpressing proteins with MHC I molecules. However, other viral antigens and types of APC still need to be further investigated. The innate signaling pathways involved in activating the cross-presentation of MVA antigens and blocked byAraC, will also be investigated in future studies.

References

Aleyas, AG., Han, YW., Patil, AM., Kim, SB., Kim, K., Eo, SK. *Impaired cross-presentation of CD8α+ CD11c+ dendritic cells by Japanese encephalitis virus in a TLR2/MyD88 signal pathway-dependent manner.* Eur J Immunol, 2012; 42(10): 2655-2666.

Amiset, L., Fend, L., Gatard-Scheikl, T., Rittner, K., Duong, V., Rooke, R., Muller, S., Bonnefoy, JY., Préville, X., Haegel, H. *TLR2 ligation protects effector T cells from regulatory T-cell mediated suppression and repolarizes T helper responses following MVA-based cancer immunotherapy*. Oncoimmunology, 2012; 1(8): 1271-1280.

Antoine, G., Scheiflinger, F., Dorner, F., Falkner, FG. *The complete genomic sequence of the modified vaccinia Ankara strain: comparison with other orthopoxviruses.* Virology, 1998; 244: 365-395.

Assarsson, E., Sidney, J., Oseroff, C., Pasquetto, V., Bui, HH., Frahm, N., Brander, C., Peters, B., Grey, H., Sette, A. *A quantitative analysis of the variables affecting the repertoire of T cell specificities recognized after vaccinia virus infection*. J. Immunol, 2007; 178: 7890–7901.

Bachem, A., Hartung, E., Güttler, S., Mora, A., Zhou, X., Hegemann, A., Plantinga, M., Mazzini, E., Stoitzner, P., Gurka, S., Henn, V., Mages, HW., Kroczek, RA. *Expression of XCR1 Characterizes the Batf3-Dependent Lineage of Dendritic Cells Capable of Antigen Cross-Presentation*. Front Immunol, 2012; 3: 214.

Banks, L., Pim, D., Thomas, M. *Viruses and the 26S proteasome: hacking into destruction*. Trends Biochem. Sci, 2003; 28: 452-459.

Beeton, C. and K.G. Chandy, *Preparing T cell growth factor from rat splenocytes.* J Vis Exp, 2007(10): 402.

Belz, GT., Bedoui, S., Kupresanin, F., Carbone, FR., Heath, WR. *Minimal activation of memory CD8+ T cell by tissue-derived dendrite cells favors the stimulation of naïve CD8+ T cell.* Nat Immunol, 2007; 8: 1060-1066.

Bennink, JR., Yewdell, JW. *Recombinant vaccinia viruses as vectors for studying T lymphocyte specificity and function*. Curr Top Microbiol Immunol, 1990; 163: 153-184.

Berkers, CR., Van Leeuwen, FWB., Groothius, TA., Peperzak, V., Van Tilburg, EW., Borst, J., Neefjes, JJ., Ovaa, H. *Profiling Proteasome Activity in Tissue with Fluorescent Probes*. Melocular Pharmaceutics, 2007; 4(5): 739-748.

Betts, MR., Nason, MC., West, SM., De Rosa, SC., Migueles, SA., Abraham, J., Lederman, MM., Benito, JM., Goepfert, PA., Connors, M. *HIV nonprogressors preferentially maintain highly functional HIV-specific CD8+ T cells.* Blood, 2006; 107: 4781–4789.

Blum, JS., Wearsch, PA., Cresswell, P. *Pathways of antigen processing*. Annu Rev Immunol. 2013; 31: 443-473.

Brandler, S., Lepelley, A., Desdouits, M., Guivel-Benhassine, F., Ceccaldi, PE., Lévy, Y., Schwartz, O., Moris, A. *Preclinical studies of a modified vaccinia virus Ankara-based HIV candidate vaccine: antigen presentation and antiviral effect*. J Virol, 2010; 84(10): 5314-5328.

Budimir, N., Huckriede, A., Meijerhof, T., Boon, L., Gostick, E., Price, DA., Wilschut, J., de Haan, A. *Induction of heterosubtypic cross-protection against influenza by a whole inactivated virus vaccine: the role of viral membrane fusion activity.* PLoS One, 2012; 7(1): e30898.

Burgdorf, S., Kautz, A., Bohnert, V., Knolle, PA., Kurts, C. *Distinct pathways of antigen uptake and intracellular routing in CD4 and CD8 T cell activation.* Science, 2007; 316: 612-616.

Burgdorf, S., Scholz, C., Kautz, A., Tampe, R. Kurts, C. *Spatial and mechanistic separation of cross-presentation and endogenous antigen presentation.* Nature Immunol, 2008; 9: 558–566.

Busche, A., Jirmo, AC., Welten, SP., Zischke, J., Noack, J., Constabel, H., Gatzke, AK., Keyser, KA., Arens, R., Behrens, GM., Messerle, M. *Priming of CD8+ T cells against cytomegalovirus-encoded antigens is dominated by cross-presentation*. J Immunol, 2013; 190(6): 2767-2777.

Byun, M., Wang, X., Pak, M., Hansen, TH., Yokoyama, WM. *Cowpox virus exploits the endoplasmic reticulum retention pathway to inhibit MHC class I transport to the cell surface*. Cell Host Microbr, 2007; 2: 306-315.

Cebrian, I., Visentin, G., Blanchard, N., Jouve, M., Bobard, A., Moita, C., Enninga, J., Moita, L., Amigorena, S., Savina, A. *Sec22b regulates phagosomal maturation and antigen crosspresentation by dendritic cells.* Cell, 2011; 147: 1355-1368.

Chang, S., Chang, Y., Izmailyan, R., Tang, Y., Chang, W. *Vaccinia virus A25 and A26 proteins are fusion suppressors for mature virions and determine strain-specific virus entry pathways into HeLa, CHO-K1 and L cells.* Journal of Virology, 2010; 84(17): 8422-8432.

Chicha, L., Jarrossay, D., Manz, M.G. *Clonal type I interferon-producing and dendritic cell precursors are contained in both human lymphoid and myeloid progenitor populations.* J. Exp. Med, 2004; 200: 1519-1524.

Cohn, L., Chatterjee, B., Esselborn, F., Smed-Sörensen, A., Nakamura, N., Chalouni, C., Lee, BC., Vandlen, R., Keler, T., Lauer, P., Brockstedt, D., Mellman, I., Delamarre,

L. *Antigen delivery to early endosomes eliminates the superiority of human blood BDCA3+ dendritic cells at cross presentation*. J Exp Med, 2013; Epub ahead of print

Choi, EM., Palmowski, M., Chen, J., Cerundolo, V. *The use of chimeric A2K(b) tetramers to monitor HLA A2 immune responses in HLA A2 transgenic mice*. J Immunol Methods, 2002; 268(1): 35-41.

Chomczynski, P, Sacchi, N. *Single-step method of RNA isolation by acid guanidinium thiocyanate-phenol-chloroform extraction.* Anal. Biochem. 1987; 162: 156 –159.

Chu, CC., Ali, N., Karagiannis, P., Di Meglio, P., Skowera, A., Napolitano, L., Barinaga, G., Grys, K., Sharif-Paghaleh, E., Karagiannis, SN., Peakman, M., Lombardi, G., Nestle, FO. *Resident CD141 (BDCA3)+ dendritic cells in human skin produce IL-10 and induce regulatory T cells that suppress skin inflammation*. J Exp Med, 2012; 209(5): 935-945.

Compeer, EB., Flinsenberg, TW., van der Grein, SG., Boes, M. *Antigen processing and remodeling of the endosomal pathway: requirements for antigen cross-presentation*. Front Immunol, 2012; 3: 37.

Condit, R.C., Moussatche, N., Traktman, P. *In a nutshell: structure and assembly of vaccinia virion.* Adv Virus Res, 2006; 66: 31-124.

Cottingham, MG., Carroll, MW. *Recombinant MVA vaccines: dispelling the myths.* Vaccine, 2013; Epub ahead of print

Coupar, BE., Andrew, ME., Both, GW., Boyle, DB. *Temporal regulation of influenza hemagglutinin expression in vaccinia virus recombinants and effects on the immune response*. Eur. J. Immunol, 1986; 16: 1479–1487.

Damico, A., Wu, L. *The early progenitors of mouse dendritic cells and plasmacytoid predendritic cells within the bone marrow hemopoietic precursors expressing Flt3.* J. Exp. Med, 2003; 198: 293-303

Dangoor, A., Lorigan, P., Keilholz, U., Schadendorf, D., Harris, A., Ottensmeier, C., Smyth, J., Hoffmann, K., Anderson, R., Cripps, M., Schneider, J., Hawkins, R. *Clinical and immunological responses in metastatic melanoma patients vaccinated with a high-dose poly-epitope vaccine*. Cancer Immunol Immunother, 2010; 59(6): 863-873.

Dasgupta, A., Hammarlund, E., Slifka, MK., Fruh, K. *Cowpox virus evades CTL recognition and inhibits the intracellular transport of MHC class I molecules*. J Immunol, 2007; 178: 1654-1661.

Delaloye, J., Roger, T., Steiner-Tardivel, Q., Le Roy, D., Reymond, MK., Akira, S., Petrilli, V., Gomez, CE., Perdiguero, B., Tschopp, J., Pantaleo, G., Esteban, M., Calandra,

T. *Innate Immune Sensing of Modified Vaccinia Virus Ankara (MVA) Is Mediated by TLR2-TLR6, MDA-5 and the NALP3 Inflammasome*. PLoS Pathog, 2009; 5(6): 1000480.

Demoulin, S., Herfs, M., Delvenne, P., Hubert, P. *Tumor microenvironment converts plasmacytoid dendritic cells into immunosuppressive/tolerogenic cells: insight into the molecular mechanisms*. J Leukoc Biol, 2013; 93(3): 343-352.

Deng, Y., Gibbs, J., Bacík, I., Porgador, A., Copeman, J., Lehner, P., Ortmann, B., Cresswell, P., Bennink, JR., Yewdell, JW. *Assembly of MHC class I molecules with biosynthesized endoplasmic reticulum-targeted peptides is inefficient in insect cells and can be enhanced by protease inhibitors*. J Immunol, 1998; 161 (4): 1677-1685.

Depla, E., Van der Aa, A., Livingston, BD., Crimi, C., Allosery, K., De Brabandere, V., Krakover, J., Murthy, S., Huang, M., Power, S., Babé, L., Dahlberg, C., McKinney, D., Sette, A., Southwood, S., Philip, R., Newman, MJ., Meheus, L. *Rational design of a multiepitope vaccine encoding T-lymphocyte epitopes for treatment of chronic hepatitis B virus infections*. J Virol, 2008; 82(1): 435-450.

Desch, AN., Randolph, GJ., Murphy, K., Gautier, EL., Kedl, RM., Lahoud, MH., Caminschi, I., Shortman, K., Henson, PM., Jakubzick, CV. *CD103+ pulmonary dendritic cells preferentially acquire and present apoptotic cell-associated antigen.* J Exp Med, 2011; 208(9): 1789-1797.

Dominguez, PM., Ardavin, C. *Differentiation and function of mouse monocyte-derived dendritic cells in steady state and inflammation.* Immunol Rav, 2010; 234: 90-104.

Dresch, C., Leverrier, Y., Marvel, J., Shortman, K. *Development of antigen cross-presentation capacity in dendritic cells.* Trends Immunol, 2012; 33(8): 381-388.

Drexler, I., Staib, C., Kastenmuller, W., Stevanovic, S., Schmidt, B., Lemonnier, FA., Rammensee, HG., Busch, DH., Bernhard, H., Erfle, V., Sutter, G. *Identification of vaccinia virus epitope-specific HLA-A*0201-restricted T cells and comparative analysis of smallpox vaccines.* Proc Natl Acad Sci USA. 2003; 100(1): 217-222.

Drexler, I., Staib, C., Sutter, G. *Modified vaccinia virus Ankara as antigen delivery system: how can we best use its potential?* Current Opinion in Biotechnology, 2004; 15: 506-512.

Drillien, R., Spehner, D., Hanau, D. *Modified vaccinia virus Ankara induces moderate activation of human dendritic cells.* Journal of General Virology, 2004; 85: 2167-2175.

Duluc, D., Gannevat, J., Anguiano, E., Zurawski, S., Carley, M., Boreham, M., Stecher, J., Dullaers, M., Banchereau, J., Oh, S. *Functional diversity of human vaginal APC subsets in directing T-cell responses.* Mucosal Immunol, 2012; 7

Eitz Ferrer, P., Potthoff, S., Kirschnek, S., Gasteiger, G., Kastenmüller, W., Ludwig, H., Paschen, SA., Villunger, A., Sutter, G., Drexler, I., Häcker, G. *Induction of Noxa-mediated apoptosis by modified vaccinia virus Ankara depends on viral recognition by cytosolic helicases, leading to IRF-3/IFN-β-dependent induction of pro-apoptotic Noxa*. PLoS Pathog, 2011; 7(6): e1002083.

Flechsig, C., Suezer, Y., Kapp, M., Tan, SM., Löffler, J., Sutter, G., Einsele, H., Grigoleit, GU. *Uptake of antigens from modified vaccinia Ankara virus-infected leukocytes enhances the immunostimulatory capacity of dendritic cells*. Cytotherapy, 2011; 13(6): 739-752.

Frenz, T., Waibler, Z., Hofmann, J., Hamdorf, M., Lantermann, M., Reizis, B., Tovey, MG., Aichele, P., Sutter, G., Kalinke, U. *Concomitant type I IFN receptor-triggering of T cells and of DC is required to promote maximal modified vaccinia virus Ankara-induced T-cell expansion*. Eur J Immunol, 2010; 40: 2769–2777.

Gasteiger, G., Kastenmuller, W., Ljapoci, R., Sutter, G., Drexler, I. *Cross-priming of cytotoxic T cells dictates antigen requisites for modified vaccinia virus Ankara vector vaccines.* Journal of Virology, 2007; 81(21): 11925-11936.

GeurtsvanKessel, CH., Willart, MA., van Rijt, LS., Muskens, F., Kool, M., Baas, C., Thielemans, K., Bennett, C., Clausen, BE., Hoogsteden, HC., Osterhaus, AD., Rimmelzwaan, GF., Lambrecht, BN. *Clearance of influenza virus from the lung depends on migratory langerin+CD11b- but not plasmacytoid dendritic cells*. J Exp Med, 2008; 205(7): 1621-1634.

Gijzen, K., Cambi, A., Torensma, R., Figdor, CG. *C-type lectins on dendritic cells and their interaction with pathogen-derived and endogenous glycoconjugates*. Curr Protein Pept Sci, 2006; 7(4): 283-294.

Gilbert, SC. *Clinical development of Modified Vaccinia virus Ankara vaccines*. Vaccine, 2013; Mar 21.

Gómez, CE., Perdiguero, B., Cepeda, MV., Mingorance, L., García-Arriaza, J., Vandermeeren, A., Sorzano, CO., Esteban, M. *High, broad, polyfunctional and durable T cell immune responses induced in mice by a novel hepatitis C virus (HCV) vaccine candidate based on MVA expressing the near full-length HCV genome (MVA-HCV)*. J Virol, 2013; Epub ahead of print

Gregg, B., Dzierszinski, F., Tait, E., Jordan, KA., Hunter, CA., Roos, DS. *Subcellular antigen location influences T-cell activation during acute infection with Toxoplasma gondii.* PLoS One, 2011; 6(7): e22936.

Guillerme, JB., Boisgerault, N., Roulois, D., Ménager, J., Combredet, C., Tangy, F., Fonteneau, JF., Gregoire, M. *Measles virus vaccine-infected tumor cells induce tumor*

antigen cross-presentation by human plasmacytoid dendritic cells. Clin Cancer Res, 2013; 19(5): 1147-1158.

Guzman, E., Cubillos-Zapata, C., Cottingham, MG., Gilbert, SC., Prentice, H., Charleston, B., Hope, JC. *Modified vaccinia virus Ankara-based vaccine vectors induce apoptosis in dendritic cells draining from the skin via both the extrinsic and intrinsic caspase pathways, preventing efficient antigen presentation*. J Virol, 2012; 86(10): 5452-5466.

Haniffa, M., Collin, M., Ginhoux, F. *Identification of human tissue cross-presenting dendritic cells: A new target for cancer vaccines.* Oncoimmunology, 2013; 2(3): e23140.

Hanwell, DG., McNeil, B., Visan, L., Rodrigues, L., Dunn, P., Shewen, PE., Macallum, GE., Turner, PV., Vogel, TU. *Murine Responses to Recombinant MVA Versus ALVAC Vaccines Against Tumor-associated Antigens, gp100 and 5T4*. J Immunother, 2013; 36(4): 238-247.

Hayes, P., Gilmour, J., von Lieven, A., Gill, D., Clark, L., Kopycinski, J., Cheeseman, H., Chung, A., Alter, G., Dally, L., Zachariah, D., Lombardo, A., Ackland, J., Sayeed, E., Jackson, A., Boffito, M., Gazzard, B., Fast, PE., Cox, JH., Laufer, D. *Safety and immunogenicity of DNA prime and modified vaccinia ankara virus-HIV subtype C vaccine boost in healthy adults*. Clin Vaccine Immunol, 2013; 20(3): 397-408.

He, Y., Zhang, J., Donahue, C., Falo, LD J. *Skin-Derived Dendritic Cells Induce Potent CD8+ T Cell Immunity in Recombinant Lentivector-Mediated Genetic Immunization.* Immunity, 2006; 24: 643-656.

Helft, J., Manicassamy, B., Guermonprez, P., Hashimoto, D., Silvin, A., Agudo, J., Brown, BD., Schmolke, M., Miller, JC., Leboeuf, M., Murphy, KM., García-Sastre, A., Merad, M. *Cross-presenting CD103+ dendritic cells are protected from influenza virus infection*. J Clin Invest, 2012; 122(11): 4037-4047.

Henry, JY., Labarthe, MC., Meyer, B., Dasgupta, P., Dalgleish, AG., Galustian, C. *Enhanced cross-priming of naive CD8+ T cells by DCs treated by the IMiDs immunomodulatory compounds Lenalidomide and Pomalidomide.* Immunology, 2013; Epub ahead of print.

Hesse, J., Reyda, S., Tenzer, S., Besold, K., Reuter, N., Krauter, S., Büscher, N., Stamminger, T., Plachter, B. *Human Cytomegalovirus pp71 Stimulates Major Histocompatibility Complex Class I Presentation of IE1-Derived Peptides at Immediate Early Times of Infection*. J Virol, 2013; 87(9): 5229-5238.

Hopkins RA, Connolly JE. *The specialized roles of immature and mature dendritic cells in antigen cross-presentation*. Immunol Res, 2012; 53(1-3): 91-107.

Hotta, C., Fujimaki, H., Yoshinari, M., Nakazawa, M., Minami, M. *The delivery of an antigen from the endocytic compartment into the cytosol for cross-presentation is restricted to early immature dendritic cells*. Immunology, 2006; 117(1): 97-107.

Houde, M., Bertholet, S., Gagnon, E., Brunet, S., Goyette, G., Laplante, A., Princiotta, MF., Thibault, P., Sacks, D., Desjardins, M. *Phagosomes are compartment organelles for antigen cross-presentation.* Nature, 2003; 425(6956): 402-406.

Husain, M., Weisberg, AS., Moss, B. *Sequence-independent targeting of transmembrane proteins synthesized within vaccinia virus factories to nascent viral membranes*. J Virol, 2007; 81(6): 2646-2655.

Hwang, ST. *Homeward Bound: How Do Skin Dendritic Cells Find Their Way into the Lymph System?* Journal of Investigative Dermatology, 2012; 132(4): 1070–1073.

Iborra, S., Izquierdo, H., Martinez-Lopez, M., Blanco-Menendez, N., Sousa, C., Sancho, D. *The DC receptor DNGR-1 mediates cross-priming of CTL during vaccinia virus infection in mice.* The Journal of Clinical Investigation, 2012; 122(5): 1628-1643.

Ikeuchi, N., Futami, J., Hosoi, A., Noji, S., Kurachi, M., Ueha, S., Fujii, S., Yamada, H., Matsushima, K., Moriyasu, F., Kakimi. K. *Efficient cross-presentation of soluble exogenous antigens introduced into dendritic cells using a weak-based amphiphilic peptide.* Biochemical and Biophysical Research Communications, 2010; 392: 217-222.

Jing, L., Chong, TM., McClurkan, CL., Huang, J., Story, BT., Koelle, DM. *Diversity in the acute CD8 T cell response to vaccinia virus in humans.* J. Immunol, 2005; 175: 7550–7559.

Joffre, OP., Sequra, E., Savina A., Amigorena S. *Cross-presentation by dendritic cells.* Nature Reviews Immunology, 2012; 12(8): 557-569.

Kastenmuller, W., Drexler, I., Ludwig, H., Erfle, V., Peschel, C., Bernhard, H., Sutter, G. *Infection of human dendritic cells with recombinant vaccinia virus MVA reveals general persistence of viral early transcription but distinct maturation-dependent cytopathogenicity.* Virology, 2006; 350(2): 276-288.

Kastenmuller, W., Gasteiger, G., Gronau, JH., Baier, R., Ljapoci, R., Busch, DH., Drexler, I. *Cross-competition of CD8+ T cells shapes the immunodominance hierarchy during boost vaccination.* J Exp Med, 2007; 204(9): 2187-2198.

Kastenmuller, W., Brandes, M., Wang, Z., Herz, J., Egen, JG., Germain, RN. *Peripheral Prepositioning and Local CXCL9 Chemokine-Mediated Guidance Orchestrate Rapid Memory CD8(+) T Cell Responses in the Lymph Node*. Immunity, 2013; 38(3): 502-13.

Katsafanas, G., Moss, B. *Colocalization of transcription and translation within cytoplasmic poxvirus factories coordinates viral expression and subjugates host functions.* Cell Host & Microbe, 2007; 2: 221-228.

Kauffmann, S., Thomsen, AR., Christensen, JP. *Role of very late antigen-1 in T-cell-mediated immunity to systemic viral infection*. Scand J Immunol, 2006; 63(4): 290-298.

Kim, E., Kwak, H., Ahn, K. *Cytosolic aminopeptidases influence MHC class I-mediated antigen presentation in an allele-dependent manner*. J Immunol, 2009; 183 (11): 7379-7387.

Kitchen, SG., Levin, BR., Bristol, G., Rezek, V., Kim, S., Aguilera-Sandoval, C., Balamurugan, A., Yang, OO., Zack, JA. *In vivo suppression of HIV by antigen specific T cells derived from engineered hematopoietic stem cells*. PLoS Pathog, 2012; 8(4): e1002649.

Klechevsky, E., Morita, R., Liu, M., Cao, Y., Coquery, S., Thompson-Snipes, L., Briere, F., Chaussabel, D., Zurawski, G., Palucka, AK., Reiter, Y., Banchereau, J., Ueno, H. *Functional specializations of human epidermal Langerhans cells and CD14+ dermal dendritic cells.* Immunity, 2008; 29(3): 497-510.

Khanna, KM., Aguila, CC., Redman, JM., Suarez-Ramirez, JE., Lefrancois, L., Cauley, LS. *In situ imaging reveals different reponses by naïve and memory CD8 T cells to late antigen presentation by lymph node DC after influenza virus infection.* Eur J Immunol, 2008; 38: 3304-3315.

Kratzer, R., Mauvais, FX., Burgevin, A., Barilleau, E., van Endert, P. *Fusion proteins for versatile antigen targeting to cell surface receptors reveal differential capacity to prime immune responses.* J Immunol, 2010; 184(12): 6855-6864.

Lambe, T., Carey, JB., Li, Y., Spencer, AJ., van Laarhoven, A., Mullarkey, CE., Vrdoljak, A., Moore, AC., Gilbert, SC. *Immunity against heterosubtypic influenza virus induced by adenovirus and MVA expressing nucleoprotein and matrix protein-1.* Sci Rep, 2013; 3: 1443.

Lehmann, MH., Kastenmuller, W., Kandemir, JD., Brandt, F., Suezer, Y., Sutter, G. *Modified vaccinia virus ankara triggers chemotaxis of monocytes and early respiratory immigration of leukocytes by induction of CCL2 expression*. J Virol, 2009; 83: 2540–2552.

Li, L., Kim, S., Herndon, JM., Goedegebuure, P., Belt, BA., Satpathy, AT., Fleming, TP., Hansen, TH., Murphy, KM., Gillanders, WE. *Cross-dressed CD8α+/CD103+ dendritic cells prime CD8+ T cells following vaccination.* Proc Natl Acad Sci USA, 2012; 109(31): 12716-12721.

Liu, L., Chavan, R., Feinberg, MB. *Dendritic Cells are preferentially targeted among hematolymphocytes by Modified Vaccinia Virus Ankara and play a key role in the induction of virus-specific T cell responses in vivo*. BMC Immunology, 2008; 9: 15.

Lu, X., Gibbs, JS., Hickman, HD., David, A., Dolan, BP., Jin, Y., Kranz, DM., Bennink, JR., Yewdell, JW., Varma, R. *Endogenous viral antigen processing generates peptide-specific MHC class I cell-surface clusters*. Proc Natl Acad Sci USA, 2012; 109(38): 15407-15412.

Mantegazza, AR., Magalhaes, JG., Amigorena, S., Marks, MS. *Presentation of phagocytosed antigens by MHC class I and II.* Traffic, 2013; 14(2): 135-152.

Martin, H., Mandron, M., Davrinche, C. *Interplay between human cytomegalovirus and dendritic cells in T cell activation*. Med Microbiol Immunol, 2008; 197(2): 179-184.

Martinez-Pomares, L. *The mannose receptor*. J Leukoc Biol, 2012; 92(6): 1177-1186.

McGill, J., Van Rooijen, N., Legge, K.L. *Protective influenza-specific CD8 T cell responses require interactions with dendritic cells in the lungs*. J. Exp. Med. 2008; 205: 1635–1646.

Meng, X., Embry, A., Rose, L., Yan, B., Xu, C., Xiang, Y. *Vaccinia virus A6 is essential for virion membrane biogenesis and localization of virion membrane proteins to sites of virion assembly*. J Virol, 2012; 86(10): 5603-5613.

Mercer, AA., Ueda, N., Friederichs, SM., Hofmann, K., Fraser, KM., Bateman, T., Fleming, SB. *Comparative analysis of genome sequences of three isolates of rf virus reveals unexpected sequence variation*. Vrus Research, 2006; 116: 146-158.

Mercer, J., Snijder, B., Sacher, R., Burkard, C., Bleck, CK., Stahlberg, H., Pelkmans, L., Helenius, A. *RNAi screening reveals proteasome- and Cullin3-dependent stages in vaccinia virus infection*. Cell Rep, 2012; 2(4): 1036-47.

Merzougui, N., Kratzer, R., Saveanu, L., van Endert, P. *A proteasome-dependent, TAP-independent pathway for cross-presentation of phagocytosed antigen*. EMBO Rep., 2011; 12: 1257–1264.

Meyer, VS., Kastenmulle,r W., Gasteige,r G., Franz-Wachtel, M., Lamkemeyer, T., Rammensee, HG., Stevanovic, S., Sigurdardottir, D., Drexler, I. *Long-term immunity against actual poxviral HLA ligands as identified by differential stable isotope labelin*g. J Immunol, 2008; 181(9): 6371-6383.

Moffat, JM., Cheong, WS., Villadangos, JA., Mintern, JD., Netter, HJ. *Hepatitis B virus-like particles access major histocompatibility class I and II antigen presentation pathways in primary dendritic cells*. Vaccine, 2013; 31(18): 2310-2316.

Moss, B. *Poxviridae: the viruses and their replication.* Fields Virology, Knipe, D.M., Howley, P.M., Eds. Lippincott Williams & Wilkins, Philadelphia, PA, USA, 2007; Volume 2: 2905-2946.

Moutaftsi, M., Peters, B., Pasquetto, V., Tscharke, DC., Sidney, J., Bui, HH., Grey, H., Sette, A. *A consensus epitope prediction approach identifies the breadth of murine T(CD8+)-cell responses to vaccinia virus*. Nat. Biotechnol, 2006; 24: 817–819.

Moutaftsi, M., Bui, HH., Peters, B., Sidney, J., Salek-Ardakani, S., Oseroff, C., Pasquetto, V., Crotty, S., Croft, M., Lefkowitz, EJ., Grey, H., Sette, A. *Vaccinia virus-specific CD4+ T cell responses target a set of antigens largely distinct from those targeted by CD8+ T cell responses*. J. Immunol, 2007; 178: 6814–6820.

Moutaftsi, M., Tscharke, DC., Vaughan, K., Koelle, DM., Stern, L., Calvo-Calle, M., Ennis, F., Terajima, M., Sutter, G., Crotty, S., Drexler, I., Fanchini, G., Yewdell, JW. *Uncovering the interplay between CD8, CD4 and antibody responses to complex pathogens.* Future Microbiol., 2010; 5(2): 221-239.

Mullarkey, CE., Boyd, A., van Laarhoven, A., Lefevre, EA., Carr, BV., Baratelli, M., Molesti, E., Temperton, NJ., Butter, C., Charleston, B., Lambe, T., Gilbert, SC. *Improved adjuvanting of seasonal influenza vaccines: Pre-clinical studies of MVA-NP+M1 co-administration with inactivated influenza vaccine*. Eur J Immunol. 2013; Epub ahead of print

Naik, S., Proietto, A., Wilson, N., Dakic A., Schnorrer, P., Fuchsberger, M,. Lahoud, M., O'Keeffe, M., Shao, Q., Chen, W., Villadangos, J., Shortman, K., Wu, L. *Generation of splenic CD8+ and CD8- dendritic cell equivalents in fms-like tyrosine kinase 3 ligand bone marrow cultures.* The Journal of Immunology, 2005; 174: 6592-6597.

Neefjes, J., Jongsma, LM., Paul, P., Bakke, O. *Towards a systems understanding of MHC class I and MHC class II antigen presentation.* Nat Rev Immunol, 2011; 11(12): 823-836.

Nerenberg, BT., Taylor, J., Bartee, E., Gouveia, K., Barry, M., Früh,K. *The poxviral RING protein p28 is a ubiquitin ligase that targets ubiquitin to viral replication factories*. J. Virol, 2005; 79: 597-601.

Nierkens, S., Tel, J., Janssen, E., Adema, GJ. *Antigen cross-presentation by dendritic cell subsets: one general or all sergeants?* Trends Immunol, 2013; Epub ahead of print.

Nopora, K., Bernhard, CA., Ried, C., Castello, AA., Murphy, KM., Marconi, P., Koszinowski, U., Brocker, T. *MHC class I cross-presentation by dendritic cells counteracts viral immune evasion*. Front Immunol, 2012; 3: 348.

Olivier, M., Foret, B., Le Vern, Y., Guilloteau, LA. *Capacities of migrating CD1b+ lymph dendritic cells to present Salmonella antigens to naive T cells*. PLoS One, 2012; 7(1): e30430.

Oseroff, C., Kos, F., Bui, HH., Peters, B., Pasquetto, V., Glenn, J., Palmore, T., Sidney, J., Tscharke, DC., Bennink, JR., Southwood, S., Grey, HM., Yewdell, JW., Sette, A. *HLA class I-restricted responses to vaccinia recognize a broad array of proteins mainly involved in virulence and viral gene regulation*. Proc. Natl Acad. Sci. USA, 2005; 102: 13980–13985.

Oseroff, C., Peters, B., Pasquetto, V., Moutaftsi, M., Sidney, J., Panchanathan, V., Tscharke, DC., Maillere, B., Grey, H., Sette, A. *Dissociation between epitope hierarchy and immunoprevalence in CD8 responses to vaccinia virus western reserve*. J. Immunol, 2008; 180: 7193–7202.

Paran, N., Suezer, Y., Lustig, S., Israely, T., Schwantes, A., Melamed, S., Katz, L., Preuss, T., Hanschmann, KM., Kalinke, U., Erez, N., Levin, R., Velan, B., Löwer, J., Shafferman, A., Sutter, G. *Postexposure immunization with Modified Vaccinia Virus Ankara or conventional Lister vaccine provides solid protection in a murine model of human smallpox*. J Infect Dis, 2009; 199: 39–48.

Pascutti, MF., Rodríguez, AM., Falivene, J., Giavedoni, L., Drexler, I., Gherardi, MM. *Interplay between modified vaccinia virus Ankara and dendritic cells: phenotypic and functional maturation of bystander dendritic cells*. J Virol, 2011; 85(11): 5532-5545.

Pasquetto, V., Bui, HH., Giannino, R., Banh, C., Mirza, F., Sidney, J., Oseroff, C., Tscharke, DC., Irvine, K., Bennink, JR., Peters, B., Southwood, S., Cerundolo, V., Grey, H., Yewdell, JW., Sette, A. *HLA-A*0201, HLA-A*1101, and HLA-B*0702 transgenic mice recognize numerous poxvirus determinants from a wide variety of viral gene products*. J. Immunol, 2005; 175: 5504–5515.

Platt, CD., Ma, JK., Chalouni, C., Ebersold, M., Bou-Reslan, H., Carano, RA., Mellman, I., Delamarre, L. *Mature dendritic cells use endocytic receptors to capture and present antigens*. Proc Natl Acad Sci (PNAS) USA, 2010; 107(9): 4287-4292.

Poulin, LF., Salio, M., Griessinger, E., Anjos-Afonso, F., Craciun, L., Chen, JL., Keller, AM., Joffre, O., Zelenay, S., Nye, E., Le Moine, A., Faure, F., Donckier, V., Sancho, D., Cerundolo, V., Bonnet, D., Reis e Sousa, C. *Characterization of human DNGR-1+ BDCA3+ leukocytes as putative equivalents of mouse CD8alpha+ dendritic cells*. J Exp Med. 2010; 207(6): 1261–1271.

Poulin, LF., Reyal, Y., Uronen-Hansson, H., Schraml, BU., Sancho, D., Murphy, KM., Håkansson, UK., Moita, LF., Agace, WW., Bonne,t D., Reis e Sousa, C. *DNGR-1 is a specific and universal marker of mouse and human Batf3-dependent dendritic cells in lymphoid and nonlymphoid tissues.* Blood, 2012; 119(25): 6052-62.

Price, PJ., Torres-Domínguez, LE., Brandmüller, C., Sutter, G., Lehmann, MH. *Modified vaccinia virus Ankara: Innate immune activation and induction of cellular signalling.* Vaccine, 2013; Epub ahead of print.

Ramirez, MC., Sigal, LJ. *Macrophages and dendritic cells use the cytosolic pathway to rapidly cross-present antigen from live, vaccinia-infected cells*. J Immunol, 2002; 169(12): 6733-6742.

Razvi, ES., Welsh, RM., McFarland, HI. *In vivo state of antiviral CTL precursors. Characterization of a cycling cell population containing CTL precursors in immune mice*. J Immunol, 1995; 154(2): 620-632.

Rehermann, B., Ferrari, C., Pasquinelli, C. & Chisari, F. V. *The hepatitis B virus persists for decades after patients' recovery from acute viral hepatitis despite active maintenance of a cytotoxic T-lymphocyte response*. Nat Med, 1996a; 2: 1104–1108.

Rehermann, B., Lau, D., Hoofnagle, J. H. & Chisari, F. V. (1996b). *Cytotoxic T lymphocyte responsiveness after resolution of chronic hepatitis B virus infection*. J Clin Invest, 1996b; 97: 1655–1665.

Ricklin Gutzwiller, ME., Moulin, HR., Zurbriggen, A., Roosje, P., Summerfield, A. *Comparative analysis of canine monocyte- and bone-marrow-derived dendritic cells*. Vet Res, 2010; 41(4): 40.

Risco, C., Rodríguez, JR., Demkowicz, W., Heljasvaara, R., Carrascosa, JL., Esteban, M., Rodríguez, D. *The vaccinia virus 39-kDa protein forms a stable complex with the p4a/4a major core protein early in morphogenesis*. Virology, 1999; 265(2): 375-386.

Rizzitelli, A., Meuter, S., Vega Ramos, J., Bird, CH., Mintern, JD., Mangan, MS., Villadangos, J., Bird, PI. *Serpinb9 (Spi6)-deficient mice are impaired in dendritic cell-mediated antigen cross-presentation.* Immunol Cell Biol, 2012; 90(9): 841-851.

Rubinstein, MP., Kovar, M., Purton, JF., Cho, JH., Boyman, O., Surh, CD., Sprent, J. *Converting IL-15 to a superagonist by binding to soluble IL-15R* α. Proc Natl Acad Sci USA, 2006; 103: 9166-9171.

Sallusto, F., Lenig, D., Forster, R., Lipp, M., Lanzavecchia, A. *Two subsetsof memory T lymphocytes with distincthoming potentials and effector functions*. Nature, 1999; 401: 708–712.

Sallusto, F., Langenkamp, A., Geginat, J., Lanzavecchia, A. *Functional subsetsof memory T cells identified by CCR7 expression*. Curr. Top. Microbiol. Immunol, 2000; 251: 167–171.

Sánchez-Sampedro, L., Gómez, CE., Mejías-Pérez, E., Sorzano, CO., Esteban, M. *High quality long-term CD4+ and CD8+ effector memory populations stimulated by DNA-LACK/MVA-LACK regimen in Leishmania major BALB/c model of infection*. PLoS One, 2012; 7(6): e38859.

Sancho, D., Joffre, OP., Keller, AM., Rogers, NC., Martínez, D., Hernanz-Falcón, P., Rosewell, I., Reis e Sousa, C. *Identification of a dendritic cell receptor that couples sensing of necrosis to immunity.* Nature, 2009; 458(7240): 899–903.

Satheshkumar PS, Weisberg AS, Moss B. *Vaccinia virus A19 protein participates in the transformation of spherical immature particles to barrel shaped infectious virions.* J Virol. 2013 Jul 24. [Epub ahead of print]

Satpathy, AT., Wu, X., Albring, JC., Murphy, KM. *Re(de)fining the dendritic cell lineage*. Nat Immunol, 2012; 13(12): 1145-1154.

Saveanu, L., Carroll, O., Weimershaus, M., Guermonprez, P., Firat, E., Lindo, V., Greer, F., Davoust, J., Kratzer, R., Keller, SR., Niedermann, G., van Endert, P. *IRAP identifies an endosomal compartment required for MHC class I cross-presentation.* Science,2009; 325: 213–217.

Savina, A., Jancic, C., Hugues, G., Guermonprez, P., Vargas, P., Moura, IC., Lennon-Dumenil, AM., Seabra, MC., Raposo, G., Amigorena, S. *NOX2 controls phagosomal pH to regulate antigen processing during crosspresentation by dendritic cells.* Cell, 2006; 126: 205-218.

Segura, E., Albiston, AL., Wicks, IP., Chai, SY., Villadangos, JA. *Different cross-presentation pathways in steady-stateand inflammatory dendritic cells.* Proc. Natl Acad. Sci. USA, 2009; 106: 20377-20381.

Segura, E., Villadangos, JA. *A modular and combinatorial view of the antigen cross-presentation pathway in dendritic cells*. Traffic, 2011; 12(12): 1677-1685.

Segura, E., Valladeau-Guilemond, J., Donnadieu, MH., Sastre-Garau, X., Soumelis, V., Amigorena, S. *Characterization of resident and migratory dendritic cells in human lymph nodes*. J Exp Med, 2012; 209(4): 653-660.

Segura, E., Durand, M., Amigorena, S. *Similar antigen cross-presentation capacity and phagocytic functions in all freshly isolated human lymphoid organ-resident dendritic cells*. J Exp Med, 2013; 210(5): 1035-1047.

Serna, A., Ramirez, MC., Soukhanova, A., Sigal, LJ. *Efficient MHC class I cross-presentatio during early vaccinia infection requires the transfer of proteasomal intermediates between antigen donor and presenting cells*. J Immunol, 2003; 171: 5668-5672.

Sette, A., Grey, H., Oseroff, C., Peters, B., Moutaftsi, M., Crotty, S., Assarsson, E., Greenbaum, J., Kim, Y., Kolla, R., Tscharke, D., Koelle, D., Johnson, RP., Blum, J., Head, S., Sidney, J. *Definition of epitopes and antigens recognized by vaccinia specific immune responses: their conservation in variola virus sequences, and use as a model system to study complex pathogens*. Vaccine, 2009; 27: Suppl 6:G21-6.

Schliwa, M. *Action of Cytochalasin D on Cytoskeletal Networks*. The Journal of Cell Biology, 1982; 92: 79-91.

Schliehe, C., Bitzer, A., van den Broek, M., Groettrup, M. *Stable antigen is most effective for eliciting CD8+ T-cell responses after DNA vaccination and infection with recombinant vaccinia virus in vivo*. J Virol, 2012; 86(18): 9782-9793.

Schramm, B., de Haan, CA., Young, J., Doglio, L., Schleich, S., Reese, C., Popov, AV., Steffen, W., Schroer, T., Locker, JK. *Vaccinia-virus-induced cellular contractility facilitates the subcellular localization of the viral replication sites*. Traffic, 2006; 7(10): 1352-1367.

Schulz, O., Reis e Sousa, C. *Cross-presentation of cell-associated antigens by CD8alpha+ dendritic cells is attributable to their ability to internalize dead cells.* Immunology, 2002; 107(2): 183–189.

Sheehy, SH., Duncan, CJ., Elias, SC., Biswas, S., Collins, KA., O'Hara, GA., Halstead, FD., Ewer, KJ., Mahungu, T., Spencer, AJ., Miura, K., Poulton, ID., Dicks, MD., Edwards, NJ., Berrie, E., Moyle, S., Colloca, S., Cortese, R., Gantlett, K., Long, CA., Lawrie, AM., Gilbert, SC., Doherty, T., Nicosia, A., Hill, AV., Draper, SJ. *Phase Ia clinical evaluation of the safety and immunogenicity of the Plasmodium falciparum blood-stage antigen AMA1 in ChAd63 and MVA vaccine vectors*. PLoS One, 2012; 7(2): e31208.

Shen, L., Rock, KL. *Cellular protein is the source of cross-priming antigen in vivo*. Proc Natl Acad Sci USA, 2004; 101: 3035-3040.

Shen, Z., Reznikoff, G., Dranoff, G., Rock, KL. *Cloned dendritic cells can present exogenous antigens on both MHC class I and class II molecules.* J Immunol. 1997; 158(6): 2723-2730.

Shortman, K., Liu, YJ. *Mouse and human dendritic cell subtypes.* Nat Rev Immunol, 2002; 2: 151-161.

Shortman, K., Naik, SH. *Steady-state and inflammatory dendritic cell development.* Nat Rev Immunol, 2007; 7: 19-30.

Shortman, K., Heath, WR. *The CD8+ dendritic cell subset.* Immunol. Rev, 2010; 234: 18-31.

Siciliano, NA., Huang, L., Eisenlohr, LC. *Recombinant poxviruses: versatile tools for immunological assays.* Methods Mol Biol, 2013; 960: 219-245.

St Leger, AJ., Peters, B., Sidney, J., Sette, A., Hendricks, RL. *Defining the herpes simplex virus-specific CD8+ T cell repertoire in C57BL/6 mice.* J Immunol, 2011; 186(7): 3927-3933.

Staib, C., I. Drexler, G. Sutter. *Construction and isolation of recombinant MVA.* Methods Mol Biol, 2004; 269: 77-100.

Stoklasek, TA., Schluns, KS., Lefrançois, L. *Combined IL-15/IL-15Ralpha immunotherapy maximizes IL-15 activity in vivo.* J Immunol, 2006; 177: 6072-6080.

Sutter, G., Moss, B. *Nonreplicating vaccinia vector efficiently expresses recombinant genes.* Proc Natl Acad Sci USA, 1992; 89(22): 10847-10851.

Szatmary, Z. *Molecular biology of toll-like receptors*. Gen Physiol Biophys, 2012; 31(4): 357-366.

Tel, J., Schreibelt, G., Sittig, SP., Mathan, TS., Buschow, SI., Cruz, LJ., Lambeck, AJ., Figdor, CG., de Vries, IJ. *Human plasmacytoid dendritic cells efficiently cross-present exogenous Ags to CD8+ T cells despite lower Ag uptake than myeloid dendritic cell subsets*. Blood, 2013; 121(3): 459-467.

Terajima, M., Cruz, J., Raines, G., Kilpatrick, ED., Kennedy, JS., Rothman, AL., Ennis, FA. *Quantitation of CD8+ T cell responses to newly identified HLA-A*0201-restricted T cell epitopes conserved among vaccinia and variola (smallpox) viruses*. J Exp Med, 2003; 197(7): 927-932.

Terajima, M., Orphin, L., Leporati, AM., Pazoles, P., Cruz, J., Rothman, AL., Ennis, FA. *Vaccinia virus-specific CD8+ T-cell reponses target a group of epitope without a strong immunodominance hierarchy in humans.* Hum Immunol, 2008; 69: 815-825.

Tewalt, EF., Grant, JM., Granger, EL., Palmer, DC., Heuss, ND., Gregerson, DS., Restifo, NP., Norbury, CC. *Viral sequestration of antigen subverts cross presentation to CD8(+) T cells*. PLoS Pathog, 2009; 5(5): e1000457.

Tolonen, N., Doglio, L., Schleich, S., Krijnse Locker, J. *Vaccinia virus DNA replication occurs in endoplasmic reticulum-enclosed cytoplasmic mini-nuclei*. Mol Biol Cell, 2001; 12(7): 2031-2046.

Tscharke, DC., Karupiah, G., Zhou, J., Palmore, T., Irvine, KR., Haeryfar, SM., Williams, S., Sidney, J., Sette, A., Bennink, JR., Yewdell, JW. *Identification of poxvirus CD8+ T cell determinants to enable rational design and characterization of smallpox vaccines.* J Exp Med, 2005; 201(1): 95-104.

Tsung, K., Yim, JH., Marti, W., Buller, RML., Norton, JA. *Gene expression and cytopathic effect of vaccinia virus inactivated by psoralen and long-wave uv light*. Journal of Virology, 1996; 70(1): 165-171.

Unger, WW., van Kooyk, Y. *'Dressed for success' C-type lectin receptors for the delivery of glyco-vaccines to dendritic cells*. Curr Opin Immunol, 2011; 23(1): 131-137.

Van der Most, RG., Murali-Krishna, K., Ahmed, R. *Prolonged presence of effector-memory CD8 T cells in the centralnervous system after dengue virus encephalitis.Int*. Immunol, 2003; 1: 119–125.

Van Vliet, SJ., García-Vallejo, JJ., Van Kooyk, Y. *Dendritic cells and C-type lectin receptors: coupling innate to adaptive immune responsesDCs and CLRs*. Immunology and Cell Biology, 2008; 86: 580-587.

Villadangos, J.A., Yong, L. *Antigen-presentation properties of plasmacytoid dendritic cells.* Immunology, 2008; 29: 352-361.

Volz, A., Sutter, G. *Protective efficacy of Modified Vaccinia virus Ankara in preclinical studies*. Vaccine, 2013; Epub ahead of print

Waibler, Z., Anzaghe, M., Ludwig, H., Akira, S., Weiss, S., Sutter, G., Kalinke, U. *Modified Vaccinia Virus Ankara induces Toll-Like Receptor-independent Type I Interferon responses*. J Virol, 2007; 81: 12102–12110.

Wagner, C., Cresswell, P. *TLR and nucleotide-binding oligomerization domain-like receptor signals differentially regulate exogenous antigen presentation.* The Journal of Immunology, 2012; 188: 686-693.

Wyatt, LS., Earl, PL., Eller, LA., Moss, B. *Highly attenuated smallpox vaccinie protects mice with and without immune deficiencies against pathogenic vaccinia virus challenge.* Proc Nat Acad Sci USA, 2004; 101: 4590-4595.

Xu, RH., Remakus, S., Ma, X., Roscoe, F., Sigal, LJ. *Direct presentation is sufficient for an efficient anti-viral CD8+ T cell response*. PLoS Pathog, 2010; 6(2): e1000768.

Yang, Z., Reunolds, S.E., Martens, C.A., Bruno, D.P., Porcella, S.F., Moss, B. *Expression profiling of the intermediate and late stages of poxvirus replication.* The Journal of Virology, 2011; 85: 9899-9908.

Yewdell, JW., Bennink, JR., Smith, GL., Moss, B. *Influenza A virus nucleoprotein is a major target antigen for cross-reactive anti-influenza A virus cytotoxic T lymphocytes*. Proceedings of the National Academy of Sciences of the United States of America, 1985; 82(6): 1785–1789.

Yewdell, JW. *DRiPs solidify: progress in understanding endogenous MHC class I antigen processing*. Trends Immunol, 2011; 32(11): 548-558.

Yoshida, R, T., Imai, K., Hieshima, J., Kusuda, M., Baba, M., Kitaura, M., Nishimura, M., Kakizaki, H., Nomiyama, O.Yoshie. *Molecular cloning of anovel human CC chemokine EBI1-ligand chemokine that is a specific functionalligand for EBI1, CCR7.* J. Biol. Chem., 1997; 272: 13803–13809.

Zaiss, DM., Sijts, AJ., Mosmann, TR. *Enumeration of cytotoxic CD8 T cells ex vivo during the response to Listeria monocytogenes infection*. Infect Immun, 2008; 76(10): 4609-4614.

Zehner, M., Burgdorf, S. *Regulation of antigen transport into the cytosol for cross-presentation by ubiquitination of the mannose receptor*. Mol Immunol, 2013; 55(2): 146-148.

Zimmerling, S., Waibler, Z., Resch, T., Sutter, G., Schwantes, A. *Interleukin-1β receptor expressed by modified vaccinia virus Ankara interferes with interleukin-1β activity produced in various virus-infected antigen-presenting cells*. Virol J, 2013; 10: 34.

Zhao, Y., De Trez, C., Flynn, R., Ware, CF., Croft, M., Salek-Ardakani, S. *The adaptor molecule MyD88 directly promotes CD8 T cell responses to vaccinia virus*. J Immunol, 2009; 182(10): 6278-6286.

Zhao, RY., Mifsud, NA., Xiao, K., Chan, KF., Oveissi, S., Jackson, HM., Dimopoulos, N., Guillaume, P., Knights, AJ., Lowen, T., Robson, NC., Russell, SE., Scotet, E., Davis, ID., Maraskovsky, E., Cebon, J., Luescher, IF., Chen, W. *A novel HLA-B18 restricted CD8+ T cell epitope is efficiently cross-presented by dendritic cells from soluble tumor antigen*. PLoS One, 2012; 7(9): e44707.

Zhang, N., Bevan, MJ. *CD8(+) T cells: foot soldiers of the immune system*. Immunity, 2011; 35(2): 161-168.

Acknowledgements

This dissertation would not have been possible without the help and support of so many people in so many ways, to only some of whom it is possible to give particular mention here.

First and foremost, I would like to express my deep gratitude to my supervisor Prof. Ingo Drexler, for his patient guidance, enthusiastic encouragement and valuable advices with unsurpassed knowledge for this research work. He has not only opened the door of scientific research for me, but also guides me to get into the way for being a scientist. He has been invaluable on both academic and personal level, for which I am extremely grateful.

My special great appreciation goes to Ronny Ljapoci, for his willingness to give his time so generously for most of the methods, generation of the viruses and the long kinetic experiments which can not be done without his help. His assistance has always been my inspiration as I hurdle all the obstacles in the completion of this research work.

Furthermore, I would like to thank Georg Gasteiger for introducing me to the topic as well for the support and development of this research work on the way.

My thanks also addressed to my committee membes, Prof. Dr. Volker Bruss and PD Dr. Oliver Ebert, for their advices and assistances in keeping my progress on schedule.

My grateful thanks are also extended to my colleagues and friends in the former institute in Helmholtz Zentrum München (Container), who gave me a nice working atmosphere. Thanks Andreas Muschaweckh for showing the BMDC preparation; Annie

Zhang and Xiaoming Cheng for sharing the experiences for the Confocal microscopy. Many thanks also go to the present colleges in Düsseldorf, especially, Mirko Trilling and Benjamin Katschinski for their guidance in IP experiments and Marek Widera for the q-PCR experiments.

Last, but not the least, I would like to thank my family who boosted me morally throughout and my friends, Yuchen Xia, Ke Zhang and our secretary Andrea Schmidbauer in Munich who provided me great information resources and the support and encouragement when I came to Germany.